TESLA - COLLABORATION

R & D Issues in the Field of Superconducting Cavities

March 6 - 8, 1995
DESY

Editor: D. Proch, DESY, MHF-sl

DESY Print May 1995, TESLA 95-09

Contents, Page I

Talks:

Contents, Page II

Reports from Working Groups

D.Proch
MHF-SL

DESY, 05.01.95

Workshop on Cavity Fabrication Techniques

Mon. to Wed., 6 to 8 March, 1995
DESY

In this workshop alternative fabrication methods of Niobium resonators will be discussed. At present resonators from solid Niobium are produced by forming cups (spinning, deep drawing, etc.) and welding at the iris and equator. For TESLA needs this fabrication method is expensive and may produce large spread of performance at the welded area. Different fabrication methods have been tried out in the past, for example spinning or hydraulic forming of the whole cavity. The final aim is to find a fabrication method for seamless Niobium cavities. It is the idea of this workshop to bring interested people together to

- report about past experiments,
- discuss the understanding of success or failure,
- collect all available information about metallurgical properties of Niobium
- review principal fabrication methods
- report/discuss present activities in development of new fabrication methods
- have time to brainstorm on new ideas
- organize/coordinate joined effort in different labs or companies

An agenda will be distributed after confirmation of attendees.

Below you find a list of people who will be invited. If you know further experts who might be interested, please let me know. Also for comments or proposals, please contact me via

e-mail: Proch@Proch.Desy.de
or fax: (0049/40) 8994 4302
or phone: (0049/40) 8998 3273

<u>Please indicate your attendance as soon as possible</u>

For housing arrangement please contact Katrin Lando via
E-mail: Lando@Lando.Desy.de
or fax (0049/40) 8994 4302

D. Proch, MHF-SL

DESY, 24.2.95

Workshop on cavity fabrication

Agenda

Monday, 6. March 95, Building 30B, Room 459

09:00 - 09:20	Welcome and Introduction	Wiik
09:20 - 09:30	Organizing Remarks	Proch
	Tutorials:	
09:30 - 10:15	On the microstructure and mechanical properties of metallic materials	Müller
10:15 - 10:45	Coffee break	
10:45 - 11:30	Niobium production: from ore to high quality sheet material	Schölz
11:30 - 12:15	Superplastic forming (to be confirmed)	Schleinzer
12:15 - 14:00	Lunch	
14:00 - 14:30	Mechanical data of Niobium	Rao
14:30 - 15:00	Electrical data of Niobium	Matheisen
15:00 - 15:45	Experience with hydroforming of cavities	Hauviller
15:45 - 16:15	Coffee break	
16:15 - 17:00	Experience with spinning of cavities	Palmieri
17:00 - 17:45	Experience with alternative methods of cavity fabrication	Padamsee
19:00	Social event (Desy canteen)	

IV

Workshop on cavity fabrication

Agenda

Tuesday, 7. March 95, Building 30B, room 459:

09:00 - 09:20	Experiments with hydroforming at INR	Jelezov, Singer
09:20 - 09:40	Experiments with hydroforming at DESY	Stepanov, Singer
09:40 - 10:00	Experiments with hydroforming at Butting	Schüller
10:00 - 12:30	Reports/discussion about further experience with forming techniques, also unsuccessful experiments	Kneisel
10:40 - 11:00	Coffee break	
12:30 - 14:00	Lunch	
14:00 - 14:10	Organization of discussion/ working groups:	Proch
	- Cavity fabrication	Kneisel
	- Niob properties	Bonin
14:10 - 16:00	Working groups (rm 362, bldg. 30B, rm 204, bldg. 55, kleiner Gästespeiseraum, canteen)	
16:00 - 16:30	Coffee break	
16:30 - 18:00	Continue of working groups	

==================================

Wednesday, 8. March 95,

09:00 - 10:45	Continue of working groups (rm 362, bldg. 30B, rm 292, bldg. 1D, rm 204, bldg. 55)	
	Building 1, Sem. Room 1:	
10:45 - 11:15	Coffee break	
11:15 - 12:30	Continue of working groups	Kneisel, Bonin
12:30 - 14:00	Lunch	
14:00 - 16:00	Plenary:	
	- Reports from Working groups	Kneisel, Bonin
	- Closing remarks	Proch

==================================

Appendix: Yield strength measurements

Attendees Cavity Fabrication Techniques Workshop, March 6 - 8, 1995, DESY

Vorname	Name	Institut	Abteilung	Straße	Stadt	Land	fax	tel	e-mail
Claire	Antoine	Saclay	DAPNIA/SEA - Bat. 701		F-91191 Gif sur Yvette	FRANCE	33-1-69 08 64 42		
B.	Aune	Saclay	DAPNIA/SEA - Bat. 701		F-91191 Gif sur Yvette	FRANCE	33-1-6908 9196		
Bernard	Bonin	Saclay	DAPNIA/SEA - Bat. 701		F-91191 Gif sur Yvette	FRANCE	33-1-69 08 64 42	33-1-6908 8451	bonin@hep.saclay.cea.fr
J.	Borne	LAL Orsay	Bat. 200	Centre d'Osay	F-91405 Orsay Cedex	FRANCE	33-1-69 07 94 04	33-1-6446 64 11	
B.	Dwersteg	DESY	MHF-sl	Notkestraße 85	D-22603 Hamburg	Germany	49-40-8994 4302	49-40-8998 3379	
Helen	Edwards	DESY	FDET	Notkestraße 85	D-22603 Hamburg	Germany	49-40-8998 3094	49-40-8998 3147	hedwards@vxdesy.desy.d
Thomas	Fuljahn	DESY	FDET	Notkestraße 85	D-22603 Hamburg	Germany	49-40-8998 3094	49-40-8998 4588	fuljahn@desy.de
Heinrich	Hartwig	DESY	MVA	Notkestraße 85	D-22603 Hamburg	Germany		49-40-8998 3457	
C.	Hauviller	CERN			CH-1211 Geneva 23	SCHWEIZ			Claude_Hauviller@macmai
Dr. Igor N.	Jelezov	INR		60th October Anniversary	117312 Moscow	Russia		7-095-334 0966	
H.	Kaiser	DESY	MPL	Notkestraße 85	D-22603 Hamburg	Germany	49-40-8994 4305	49-40-8998 3284	
Dr. G.	Kljatchkov	INR		60th October Anniversary	117312 Moscow	Russia	7-095-334 0966		
Peter	Kneisel	CEBAF	SRF Department	12000 Jefferson Avenue	Newport News, VA 23606	USA	1-804-249 7658	1-804-249 7646	kneisel@cebaf.gov
J.	Kouptsides	DESY	MVA	Notkestraße 85	D-22603 Hamburg	Germany		49-40-8998 3695	
G.	Kreps	DESY	MHF-sl	Notkestraße 85	D-22603 Hamburg	Germany	49-40-8994 4302	49-40-8998 2394	
Moyses	Kuchnir	FNAL		P.O.Box 500	Batavia, IL 60510	USA	1-708-840 3756	1-708-840 3368	kuchnir@fnalv.fnal.gov
Jozef	Kuzminski	DESY	MHF-sl	Notkestraße 85	D-22603 Hamburg	Germany	49-40-8994 4302	49-40-8998 2047	jozefk@vxdesy.desy.de
Dr. Adamo	Laurenti	Ansaldo	PMA	Via N. Lorenzi, 8	I-16152 Genoa	ITALY	39-10-655 6485	39-10-655 6232	
P.	Maccioni	Cerca		Les Berauds - B.P. 1114	F-26104 ROMANS Cedex	France	33-75 05 39 58	33-75 05 60 92	
Jean	Marini	LAL Orsay	Bat. 200	Centre d'Osay	F-91405 Orsay Cedex	FRANCE	33-1-69 07 94 04	33-1-64 46 83 03	
A.	Matheisen	DESY	MHF-sl	Notkestraße 85	D-22603 Hamburg	Germany	49-40-8994 4302	49-40-8998 2774	
Frank	Meyer	Meyer Tool		4601 W Southwest Hwy	Oaklawn, IL 60453	USA	1-708-425 7612	1-708-425 9080	
Marina	Minestrini	INFN Frascati	LNF	Via E. Fermi 40	I-00044 Frascati (Roma)	ITALY	39-6-9403 565	39-6-9403 336	marinam@vaxlnf.lnf.infn.it
D.	Moffat	Saclay	DAPNIA/SEA - Bat. 701		F-91191 Gif sur Yvette	FRANCE	33-1-69 08 64 42		moffat@hep.saclay.cea.fr
W.-D.	Möller	DESY	MHF-sl	Notkestraße 85	D-22603 Hamburg	Germany	49-40-8994 4302	49-40-8998 2515	wolf@moeller.desy.de
F.	Müller	HdBW	FB Maschinenbau	Hostenhofweg 85	22043 Hamburg		49-40-6541 2737	49-40-6541 3379	
H.	Nadal	Cerca		Tour Fian Cedex 16	F-92084 Paris la Defense	FRANCE	33-1-4796 5892	33-1-4796 5886	
Hasan	Padamsee	Cornell	Newman Lab		Ithaca, NY 14853	USA			hsp@cesr10.lns.cornell.ed
Carlo	Pagani	INFN Milano	L.A.S.A.	Via Fratelli Cervi 201	I-20090 Segrate (Milano)	ITALY	39-2-2392 543	39-2-2392 561	pagani@mvlasa.mi.infn.it
V.	Palmieri	INFN Legnaro		Via Romea 4	I-35020 Legnaro (Padova)	ITALY	39-49-64 19 25	39-49-8292 321	
Michael	Peiniger	ACCEL Instruments		Friedrich-Ebert-Str. 1	51429 Bergisch-Gladbach		49-2204-84 25 01	49-2204-84 36 76	
Michael	Pekeler	DESY	FDET	Notkestraße 85	D-22603 Hamburg	Germany	49-40-8998 3094	49-40-8998 3950	michael@pekeler.desy.de
J.P.	Poupeau	Saclay	DAPNIA/SEA - Bat. 701		F-91191 Gif sur Yvette	FRANCE	33-1-69 08 64 42		
Dieter	Proch	DESY	MHF-sl	Notkestraße 85	D-22603 Hamburg	Germany	49-40-8994 4302	49-40-8998 3273	proch@proch.desy.de
G.	Rao	CEBAF		12000 Jefferson Avenue	Newport News, VA 23606	USA	1-804-249 7658	1-804-249 7651	rao@cebaf.gov
J.P.	Rodriguez	Saclay	DAPNIA/SEA - Bat. 701		F-91191 Gif sur Yvette	FRANCE	33-1-69 08 64 42		
Th.	Schilcher	DESY	MHF-sl	Notkestraße 85	D-22603 Hamburg	Germany	49-40-8994 4302	49-40-8998 4584	mhfsil@dsyibm.desy.de
	Schleinzer	Dornier GmbH	Postfach 1360		88039 Friedrichshafen	Germany	49-7545-88548	07545-88695	
P.	Schmüser	DESY	FDET	Notkestraße 85	D-22603 Hamburg	Germany	49-40-8998 3094		
Friedhold	Schölz	W.C. Heraeus GmbH		Heraeusstr. 12-14	63450 Hanau	D	49-6181-35 59 75	06181-35 54 60	
Thomas	Schüller	Fa. H. Butting (	Röhren- und Metallwerk	Gifhornerstr. 59	29377 Wittingen-Knesebeck		05834-50436	05834-50 391	
Q.S.	Shu	DESY	MHF-sl	Notkestraße 85	D-22603 Hamburg	Germany	49-40-8994 4302	49-40-8998 2775	
W.	Singer	DESY	MHF-sl	Notkestraße 85	D-22603 Hamburg	Germany	49-40-8994 4302	49-40-8998 2775	
	Stephan	FZ Rossendorf		Postfach 510 119	D-01314 Dresden	Germany			
A.	Stephanov	INR/DESY	MVA	Notkestraße 85	22603 Hamburg	D	7-095-3340 968	49-40-8998 234 4	
Christoph	Stolzenburg	DESY	FDET	Notkestraße 85	D-22603 Hamburg	Germany	49-40-8998 3094	49-40-8998 3950	stol@teslahc.desy.de
J.	Susta	CEBAF	SRF Department	12000 Jefferson Avenue	Newport News, VA 23606	USA	1-804-249 7658	1-804-249 7651	
B.H.	Wiik	DESY	GD	Notkestraße 85	D-22603 Hamburg	Germany	49-40-8994 4304	40-40-8998 2407	wiik@desy.de
Siegfried	Wolff	DESY	B1	Notkestraße 85	D-22603 Hamburg	Germany	49-40-8998 3094	49-40-8998 3409	swolff@desy.de

D. Proch, DESY

Conclusion of fabrication workshop

1. SPINNING

The spinning technique is most advanced to make seamless cavities. After making some single cavities by spinning, now the RF performance of the heavily deformed Nb materiel has to be measured.

Action points:
- Prepare and carry out the cold measurement of the single cell cavity made by Palmieri. Help is offered by DESY to make the cold measurement (frequency is 1.5 GHz, not 1.3 GHz!!).
- Make second cavity at Heraeus (first was cut for metallurgical investigation)
  Prepare beam pipes and stiffening rig (wall thickness thins down from 2.5 to .8 mm)

2. HYDRAULIC FORMING

Hydraulic forming seems to be very promising. Investigations must be carried out to reduce the number of intermittent heating.

Action points:
- Finish design and start construction of INR-DESY machine. Next meeting at INR (KW 21) to discuss the layout and prepare spec./order of hydraulic system
- Fix dimension of tube for optimal hydroforming. Proposal by INR: OD 110 mm, wall thickness 5 mm, not optimized , is equal to available test pipe of Cu at INR.
- Send Nb material to Palmieri to make seamless Nb tube. Outer dia of 136 mm, wall thickness about 3 mm
- Continue investigation of welded pipe (longitudinal weld). Make cuts to be investigated by Prof. Kreye. (weld should have same metallurgical properties as bulk material.)
- Reserve or order Nb sheets for 10 tubes
- Get offer from companies for forming and welding 10 tubes, od of 136 mm, thickness 3 mm
- Contact Schleinzer, Dornier, for Addresses of German companies with magnetic forming equipment.
- Contact Prof. Dormann, Institute for Hydroforming, to discuss/organize collaboration on seamless cavity production (first meeting at Paderborn at 20.April 95).

3. EXPLOSIVE FORMING

At KEK efforts are started for explosive forming.

Action points:
- Establish contact for exchange of experience.
- Is there an institute for explosive forming techniques? Also try Dynamite Nobel to get possible addresses.

4. SUPER PLASTIC FORMING

Super plastic forming might be possible with Nb.

Action points:
- Contact Schleinzer, Dornier, for Russian paper about super plasticity of Nb.
- Contact Schleinzer, Dornier, to organize experiments at Dornier/DESY to investigate super plastic properties of Nb.

5. INNER SPINNING

Inner spinning was proposed and discussed as simple alternative method for fabrication.

Action points:
- Contact Dornier, ACCEL, Heraeus, for addresses of competent spinning companies.

6. DATA BASE

A data base is needed to compile all electrical and mechanical data on Nb. There was agreement that Rao`s compiled data will be extended by further measurements at CEBAF (also DESY?) and published. Bonin will extend and publish his data base also.

Action points:
- Regular contact/exchange of information should be organized (CEBAF, DESY, Saclay) at R&D discussions during TTF meetings.
- A recent Ph.D. work at Saclay about Nb properties should be distributed (CEBAF, DESY, ...?)

DESY

Founded in 1959.

- Charge:

  Develop, design and construct large accelerator facilities and to use these facilities in collaboration with universit[y] groups to explore the structure of matter at short distances and for research based on synchrotron radiation

- Status:

  Two laboratories – Hamburg / Zeuthe[n]

  Budget: 270 MDM

  Employies: 1600

  Users : 2600 from 31 Nations

- Particle Physics → HERA

  Users : 260 from 21 German Institutio[ns]
  990 from 91 Univ. in 21 Count[ries]

- Synchrotron Radiation

  Users : 770 from 95 German Instituti[ons]
  580 from 140 Univ. in 26 Count[ries]

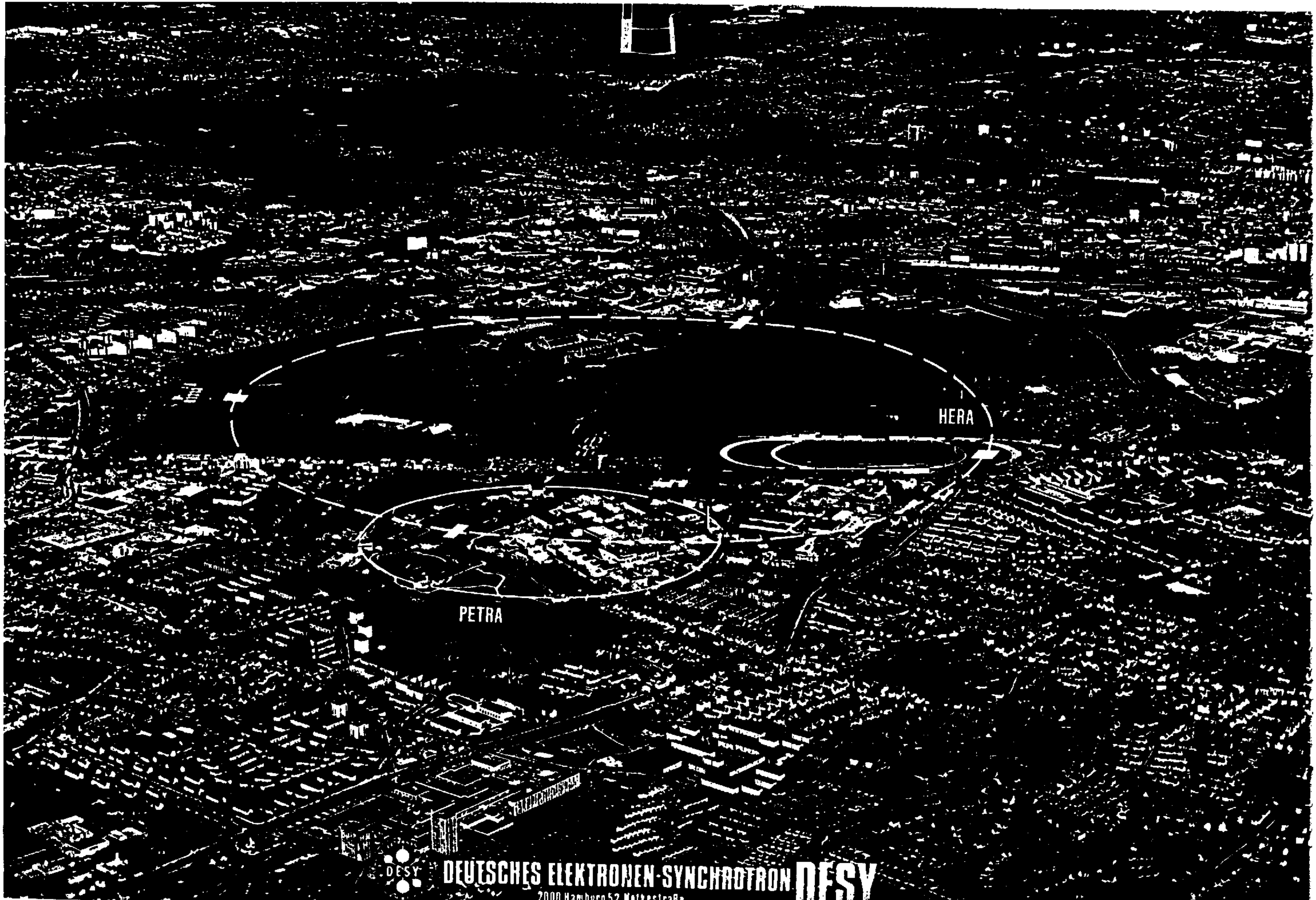
HERA
PETRA
DESY
DEUTSCHES ELEKTRONEN-SYNCHROTRON DESY
2000 Hamburg 52 Notkestraße

TESLA 1995-09

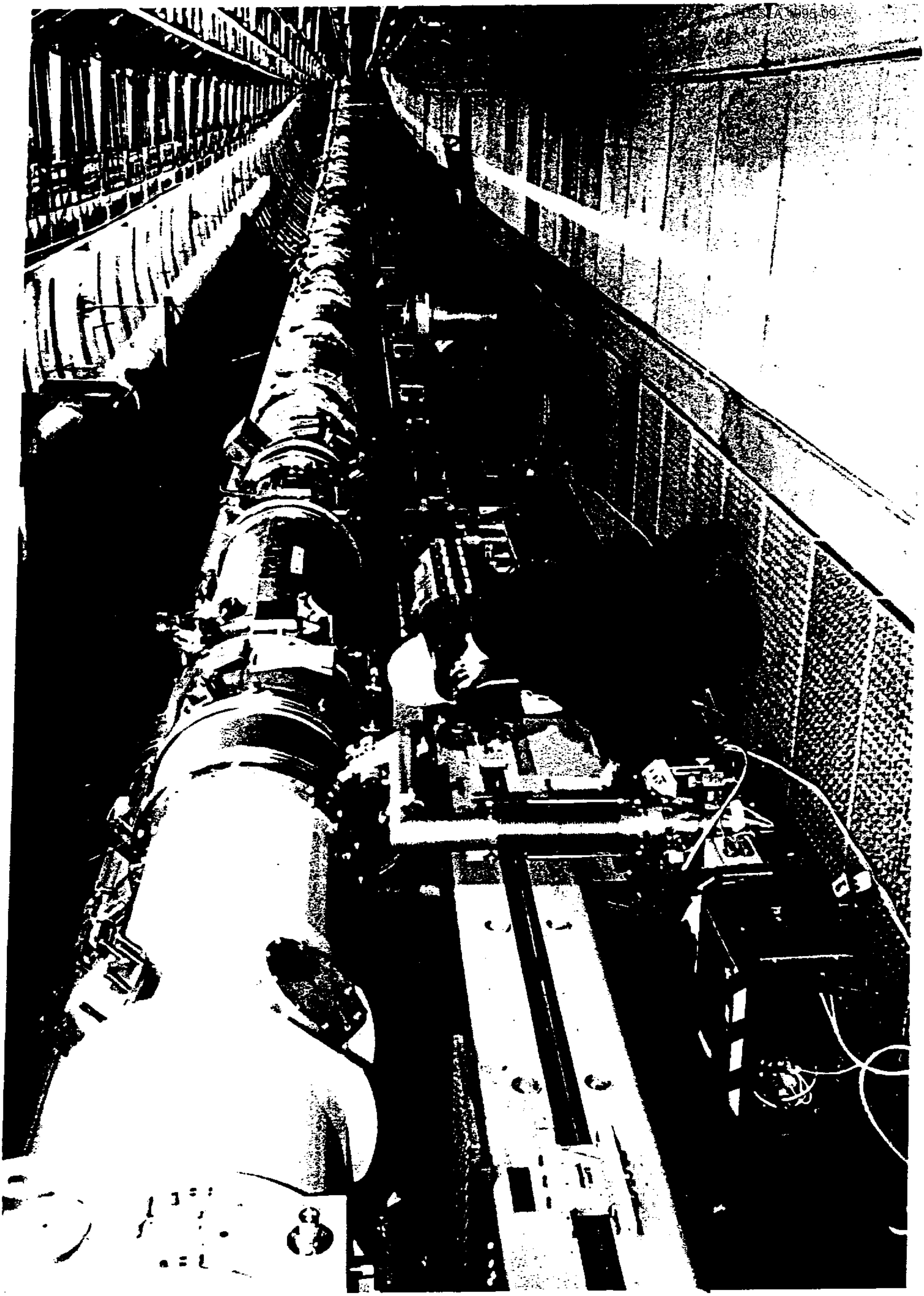

TESLA 1995-09

The Future

- HERA and HASYLAB (DORIS, PETRA; FEL-Facility) will provide the basis for a front line research programme until ~ 2005.

- It takes 15-20 years from the first ideas until turn on of a large facility

- The new facility should.

  be a unique device providing physics opportunities complementar to those which will become availab at the LHC

  keep the symbiosis between particle physics and synchrotron radiation

- DESY's choice supported by the Scientifi Council

  → 500 GeV e^+e^- linear collide

$\varepsilon_y \lesssim 10^{-12}\,\pi\cdot m\,rad$

For coherent light

$\varepsilon < \lambda/4\pi$

$\lambda = 1\,\mathring{A}$

$\Rightarrow \varepsilon = 8\cdot 10^{-12}\,\pi\, m\cdot rad$

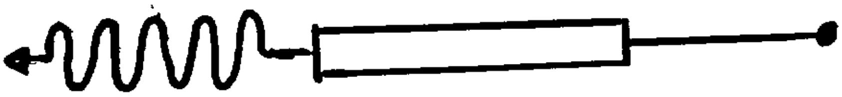

Undulator

ESRF (.94

$\varepsilon_x = 7\cdot 10^{9}\,\pi\cdot m\cdot$

$\varepsilon_y = 2\cdot 10^{-10}\,\pi\, m$

$\varepsilon_y = 10^{-13}\,\pi\, m\cdot$

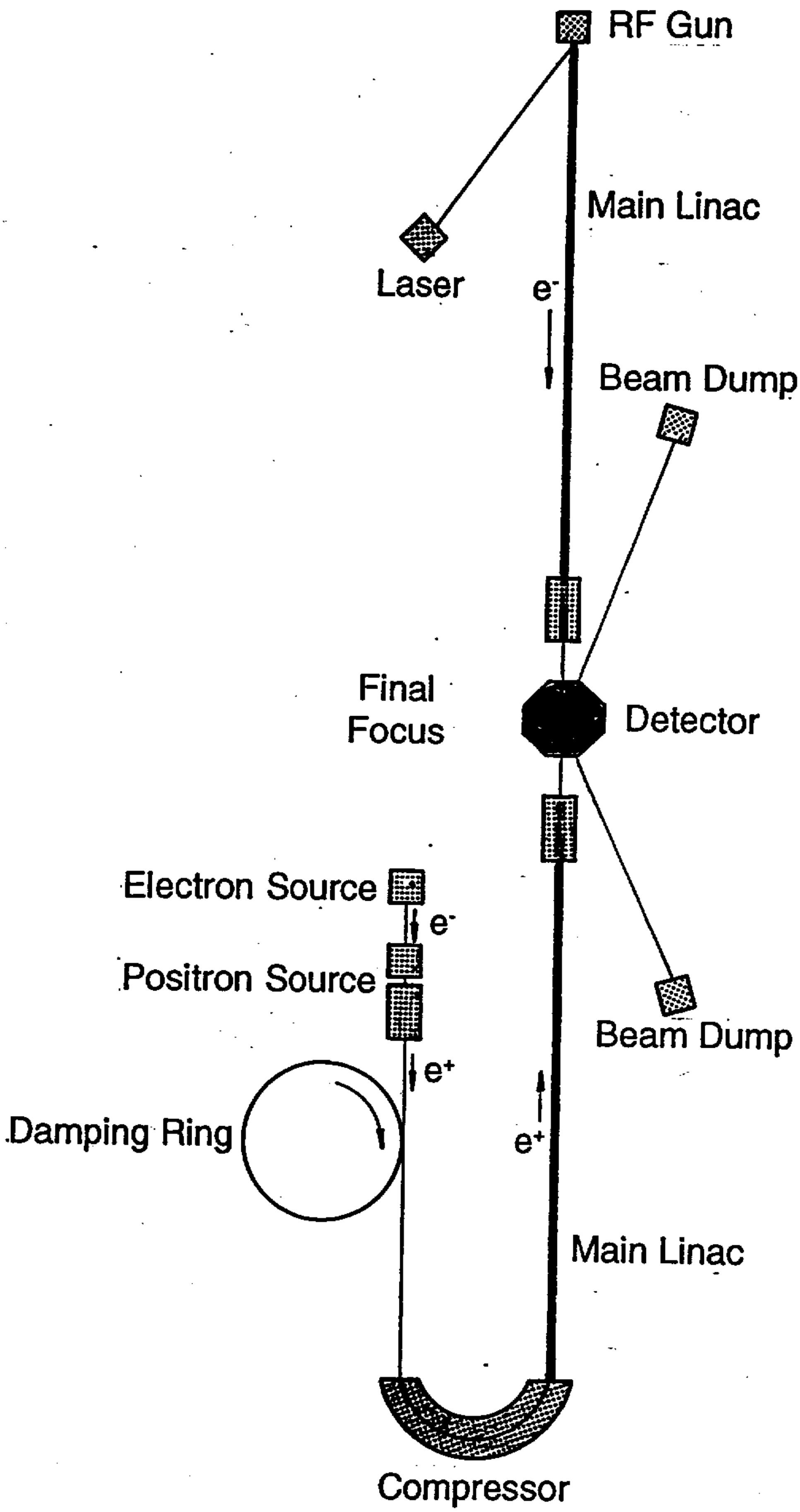
RF Gun
Laser
Main Linac
e-
Beam Dump
Final
Focus
Detector
Electron Source
e-
Positron Source
e+
Damping Ring
Beam Dump
e+
Main Linac
Compressor

Research and Development Prospects for Linear Colliers

- e^+e^- physics at energies beyond LEP II can only be explored using linear colliders

Ring:
Cost ~ E^2

Linac:
Cost ~ E

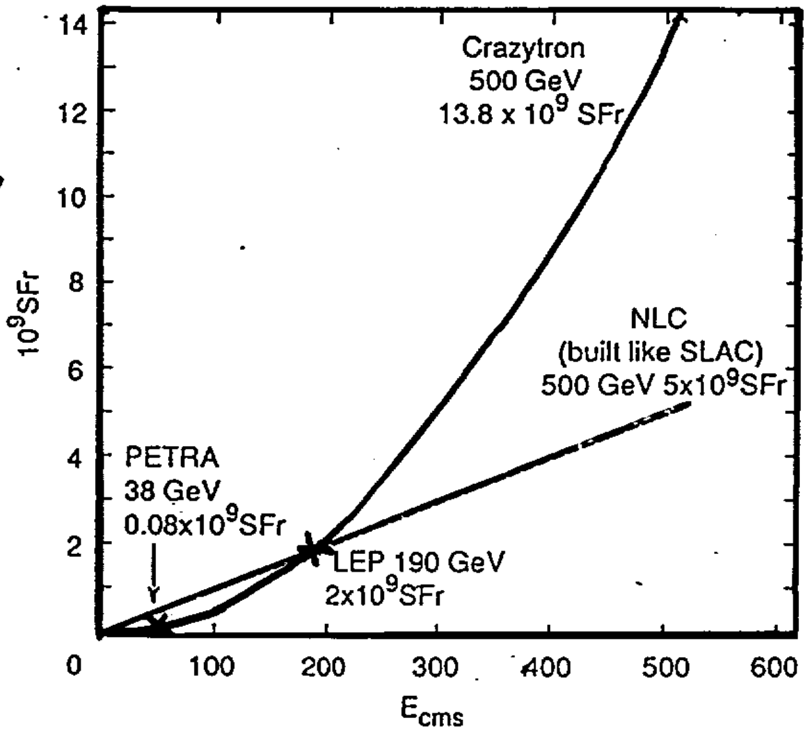

- New and demanding technology. For constant values of beam parameters:

$$L = \frac{1}{4\pi E_{CM}} \cdot \frac{N}{\langle \sigma_x^* \rangle} \cdot \frac{P_b}{\langle \sigma_y^* \rangle} \sim \gamma^{-5/2}$$

- As a compromise between physics scope and doability:

E : Z^0 - 500 GeV

Luminosity: > $2 \cdot 10^{33}$ $cm^{-2}s^{-1}$

or 20 fb^{-1} $year^{-1}$

$$L = \frac{1}{4\pi E} \cdot \frac{N \cdot \eta}{\sigma_x^*} \cdot \frac{1b}{\sigma_y^*}$$

Physics — Beam-Beam, Beam-Cavity — Collider Technology

LINEAR COLLIDER DESIGN PARAMETERS (500 GeV)

	TESLA	S-band	X-band	CLIC
RF frequency (GHz)	1.3	3.0	11.4	30.0
Luminosity (10^{33} cm^{-2} s^{-1})	6.5	3.7	8.2	~~2.2~~ 0.8
N / Bunch (10^{10})	5.2	2.9	0.65	0.6
Bunches / rf pulse	800	125	90	1
Bunch spacing (ns)	1000	16.0	1.4	-
Linac repetition rate (Hz)	10 ($4 \cdot 10^{14}$/s)	50 ($1.8 \cdot 10^{14}$/s)	180 ($1.1 \cdot 10^{14}$/s)	1700 (10^{13}/s)
Invariant emittance $\gamma\varepsilon_x / \gamma\varepsilon_y$ (10^{-5} mrad)	2000/100	1000/50	500/5	180/20
Gradient (MV/m)	25	17	38	78
Klystron peak power (MW)	3.3 (1.5ms)	150 (3 μs)	94 (1.5 μs)	-
Beam power (MW)	16.5	7.3	4.2	0.4
Mains power (MW)	137	114	152	175
Beam size at I.P.				
σ_x / σ_y (nm)	1000/64	1000/50	300/3	90/8
β_x / β_y (nm)	25/2	22/0.8	100/0.1	2.2/0.6
δ_B	2.7	3.2	3.0	36.0

- There is consensus among accelerator experts that a linear collider based on low frequency superconducting cavities has many technical advantages compared to a "warm" linac.

- However to be cost competitive the price per MeV of accelerating voltage must be reduced by a factor of ≥ 20 compared to the cost of present system

  This statement is based on:

  Gradient ~ 5 MV/m

  Linear Cost ~ 200 kDM/m.

- The TESLA Collaboration has proposed to meet this goal of a factor 20 in cost reduction by:

  Raising the gradient: 5 MV/m ⟶ 25 MV/m

  Reducing the linear cost by a factor of 5.

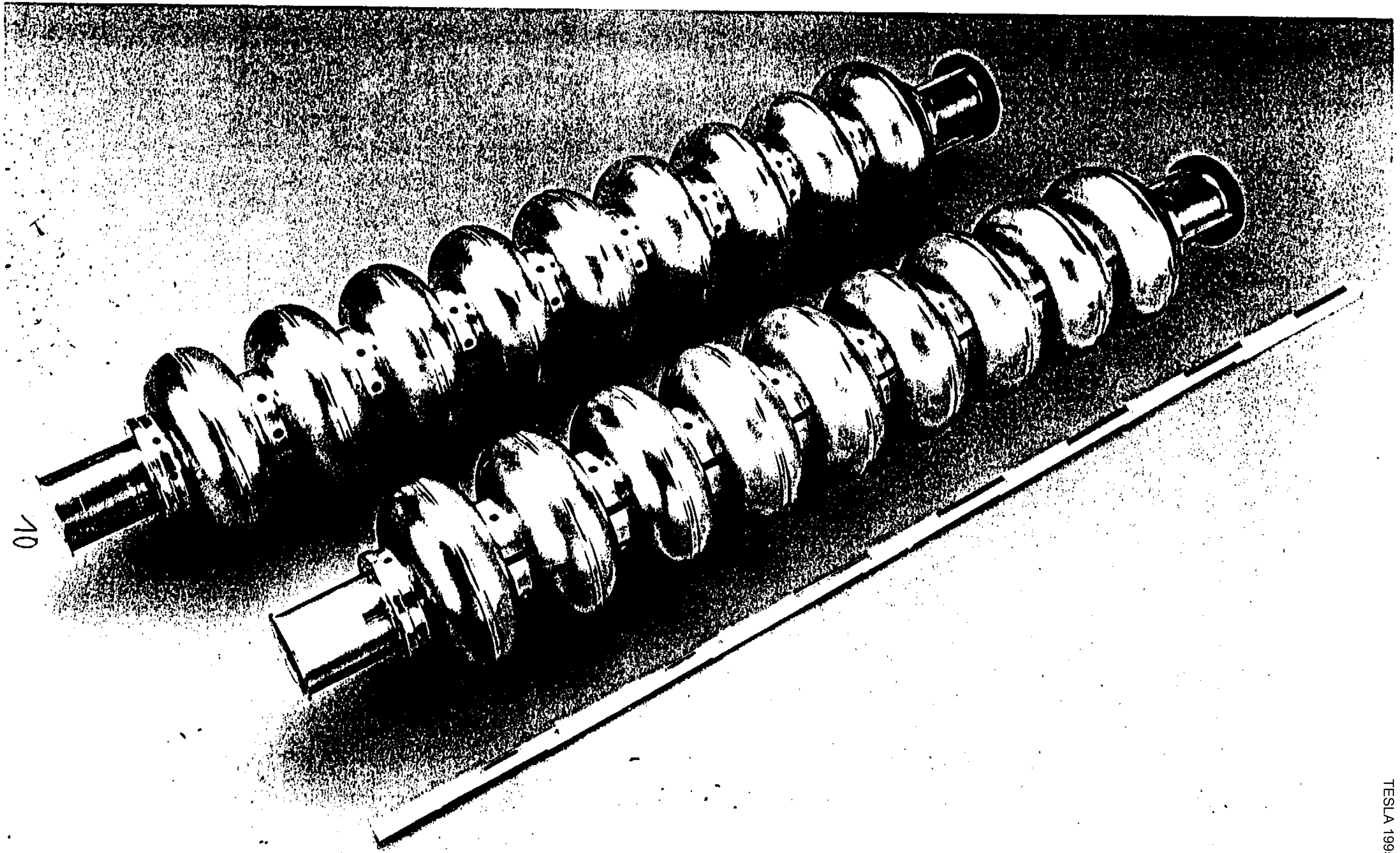

Prototype Cavities for TESLA (9-cell, 1300 MHz, Nb RRR 400)

TESLA-TEST-FACILITY
MEMBERS OF THE COLLABORATION
(April 1993)

BEIJING (IHEP)

BERLIN (TU)

• CERN

• CORNELL

DARMSTADT

• DESY

• FERMILAB

FRANKFURT

• INFN FRASCATI

INFN MILAN

• IPN-ORSAY

KARLSRUHE (KFK)

KARLSRUHE (U)

• LAL-ORSAY

• SACLAY

SEFT

WUPPERTAL

UCLA

Aim:

Develop the technological base for a 500 GeV supercon Linear collider by 97/98

Design and build prototyp multicavity modules with an estimated cost ~ 50 k$/m

Build and operate a 500M linear accelerator made of prototype S.C. multicavity structures.

Design Parameters

gradient : ≥ 25 MV/m

Q_0-value : ≥ $3 \cdot 10^9$

f : 1.3 GHz

Static heat leak : ≤ 1 W/m

9 cells / Cavity

8 cavities / cryostat.

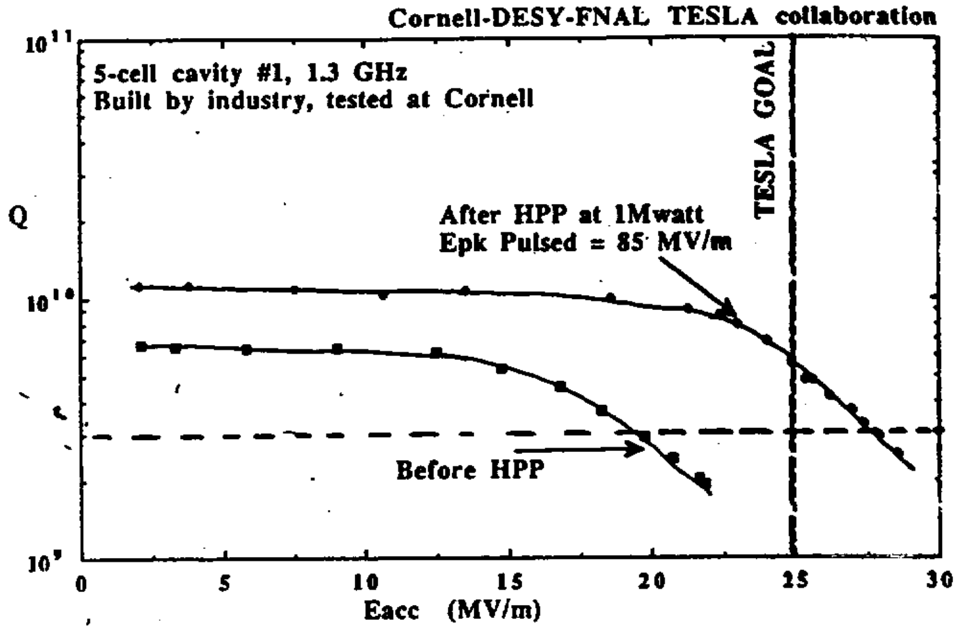
Cornell-DESY-FNAL TESLA collaboration
5-cell cavity #1, 1.3 GHz
Built by industry, tested at Cornell
TESLA GOAL
After HPP at 1Mwatt
Epk Pulsed = 85 MV/m
Before HPP
Q
10¹¹
10¹⁰
10⁹
0
5
10
15
20
25
30
Eacc (MV/m)

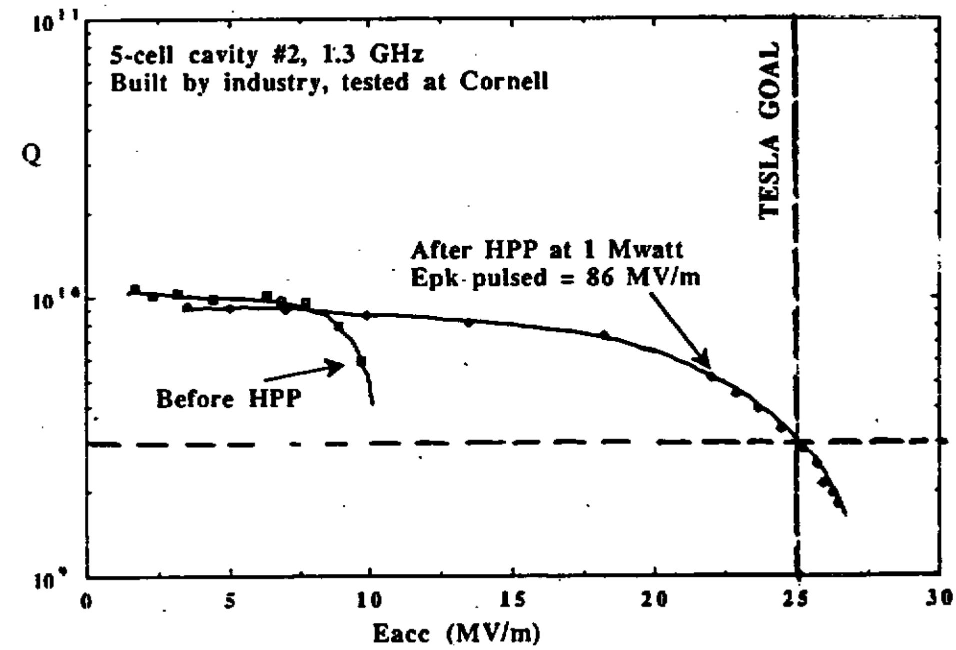
5-cell cavity #2, 1.3 GHz
Built by industry, tested at Cornell
TESLA GOAL
After HPP at 1 Mwatt
Epk pulsed = 86 MV/m
Before HPP
Q
10¹¹
10¹⁰
10⁹
0
5
10
15
20
25
30
Eacc (MV/m)

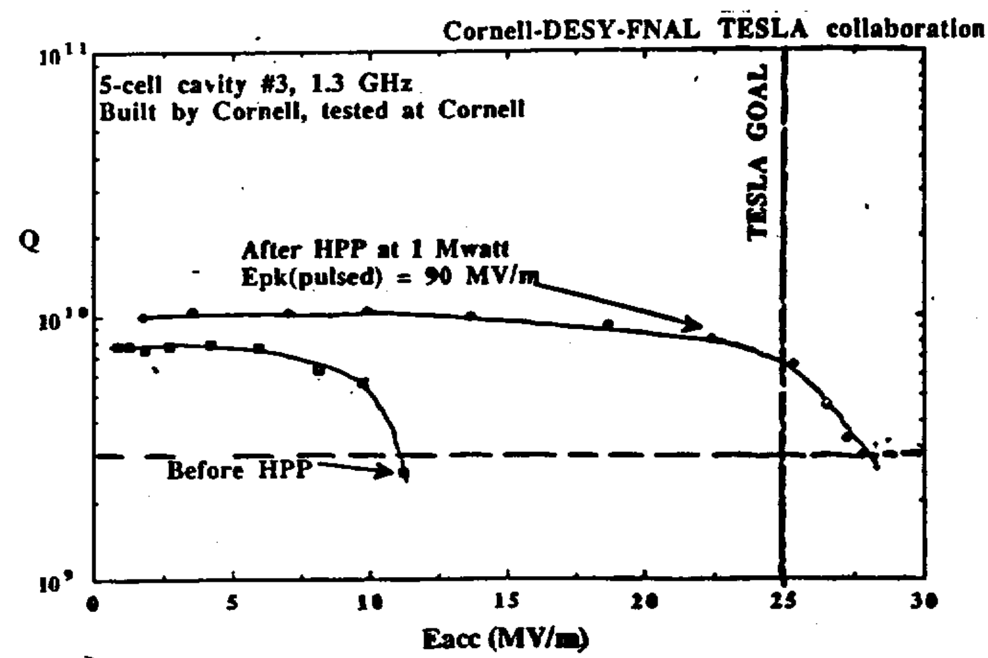
Cornell-DESY-FNAL TESLA collaboration
5-cell cavity #3, 1.3 GHz
Built by Cornell, tested at Cornell
TESLA GOAL
After HPP at 1 Mwatt
Epk(pulsed) = 90 MV/m
Before HPP
Q
10¹¹
10¹⁰
10⁹
0
5
10
15
20
25
30
Eacc (MV/m)

12

TESLA TEST FACILITY

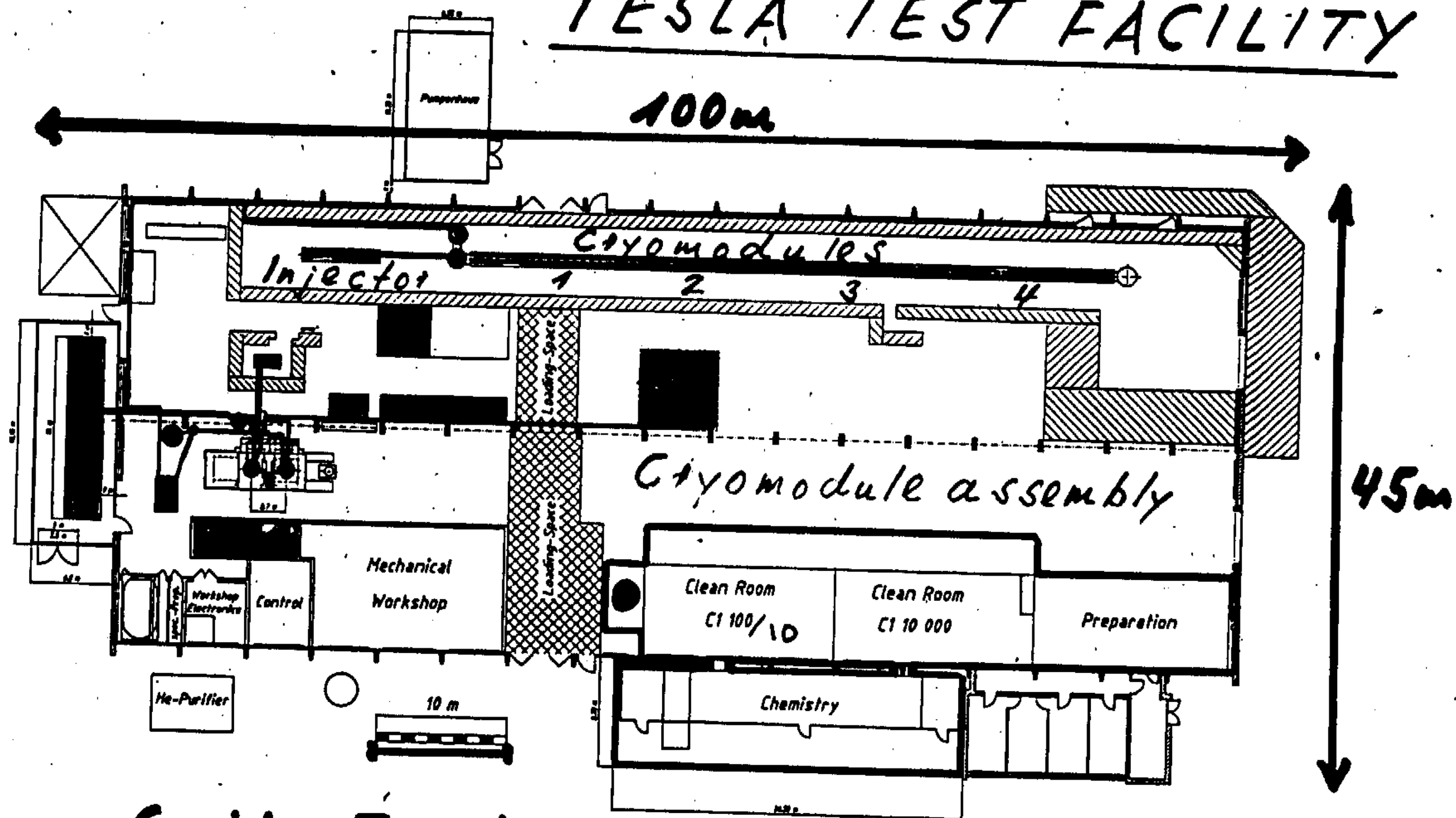

— Cavity Treatment and Assembly
— Cavity Testing (RF system, He plant)

Halle 3 (Gebäude 28)

M=1:100

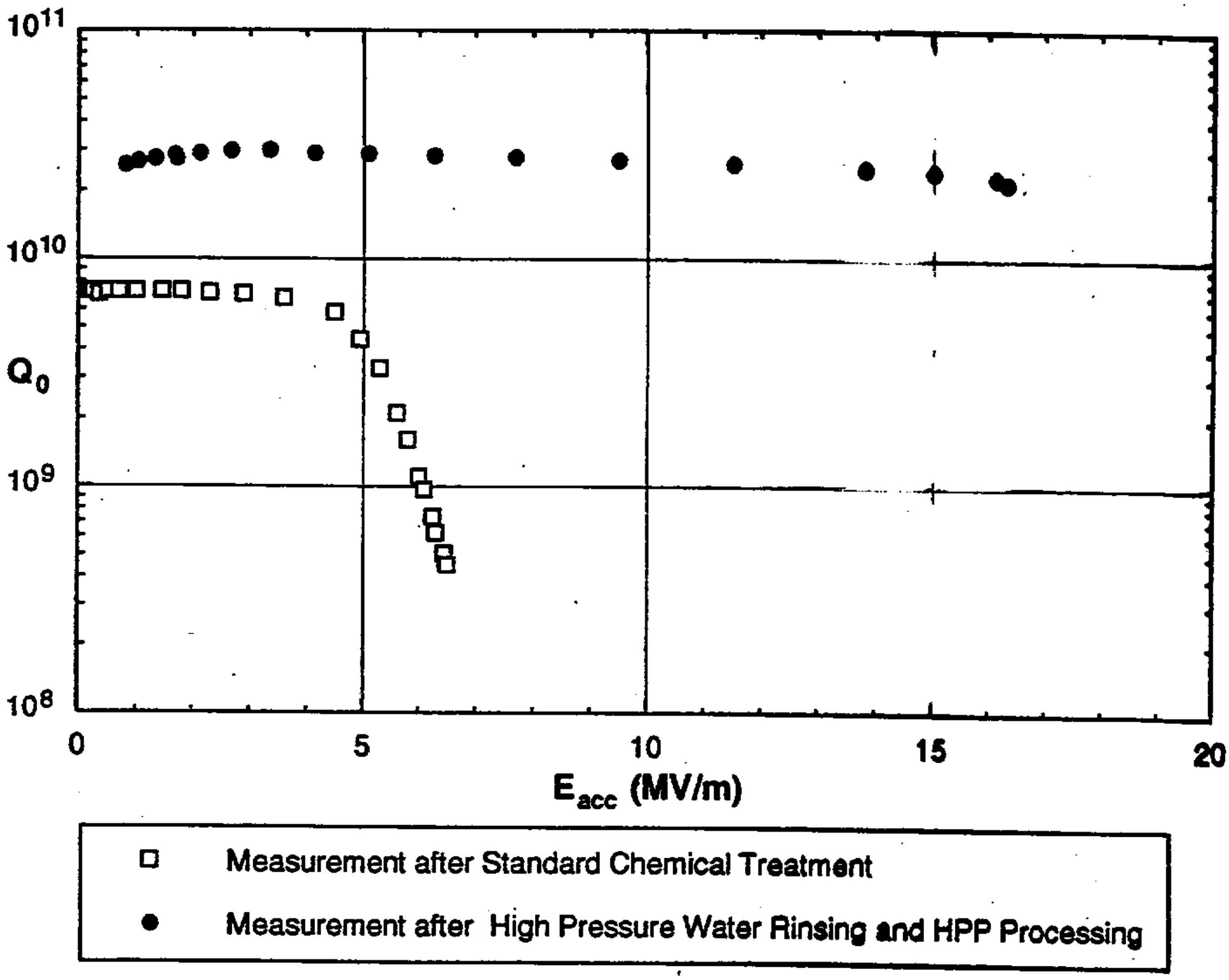

10^{11}
10^{10}
Q_0
10^{9}
10^{8}
0
5
10
15
20
E_{acc} (MV/m)
Measurement after Standard Chemical Treatment
Measurement after High Pressure Water Rinsing and HPP Processing

Workshop on Cavity Fabrication
DESY Hamburg, March 6-8, 1995

TESLA 1995-09

An Introduction to Microstructure and Mechanical Behavior of Metallic Materials

Felix Müller
Universität der Bundeswehr Hamburg
Institut für Werkstofftechnik

1. Pure Metals
   - crystal lattice, grain size
   - anisotropy grain shape, orientation distribution (texture)
   - lattice defects
   - elastic and plastic deformation
   - mechanical properties
   - effect of heating on microstructure
   - Cold and hot forming
   - Creep

2. Alloys
   - Homogeneous solid solution
   - Heterogeneous alloys

3. Embrittlement of materials (e.g. S in Ni)

Introduction

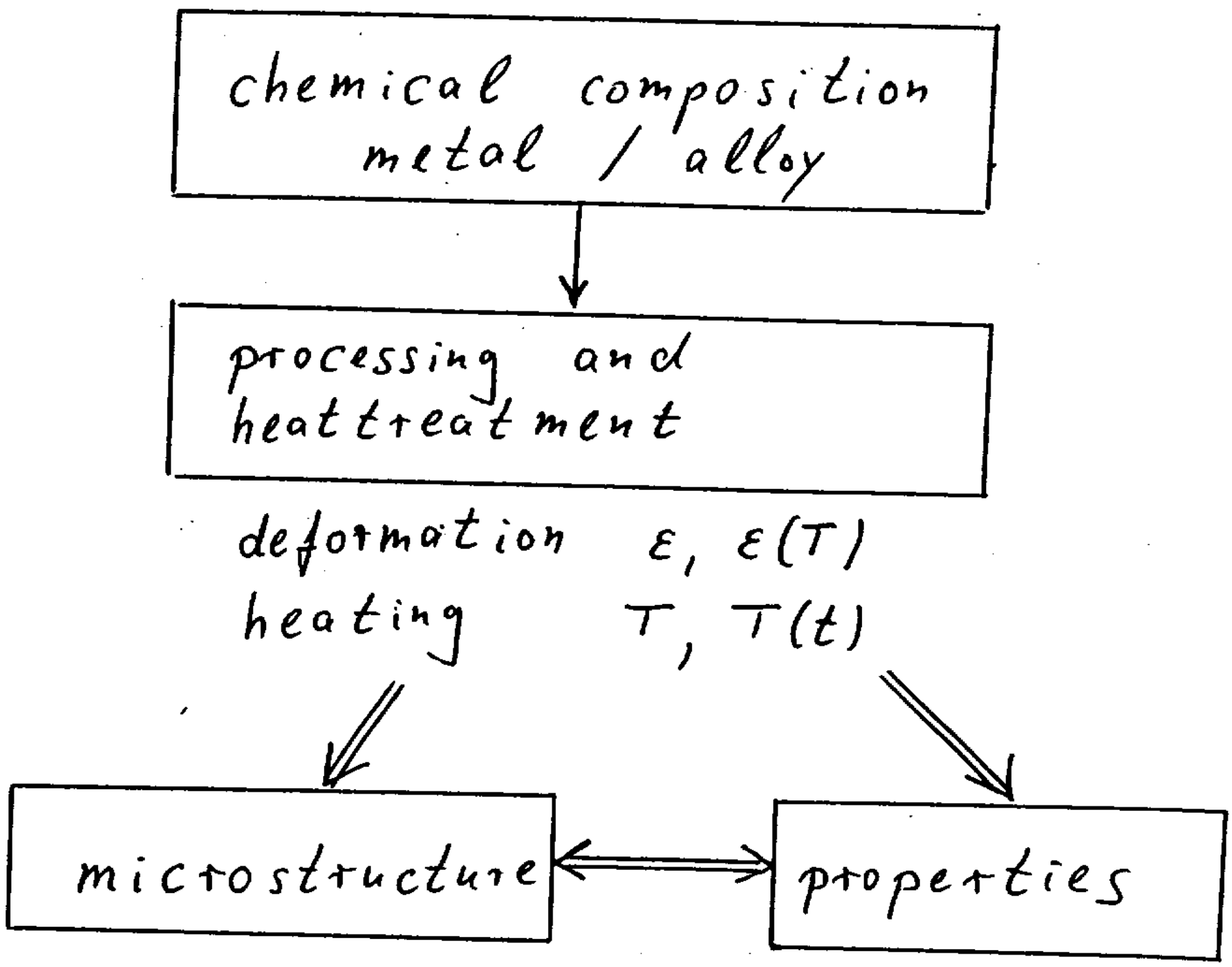

e.g.
grain size
size of phases
distribution of phases
dislocation density
defect structure

eg.
strengh hardness
formability
physical propeties

1. Pure Metals

- crystal structure, unit cells of space lattices

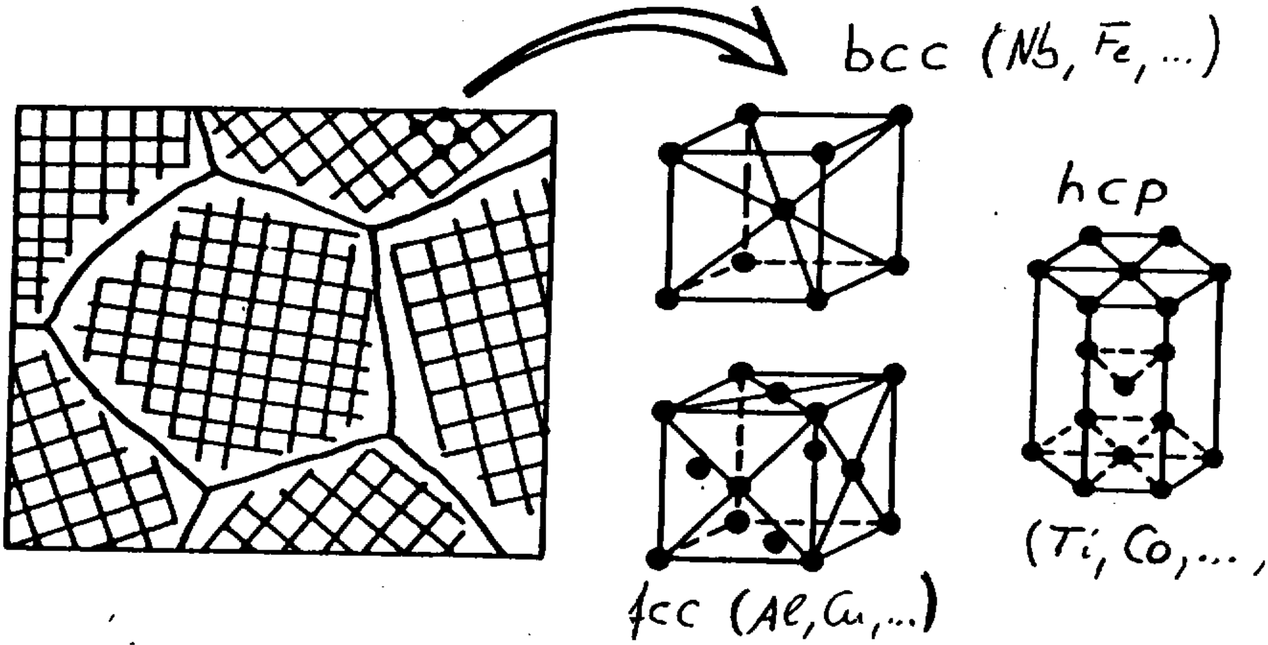

- lattice planes defined by Miller indices (hkl)

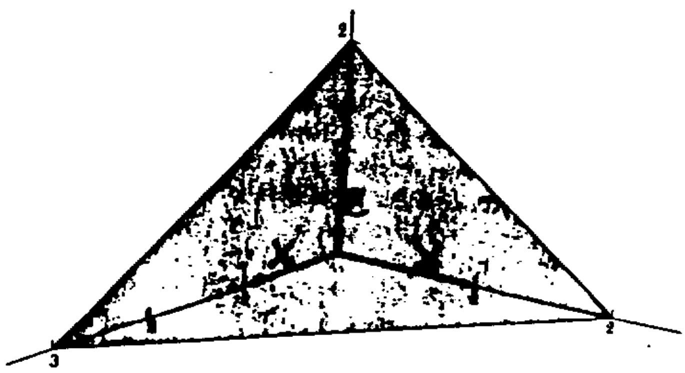

$x = 3, \ y = 2, \ z = 2$

$\frac{1}{x} = \frac{1}{3}, \ \frac{1}{y} = \frac{1}{2}, \ \frac{1}{z} = \frac{1}{2}$

$h = 2, \ k = 3, \ l = 3$

(233) plane

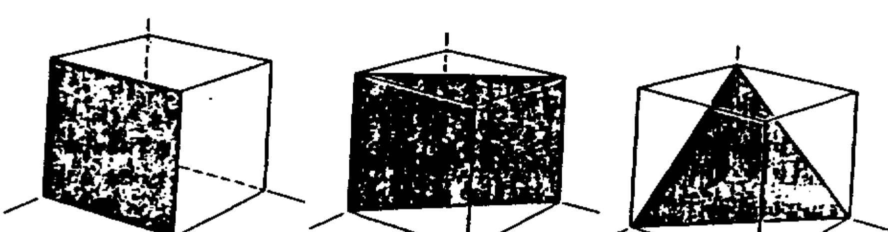

(100) (110) (111)

for cubic lattices

X-ray: $n \cdot \lambda = 2 \cdot d_{hkl} \sin\theta$, $d_{hkl} = \frac{a}{\sqrt{h^2 + k^2 + l^2}}$

- grains and grain boundaries

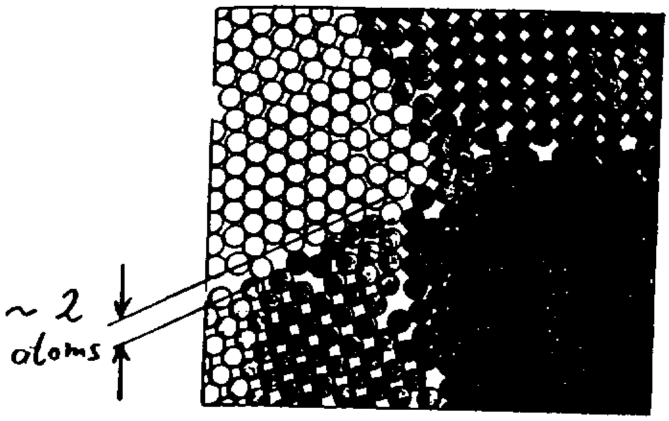

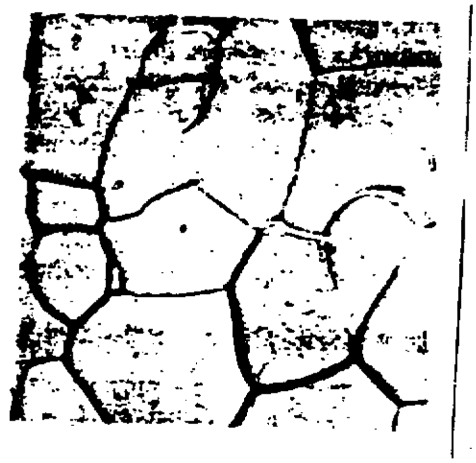

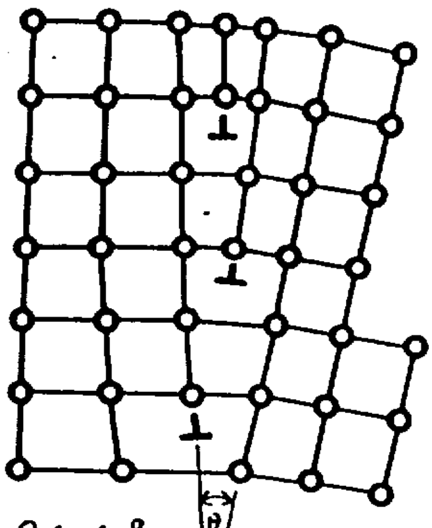

θ< 10°

small-angle grain boundary (SAGB)

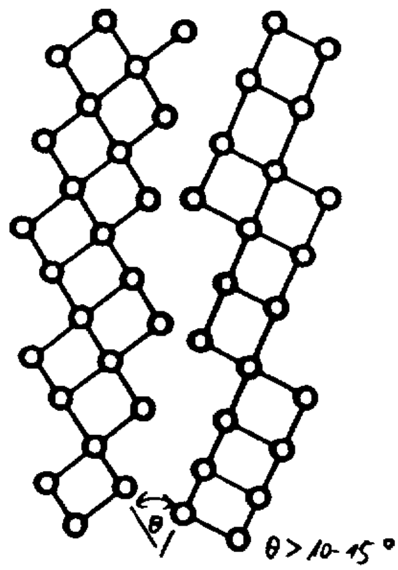

grain boundary (GB)

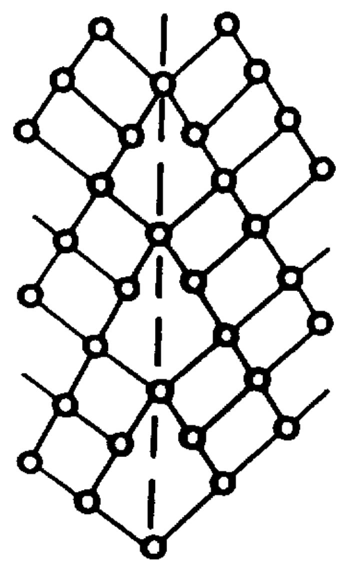

twin boundary (TB)

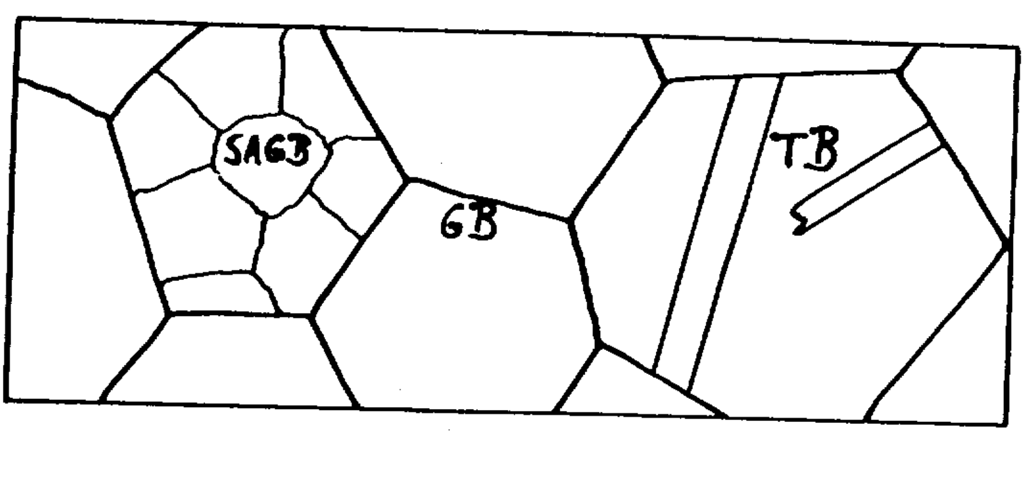

- grain size, grain shape, grain orientation distribution (texture)

ASTM grain size number : n

optical microscope at 100x

area : $(10^{-2}\ in.)^2$ or $0{,}0645\ mm^2$

Number of grains in the area : $N = 2^{n-1}$

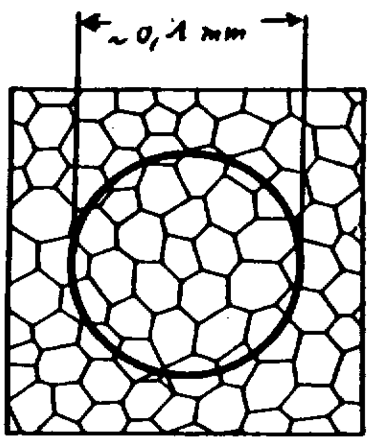

n	N /mm²	$\overline{D}$ (μm)
1	16	250
2	32	180
3	64	125
4	128	90
⋮	⋮	⋮

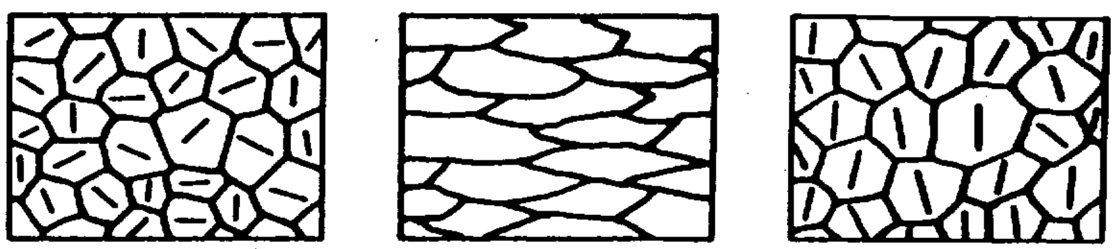

random orientation — anisotropy grain shape — preferred orientation (texture)

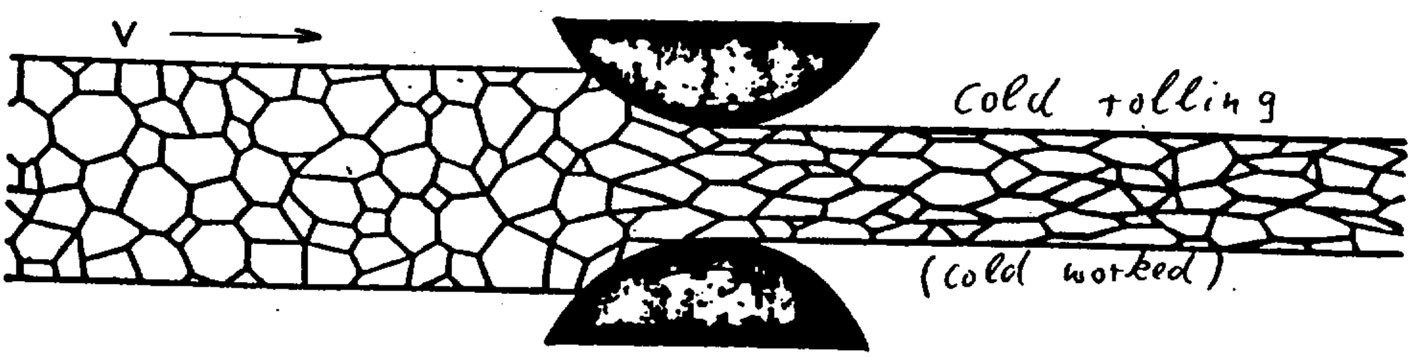

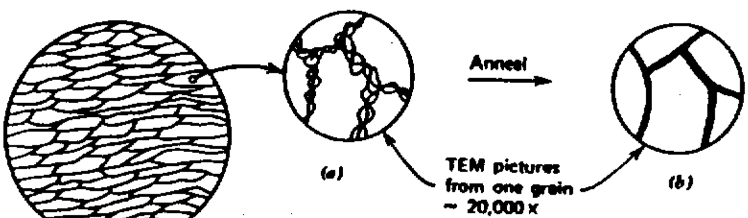

- anisotropy grain shape
- texture
- stored energy
- subgrain structure

TESLA 95-09

- # Imperfections in Crystalline Solids

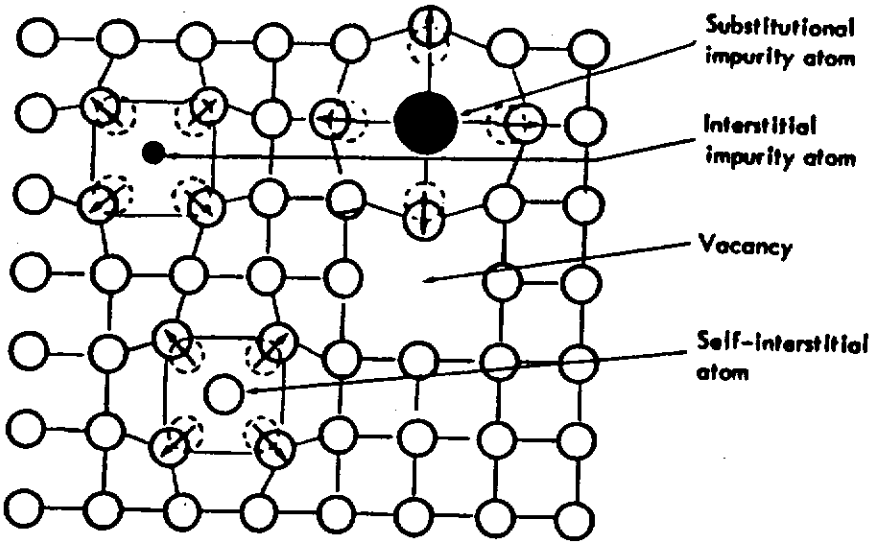

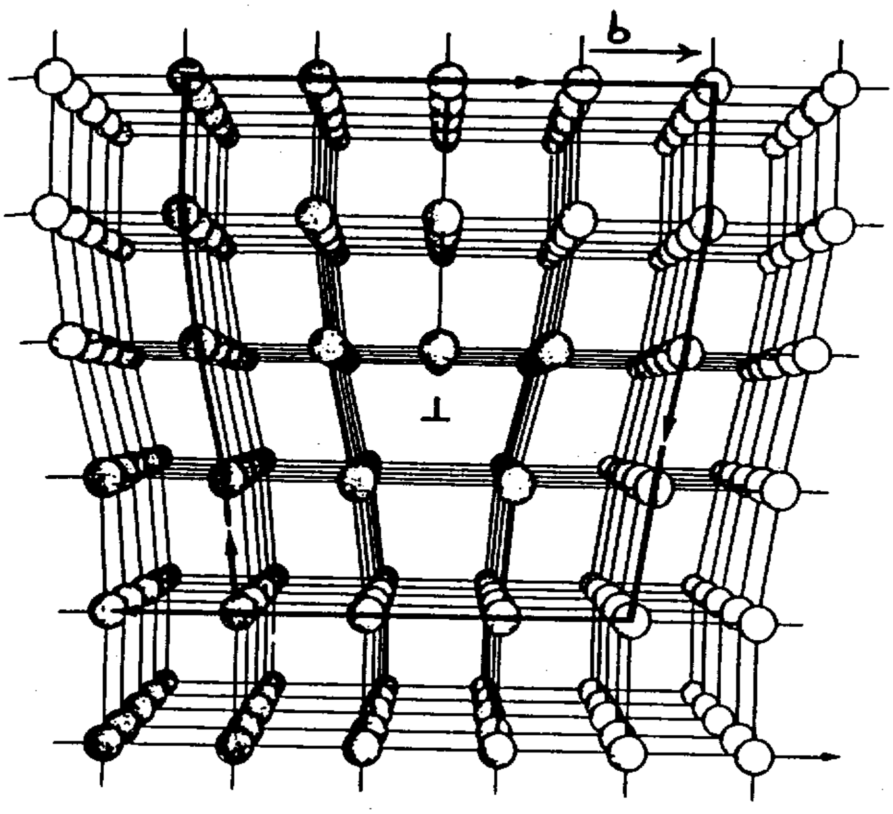

slip vector $\vec{b}$
(Burgers vector)

edge dislocation

$\vec{b} \perp$ dislocation line

disl. density

a) annealed ($T \sim T_m$)

$\sim 10^{8}\ cm^{-2}$

($\sim 10^{4}$ atomic distance)

b) cold worked

$\sim 10^{12}\ cm^{-2}$

($\sim 10^{2}$ atomic distance)

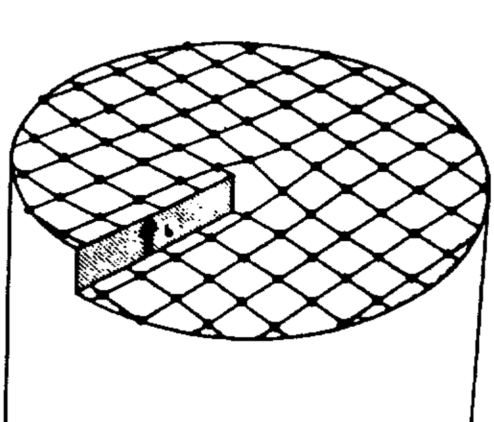

screw dislocation

$\vec{b} \parallel$ dislocation line

• Elastic and Plastic Deformation

tensile test

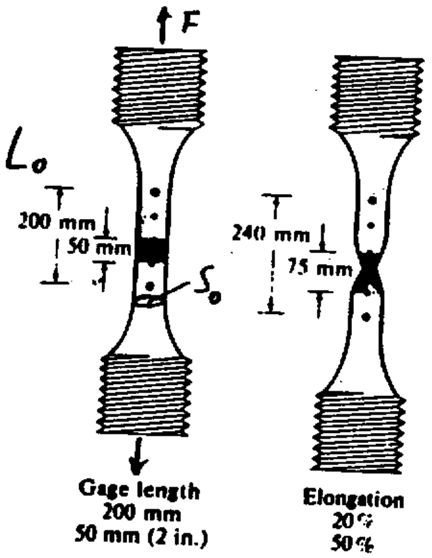

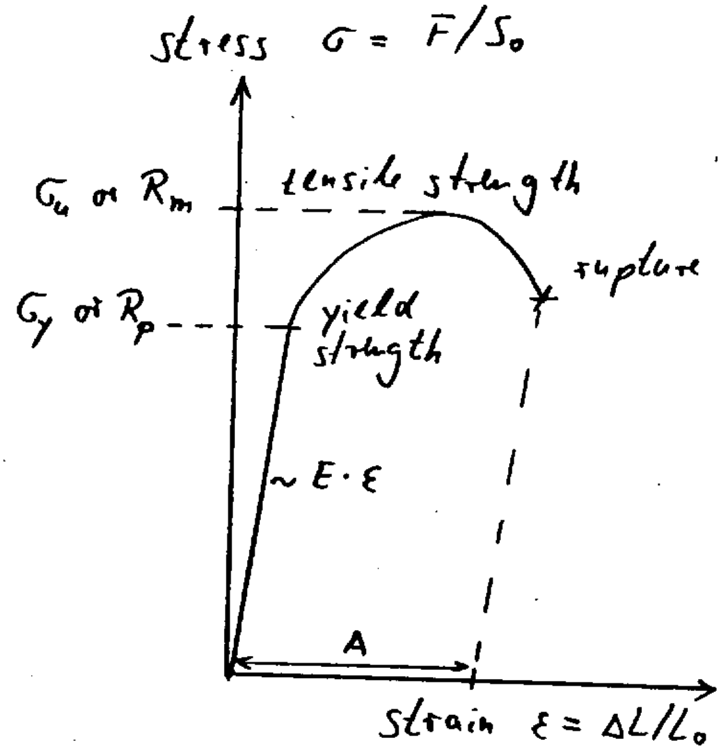

ductility :

- elongation $A = \frac{L_u - L_o}{L_o}$
- reduction of area $Z = \frac{S_o - S_u}{S_o}$

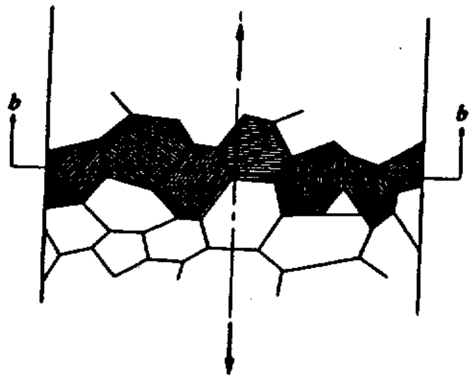

(a)

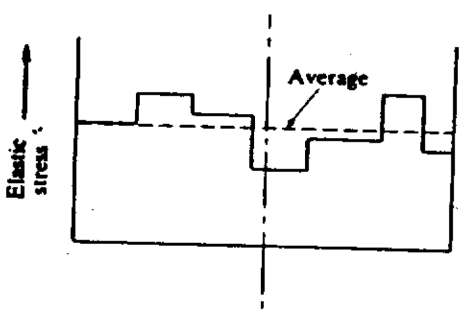

elastic stresses vary with grain orientation

$1\,GPa = 10^3\,MPa\,, \quad 1\,MPa = 1\,\frac{N}{mm^2}$

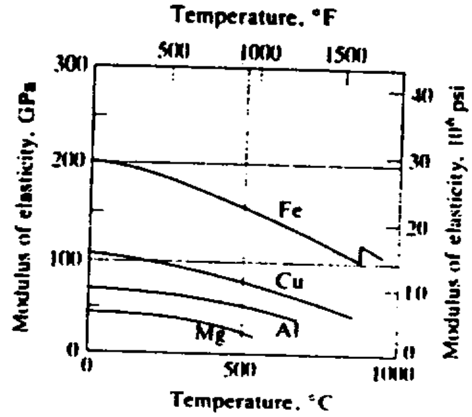

young's modulus E

	MAXIMUM		MINIMUM	
METAL	GPa	10^6 psi	GPa	10^6 psi
Aluminum	75	11	60	9
Gold	110	16	40	6
Copper	195	28	70	10
Iron (bcc)	280	41	125	18
Tungsten	345	50	345	50

- plastic deformation (cold worked)

$\epsilon = 3\%$

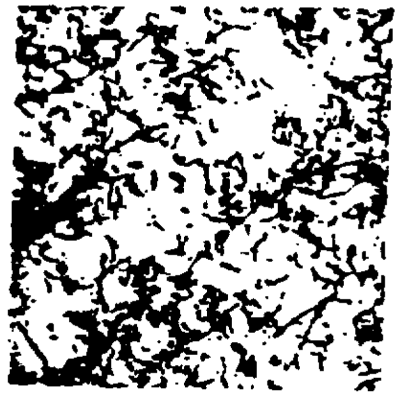

$\epsilon = 6\%$

increase in dislocation density (from 10^4 to 10^{12} cm^{-2})

decrease in ductility and formability

increase in hardness and strength

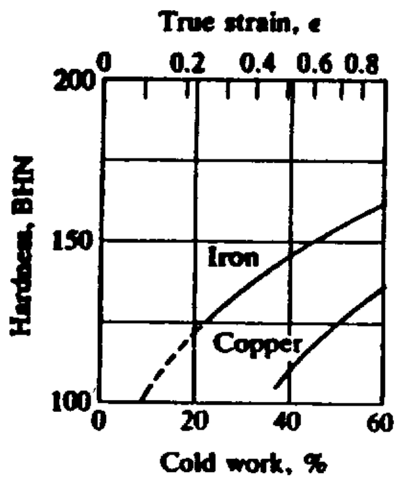

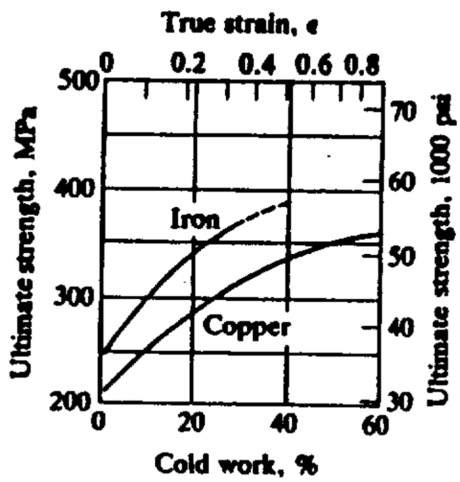

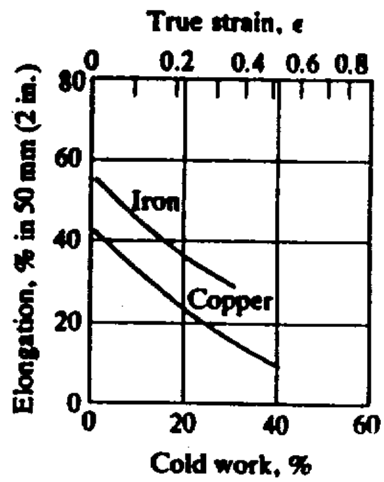

influence of temperature

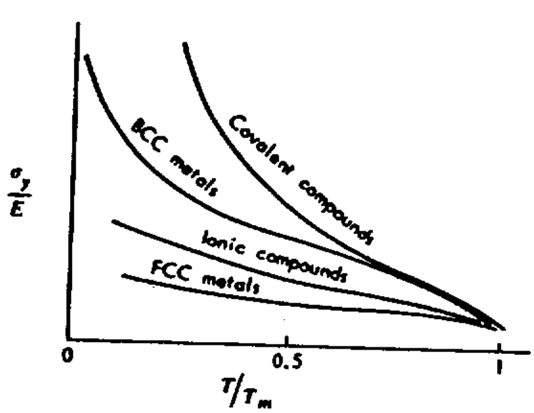

influence of strain rate

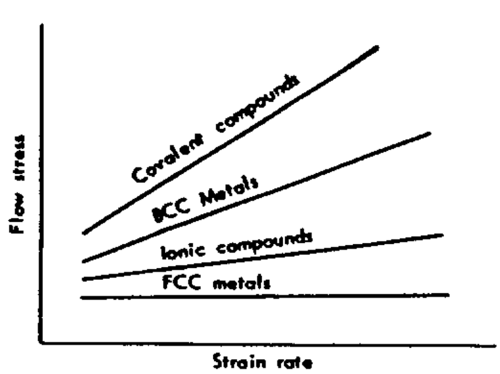

- dislocation movement on slip systems by plastic deformation

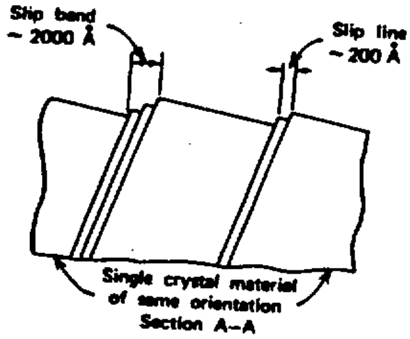

fcc : $\langle 110 \rangle$ on $\{111\}$

bcc : $\langle 111 \rangle$ on $\{101\}$, $\{211\}$ and $\{321\}$

movement in glide

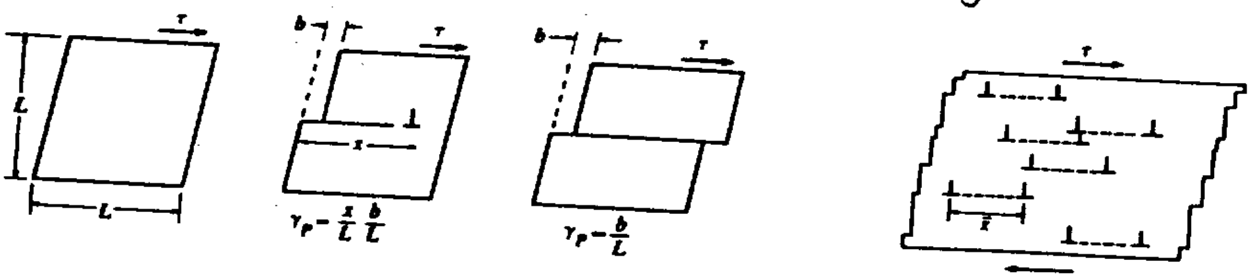

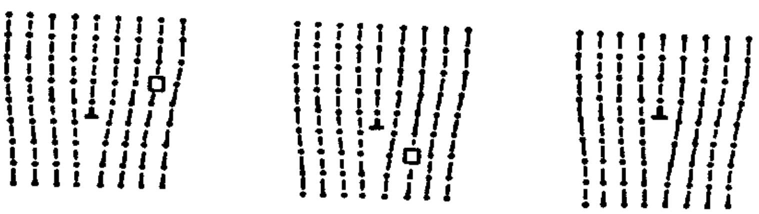

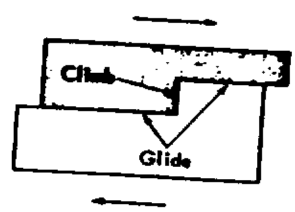

climb of edge dislocation

influence of grain size

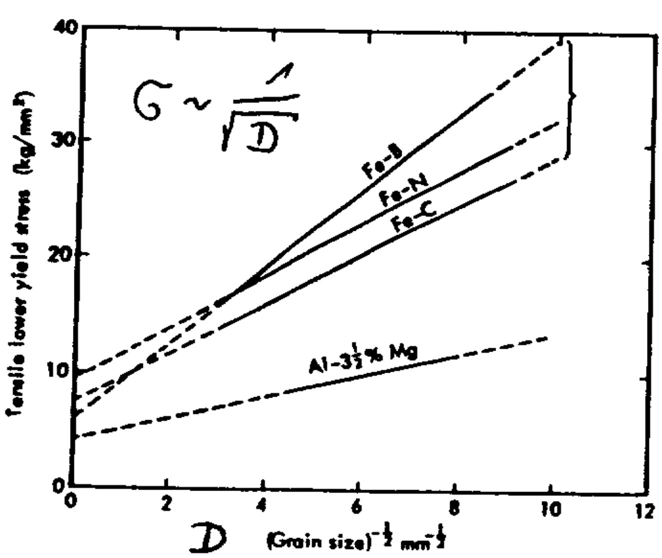

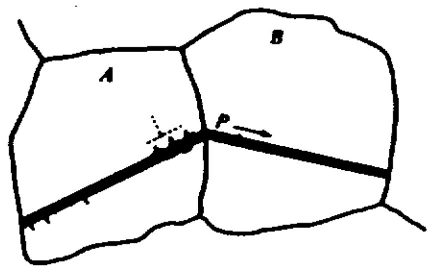

slip propagation from one grain to the next

- recovery and recrystallization

plastic deformated material (cold worked)

thermal activated phase transformation

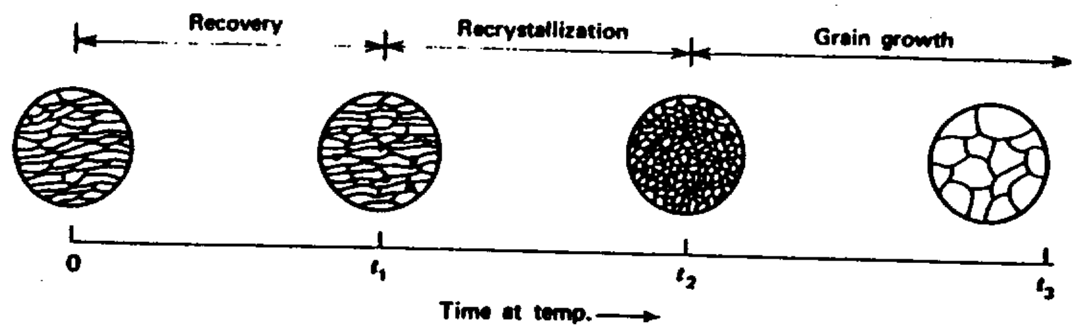

annealing out point defects and dislocations	changing of microstructure	grain size increase

changing of properties

$T_R \geq 0{,}4\ T_m$

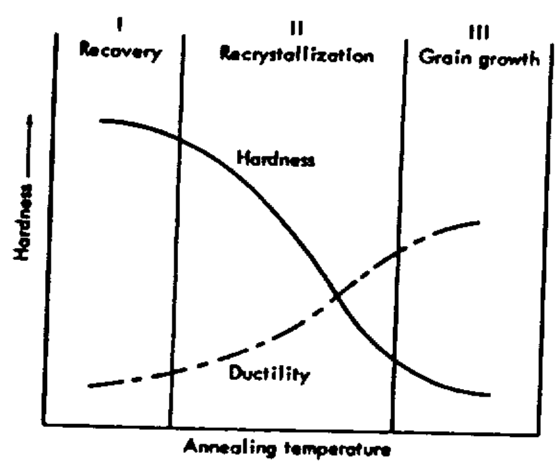

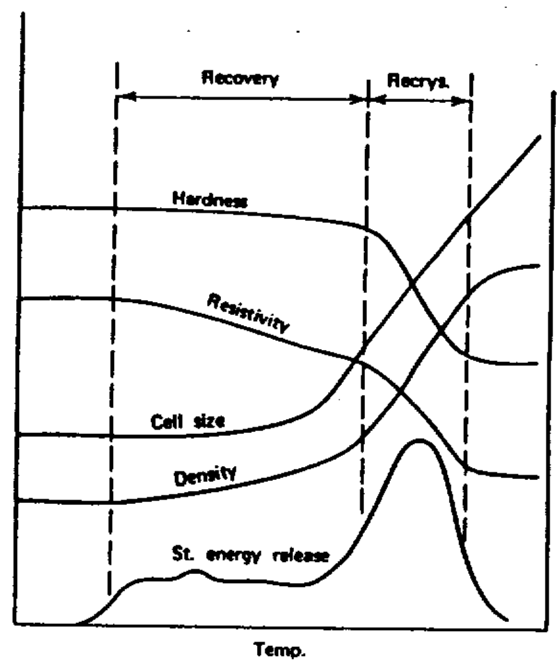

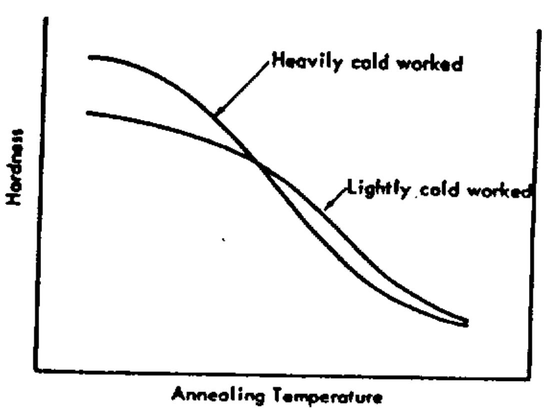

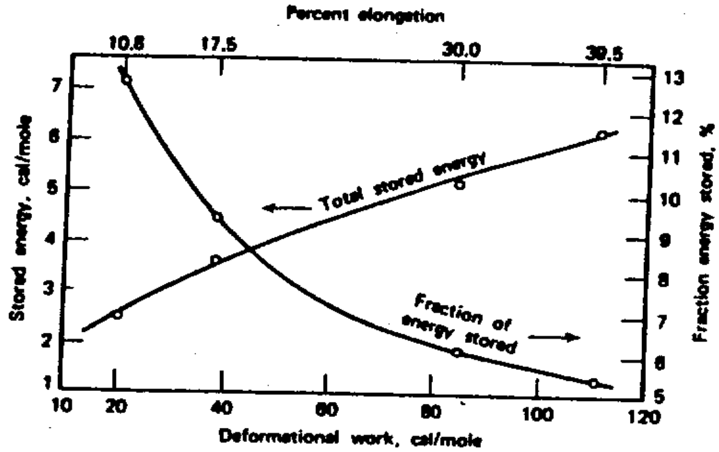

cold worked:

- stored energy during deformation $\leq 14\%$
- most goes into heat
- stored energy $\leq 6 \frac{cal}{mole}$

($\approx 25 \frac{J}{mole} \approx 0{,}3$ eV/atom

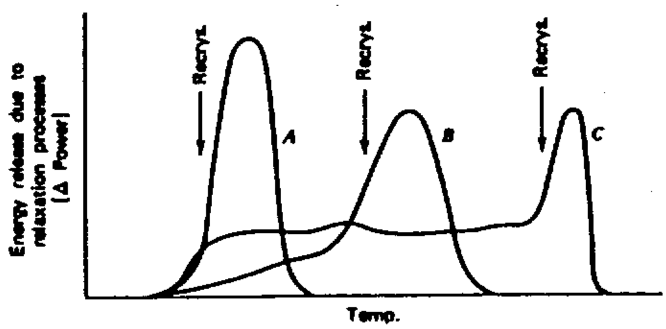

stored energy release due to thermal activation

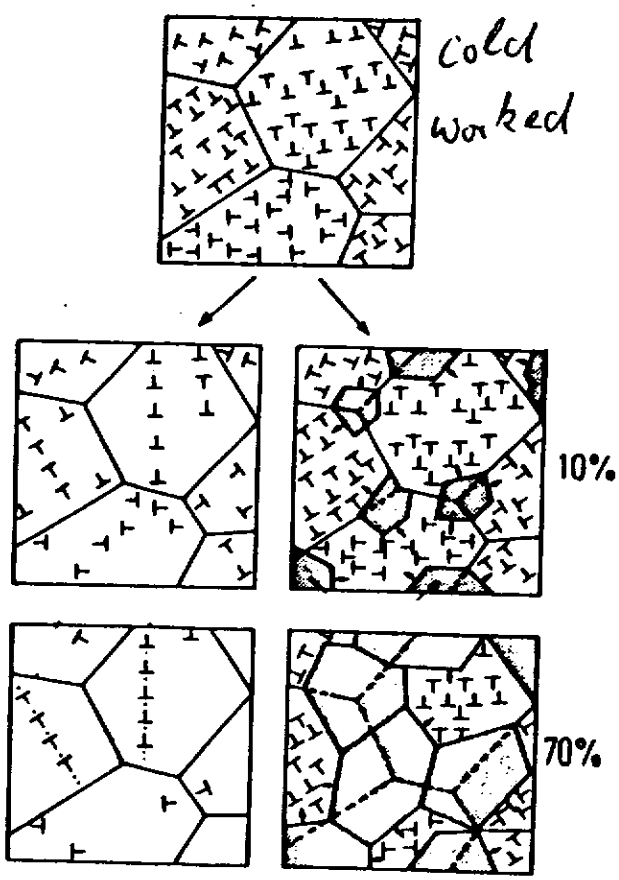

cold worked

recovery

decrease + orientation of dislocations

recrystallizatio nucleation of new grains and growing of new crystals

- time and temperature dependency of recrystallization

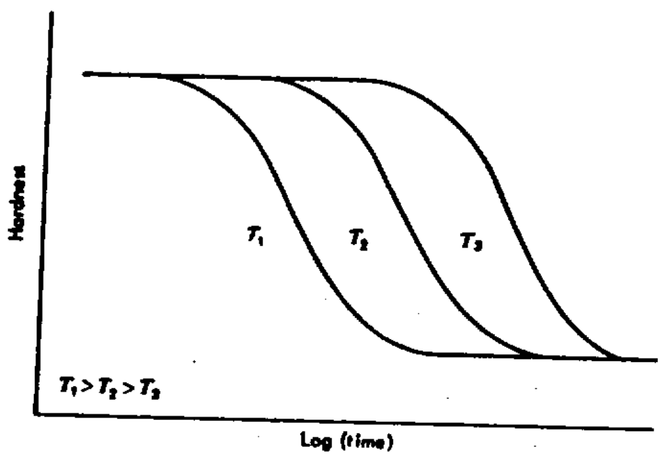

Arrhenius equation

$$t_r = t_0 \exp\left(-\frac{Q}{RT}\right)$$

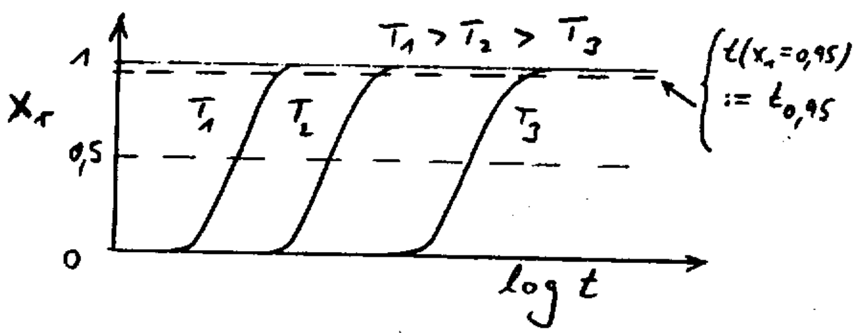

fractional transformation
Avrami equation

$$x_r = 1 - \exp(-kt^n)$$

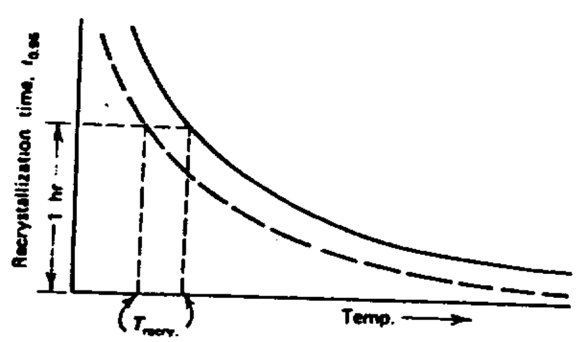

1-hour recrystallization temperature T_r

$t = 1h$, $x_r = 0{,}95$

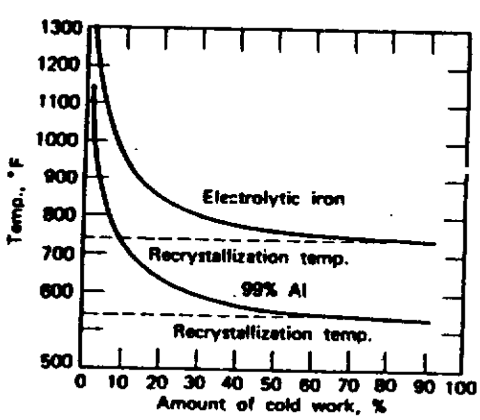

e.g. Nb

- $T_r \approx 950° - 1050°C$
- excessive grain growth:

  $T \gtrsim 1300°C$

- hot rolling (hot worked)

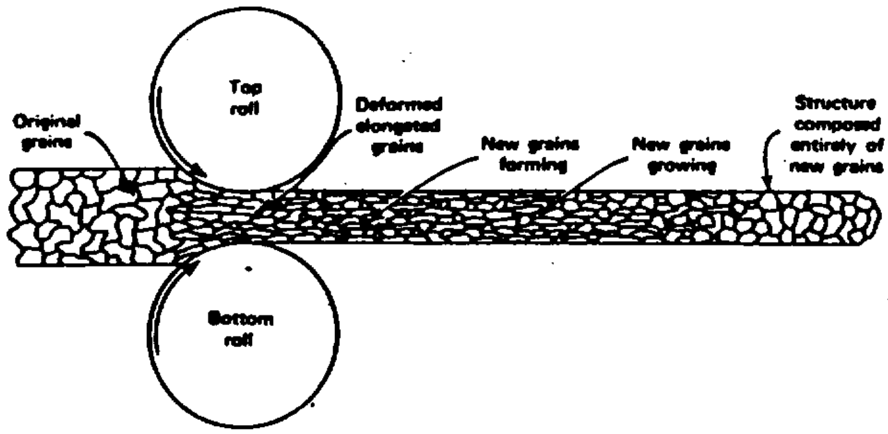

- creep ($T > 0{,}5\ T_m$)

constant stress σ → time-dependent plasticity

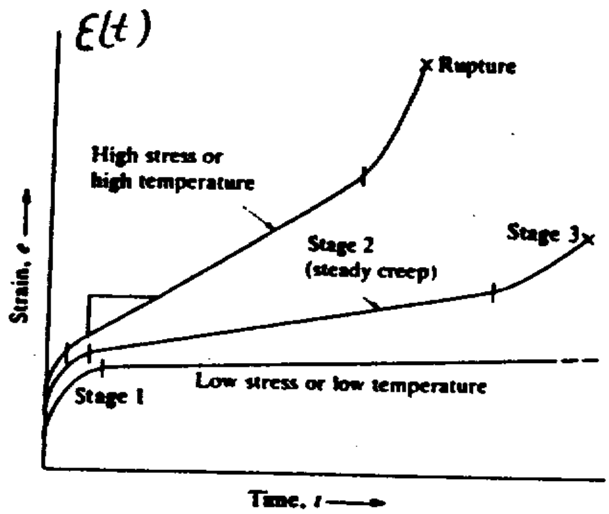

creep test: $\sigma = const,\ \varepsilon(t)$

creep mechanism
- dislocation creep
- grain boundary sliding
- vacancy migration

deformation mechanism : σ, T

(shear modulus $G = E/2(1+\nu)$)

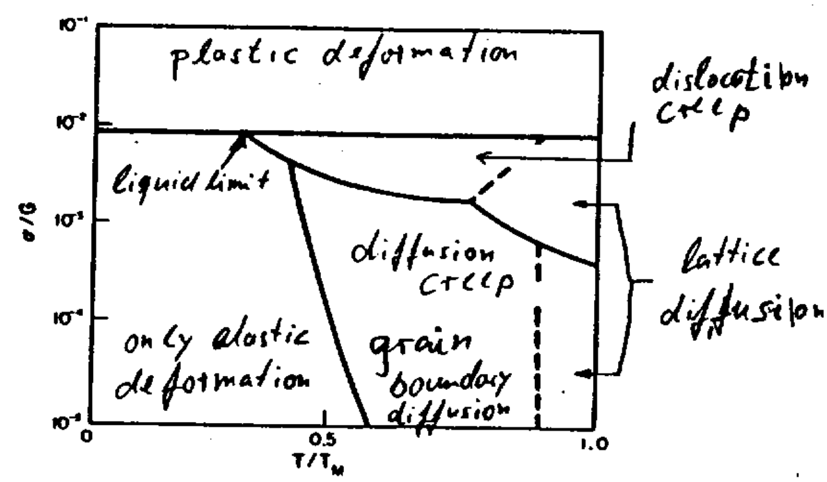

2. Alloys

elements of the microstructure of alloys are the same as for pure metals

e.g. binary phase diagram of Al-Si-alloys

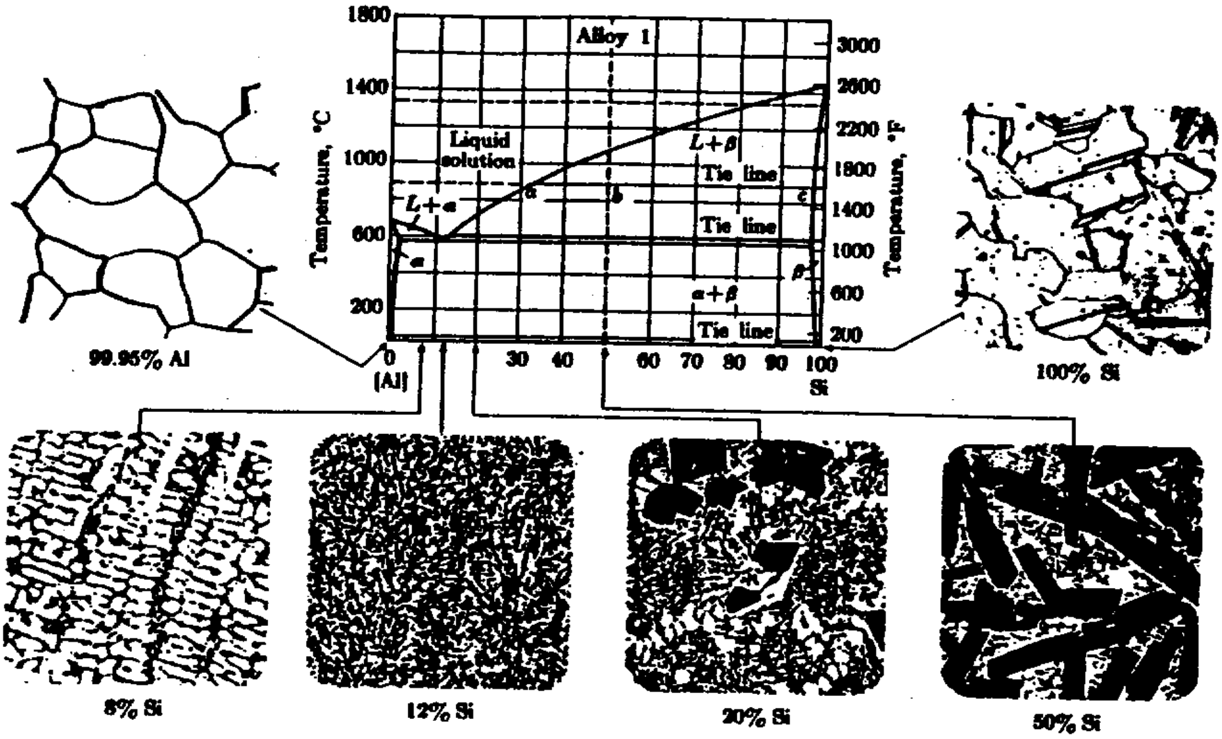

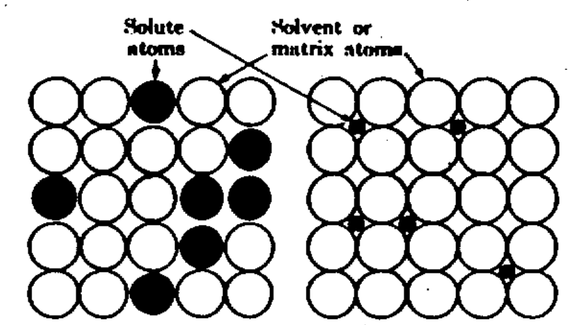

Substitutional solid solution. (h) Interstitial solid solution.

• α - phase (or β - phase)
homogeneous solid solution

statistic distribution of solute atoms ($\Delta\sigma \sim \sqrt{c}$)

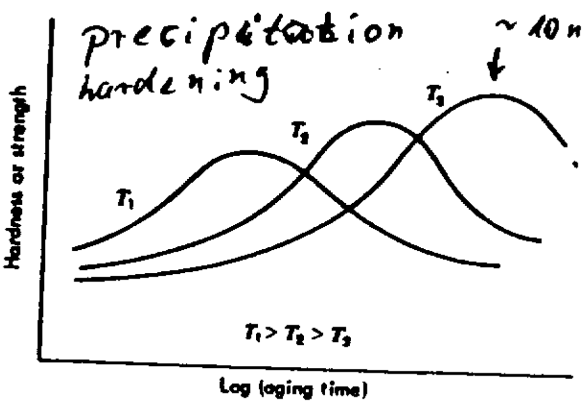

• second phase ~~particle~~ particle (α+β)
- eutectic mixture (12% Si)
lamellar structure
- fine dispersion particles

$\Delta\sigma \sim \frac{1}{\sqrt{D}}$ most effective $D \sim 10\,nm$

3. Embrittlement of materials

e.g. Ni with additions of S ($\gtrsim$ 0,01%)

- at high temperature S segegates as grain boundaries ($Ni_3 S_2$)
- $Ni_3 S_2$ forms with adjacent Ni a low melting eutetic T_m (eutetic) ≈ 630 °C as compare to T_m (Ni) ≈ 1720 °C
- when Ni(S) is hot worked at ~ 500 - 600°C it cracks along grain boundaries

our case: electroplated Ni

- electroplating of Ni with additions of Saccharin to the bath in order to increase hardness of the coatings containing ~ 0,005 - 0,05 % S
- high hardness is due to high dislocation density and small grain size of the deposition
- when the coating is heated at 300°C it recrystallizes; the moving grain boundaries collect the S
- as a consequence the ductility (elongation to fracture) does not increase as normally, in this case it decreases from 20 to < 2%

F. Schölz
W.C.Heraeus GmbH
GBM-PMT-EC
D-63450 HANAU

Workshop on cavity fabrication DESY 06.-08.03.95

Niobium production
From ore to high quality sheet material

Niobium and tantalum always occur in association with one another in nature, and this both as isomorphous niobate and tantalate of manganese and iron and in the form of higher grade niobite and tantalite. The latter contain 53 to 84% Ta_2O_5 and 47 to 78% Nb_2O_5. The most important reserves are the pyrochlorines (calcium niobate) out of brasilia (about 80%) and canada (about 10%) and zinc- or tin-slags containing niobium and tantalum out of zaire, nigeria and GUS as well as stibiotantalite from westaustralia. The complete worldraise amount to 16000 t/a Nb-metall. The price of standard grade nb amounts to 150 DM/Kg.
The most important commercial product for steel-production is the alloy Ferroniobium with a content of 66% nb. An other important production part are optical glasses which are endowed with up to 20% Nb_2O_3, because Nb_2O_3 gives glass a very high refractive index.
The ores are processed to concentrates by opening up with melted alkalis or hydrofluoric acid. Then the niobium and tantalum are separated from one another using an older process of fractionated crystallisation. Modern separating methods are based on solvent extraction with MIBK. The next step is the chlorination. Then either a distillation and reduction with hydrogen takes place or an extraction by complete fusion electrolysis is one way to produce pure nb. In industrial processes the niobium halides are converted to niobium oxide and this is reduced by carbon or aluminium to niobium powder or pellets. As a result of the high melting point of niobium of 2468 °C, whitch is much higher than that of most other materials, evaporation of impurities by electron beam melting in a vacuum typically better than $3x10^{-4}$ mbar for the first melt and $2x10^{-6}$ mbar in the last melt is very effective. Thus commercial grade niobium can be achieved by a minimum of four EB melting steps.
The production of high grade niobium for construction of superconducting high frequency cavities for accelerators in high energy particle physics, you need to know, which are the sensitive parameters. Therefor it is absolutly nessesary to have a very good analytical equipment for to detect the traceelements and a lot of exact physical test methods for to find out the correlations between them. Therefore it was the aim, to produce an extremly pure niobium in a tonnage scale based on economic process steps which are available on an industrial scale.

● Niob mining and dressing

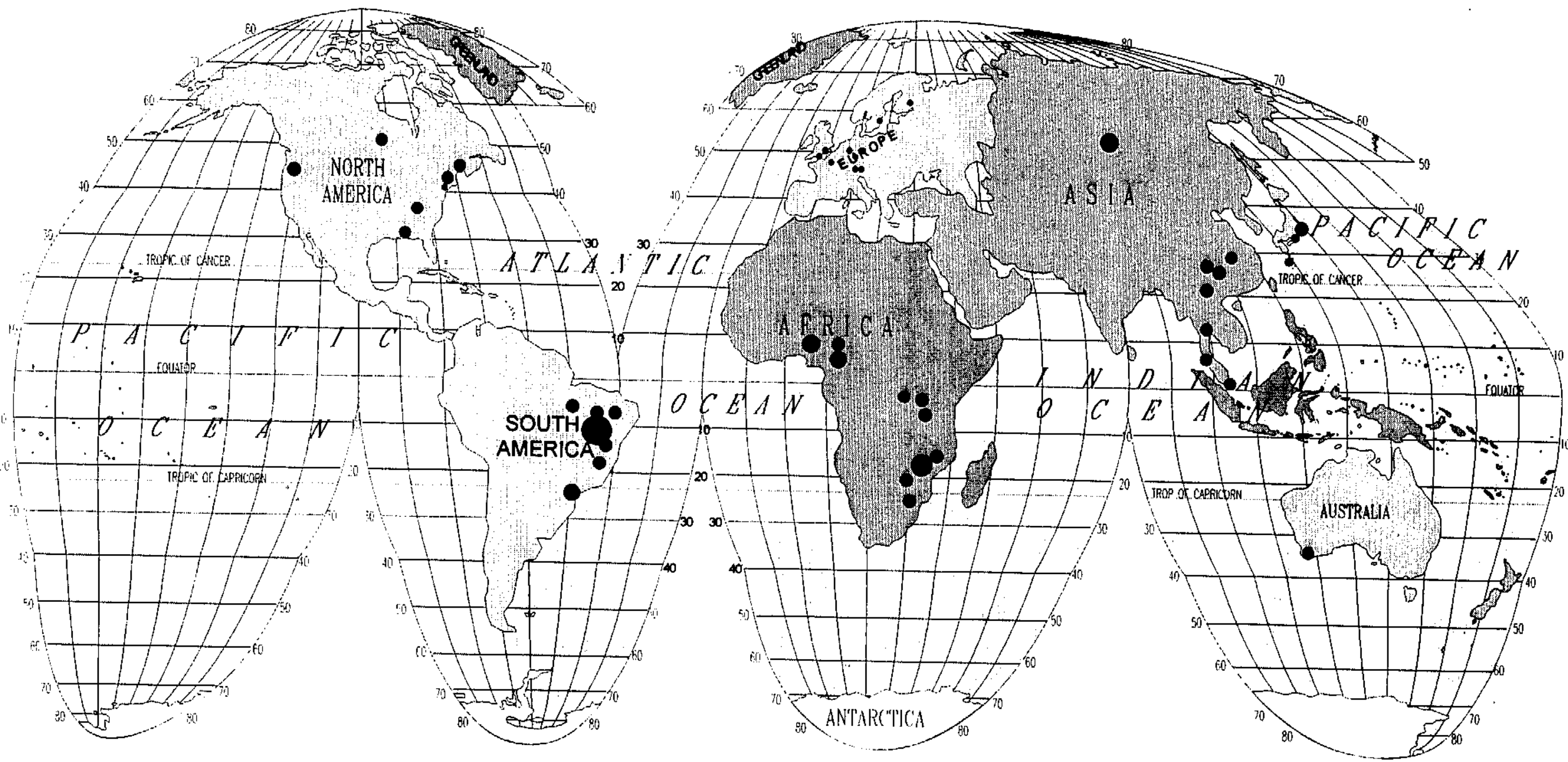

Niobium Minerals

(the most important deposits: Brasil, Canada, South Africa)

Designation	Composition	$\%Nb_2O_5+Ta_2O_5$	$\%Nb_2O_5$	$\%Ta_2O_5$
Tantalit	$(Fe,Mn)(Ta,Nb)_2O_6$	81....86	2....27	53....84
Niobit (Columbit)	$(Fe,Mn)(Nb,Ta)_2O_6$	75....81	47....78	0.1....34
Tapiolit	$FeTa_2O_6$	80....85	1....11	74....83
Pyrochlor	$NaCaNb_2O_6F$	38....73	26....73	0.2....22
Microlit	$(Na,Ca)_2Ta_2O_6(O,OH,F)$	58....80	3....30	33....77
Euxenit	$(Y,Ca,Ce,U,Th)(Nb,Ta,Ti)_2O_6$	28....31	22....29	1....5
Simpsonit	$Al_8Ta_6O_{27}$	72....73	0.3....1	72....73
Samarskit	$(Y,Ce,U,Ca,Fe,Pb,Th)(Nb,Ta,Ti,Sn)_2O_6$	43....60	28....40	2....27
Fergusonit	$(Y,Ce,Fe)(Nb,Ta,Ti)O_4$	43....53	35....47	0.1....17

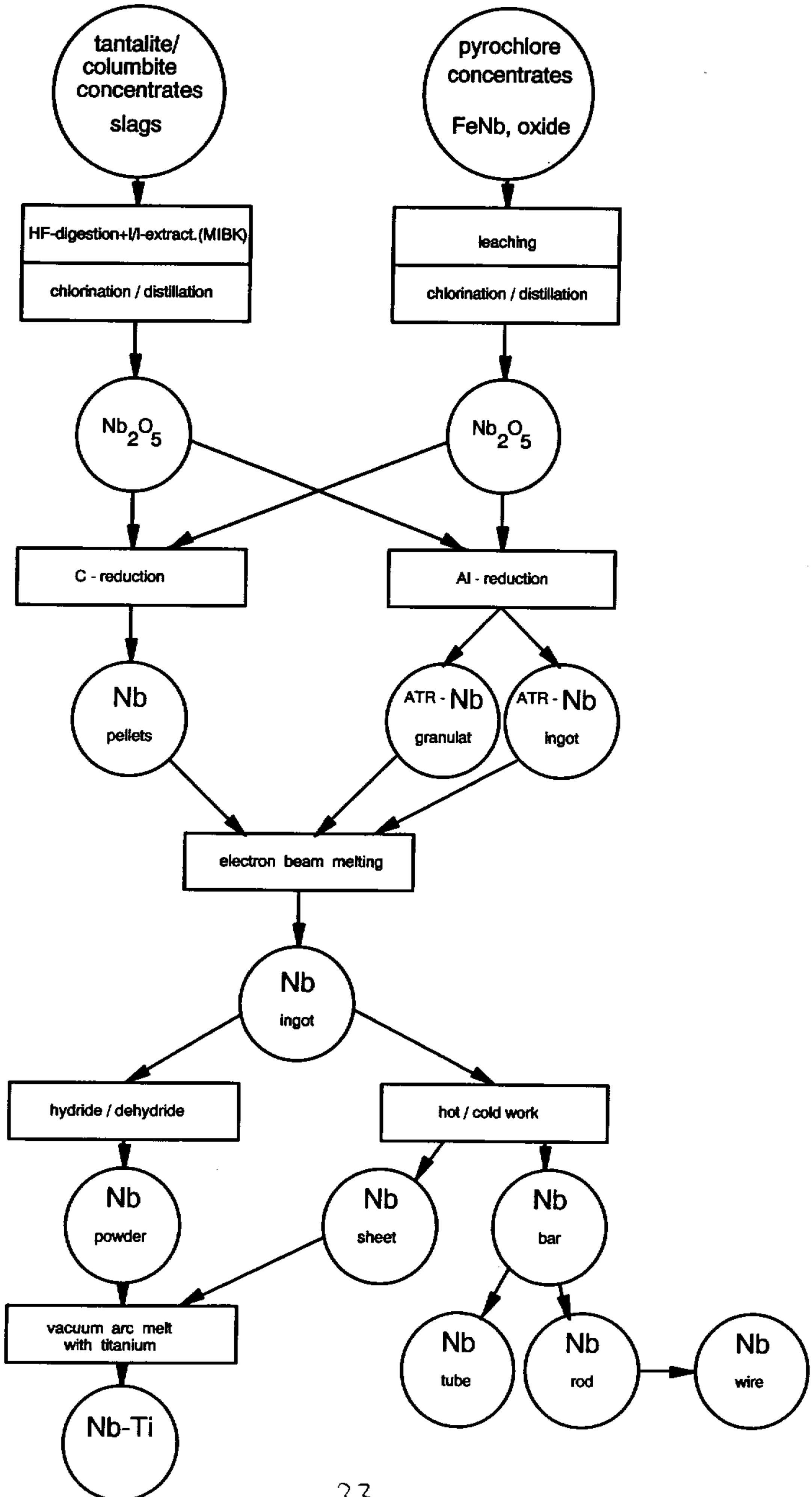
tantalite/
columbite
concentrates
slags
pyrochlore
concentrates
FeNb, oxide
HF-digestion+l/l-extract.(MIBK)
chlorination / distillation
leaching
chlorination / distillation
Nb_2O_5
Nb_2O_5
C - reduction
Al - reduction
Nb
pellets
ATR - Nb
granulat
ATR - Nb
ingot
electron beam melting
Nb
ingot
hydride / dehydride
hot / cold work
Nb
powder
Nb
sheet
Nb
bar
vacuum arc melt
with titanium
Nb
tube
Nb
rod
Nb
wire
Nb-Ti

Niobium Purification by Electron - Beam - Melting

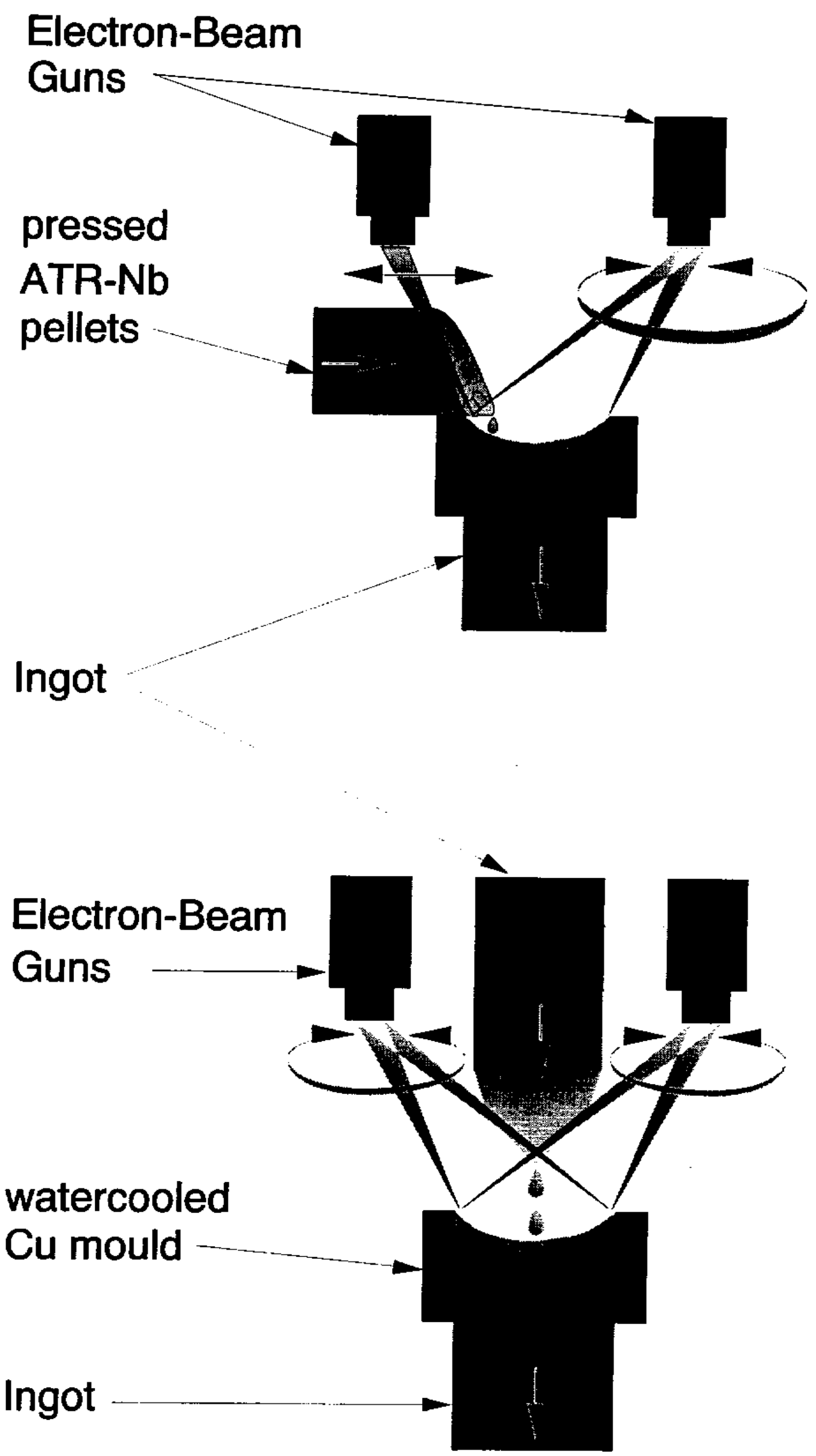

1. Melt Consolidation

2. to 6. Melt Drip Melting

Investigations of the thermal conductivity of superconducting niobium show that the thermal conductivity in the temperature range between 0.5 to 10 K is composed of phonon and electron components and between 2 and 10 K depends largely on the interstitial impurities like C, H_2, O_2 and N_2. Approatching the critical temperatur Tc, the point of transition to supraconduction, the electrons condensed to Copper-pairs, which makes no contribution to the thermal transport. That is why the phonons gain in significance for the thermoconductivity. If there are no defects in the lattice like transpositions, grainboundaries etc. a significant peak of phonones can be seen at about $T \approx 0.2 * T_c$. The range of the operating temperature of the niobium-cavities is about 2 to 4.2 K and so the importance of the phonones for the themal conductivity must be seen. Therefor the material development have to take care for both, improvement of structure and deformation as well as purity of the material. To check the interstitial contents after various processing steps like electron beam melting, forging, rolling and vacuum heat treatment, the determination of the thermal conductivity, the residual restivity ratio compared to special gas analysis methods is particulary advantageous.
For determination of the thermal conductivity λ at 4.2 K samples must be heated in liquit helium under a high vacuum. The calculation followes the equation:

$$\Delta Q/\Delta t = \lambda_{Tc} * F * \Delta T / L$$

$\Delta Q/\Delta t$	$\Rightarrow$	heat transfer
F	$\Rightarrow$	cross-sectional area
L	$\Rightarrow$	length
ΔT	$\Rightarrow$	temperature difference
t	$\Rightarrow$	time

On the basis of theoretical calculations there exists a correlation between thermal conductivity in the normal and superconductive conditions. Together with the Wiedemann-Franz-law a simplyfied correlation between the thermal conductivity and the RRR coult be deduced:

$$\lambda_{Tc} = RRR / 4 \quad | \; T=4.2\ K$$

Therefor the thermal conductivity and the RRR decreases both when the concentration of impurities is growing. The measurement of RRR is much easier than the measurement of the thermal conductivity, and this method showes a high sensitivity, accuracy and reproducibility.

It is known that the electrical resistivity is made up of partial resistances according to the following relationship (Matthiesen rule):

$$pR = pi(T) + pFA + pEF + pOF$$

pi(T)	$\Rightarrow$	resistivity from electron phonon scattering
pFA	$\Rightarrow$	impurity atom resistance
pEF	$\Rightarrow$	intrinsic defect resistance
pOF	$\Rightarrow$	surface resistance

The resistivity contributions pEF and pOF can be neglected in technical quality material in comparison with the resistivity pFA caused by impurity atoms.

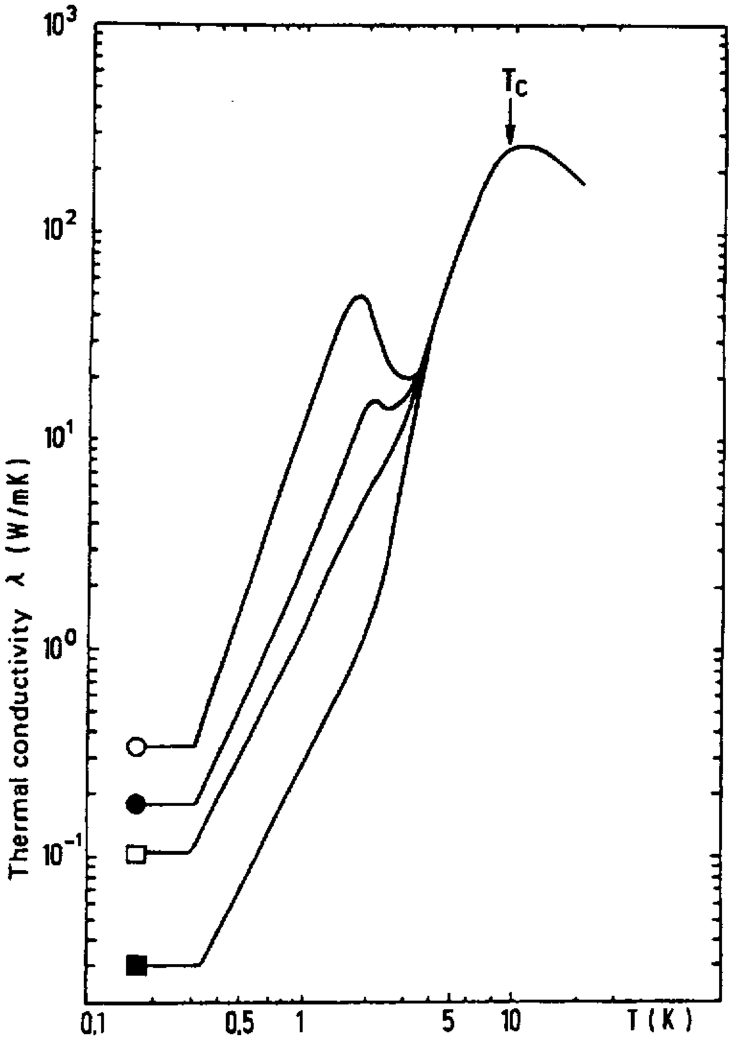

Thermal conductivity of cold deformed niobium samples (Wasserbäch)

- ○ undeformed
- ● 1.0 % deformed
- □ 2.4 % deformed
- ■ 22.0 % deformed

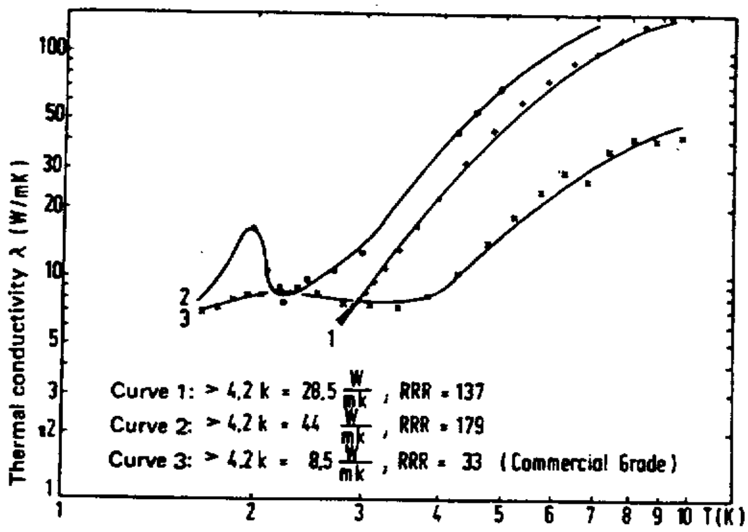

Temperature dependence of the thermal conductivity in the technical niobium qualities obtained

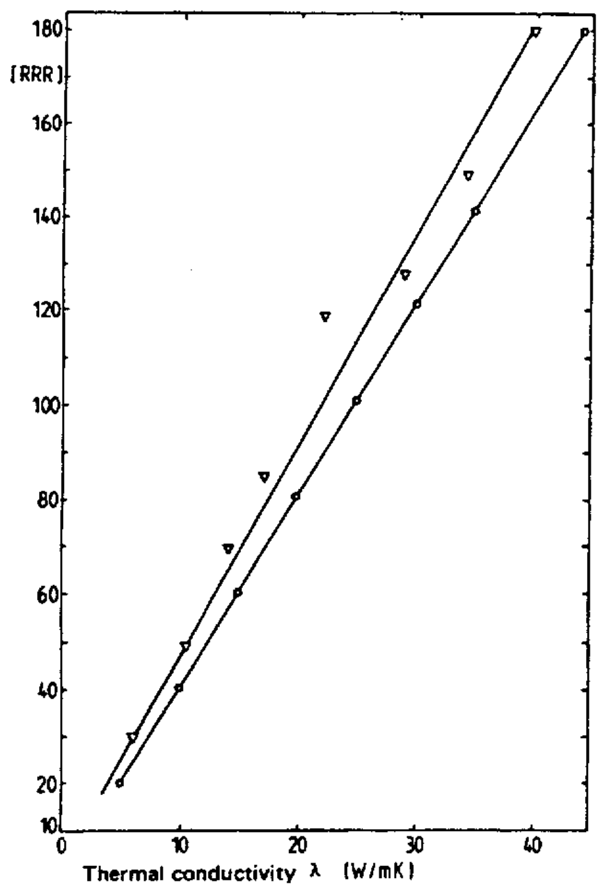

Agreement between the experimentally determined value pairs λ(4.2K) and RRR and Wiedemann-Franz law

The following relationship holds for the residual resistance pR :

$$pR = pi(T) + pFA = pi(T) + \Delta pi / \Delta Ci * Ci$$

Ci is the concentration and $\Delta pi / \Delta Ci$ the resistivity coefficients of the most important impurity atoms are given in the following Table :

Residual Resistance Coefficients of Various Impurity Atoms in Niobium

Impurity Atom	O	N	C	Ta	Zr
$\Delta pi / \Delta Ci$	2.64	3.49	3.33	0.12	0.6

(literature values converted to [Ωcm / wt.ppm.])

It can be seen, that the substitutionally dissolved impurity atoms (Ta, Zr ...) contribute much less to the electrical resistance than the interstituals (O, N, C, H ...).For practical reasons, pR is mainly measured at the boiling point of helium (4.2 K) or above the helium bath at 10 K. A measurement at 10 K offers the advantage of being able to measure above the critical temperature $Tc \approx 9.3$ K of niobium. Thus there is no need for an external magnetic field to prevent the supercontuctivity. The residual resistivity ratio RRR is then :

$$RRR = \frac{R(300\ K)}{R(10\ K)} = \frac{pi(300\ K) + pFA}{pi(10\ K) + pFA}$$

As pFA at 10 K and 300 K are practically equal and pFA << pi(300 K), you can simplify:

$$RRR = pi(300\ K) / \{ pi(10\ K) + (\Delta p/\Delta C)_O * C_O + (\Delta p/\Delta C)_N * C_N + (\Delta p/\Delta C)_C * C_C \}$$

The absolute values for pi(300 K) and pi(10 K) were taken from the literatur and are $14.58*10^{-6}$ and $8.7*10^{-9}$ [Ωcm] respectively.

Because of the marked oxygen-affinity of niobium in gas-metal reaktions, the dependence of RRR on the oxygen concentration was first calculated after writing the necessary computer programs. The diagrams shows clearly that to achieve high RRR values with decreasing oxygen concentration, the significance of low nitrogen and carbon contents becomes very marked. Examination of this supposition with production samples shows that the influence of defect structure and the metallic impurities can be neglected. Thus, a correlation between the gasanalytically determined oxygen, nitrogen and carbon contents and the RRR values could be established. The good correlation between RRR values and analytically determined gas contents for samples produced on a pilot scale provided the basis for optimizing the melting programmes on a large scale.

The analytical determinations of oxygen and nitrogen were carried out by carriergas and vacuum melt extraction with the platinum flux technique. Suitably prepared and etched samples were injekted in a platinum capsule via a sample lock into a gas-free annealed graphite crusible at about 2900 K and extracted for 25 sec.To estimate the achievable final concentrations of oxygen, nitrogen and carbon and also to control the process equipment, mass-spectrometric analyses of the residual gas atmosphere were carried out during the electron-beam melting cycles with the aid of a mass filter. The main constituents of the residual gas were detected to be mainly hydrogen with water vapour, carbon

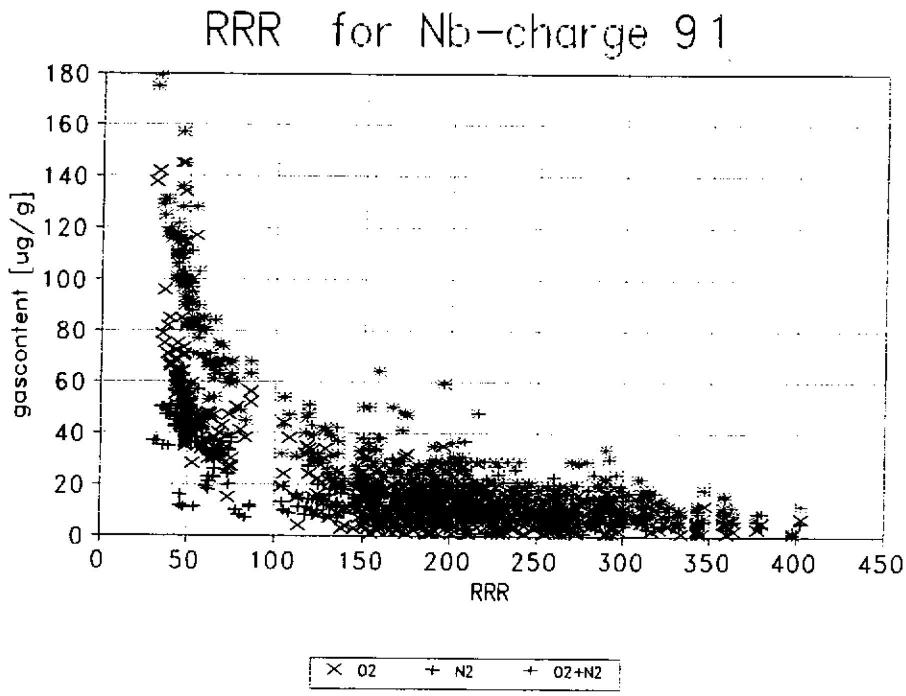
RRR for Nb-charge 91
gascontent [ug/g]
RRR
O2
N2
O2+N2

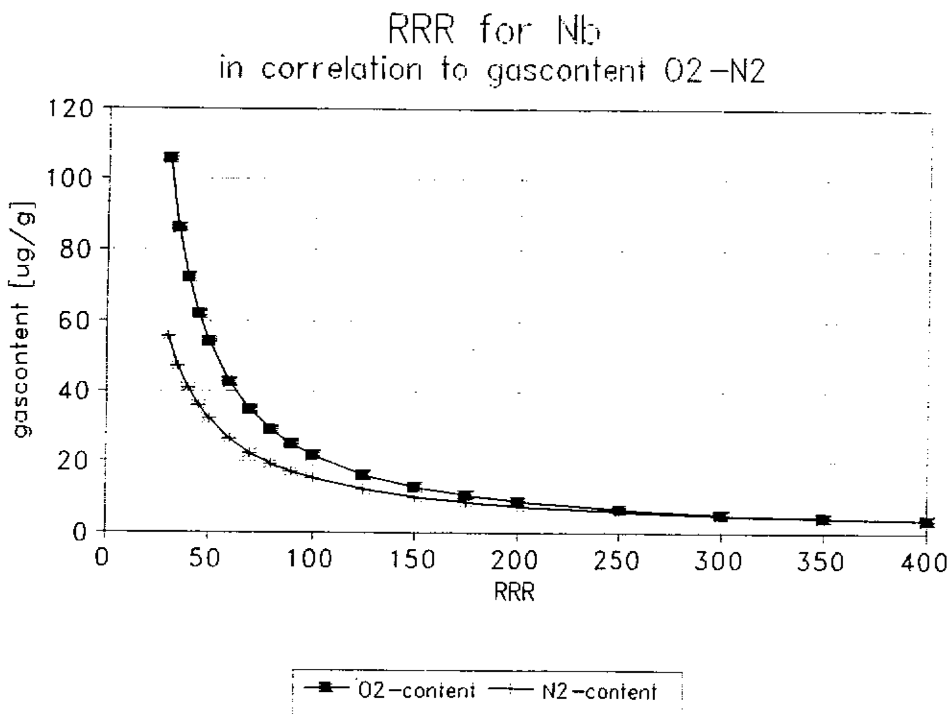
RRR for Nb
in correlation to gascontent O2-N2
gascontent [ug/g]
RRR
O2-content
N2-content

monoxide, oxygen and nitrogen. The partial pressures of CO and N_2 had to be approximated from ion currents I_{12} and I_{14} because of the small difference in mass between carbon monoxide and nitrogen.

Experimental Procedure

The starting material (aluminothermically reduced (ATR) niobium) for the electron beam melting electrodes consisted of slabs with defined interstitial and metallic impurity contents. The relatively high contents of aluminium and the interstitial impurities are associated with the process and can be varied within limits. The analytical charakterisation was carried out by sampling from the top, middle and bottom of the turned ingot.

Impurity Contents of Aluminothermically Reduced Niobium

Element	Wt %	Element	Wt ppm
Zr	<0.002	O2	6.800
Ta	0.031	N2	300
Fe	0.051	H2	10
Si	0.021		
W	<0.010	C	120
Ni	<0.002		
Mo	<0.002		
Hf	<0.003		
Ti	<0.002		
V	<0.002		
Al	5.500		

(Average values from top, middle and bottom of the ingot)

The ingots (weighing approximately 800 kg) were melted in an electronbeam furnace type ESP 100/450 from Leybold-Heraeus. A final vacuum of about $<10^{-6}$ mbar can be achieved in the cold furnace after cleaning. The effective melting power is 450 kW, and two electron guns can be used with a performance up to 400 kW each with an accelerating voltage of 30 kV. The furnace has a magazine for the continuous charging of starting material in the form of slabs. Crusible dimensions are available between 150 mm and 300 mm diameter for final ingot lengths up to 2300 mm.

Parameters for electron-beam melting

Starting material	ATR-Nb slabs
Starting quantity	≈ 800 kg
Melting cycles	6
Melting temperature	≈ 2400 °C
Melting rate	60 - 70 kg / h
Working pressure	3 x 10^{-6} mbar
Ingot diameter	225 mm
Yield	81%

Contents (µg/g) after each melting cycle

Melting cycle	1	2	3	4	5	6
C	8	8	7	10	6	8
O	675	128	54	32	17	10
H	1	1	1	1	1	1
N	128	59	45	28	26	20
Total	812	196	107	71	50	39

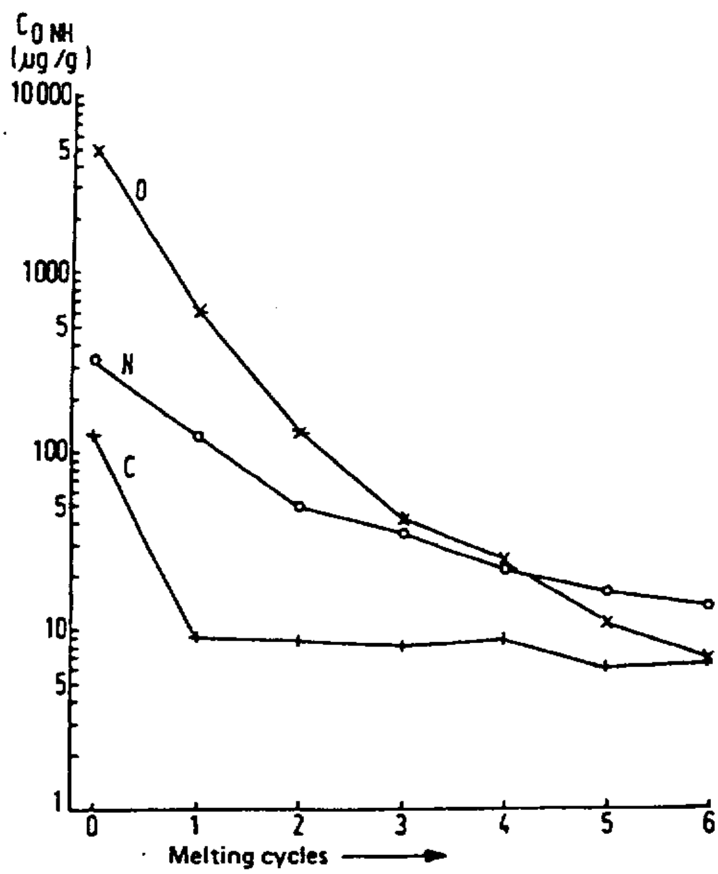

Gas contents, C_O, C_N, C_H, as a function of the number of melting cycles

The results of the mass-spectrometric determination of the residual gas components are summarised in the following table. The evaluation was carried out during the maximum degassing of the fifth remelt cycle.

Mass-spectrometrically determined partial pressures [mbar] of the residual gas components at T = 2700 K

P_{tot}	P_{O2}	P_{H2O}	P_{CO}	P_{N2}	P_{H2}
$3*10^{-4}$	$1.4*10^{-6}$	$9*10^{-5}$	$8*10^{-6}$	$9*10^{-6}$	$2*10^{-4}$

The degassing behaviour of niobium at high temperatures has been thoroughly investigated. The final contents that can be achieved are largely determined by the residual gas partial pressures during the last melting cycle. In the temperature ranges quoted, thermodynamic equilibria are established for the gases H_2, N_2, CO and stationary states for O_2, H_2O. The corresponding P-T-C relationships for solid solutions (in the α - solid solution) are known. For the thermodynamic equilibria, the following systems are valid for the temperature ranges shown:

$$\log C_H = 1/2 \log P_{H_2} + 0.03 + 1620 / T \qquad (2600 \text{ to } 2800\ °C)$$

$$\log C_N = 1/2 \log P_{N_2} + 0.02 + 9300 / T \qquad (1500 \text{ to } 2200\ °C)$$

$$\log C_C + \log C_O = \log P_{CO} - 14.55 + 14700 / T \qquad (1900 \text{ to } 2400\ °C)$$

At a carbon : oxygen ratio of 1, the following systems are valid for the temperature range 1900 to 2500 °C:

$$\log C_O = \log P_{O_2} - 3.8 + 26265 / T \qquad (1900 \text{ to } 2500\ °C)$$

$$\log C_O = \log P_{H_2O} - 4.55 + 25113 / T \qquad (1900 \text{ to } 2500\ °C)$$

The units for the concentrations C are [µg/g] , the temperature is in Kelvins and the pressure P is measured in [mbar].
The next table shows the gas contents of niobium calculated from the partial pressures with the aid of these equations. The gas impurity contents determined in this way correspond as a first approximation to the values determined by gas analysis, in particular for oxygen and nitrogen. Thus with the aid of continuous mass-spectrometric measurements during the melting process, a qualitative control of the achievable final contents is possible.

Carbon, oxygen, hydrogen and nitrogen contents [µg/g] calculated from the P-T-C relationships:

Nb-O_2	Nb-H_2O	Nb-CO	Nb-N_2	Nb-H_2
C_O	C_O	C_O	C_N	C_H
1.2	4.5	1.3	8.7	0.006

In the contrast of nitrogen, oxygen forms oxides of various compositions with the metal atoms of the melt surface during degassing at temperatures above 1600 °C. these oxides evaporate, condense on the cold walls of the vessel, and are thus removed from the reaction system. the oxygen concentration decreases at first and then adjusts itself to the value given by the stationary state. Therefor, marked metal losses result from the evaporation of oxides with very long melting times.
A comparison of the oxygen contents shown in the tables befor, shows that the oxygen content after the sixth melt has approached the stationary state of approximately 6 [μg/g]. A significant reduction of the dissolved oxygen content is not to be expected for more than six melting cycles at the given furnace pressures and the resulting partial pressure ratios (see also P_{H2O} in the table before).
The nitrogen degassing of niobium also occurs via the recombination of nitrogen atoms to nitrogen molecules at the surface of the melt. The degassing rate obeys the relationship $V_n \propto C_N^2$ and therefore decreases strongly with degreasing concentration. For this reason, the thermodynamic final content (CN = 8.7 [μg/g]) cannot be achieved with the finite melting times used. Furthermore, for a given nitrogen partial pressure which is dependent on the equipment, the solubility $C_{N,liquit} > C_{N,solid}$.
As well as the C-O-H-N contents, the RRR and the thermal conductivity λ(4.2K) and λ(10K) were measured for selected samples from the final ingot. The results are summarized in the following table. Additionally, the measured values for RRR and the corresponding values for C_O and C_N are shown in a diagram.

COHN contents, RRR and λ(4.2 K) values of a 620 kg niobium ingot after sixfold electron-beam melting

	C_O measured [μg/g]	C_{NHC}	RRR measured	calculated	λ [W/mK] measured	calculated
Top (K)	10	25	119	117	25.0	29
Middle (M)	11	30	110	97	23.5	24
Bottom (B)	15	45	--	-	-	-
Slice 1	10	25	118	117	28.0	29
2	10	30	112	110	-	-
3	15	35	110	80	24.0	20
4	10	30	-	-	-	-
5	10	35	108	117	-	-

If one considers the error limits which arise in gas analysis techniques as a result of sampling procedures and the standard deviations of the chosen analytical methods, the agreement with the physical determinations can be regarded, to a first approximation, as very good. The experimentally determined values for RRR and C_O lie within the desired "identification area", which is enclosed by the curves C_{NHC} = 20 and 30 [μg/g]. The measured values for CNHC vary between 25 and 30 [μg/g]. This demonstrates that RRR values greater than 100 and thermal conductivities λ(4.2K) > 25 [W/mK] were achieved by electron-beam melting on a technical scale in the year 1987. A horizontal slice, taken from the ingot to investigate homogeneity, illustrates the low scatter of the values measured and the good homogeneity over the cross-section and the length of the ingot.

Sheets were produced from ingots with the COHN contents and RRR values shown in the following table. The sheets had the property values which are also presented. A comparison of the values shows that the gas contents achieved by melting could be maintained during the subsequent manufacture of semifinished products, i.e. no contamination occurred during the deformation and annealing process.

Summary of RRR, λ(4.2 K) and COHN content values of the niobium samples produced

	Ingot		Sheet		
Heat No.	COHN [µg/g]	RRR	COHN [µg/g]	RRR	λ(4.2 K) [W/mK]
3042	140	38	150	33	8.5 a)
906	60	112	65	105	25.0
873/1	50	114	52	137	29.5
873/2	40	145	42	179	44.0
3074	20	350	25	300	70

a) Commercial grade Nb

The mechanical properties of these high purity niobium samples are of interest with regard to deep drawability for producing cavities. Typical values for tensile strength, yield point and elongation are summarized together with the ASTM grain size:

RRR	Tensile strength R_m [N/mm²]	Yield strength $R_{p0.2}$ [N/mm²]	Elongation A_L 30 [%]	Grain size ASTM
137 300	183	83	59	6-7

The following figures illustrate the relationship between the change in hardness (HV10) and the degree of deformation for niobium of different qualities. The individual curves show almost the same characteristic shape but are displaced parallel to each other. The initial hardness is very low (HV10 = 50 and 60) and does not increase above HV10 = 100 even with high degrees of deformation (85% to 95%). The low degree of final work hardening represents a further advantage for the deep drawability of this material.

Hardness increase as a function of degree of deformation:

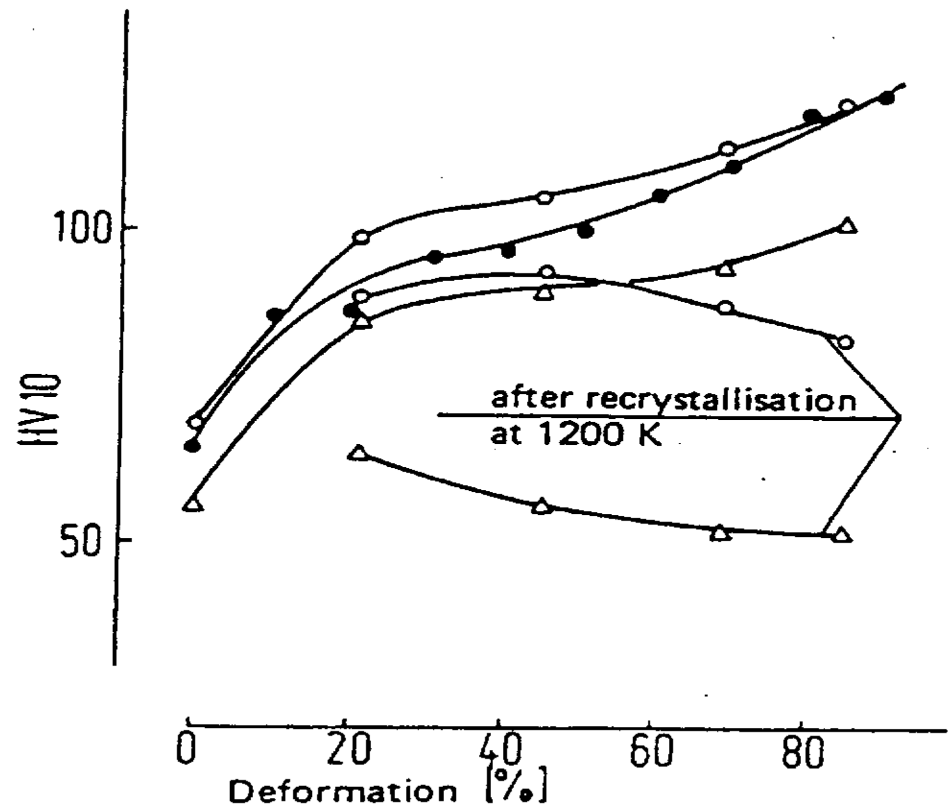

niobium , reactor grade
niobium , commercial grade
niobium , grade 100

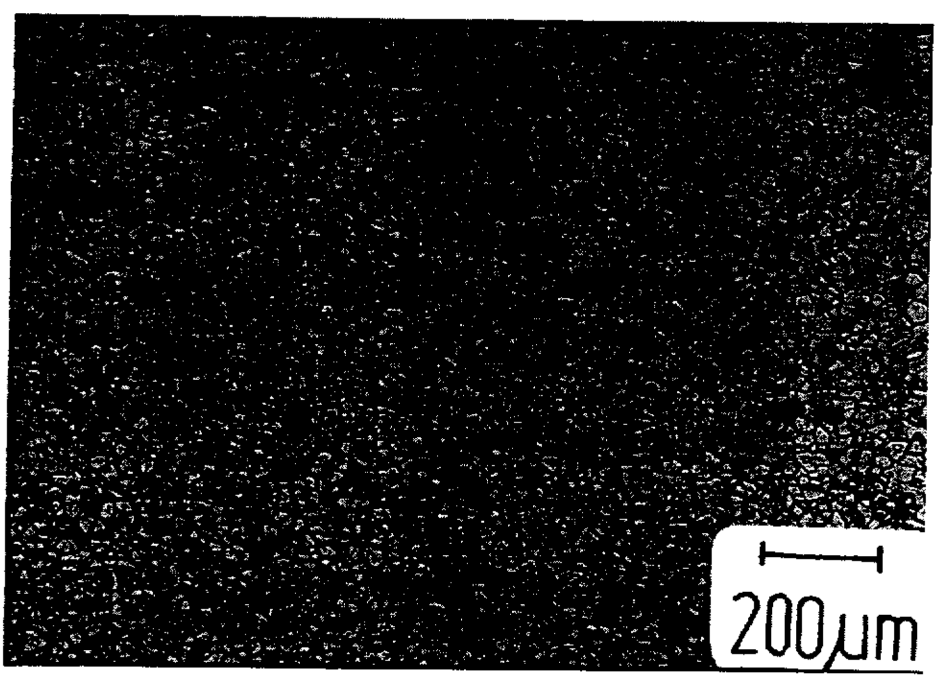

Microstructure after recristallisation

As already mentioned, microscopic surface defects, such as scratches, inclusions and rolling defects ore local impurities have a negative effect on the quality of cavities, because they represent sensitive areas of disturbance for the highfrequency superconductivity leading to local overheating. These effects could be showen in so called temperature maps. Therefor the thermoconductivity is registrated along the surface of a niobium sheet or the complete cavity.
Since 1987 the equipment of the electron beam melting furnace had been optimized by using special diffusion pump oils, reducing the leak rate and improving the pumping capacity. So RRR values better than 400 and $\lambda(4.2K)>100$ [W/mK] corresponding to acceptable mechanical parameters could be reached. As a result of the use of these pure niobium qualities, an increase in the high frequency field strength is often no longer limited by the materials but by electron field-emmission phenomena.
An essential influence becomes also some production parameters like heat treatement and pickling. To get a maximum in fine-grained structure and a maximum in healing up the lattice defects you have to make a compromise between temperature range and the length of time of annealing. If there are some defects in the lattice, the thermoconductivity will decrease. If the annealing temperatur is too high and the time is too long, the thermoconductivity also will decrease, because the niobium will getter gases out of the restgasatmosphere. Also a too high temperature during the pickling process let the oxygen and hydrogen content increase.

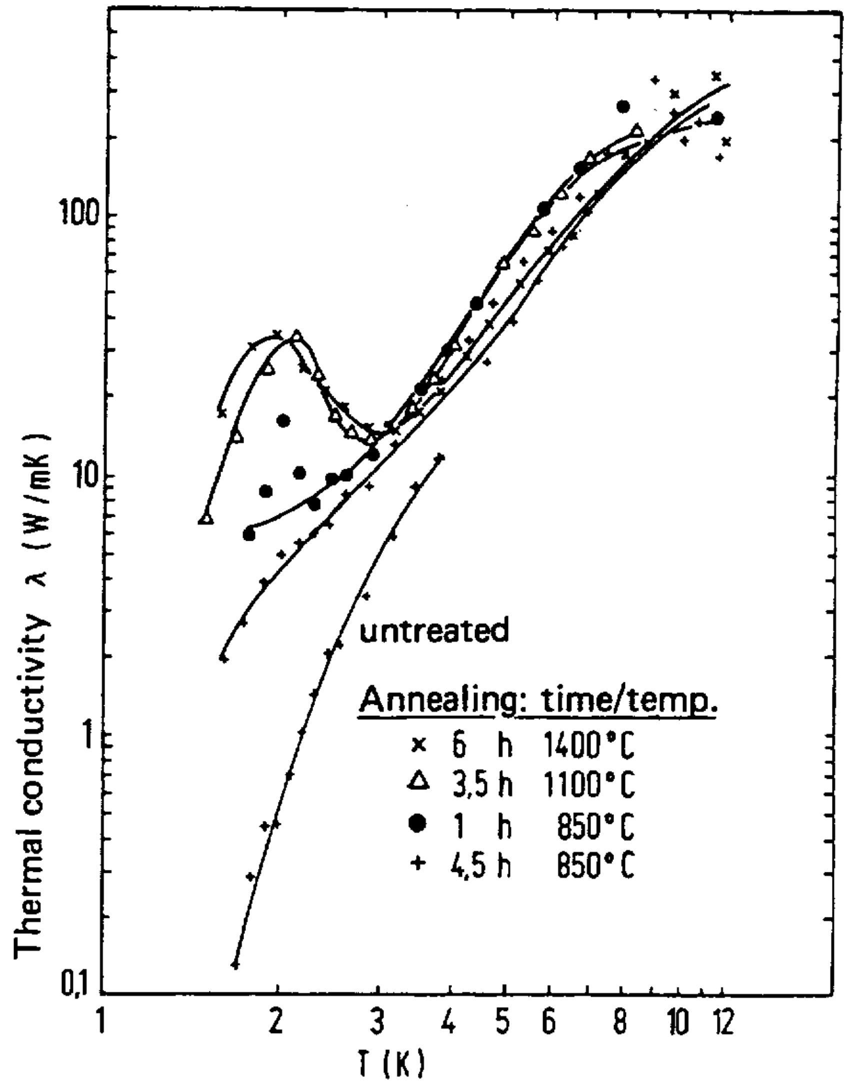

Dependence of the thermal conductivity λ(4.2K) on further recristallisation anneals

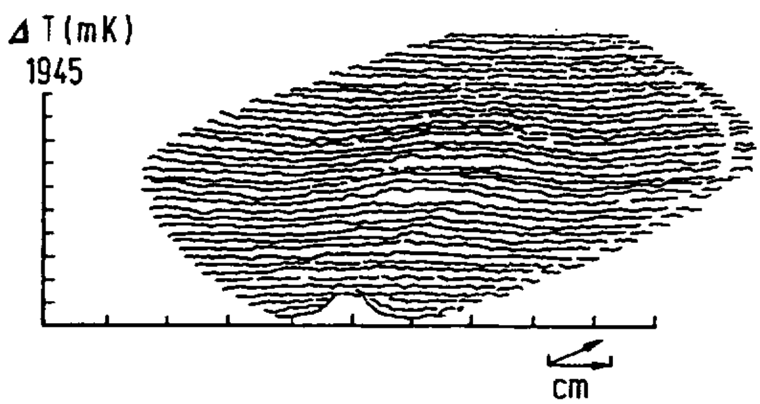

Temperature maps: ΔT vs. cavity surface

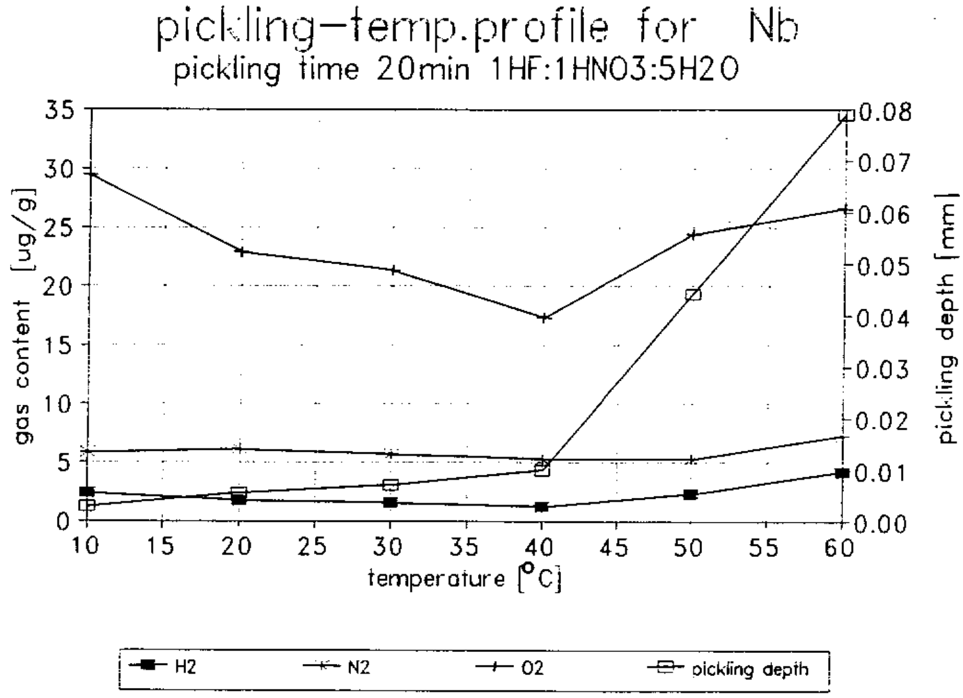
pickling-temp.profile for Nb
pickling time 20min 1HF:1HNO3:5H2O
gas content [ug/g]
pickling depth [mm]
temperature [°C]
H2
N2
O2
pickling depth

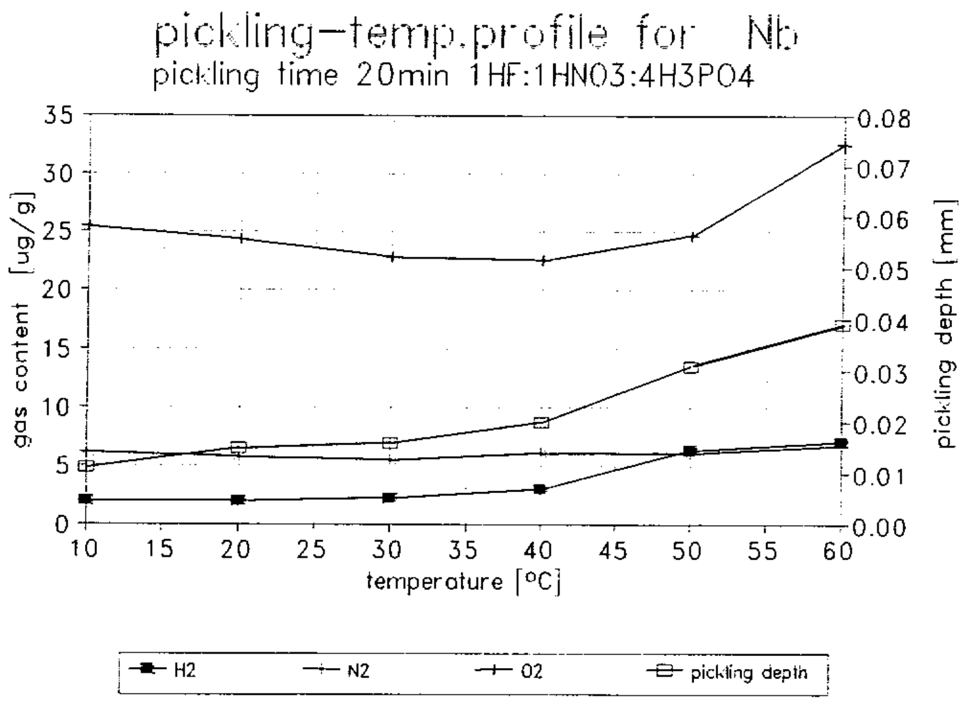
pickling-temp.profile for Nb
pickling time 20min 1HF:1HNO3:4H3PO4
gas content [ug/g]
pickling depth [mm]
temperature [°C]
H2
N2
O2
pickling depth

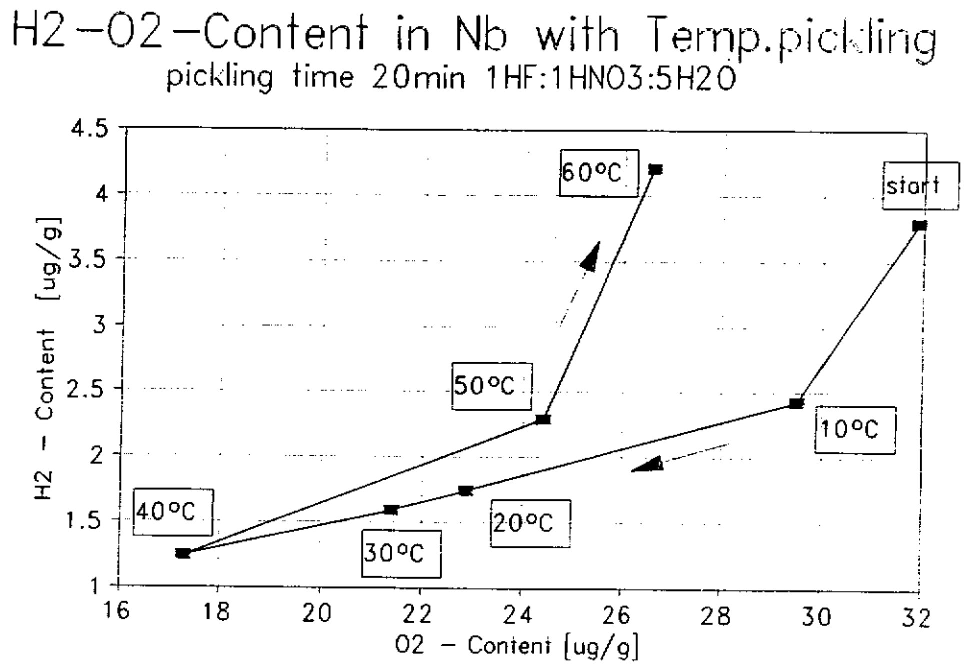
H2-O2-Content in Nb with Temp.pickling
pickling time 20min 1HF:1HNO3:5H2O
H2 - Content [ug/g]
O2 - Content [ug/g]
60°C
start
50°C
10°C
40°C
20°C
30°C
4.5
4
3.5
3
2.5
2
1.5
1
16
18
20
22
24
26
28
30
32

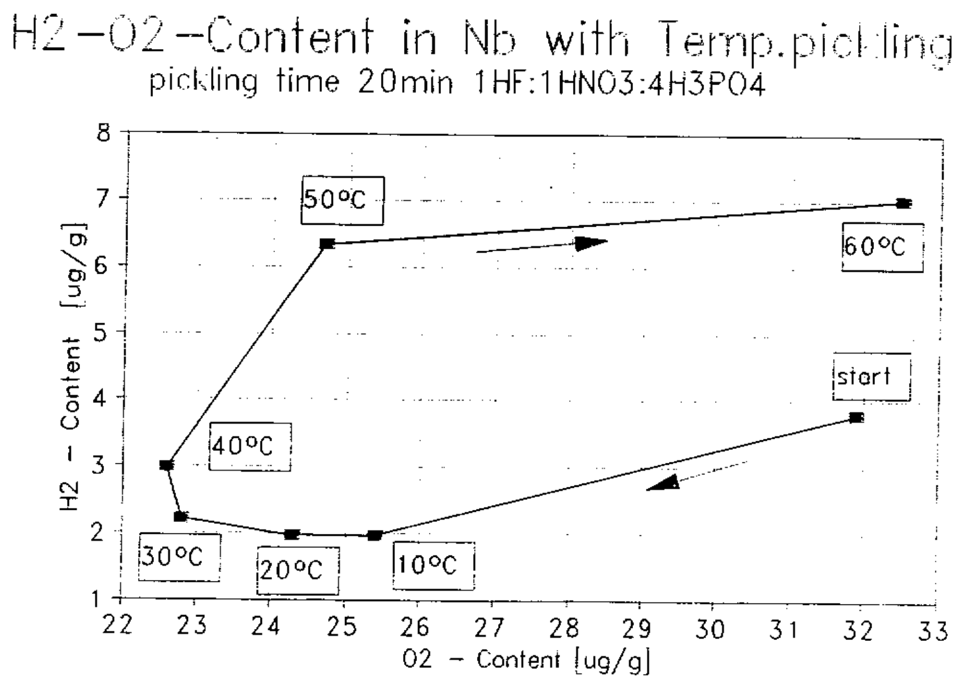
H2-O2-Content in Nb with Temp.pickling
pickling time 20min 1HF:1HNO3:4H3PO4
H2 - Content [ug/g]
O2 - Content [ug/g]
50°C
60°C
start
40°C
30°C
20°C
10°C
8
7
6
5
4
3
2
1
22
23
24
25
26
27
28
29
30
31
32
33

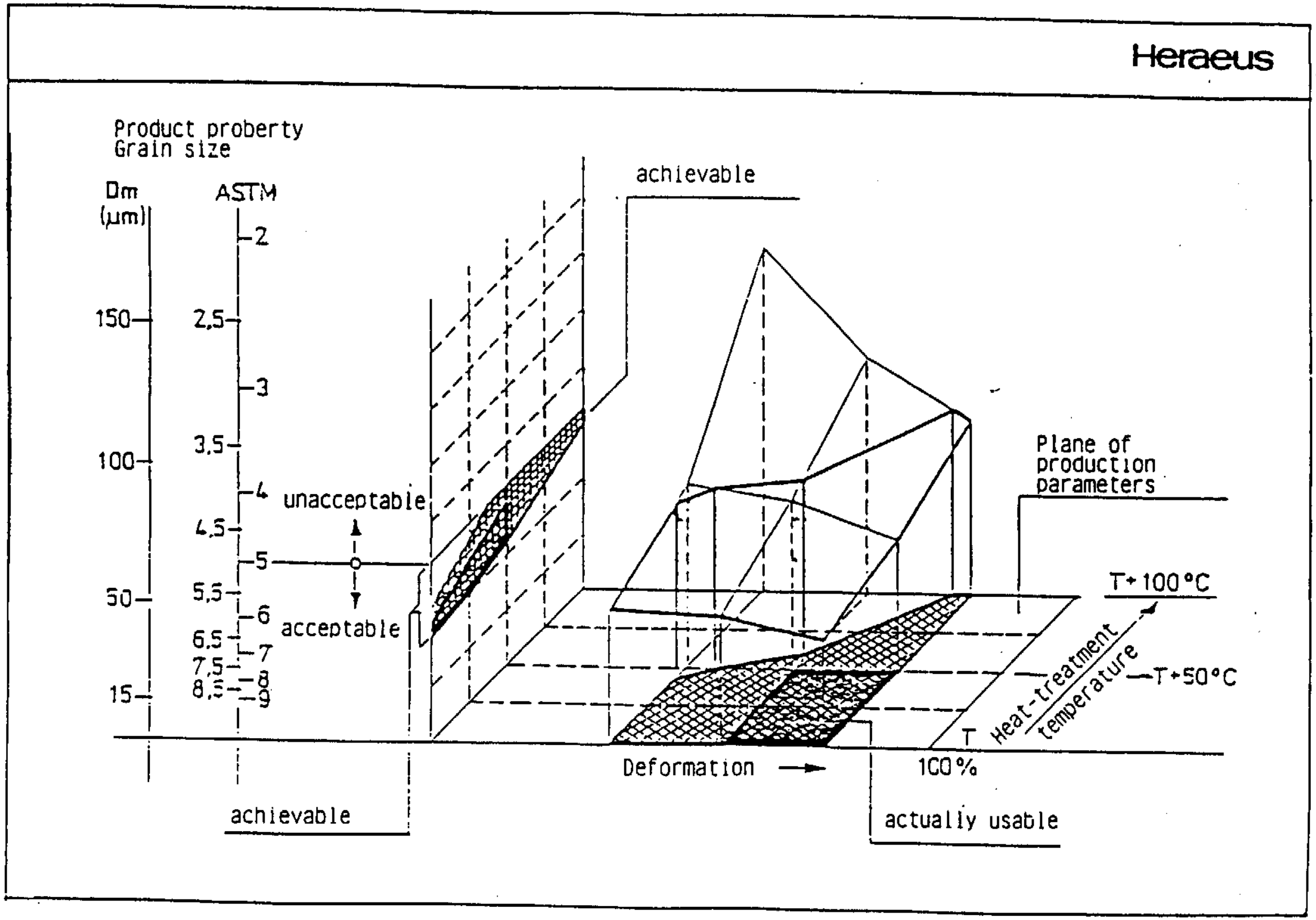

Nb 100 Recrystallization Diagram
(t = constant)

Manufacturing process for Nb semifinished products

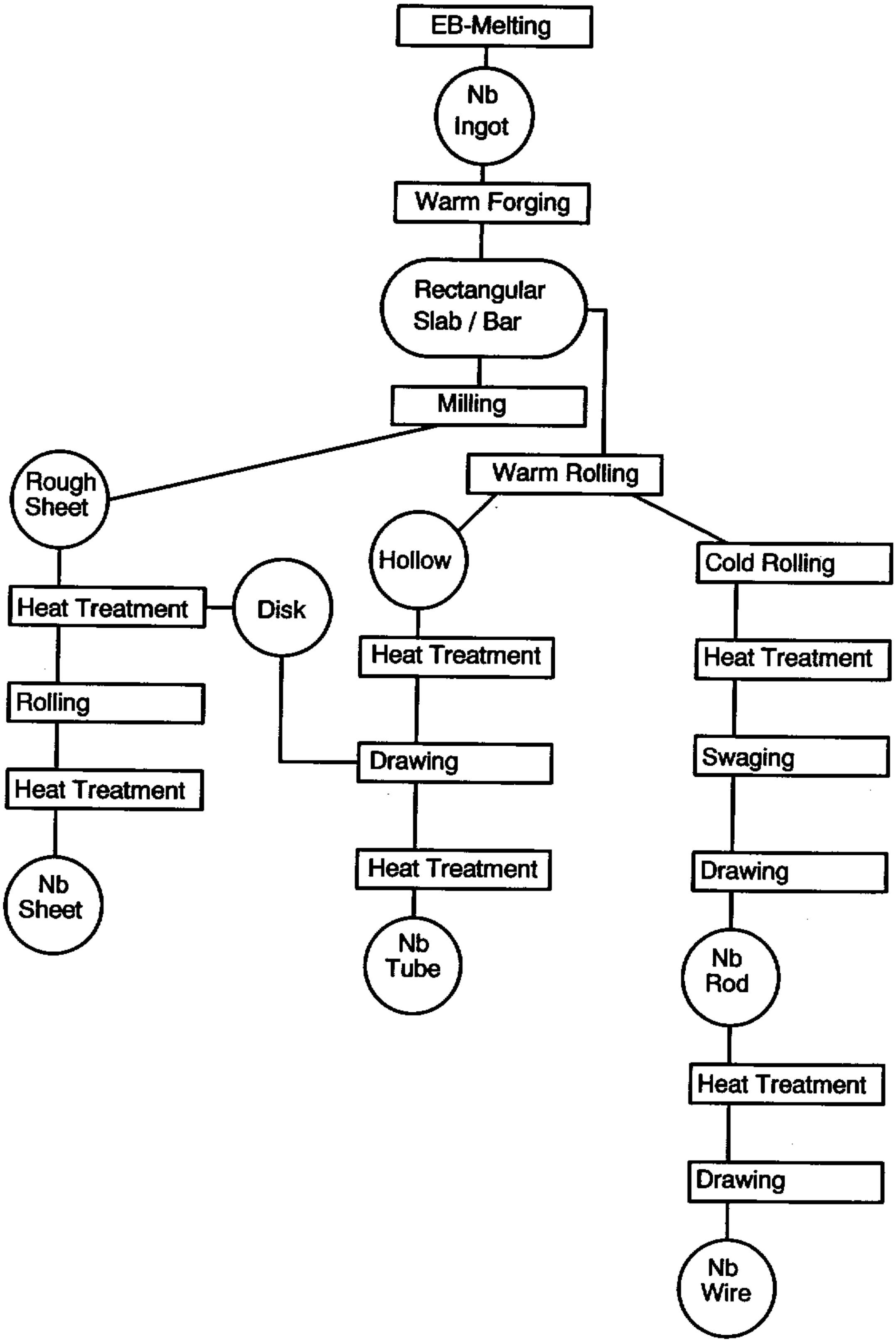

Manufacturing process for Nb sheet

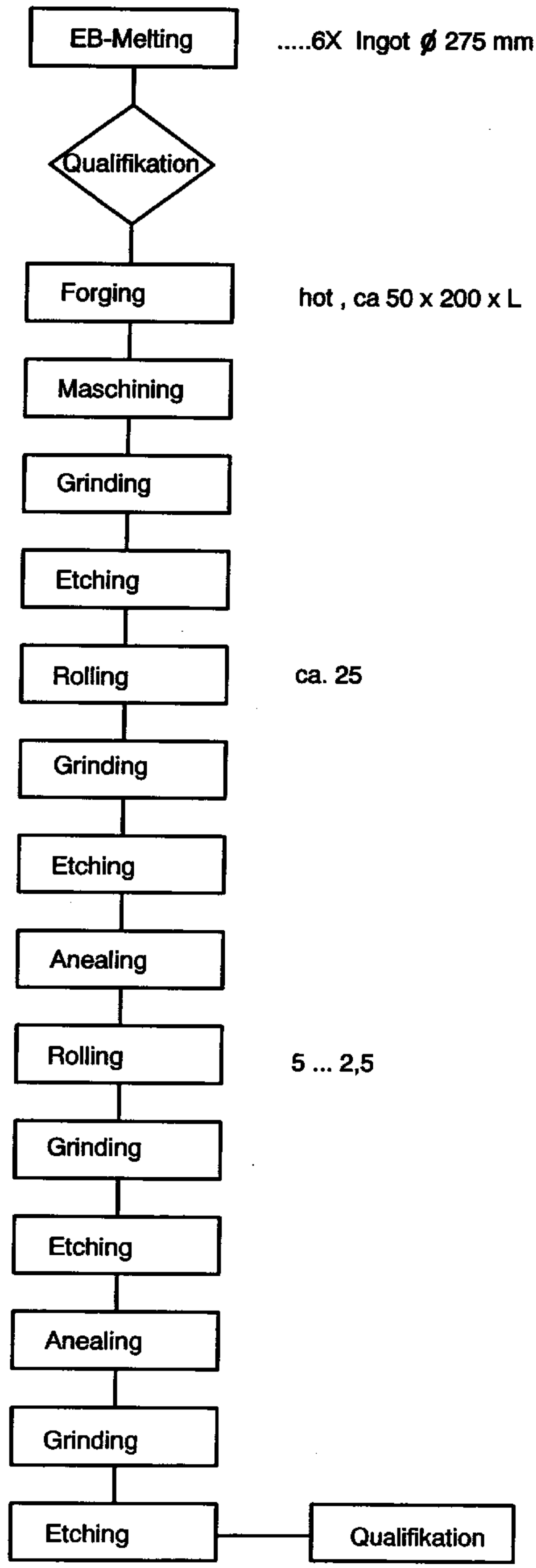

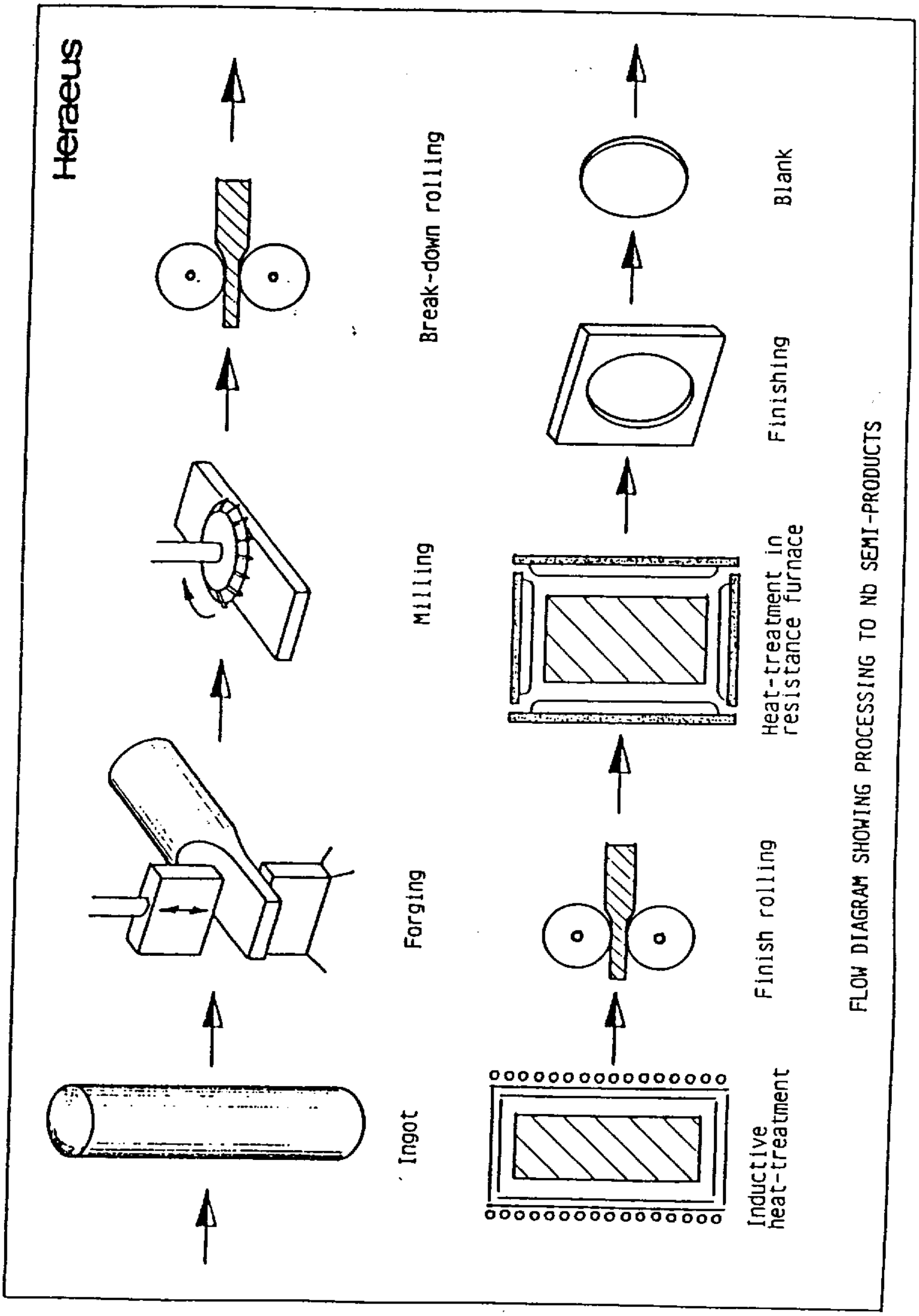

FLOW DIAGRAM SHOWING PROCESSING TO Nb SEMI-PRODUCTS

Heraeus

N I O B I U M 100, 200, 300

Material for HF-superconductor applications

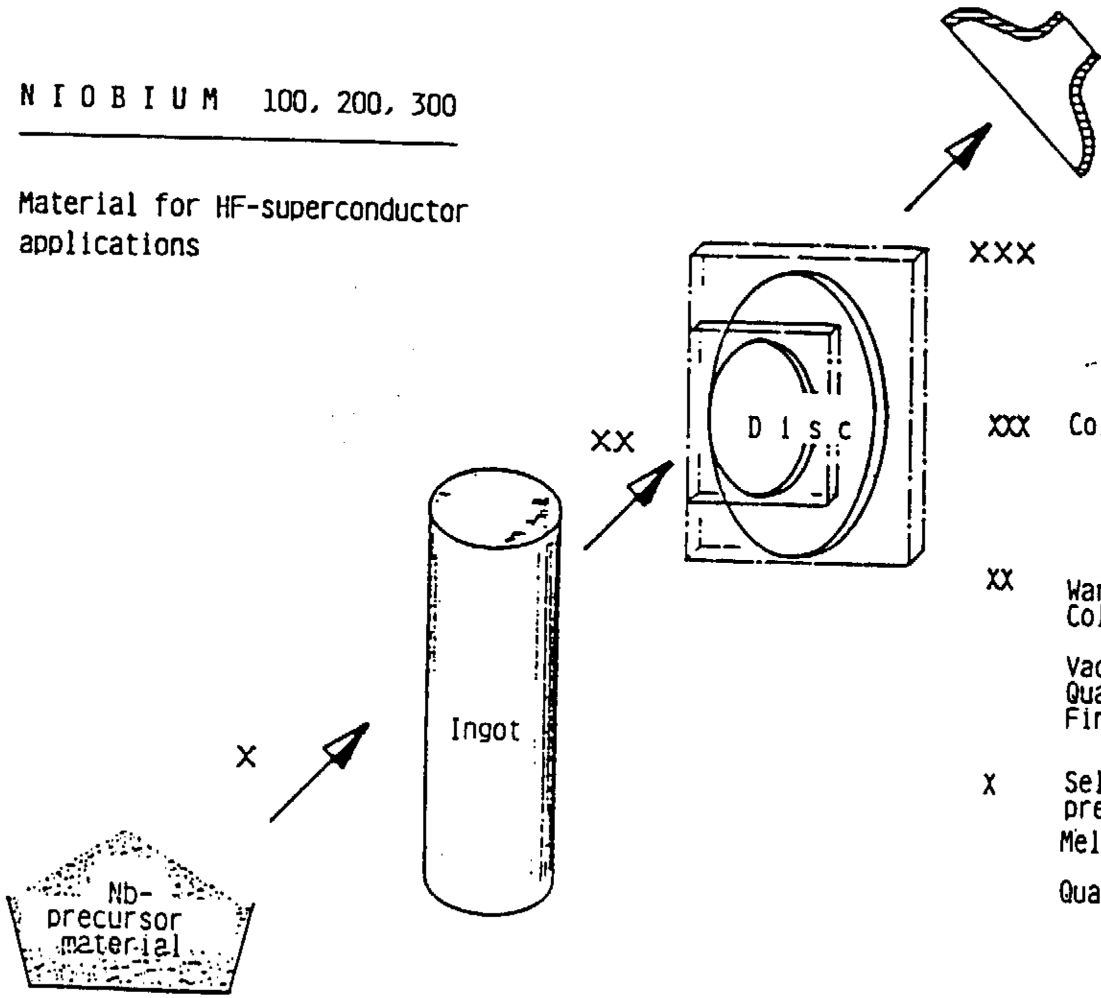

XXX Cold forming

XX Warm forming
Cold forming

Vacuum heat-treatment
Qualification
Finishing

X Selection of precursor material
Melting

Qualification

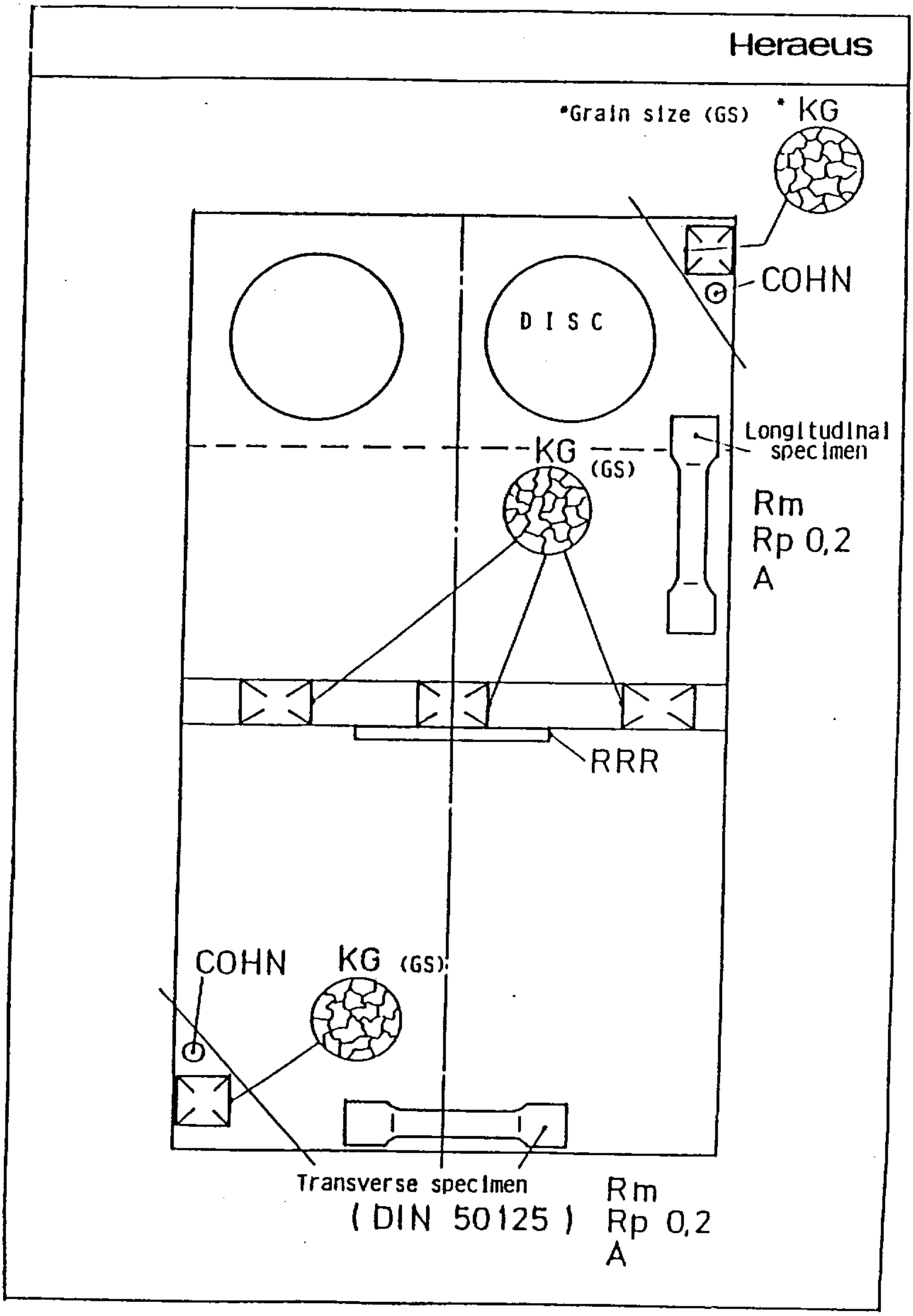

Qualification of Niobium Semi-Products

Electron Beam Melting Furnace

450 kW Leybold-Heraeus EPS 100/450

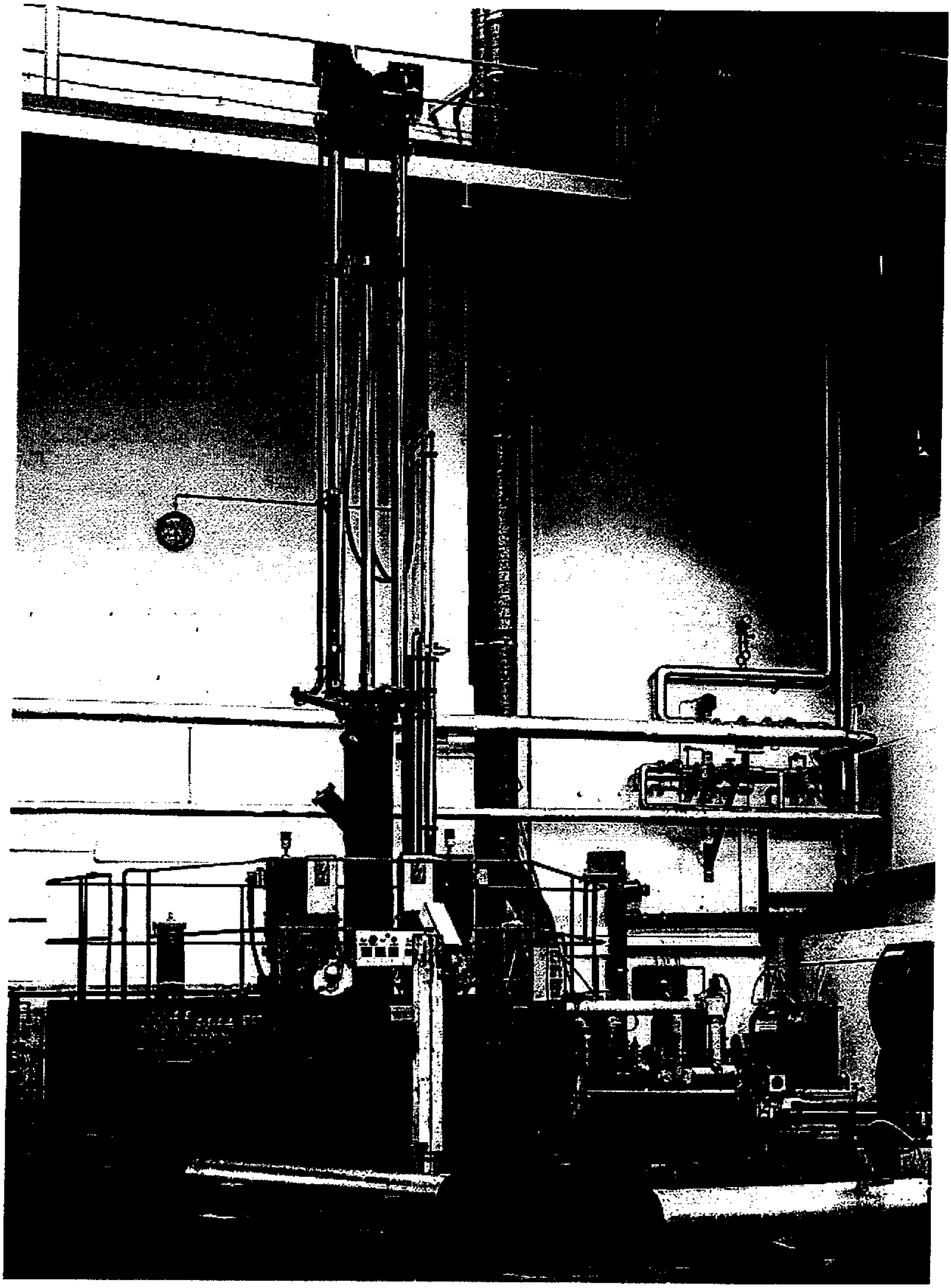

Electron Beam Melting Furnace

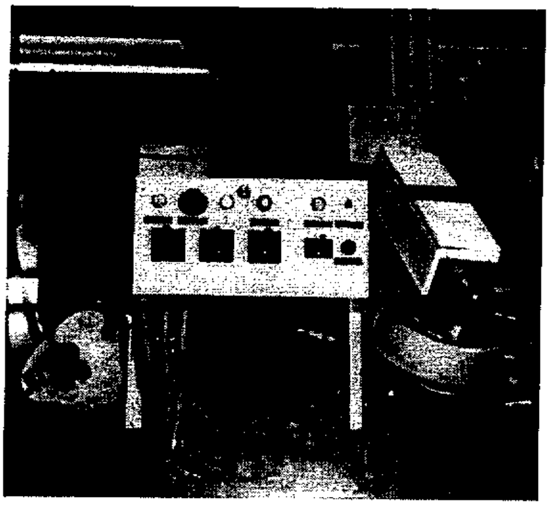

Video controll unit

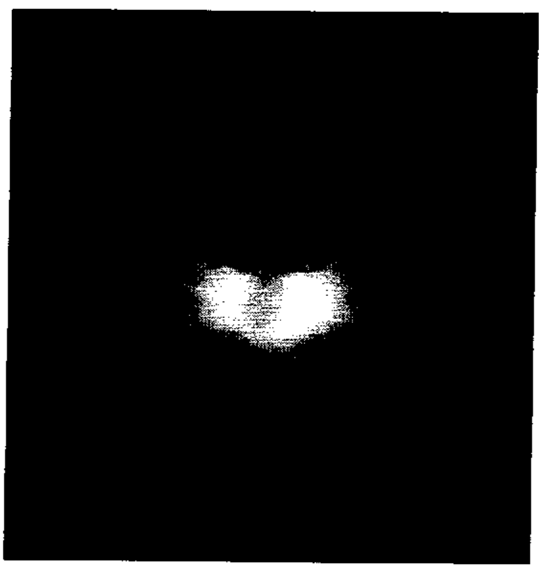

Electron Beam Focus

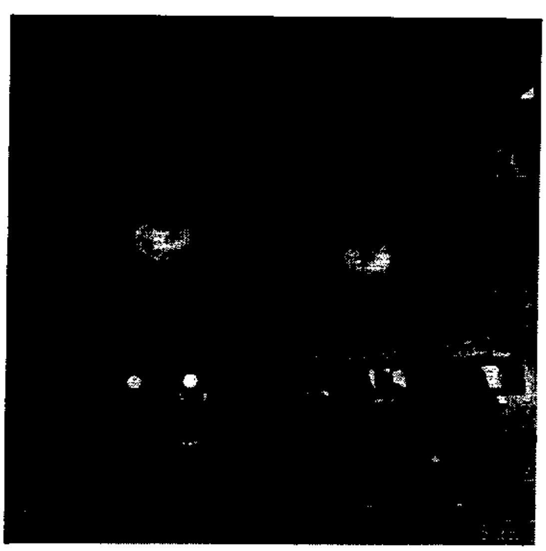

Control Desk with TV-unit

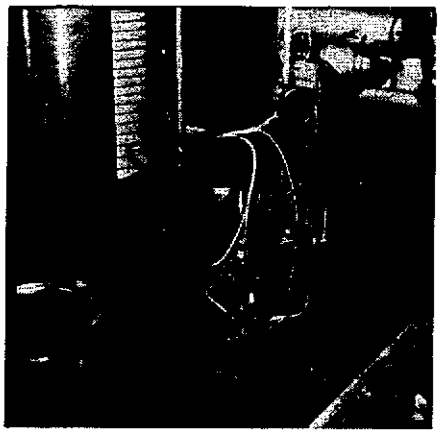

Ingot charging module at bottom of the furnace

Loading unit for ATR-Niobium

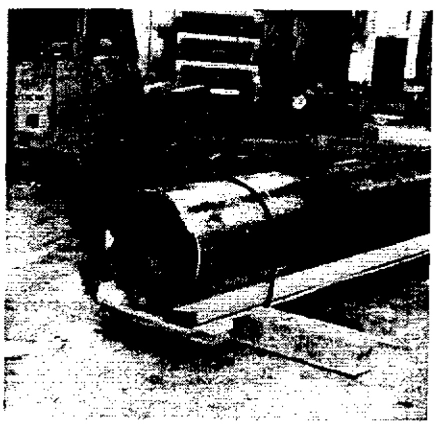

Finished Ingot

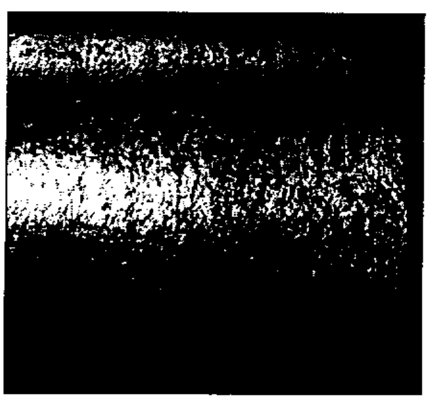

Ingot surface

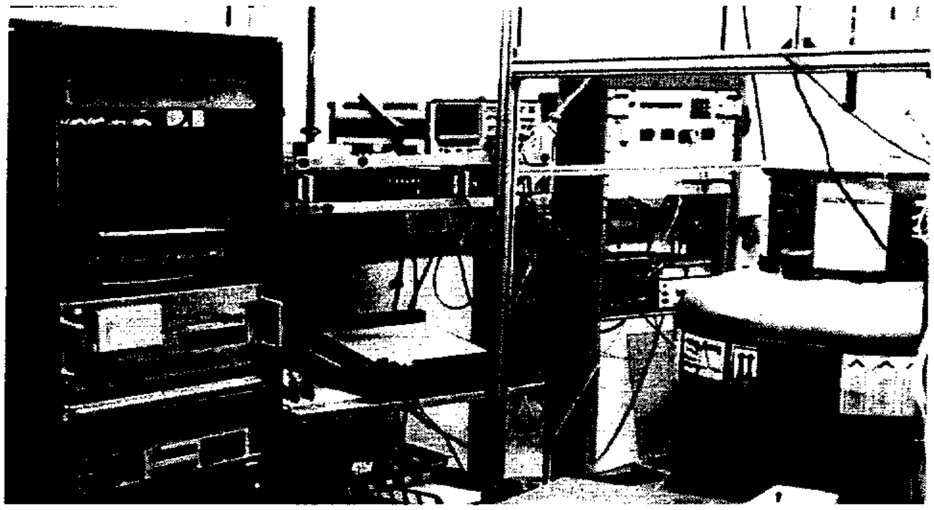

RRR and thermoconductivity measuring unit with liquit Helium container

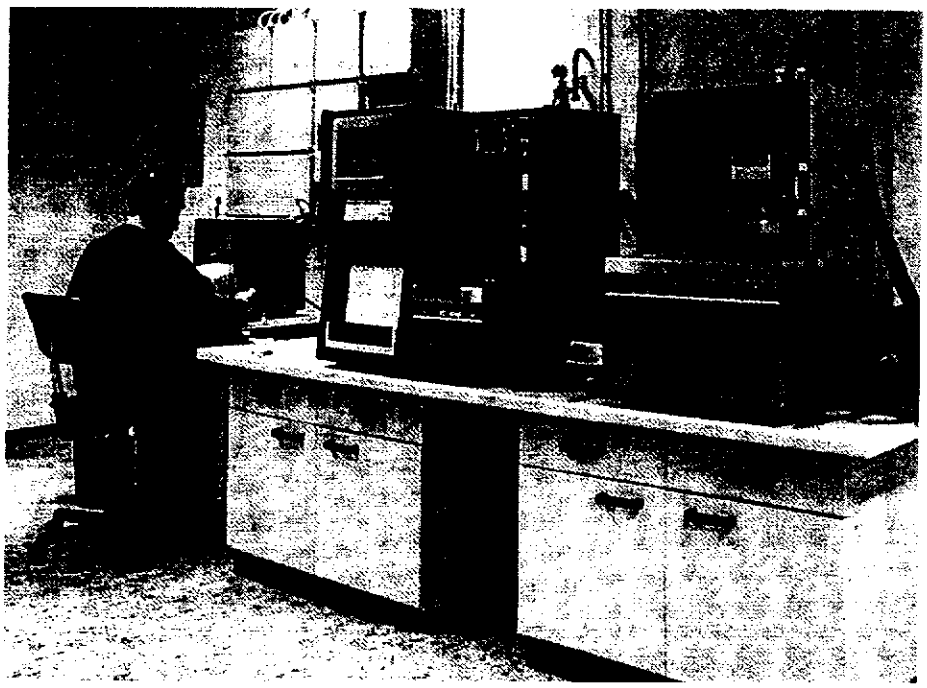

Gasanalytik laboratory for the measurement of the H_2,N_2,O_2,C and S content in niobium

Schleinzer, Dornier

SUPERPLASTIC FORMING

SPF:

- FUNDAMENTALS ABOUT SUPERPLASTICITY -

FUNDAMENTALS ABOUT SUPERPLASTICITY

- Phenomenological description
- Relevance of the m-value for superplastic formability
- Determination of m-values
- Deformation mechanisms
- Forming conditions for SPF

- Summary: materials requirements for superplastic properties

4.5

SPF – Hot Press (Schematic)

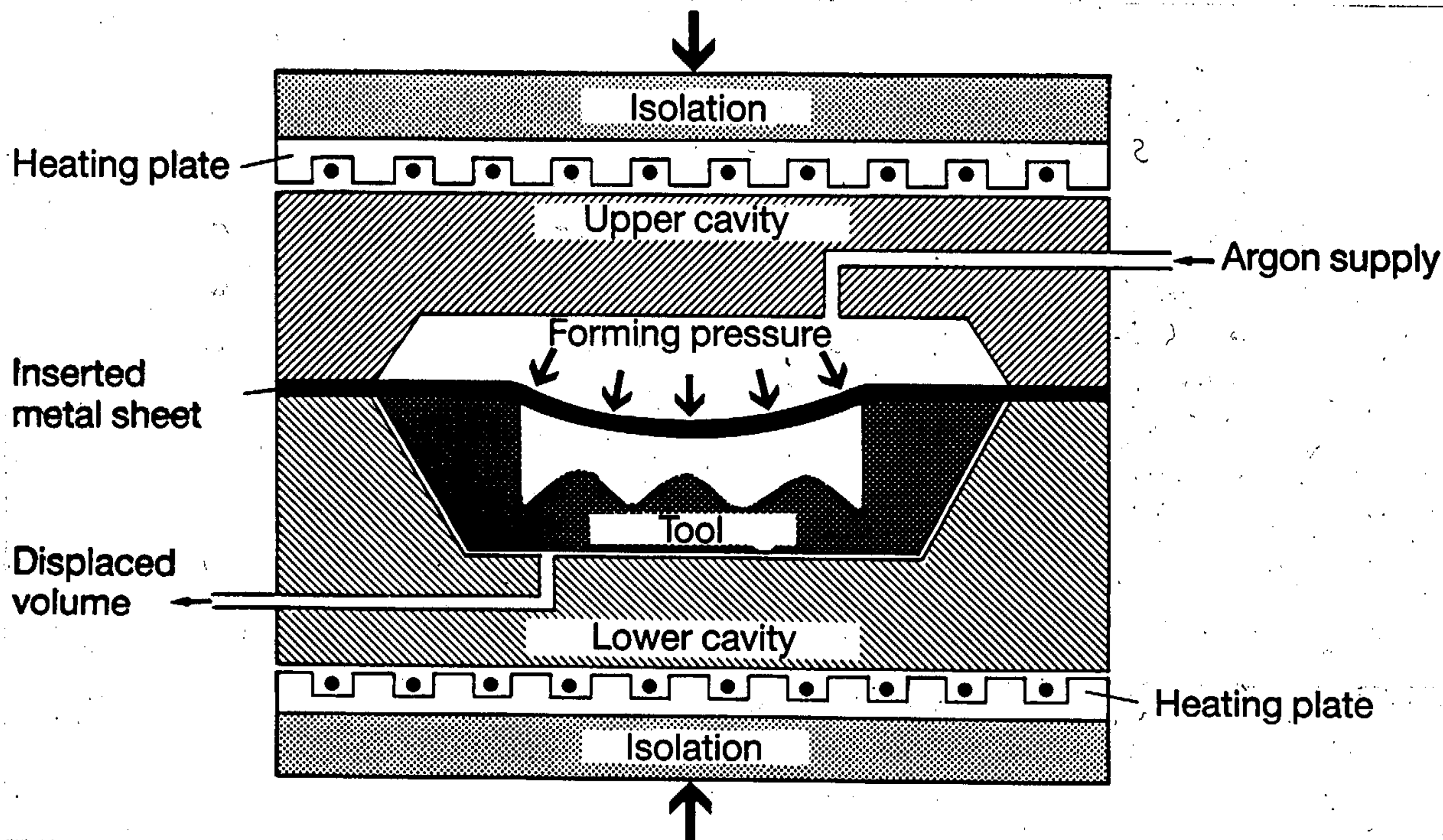

62

Dornier Luftfahrt GmbH

Dornier
Deutsche Aerospace

Dornier 328 Titanium SPF-Part

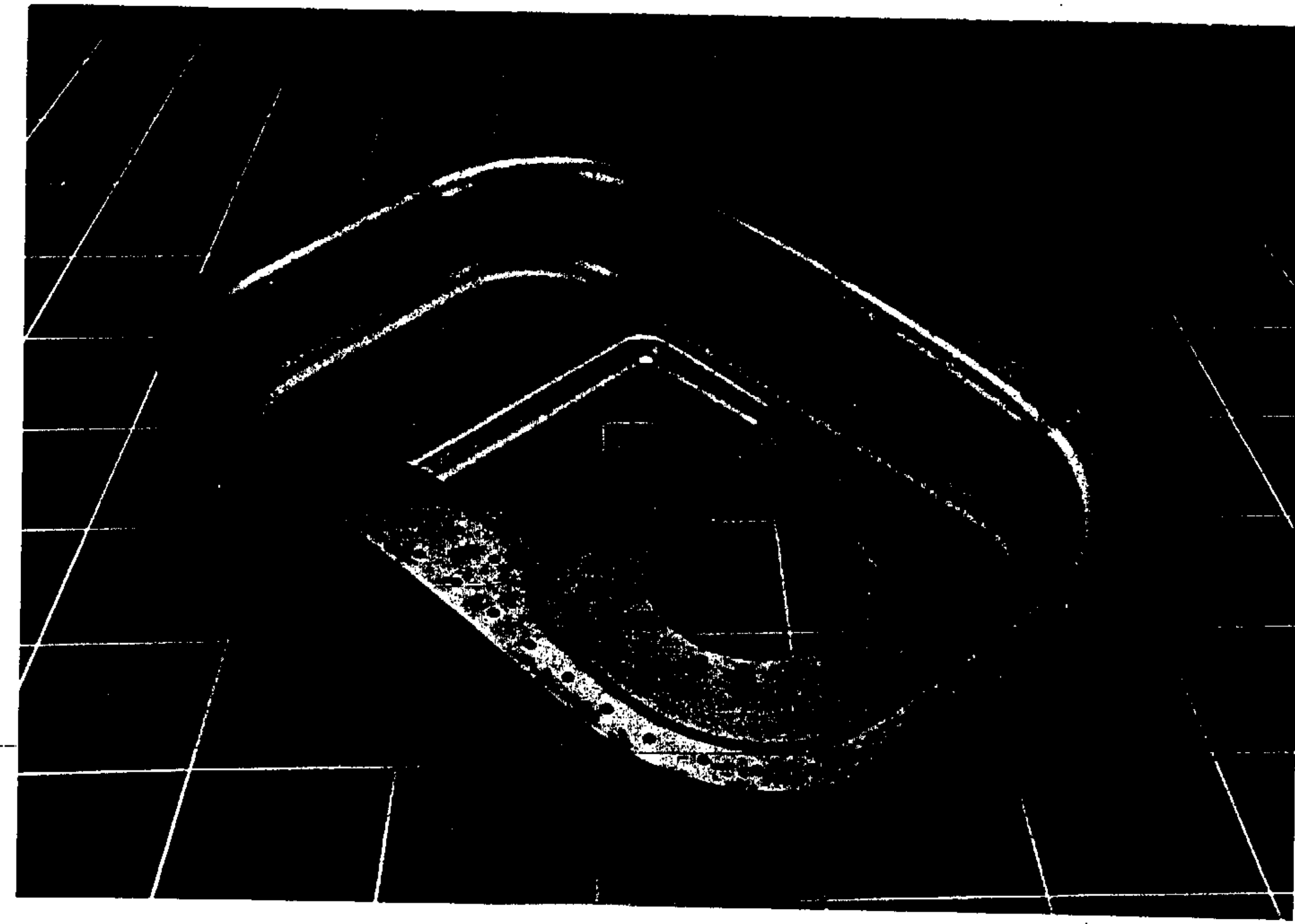

995.0889

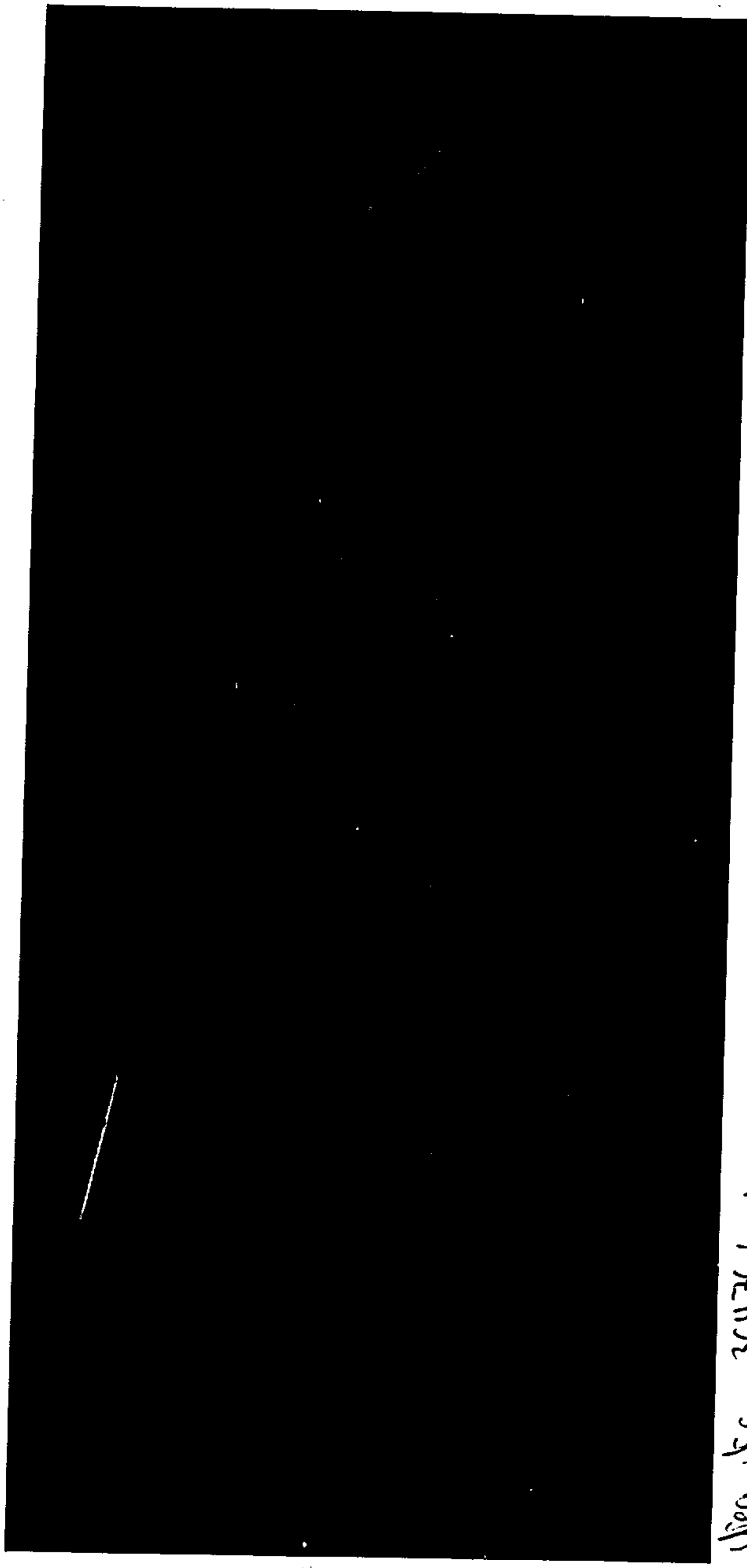

Vlieg Nr: 364761 / 1

SFF - geformte Innenversteifung Holme

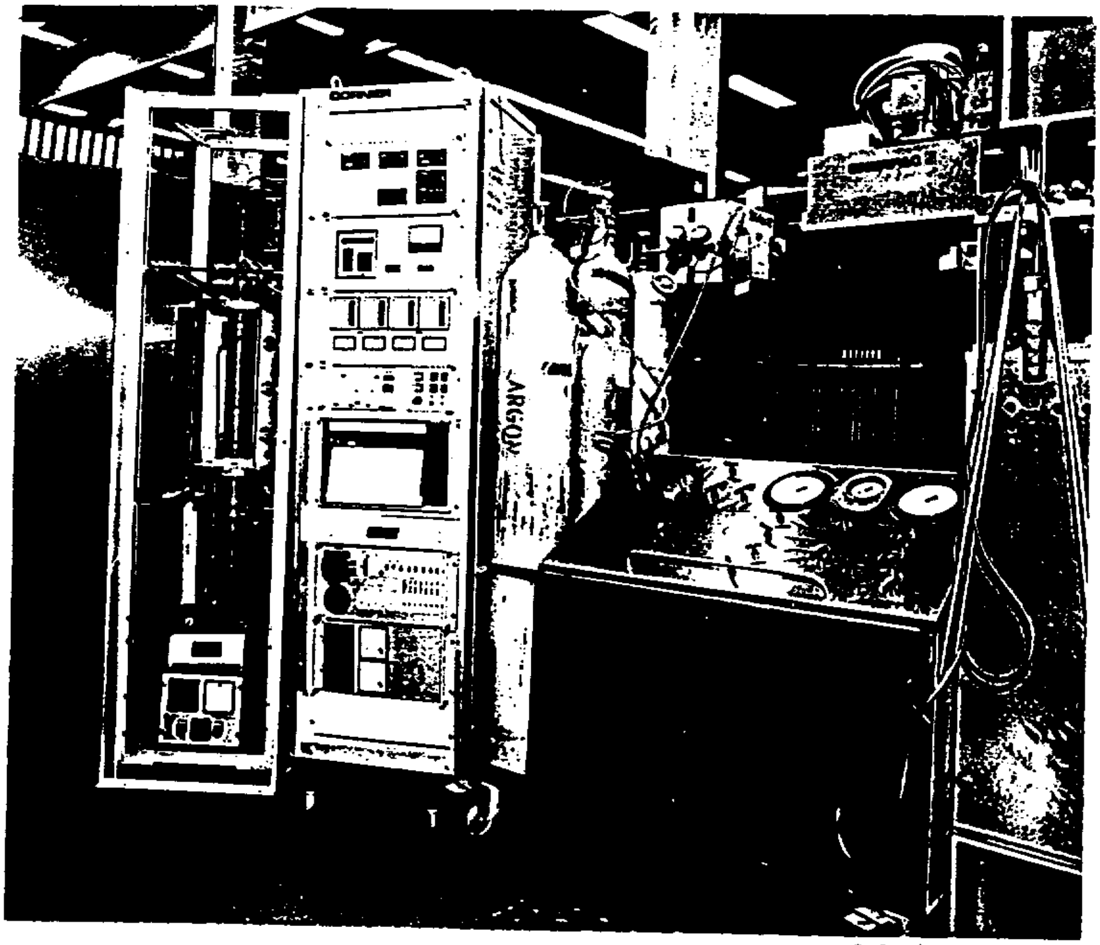

385401A

385401C

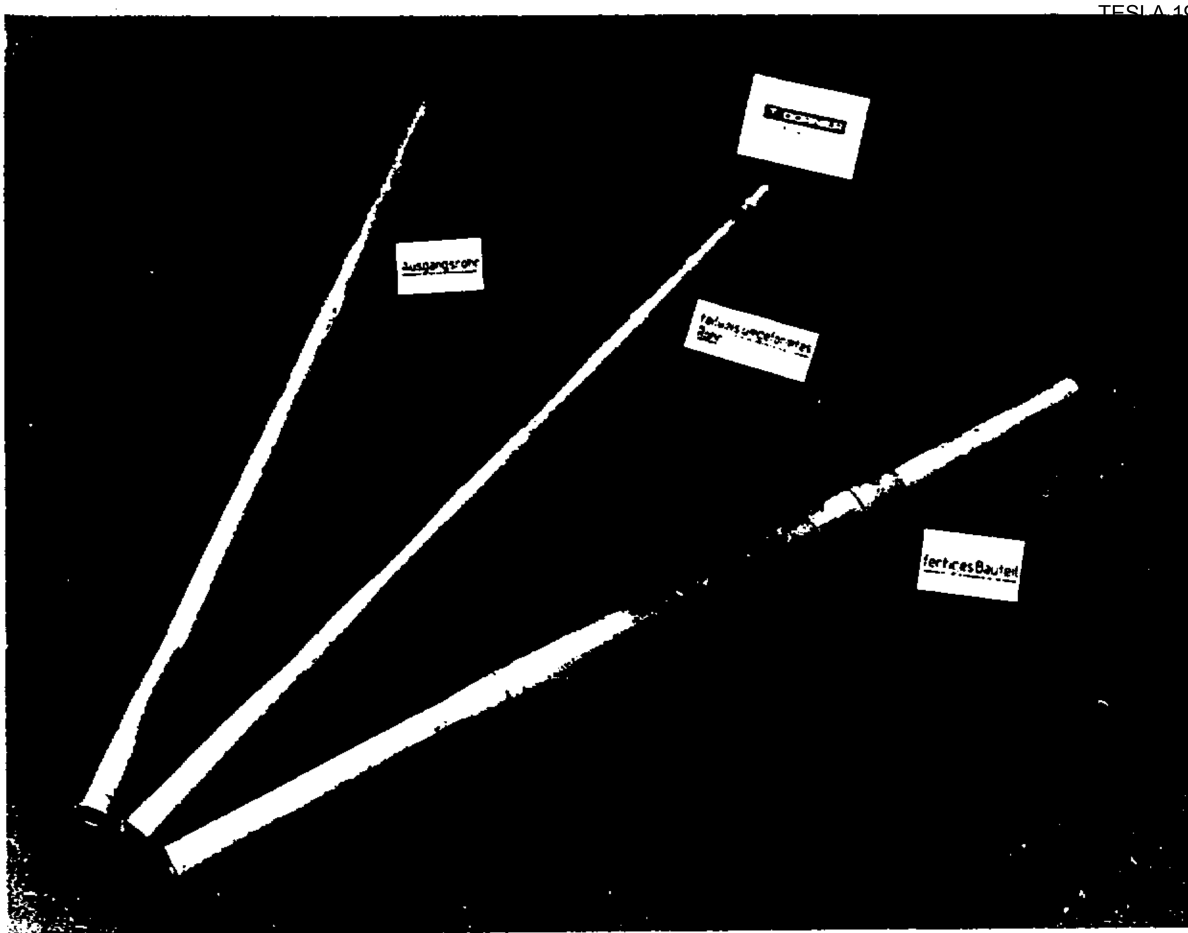
Ausgangsrohr
fertiges Bauteil

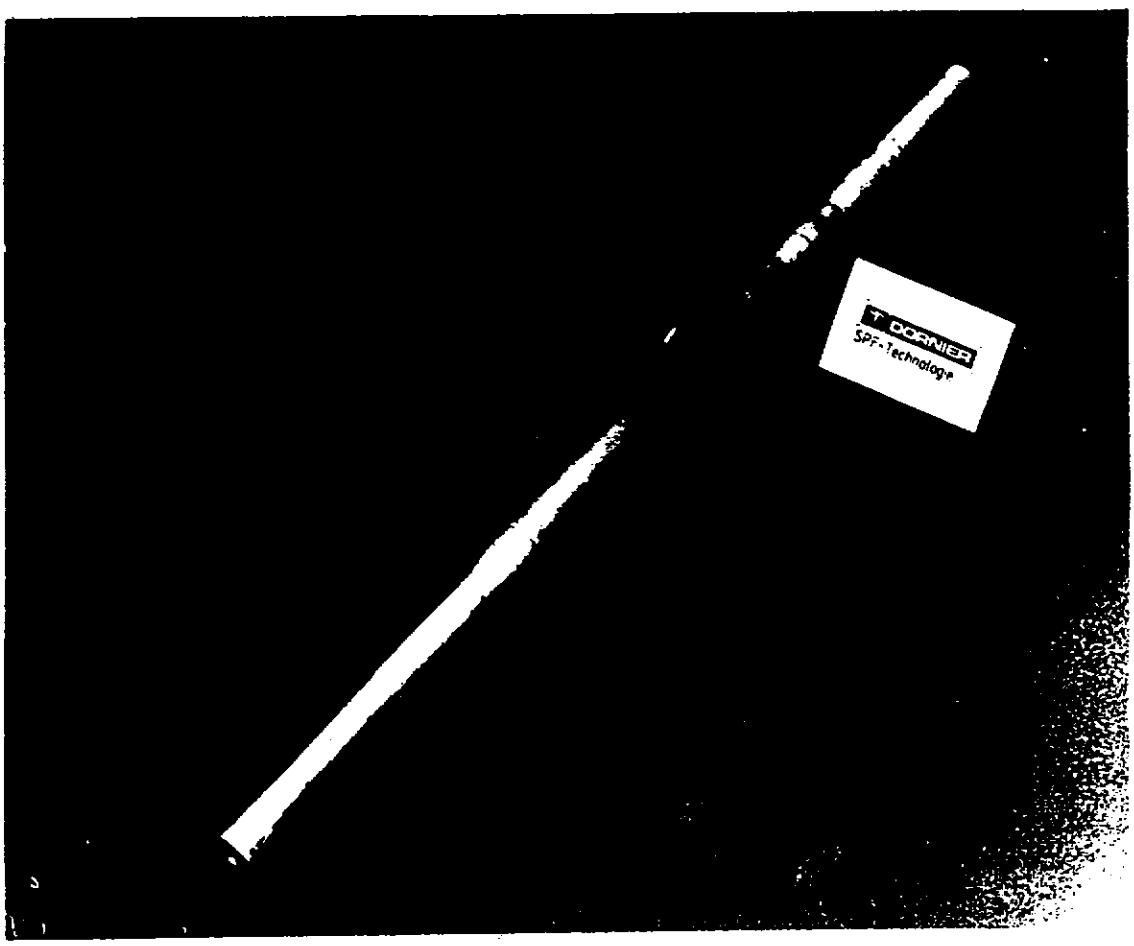
DORNIER
SPF-Technologie

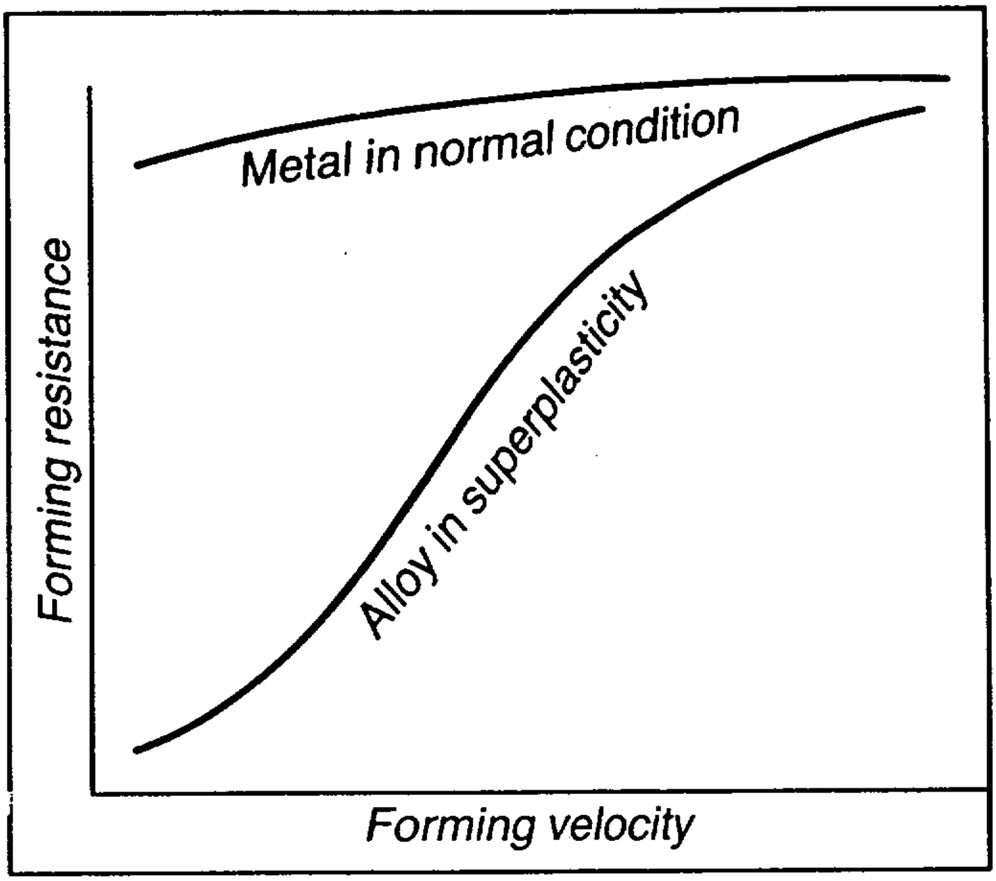

Ordinary metals show little dependance
of flow stress from forming rate.

Under certain conditions particular alloys
show “superplastic“ behaviour:

Very little force is sufficient to achieve extremely high elongations
as long as the forming velocity is low enough.

Superplasticity – a phenomenological approach

"Normal" plasticity (deformation temperature < 0.4 T_m)

$$(1) \qquad \sigma_t = k_1 \cdot \varepsilon_t^{\,n}$$

Condition for stability against local necking with subsequent fracture:

$$(2) \qquad \frac{d\sigma_t}{\sigma_t} \geq \frac{-dA}{A} = \frac{dl}{l} = d\varepsilon_t$$

From (1) and (2), the limit of uniform plastic flow is reached when

$$(3) \qquad \varepsilon_t = n$$

With n typically significantly smaller than 1, a very limited formability results.

Superplasticity – a phenomenological approach

"Super" plasticity (deformation temperature $> 0.5\,T_m$
+ special materials requirements)

$$(1) \quad \sigma_t = k_2 \cdot \dot{\varepsilon}_t^{\,m}$$

with m the "strain rate sensitivity"

For $m = 1$ (a linear viscous material), from

$$(2) \quad \dot{\varepsilon}_t = \frac{dl}{l} \cdot \frac{1}{dt} = -\frac{dA}{A} \cdot \frac{1}{dt}$$

for the change of specimen crossection A with time it follows:

$$(3) \quad \boxed{-\frac{dA}{dt} = A \cdot \dot{\varepsilon}_t = \frac{A \cdot \sigma_t}{k_2} = \frac{P}{k_2}}$$

with P the load applied to the specimen.

Therefore, independent of the local cross-section, the thinning behaviour of the specimen will be uniform over its whole length

→ no necking, very large elongations possible

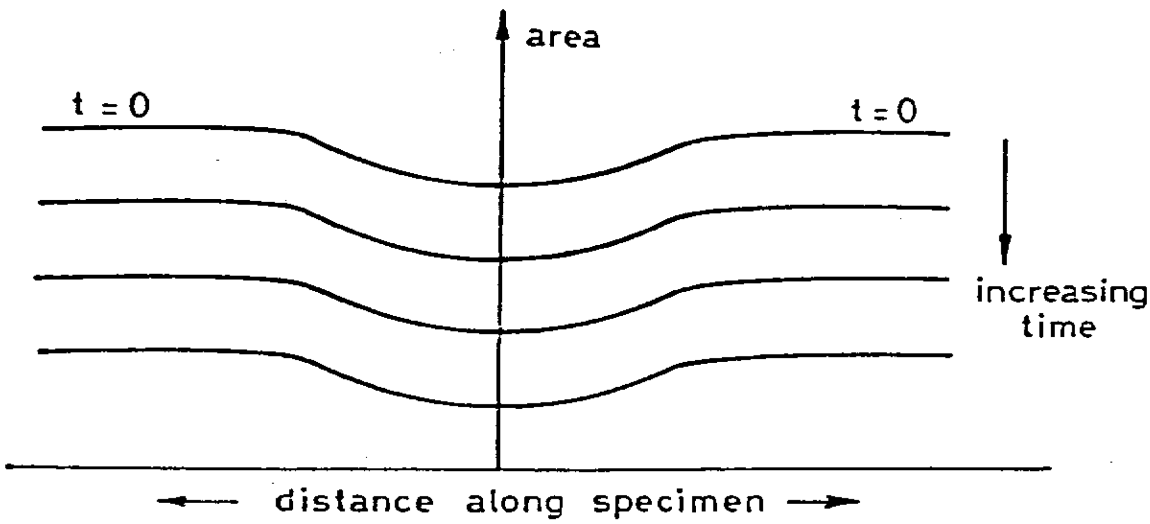

Distribution of areas in a tension bar of a viscous material

Superplasticity – an phenomenological approach

In practice the m-value of metals gets never equal to unity and the criterion for stability against necking gets therefore more complicated.

Nevertheless a clear correlation between m and the maximum elongation obtained in tension testing is experimentally well proven, and materials with a m-value of $m > 0.3$ are commonly regarded to be superplastic

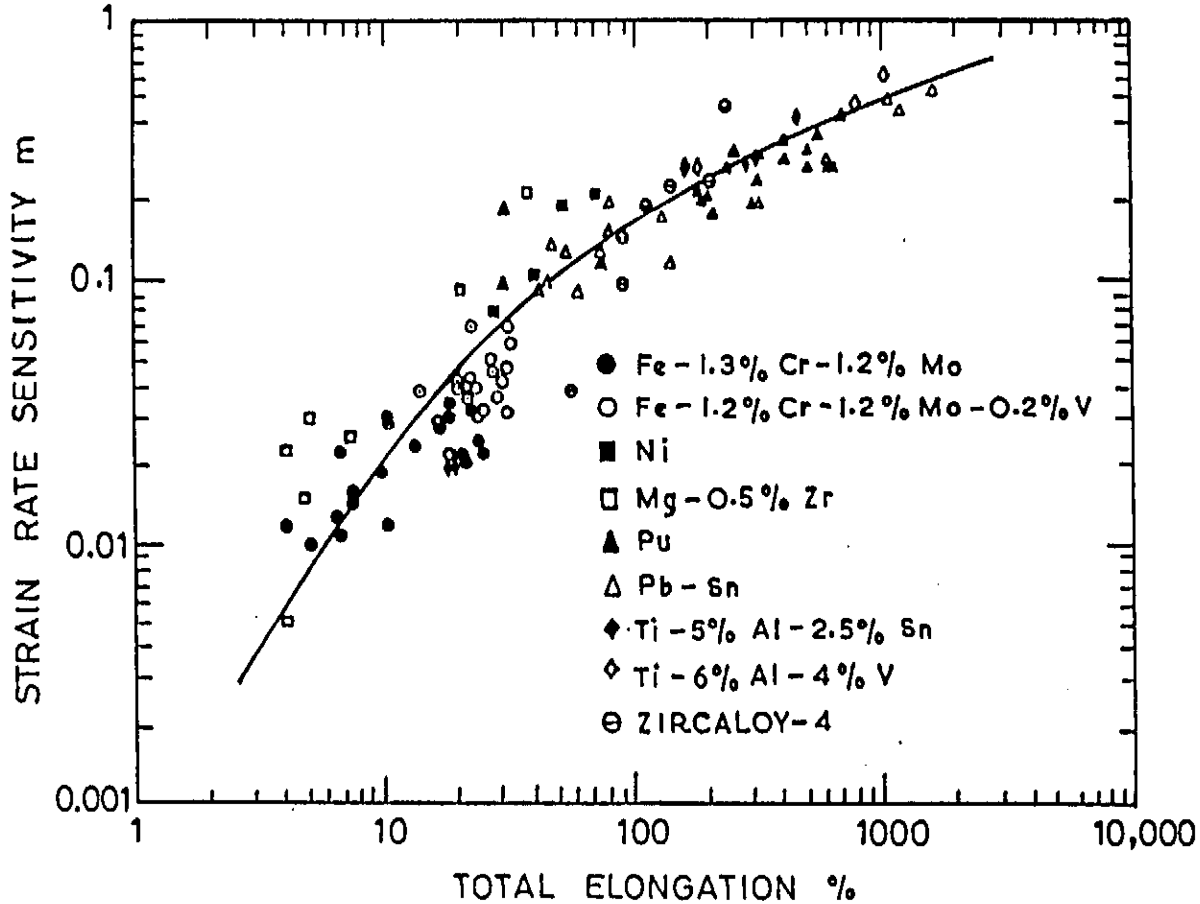

Correlation between strain-rate sensitivity and total elongation for a variety of materials (Woodford (125))

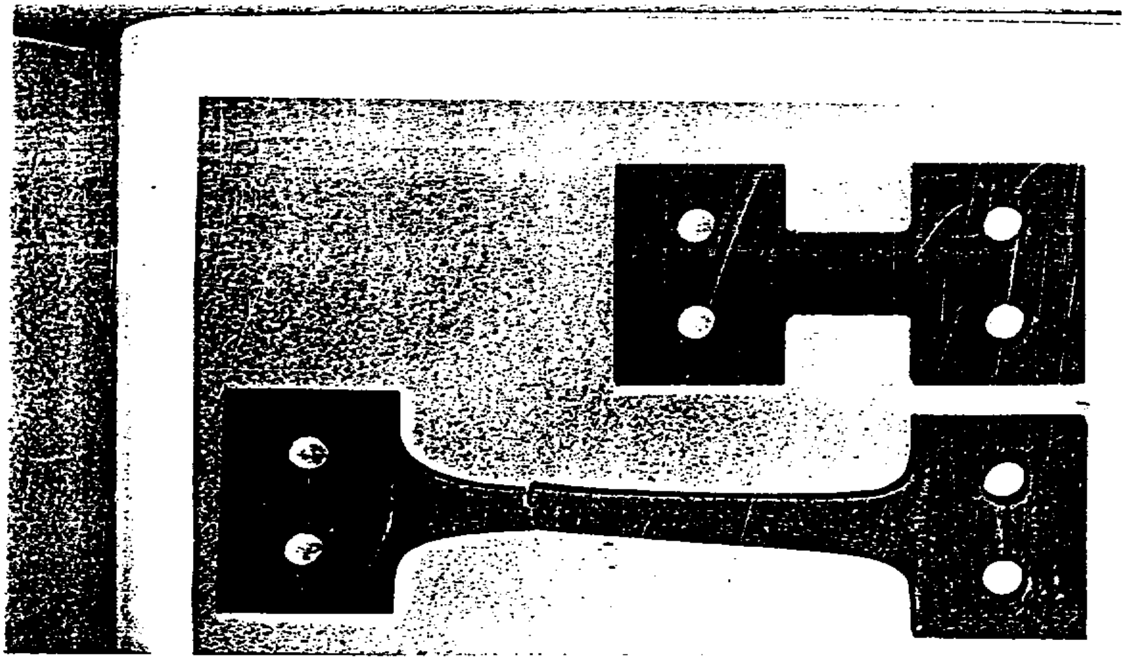

Superplasticity – an phenomenological approach

Even if a material is said to be "superplastic", it is superplastic only in a certain temperature range and in a certain strain-rate range:

The strain rate sensitivity itself is a function of the strain rate:

$$m = \frac{\partial \log \sigma_t}{\partial \log \dot{\varepsilon}_t}$$

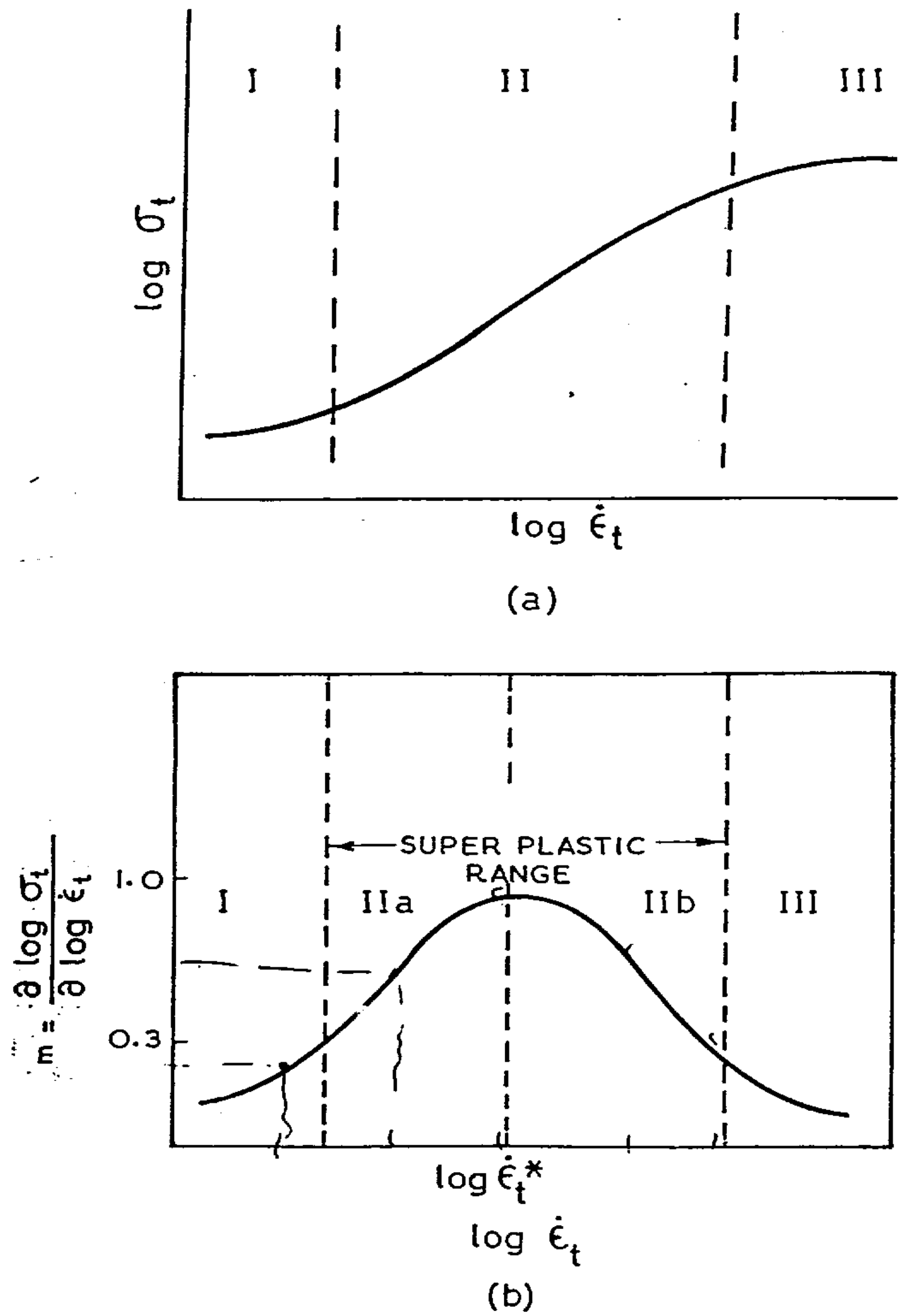

The relationship between (a) stress, σ_t, and strain rate, $\dot{\epsilon}$ and
(b) strain-rate sensitivity index, m and strain rate, for superplastic deformation (Schematic)

Determination of m-values

Three possibilities, out of many more:

1) Constant strain rate tests $\quad \dot{\varepsilon} = \frac{v}{l}$

A series of specimens is tested with each time different, but constant $\dot{\varepsilon}$. From the results, a σ - $\dot{\varepsilon}$ - curve may be plotted, from which m-values can be calculated.

2) Constant crosshead-velocity-test

results in a continues σ - $\dot{\varepsilon}$ -curve, due to continuously decreasing $\dot{\varepsilon}$. From the σ - $\dot{\varepsilon}$ - curve, m-values may be calculated.

3) Stepped strain rate testing

Suddenly increasing the crosshead velocity results in load increasements. From this, m-values can be calculated:

$$m = \frac{\ln (P_A / P_B)}{\ln (v_2 / v_1)}$$

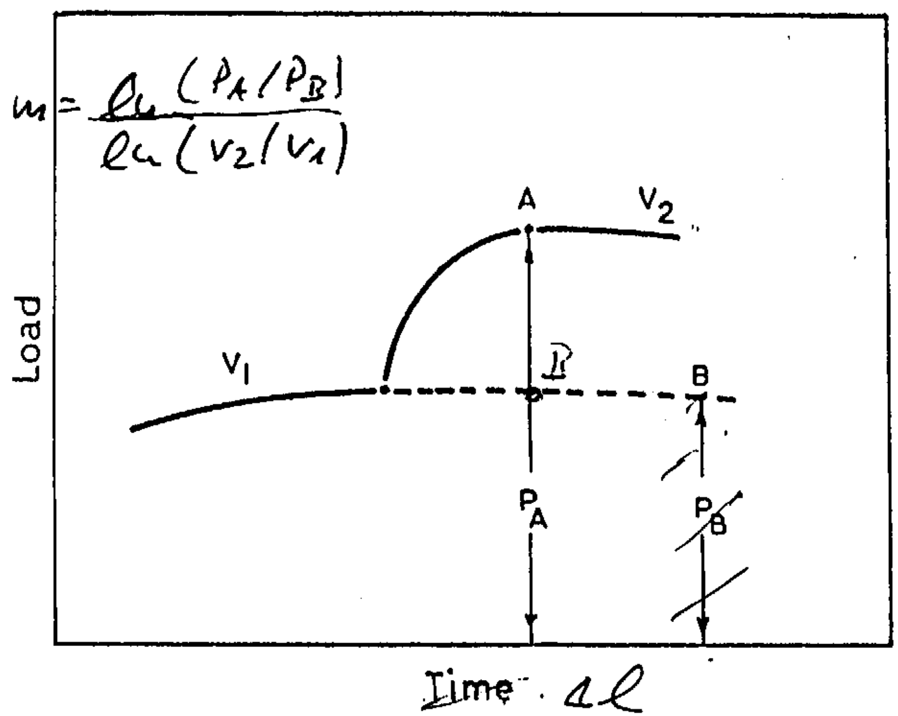

A schematic load-time diagram representing a velocity change from V_1 to V_2. Times A and B represent the same strain at the different pulling speeds (Backofen, Turner and Avery (42))

Deformation mechanisms in SPF

Deformation mechanism in cold forming:

Dislocation gliding and twinning, resulting in shear- and shape changes of the individual grains.

Deformation mechanism in SPF:

Sliding of grains relative to each other along grain boundaries without major shape changes of the grains ("grain boundary sliding").

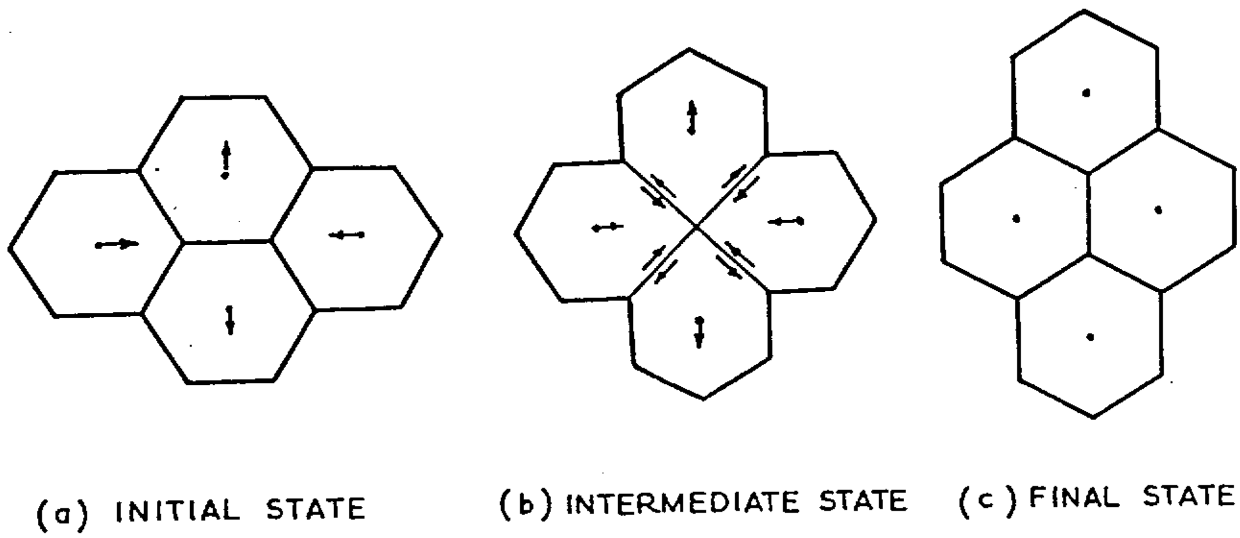

A schematic representation of the grain-switching mechanism of Ashby and Verrall. The directions of stress and relative movements between grains arrowed (Ashby and Verrall (62))

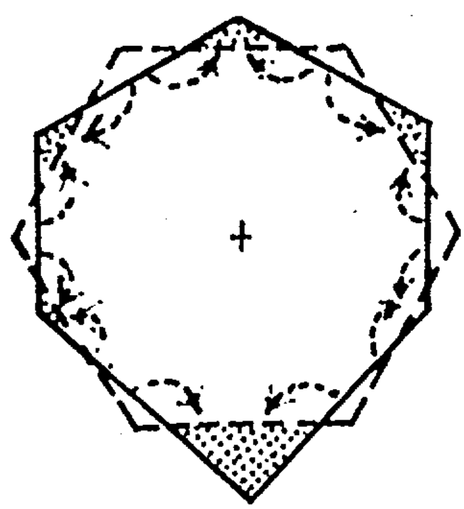

Deformation mechanisms in SPF

From the deformation mechanism:

Grain boundary sliding

with

form accommodation by diffusion

(Ashby - Verrall)

the following microstructural requirements result:

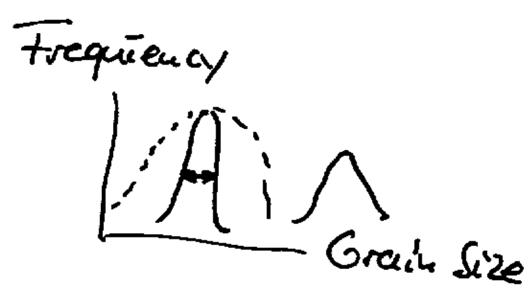

Small grain size

Unimodal and narrow grain size distribution

Stability against grain growth: two phase material; dispersoids, lamellar u.s.w.

FORMING CONDITIONS FOR SPF

FROM THE DEFORMATION MECHANISM,

GRAIN BOUNDARY SLIDING WITH
GRAIN SHAPE ACCOMODATION
MAINLY BY DIFFUSION,

THE FOLLOWING GENERAL FORMING
CONDITIONS RESULT:

- HIGH TEMPERATURE ($> 0.5 * T_m$)
- LOW STRAIN RATES ($< 10^{-3} s^{-1}$)
- LOW FLOW STRESSES ($<$ 10 MPa)

Summary: materials requirements for superplastic properties

$m > 0.3$

Grain size < ~ 10 μm and stable at working temperature.

$T > 0.5\ T_m$

Deformation mainly by grain boundary sliding

Typical strain rates: $10^{-4}\ sec^{-1}$ to $10^{-2}\ sec^{-1}$

Typical flow stresses: 2 MPa to 10 MPa

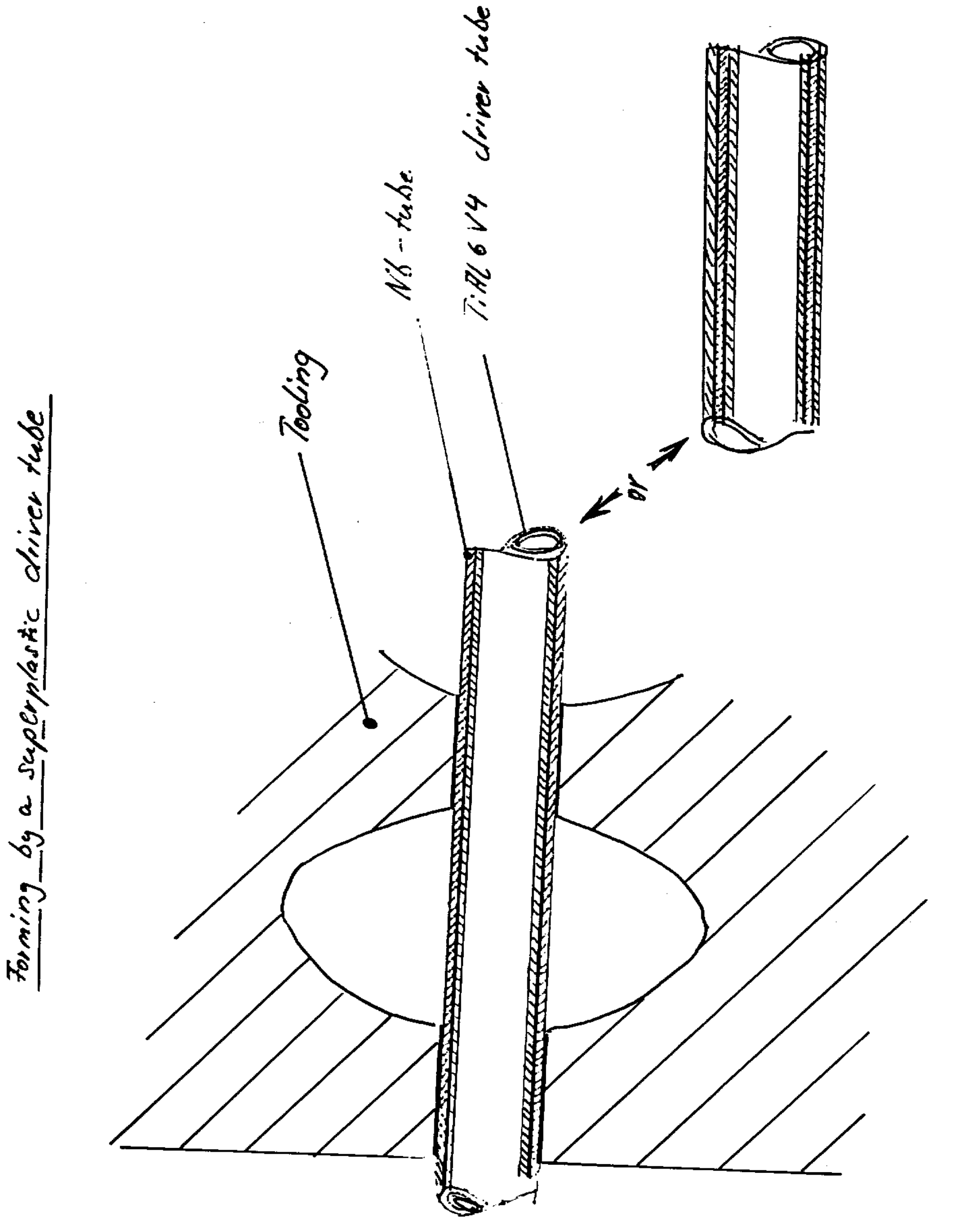
Forming by a superplastic driver tube
Tooling
Nb-tube
TiAl6V4 driver tube
or

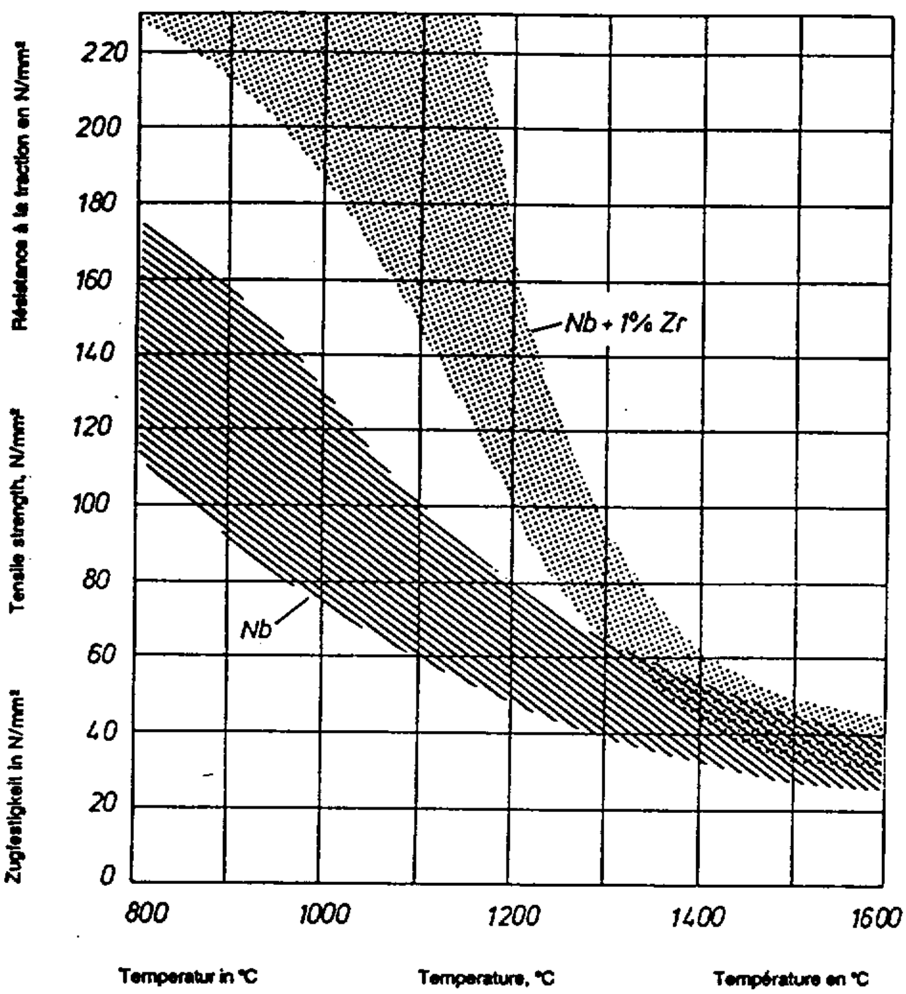

Fig. 1: Die Zugfestigkeiten von reinem Niob und der Nioblegierung Nb1Zr in Abhängigkeit von der Temperatur

Fig. 1: Tensile strengths of pure niobium and of the niobium alloy Nb1Zr versus temperature

Fig. 1: Résistances à la traction de niobium et de l'alliage Nb1Zr en fonction de la température

MECHANICAL PROPERTIES OF HIGH RRR Nb

Cavity Fabrication Techniques Workshop
DESY
March 6-8, 1995

M. G. RAO

and

P. KNEISEL

CEBAF High RRR Nb Data Base

Mechanical & Thermal Properties

- Fansteel } USA
- Teledyne } USA
- Cabot } USA
- Heraeus — Germany
- Chinese
- Russian
- Ukranian
- Brazilian } To be investigated
- Japanese } To be investigated

Overview

- Introduction to the uniaxial tensile measurements
- Description of the apparatus
- Discussion of typical stress-strain curves
- Definition of yield strength, ultimate tensile strengths
- Discussion of strain rate; slow - fast
- Presentation of the CEBAF data base
    - room temperture measurements
    - low temperature data
- Summary

TEST MACHINE

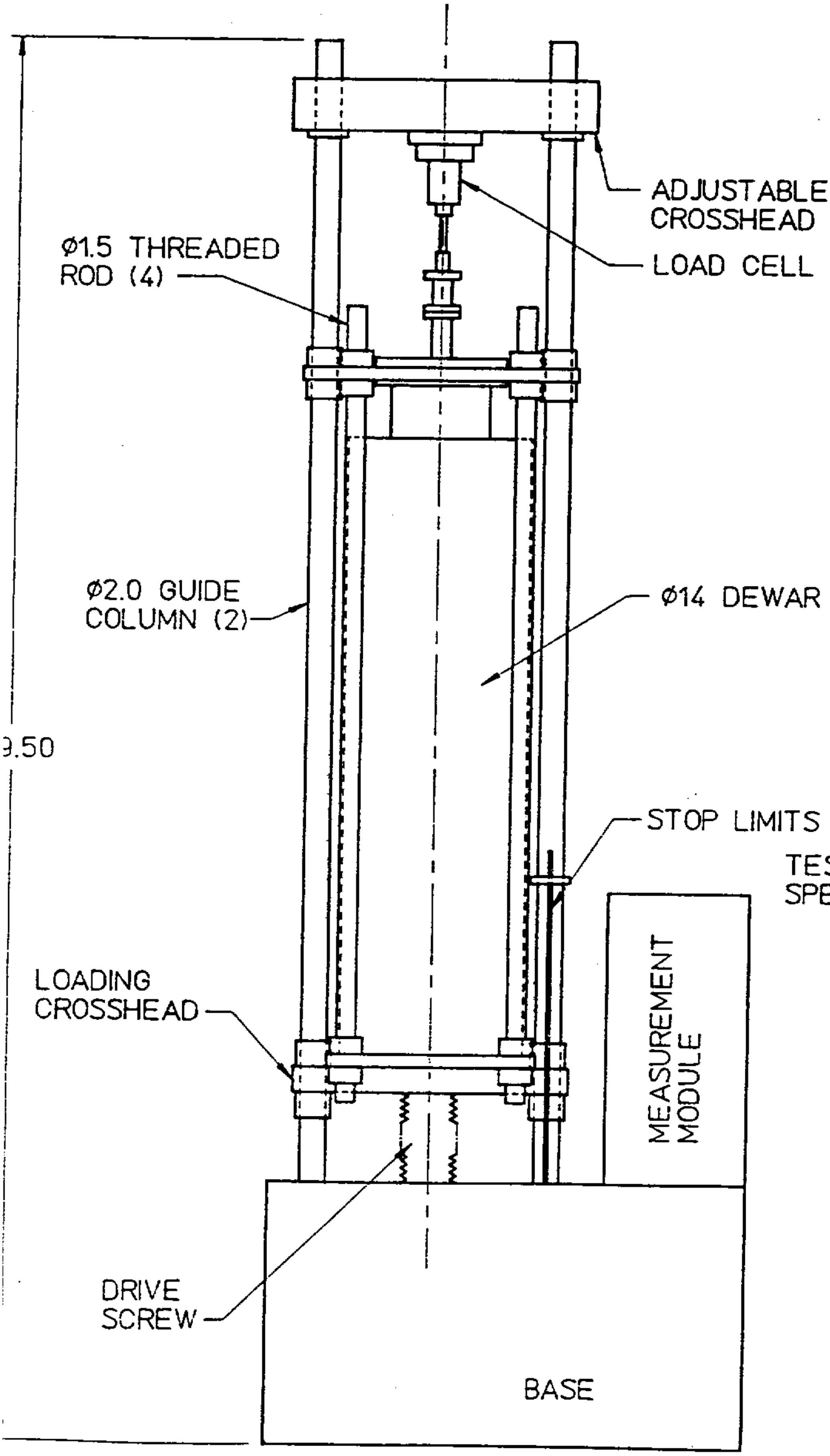

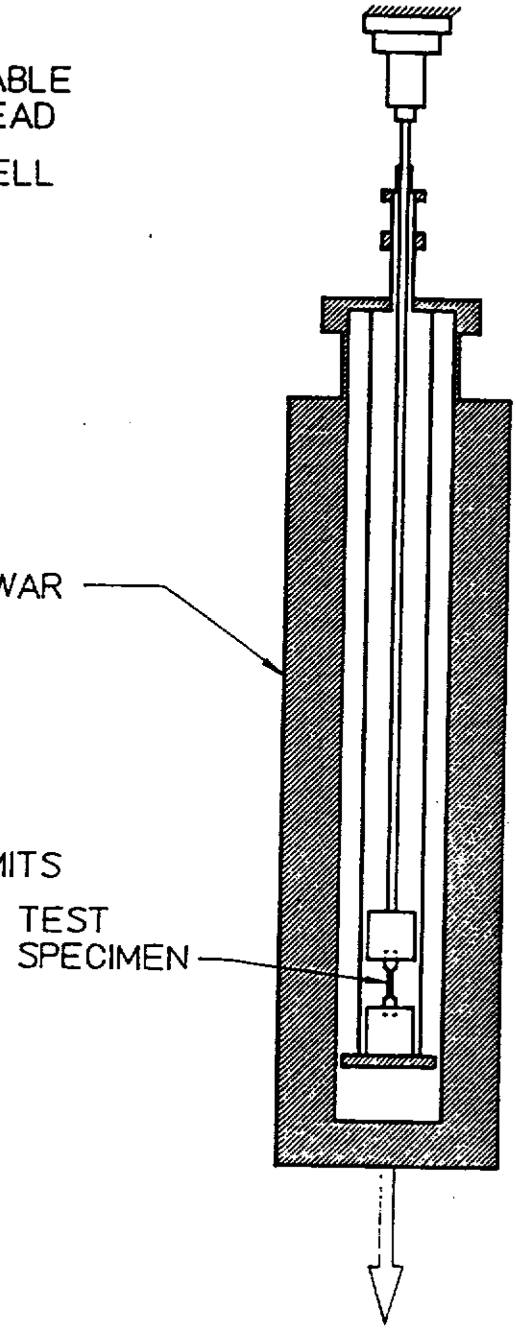

TENSILE TEST SCHEMATIC

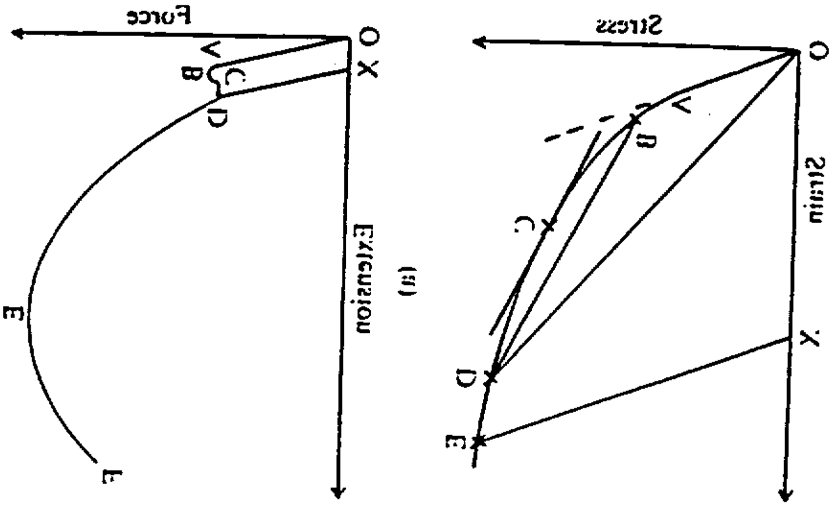

Fig. 1 (a) Schematic force-extension curve; (b) schematic stress-strain curve for small strains illustrating various moduli: 0A = Young's modulus, BD = chord modulus, C = tangent modulus, OD = secant modulus, A = limit of proportionality, and E = proof stress

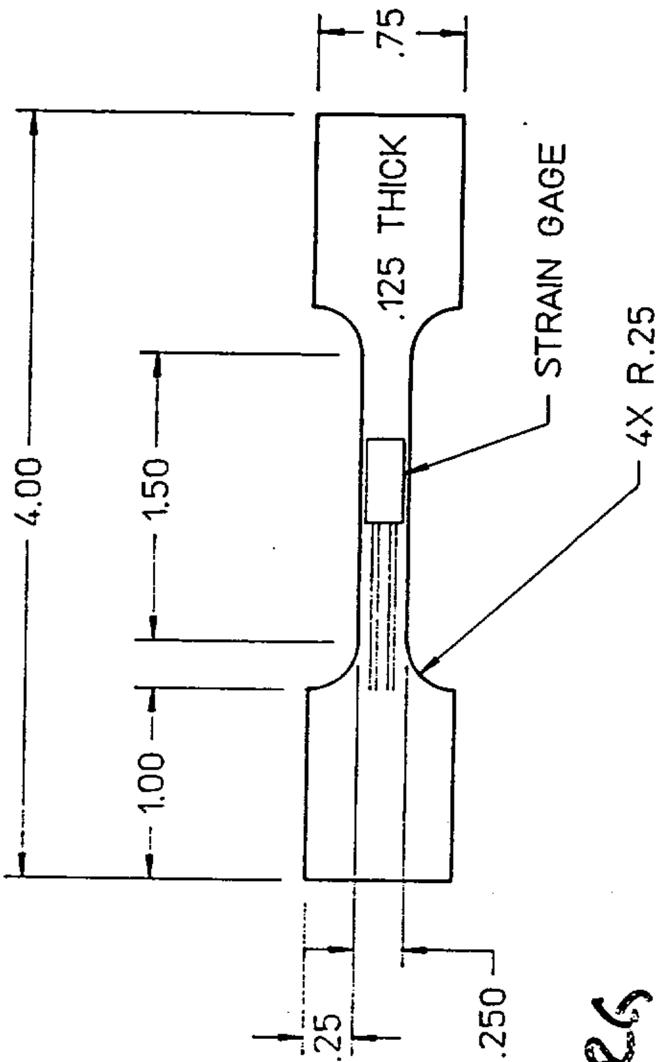

$$K = \frac{\Delta R / R_G}{\Delta L / L}$$

$$\epsilon = \frac{\Delta R}{K R_G}$$

$$\frac{1 \times 10^{-6}}{2\%}$$

Appendix II

Conversion Table for the Units Most Commonly Used to Measure Stress or Pressure*

	10^3 psi (1 ksi)	1 kg/mm²	1 ton/in.²	1 MN/m²	1 dyne/cm²	1 bar	1 atm
10^3 psi (1 ksi)	1	0.7031	0.4464	6.895	68.95×10^6	68.95	68.03
1 kg/mm²	1.422	1	0.6349	9.807	98.07×10^6	98.07	96.81
1 ton/in.²	2.240	1.575	1	15.44	154.4×10^6	154.4	152.4
1 MN/m²	0.1450	0.1020	64.75×10^{-3}	1	10×10^6	10	9.869
1 dyne/cm²	14.50×10^{-9}	10.20×10^{-9}	6.475×10^{-9}	0.1×10^{-6}	1	10^{-6}	0.9869×10^{-6}
1 bar	14.50×10^{-3}	10.20×10^{-3}	6.475×10^{-3}	0.1	10^6	1	0.9869
1 atm	14.70×10^{-3}	10.33×10^{-3}	6.562×10^{-3}	0.013	1.013×10^6	1.013	1

* 1 psi ≡ 1 lb/in.² ≡ one pound force per square inch; 1 kg/mm² ≡ one kilogram force per square millimeter; 1 ton/in.² ≡ one ton force per square inch; 1 MN/m² ≡ one meganewton per square meter; 1 dyne/cm² ≡ one dyne per square centimeter; 1 atm ≡ one standard atmosphere (≡ 760 mm Hg at 0°C, ≡ 29.92 in. Hg at 0°C).

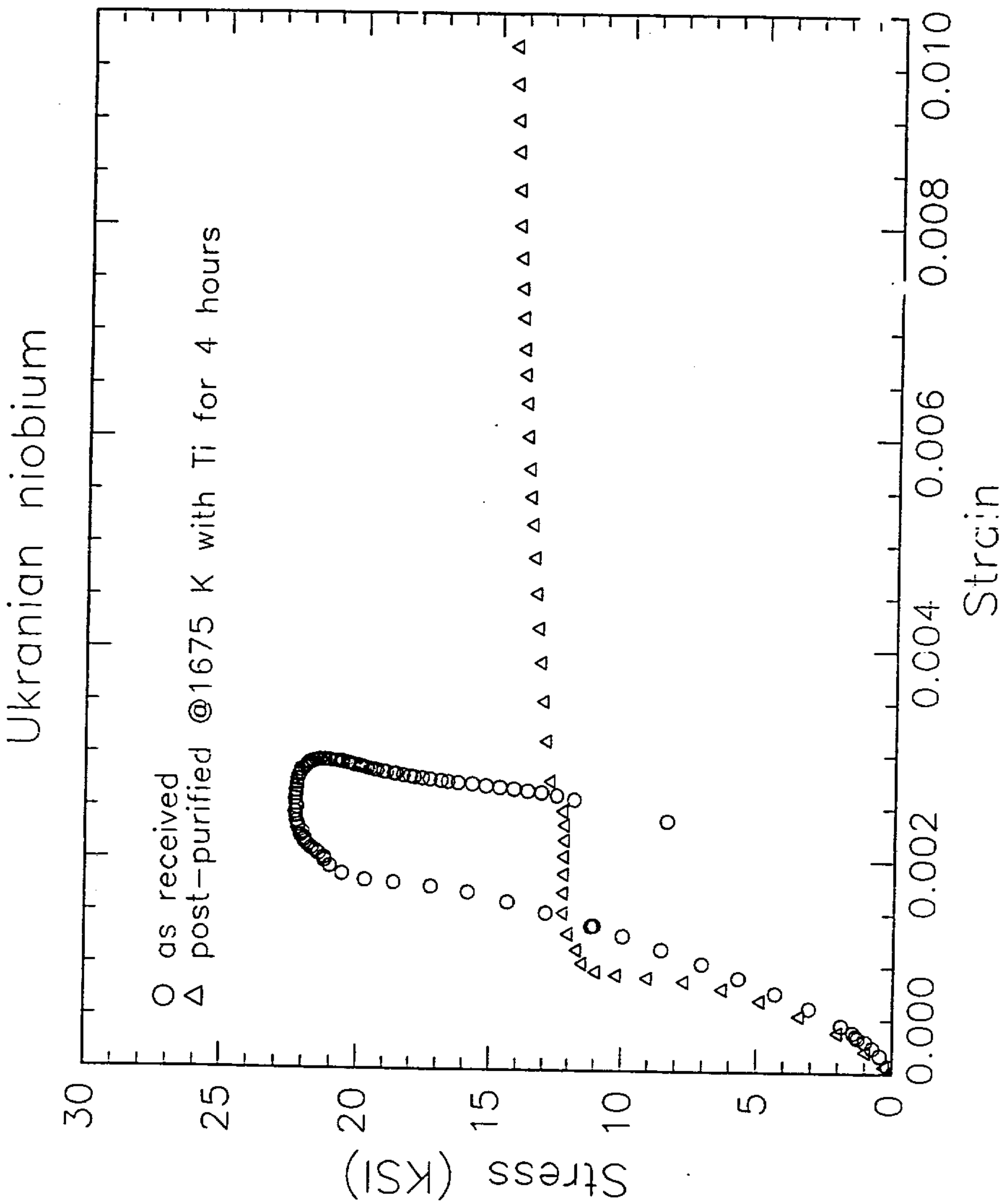
Ukranian niobium
as received
post-purified @1675 K with Ti for 4 hours
Stress (KSI)
0
5
10
15
20
25
30
Strain
0.000
0.002
0.004
0.006
0.008
0.010

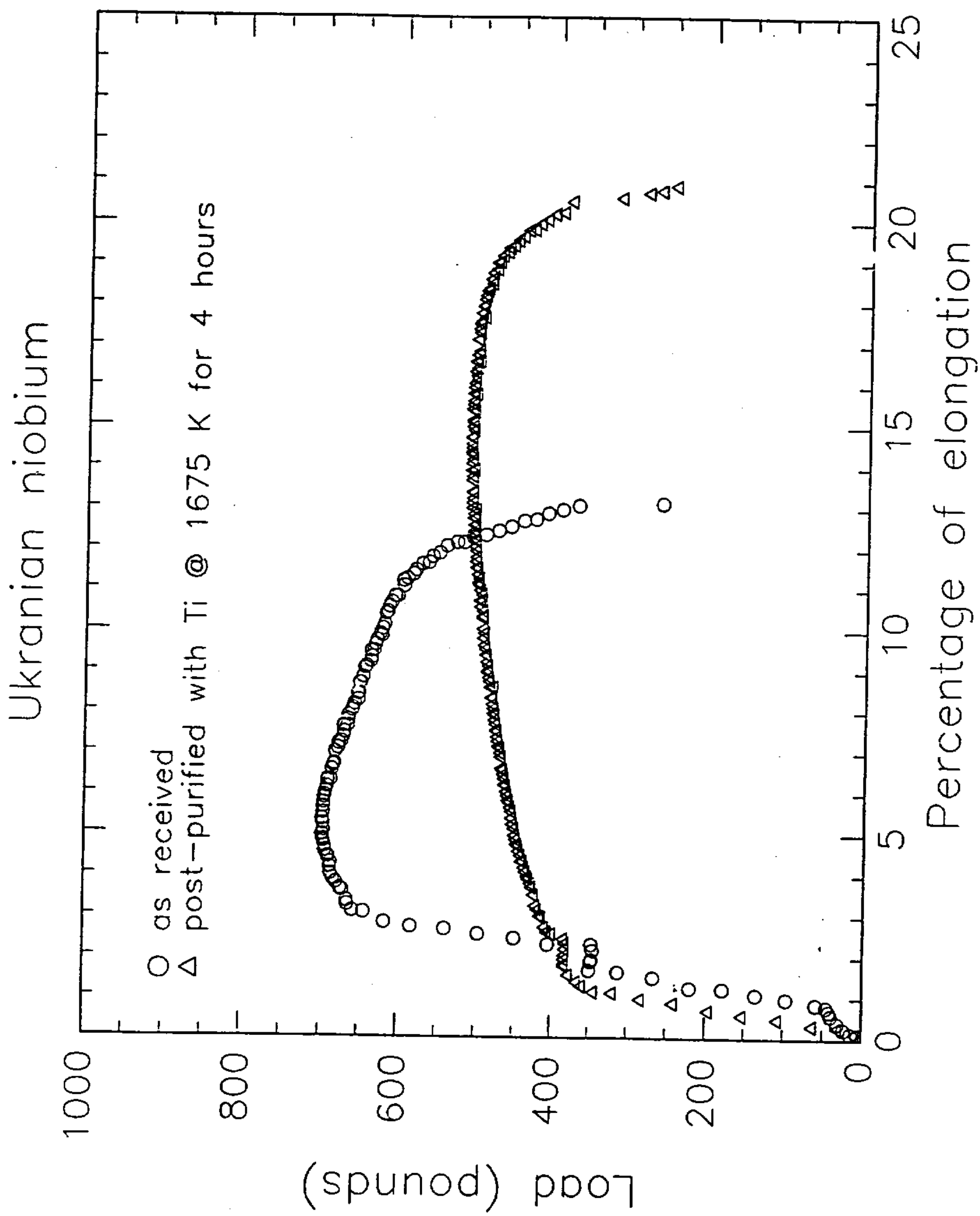
Ukranian niobium
○ as received
△ post-purified with Ti @ 1675 K for 4 hours
Load (pounds)
0
200
400
600
800
1000
Percentage of elongation
0
5
10
15
20
25

Summary of Ukrainian Nb

Status of the material	Yield Strength KSI	Tensile Strength KSI	% of Elongation
As received	21	22.8	14
Post purified @ 1675 K for 4h	13	16.7	22

Mechanical Properties of Chinese Niobium

(*Measurements done at Peking University)

Sample #	Tensile Strength [kg/mm^2]			Yield Strength [kg/mm^2]			Elongation [%]		
	as received		post-purified	as received		post-purified	as received		post purified
2	15.3*	16.5	13.74	5.5*	7.5	7.0	54*	52	34
3		21.6	13.84		11.5	8.0		42	22
4	16.5*			6.8*			54.4*		

CEBAF Cold RF Window Frame Nb Tensile Properties at 295 K (Cabot Nb)

Sample #	Yield Strength (KSI)	Tensile Strength (KSI)	% of Elongation
1	28	29.3	26.4
2	19	26.8	33
3	11	23.7	54.1

CEBAF SRF Cavity Flanges Nb Tensile Properties at 295 K (Cabot Nb)

Sample #	Yield Strength (KSI)	Tensile Strength (KSI)	% of Elongation
1	20.6	30.7	39.6
2	20.3	30.9	39.6
3	19.2	29.9	41.2

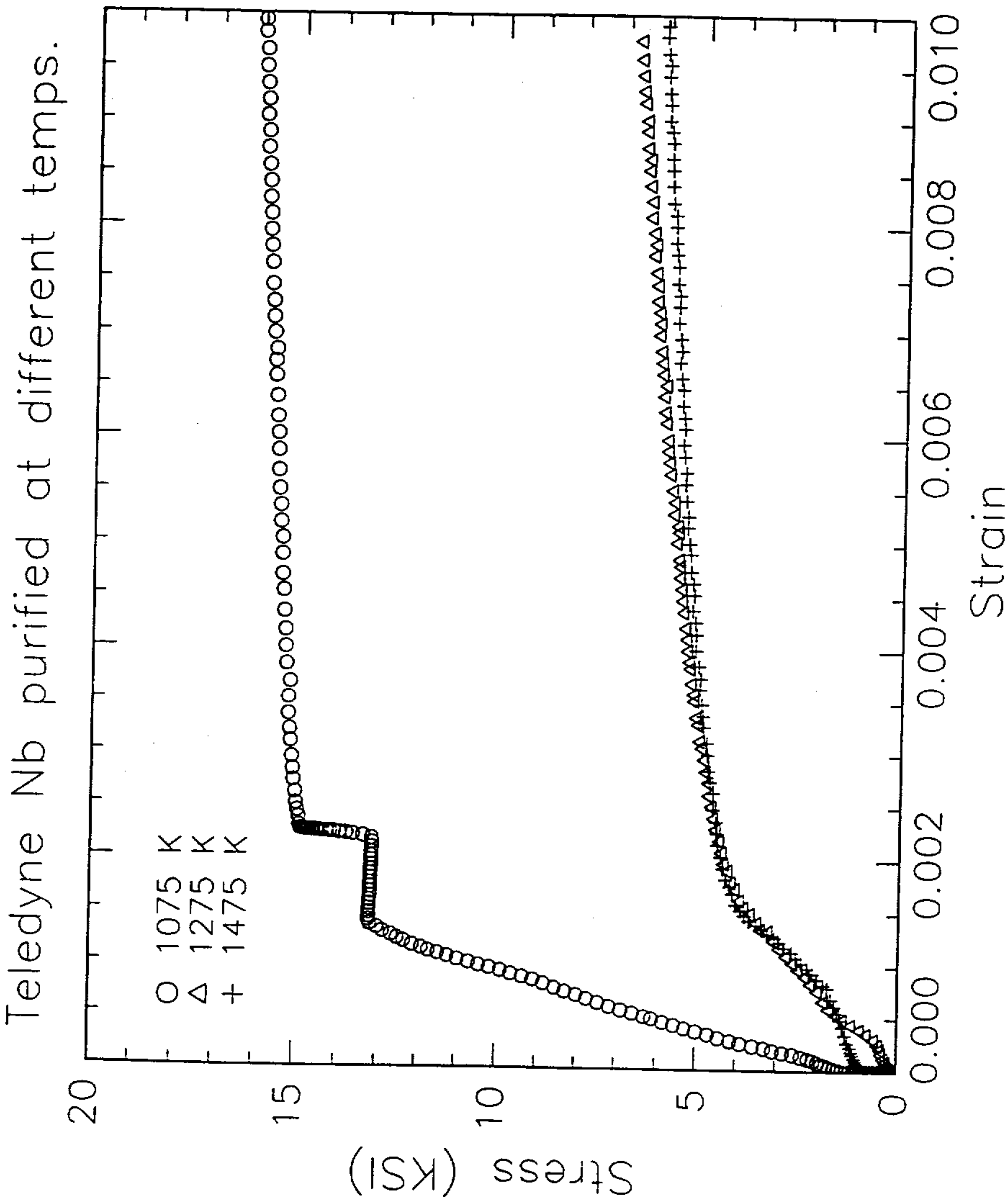
Teledyne Nb purified at different temps.
O 1075 K
Δ 1275 K
+ 1475 K
Stress (KSI)
Strain
0
5
10
15
20
0.000
0.002
0.004
0.006
0.008
0.010

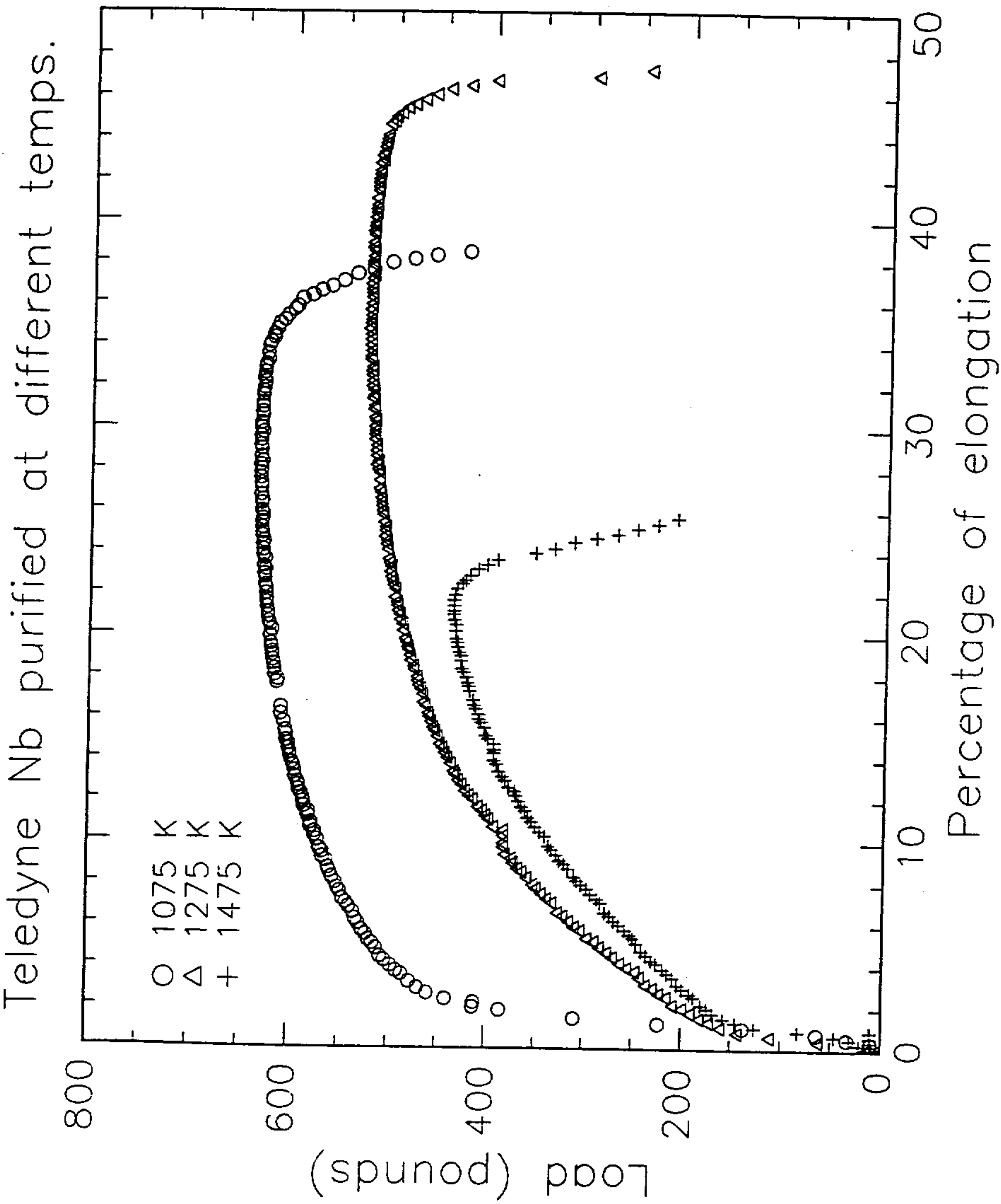
Teledyne Nb purified at different temps.
○ 1075 K
△ 1275 K
+ 1475 K
Load (pounds)
0
200
400
600
800
0
10
20
30
40
50
Percentage of elongation

Summary of Teledyne Nb Post-Purified at Different Temperatures for 2h

Purfication Temperature K	Yield Strength KSI	Tensile Strength KSI	% of Elongation
1075	15.5	20.4	40.0
1275	5.5	17.3	49.0
1475	5.0	13.8	28.3

Summary of Teledyne Nb Post-Purified for Different Times at 1675 K

Purification Time h	RRR	Yield Strenght KSI	Tensile Strength KSI	% of Elongation
1	700	4.6	12.8	28
2	670	5.5	14.8	38
4	1060	6.0	14.0	26
6	1295	6.0	13.8	26

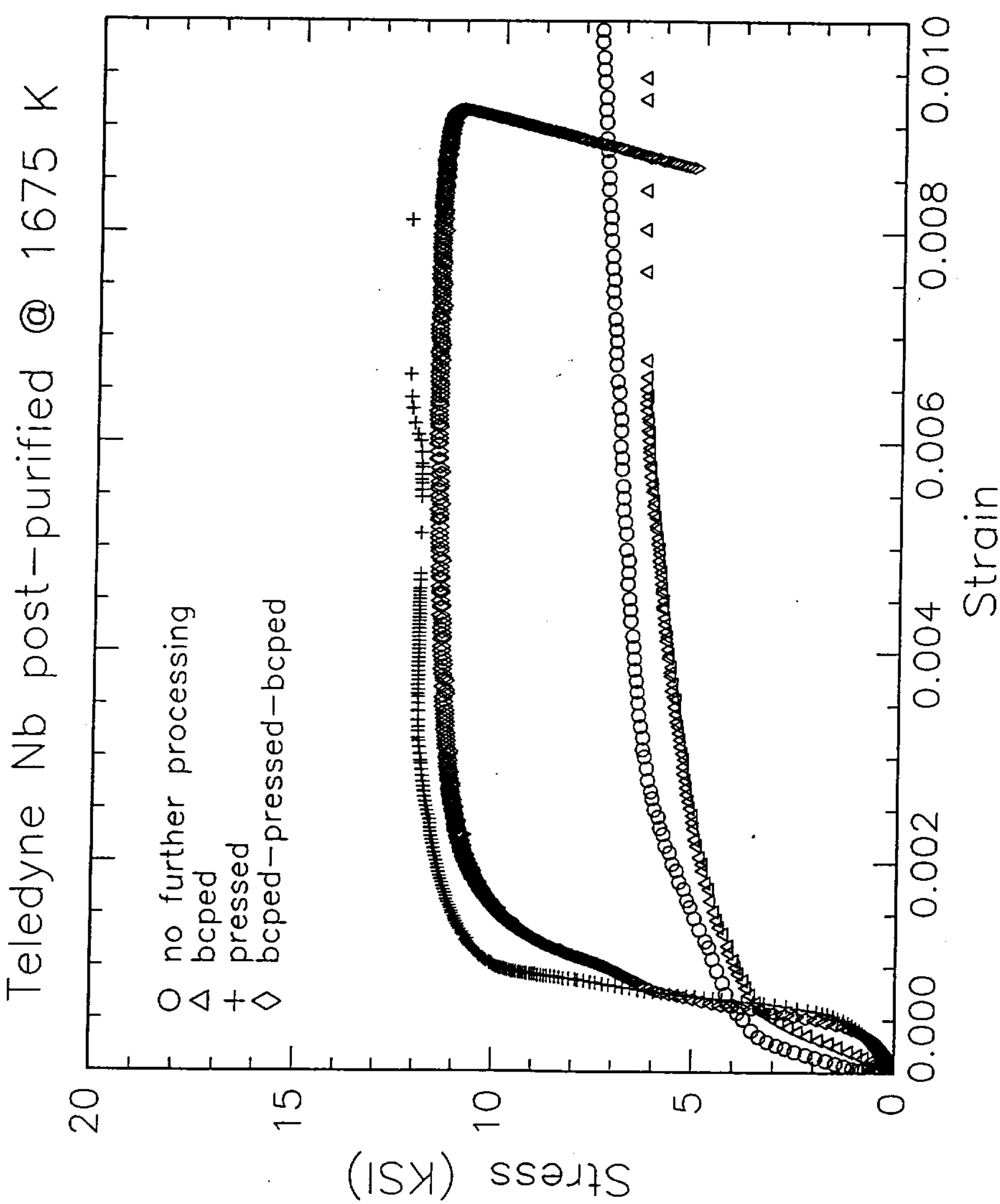
Teledyne Nb post-purified @ 1675 K
O no further processing
Δ bcped
+ pressed
◇ bcped-pressed-bcped
Stress (KSI)
0
5
10
15
20
Strain
0.000
0.002
0.004
0.006
0.008
0.010

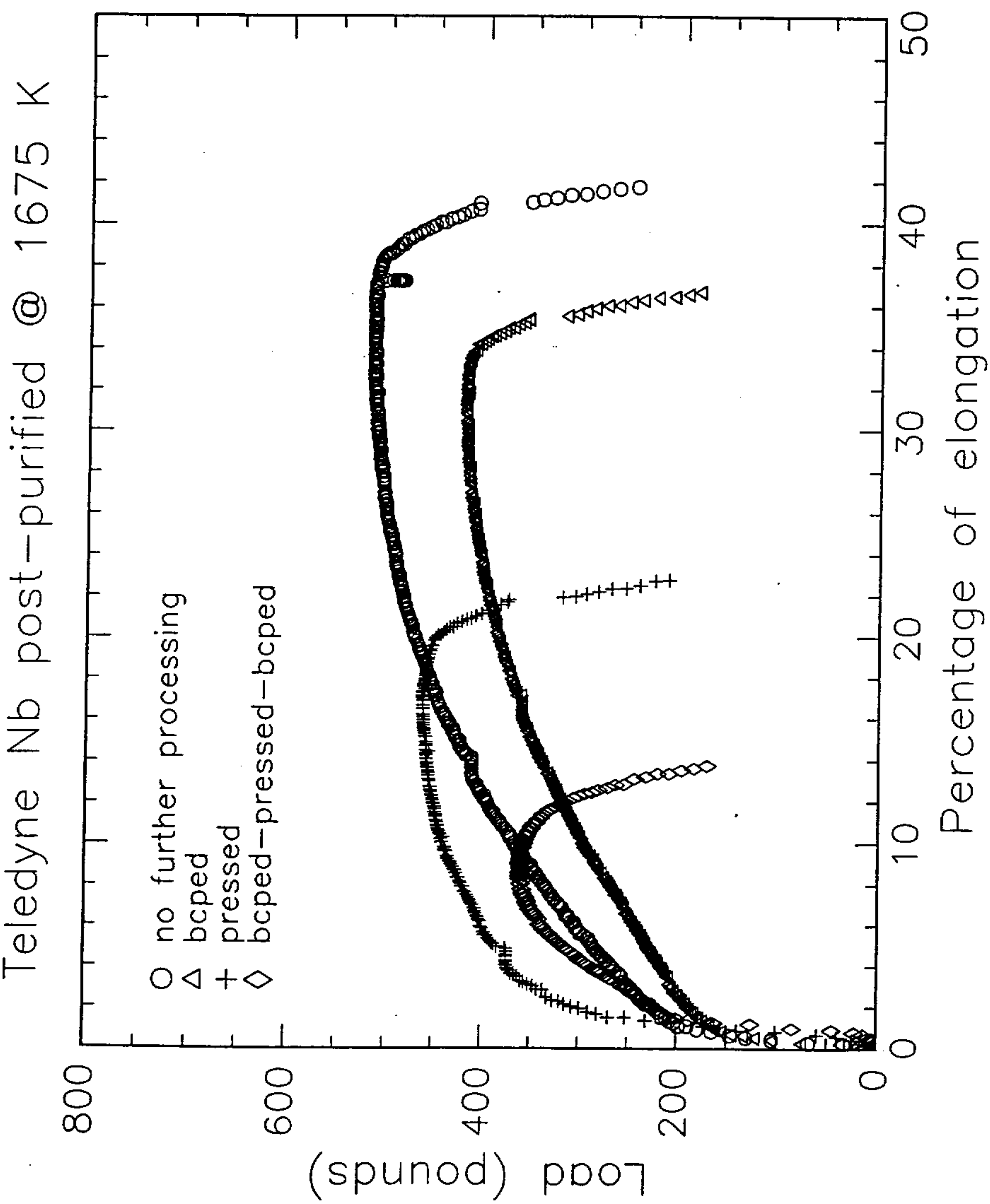
Teledyne Nb post-purified @ 1675 K
○ no further processing
△ bcped
+ pressed
◇ bcped-pressed-bcped
Load (pounds)
0
200
400
600
800
Percentage of elongation
0
10
20
30
40
50

Summary of Post-Purified (1675 K for 4h) Teledyne Nb

Status of the material	Yield Strentgh KSI	Tensile Strength KSI	% of Elongation
No futher processing	6	16.8	42
Bcped	5	13.6	37
Pressed	12	15.2	23
Bcped - pressed - bcped	11.5	11.5	14

TABLE 2
SUMMARY OF TENSILE PROPERTIES OF THE TESLA Nb†
(Thickness = 1.59 mm)

Niobium	At 293K YS (MPa)	At 293K TS (MPa)	% Elongation	At 4.2K YS (MPa)	At 4.2K TS (MPa)	% Elongation
As received	165	186	42	896	903	>1
Heat treated with Ti at 1400° for 4 h	102	128	30.2	—*	779	15.2
Welded & heat treated with Ti at 1400° C for 4 h	79	115	25.6	—*	807	6.6

†Samples were provide by Cornell University

*Serration started before reaching 0.2% offset yield

105

TABLE I
TENSILE TESTS OF NIOBIUM

SAMPLE	0.2% YIELD STRESS #/in^2	PROPOR LIMIT #/in^2	% ELONGATION	ULTIMATE TENSILE STRENGTH #/in^2
1	6310	3000	--	22410
2	6550	2500	50	23310
3	6300	2000	50	23410
4H	6450	4000	45	18330
5H	--	--	--	---
6H	6440	4400	--	15450
7HC	5970	2300	26	14720
8HC	5890	3000	47	19450
9HC	5780	1800	38	14960
10C	5790	2100	50	21880
11C	5780	2000	45	21710
12C	5500	2000	50	21230
21	5630		41	22100
22	5420		39	21390
23	5410		38	22370
24H	5370		35	14240
25H	6230		29	15590
26H	5580		32	16150
27HC	5000		28	14880
28HC	6230		29	15040
29HC	--		---	---
30C	4850		43	21130
31C	5080		44	21650
32C	--		---	---
33 ⊥	7980		33	23440
34 ⊥	5910		43	22900
35 ⊥	6210		27	24010
36H⊥	6560		28	15640
37H⊥	6710		19	16560
38H⊥	6030		19	16790
AVERAGES				
as-delivered	6000	2270	43	22350
heat-treated	5950	3100	31	15980

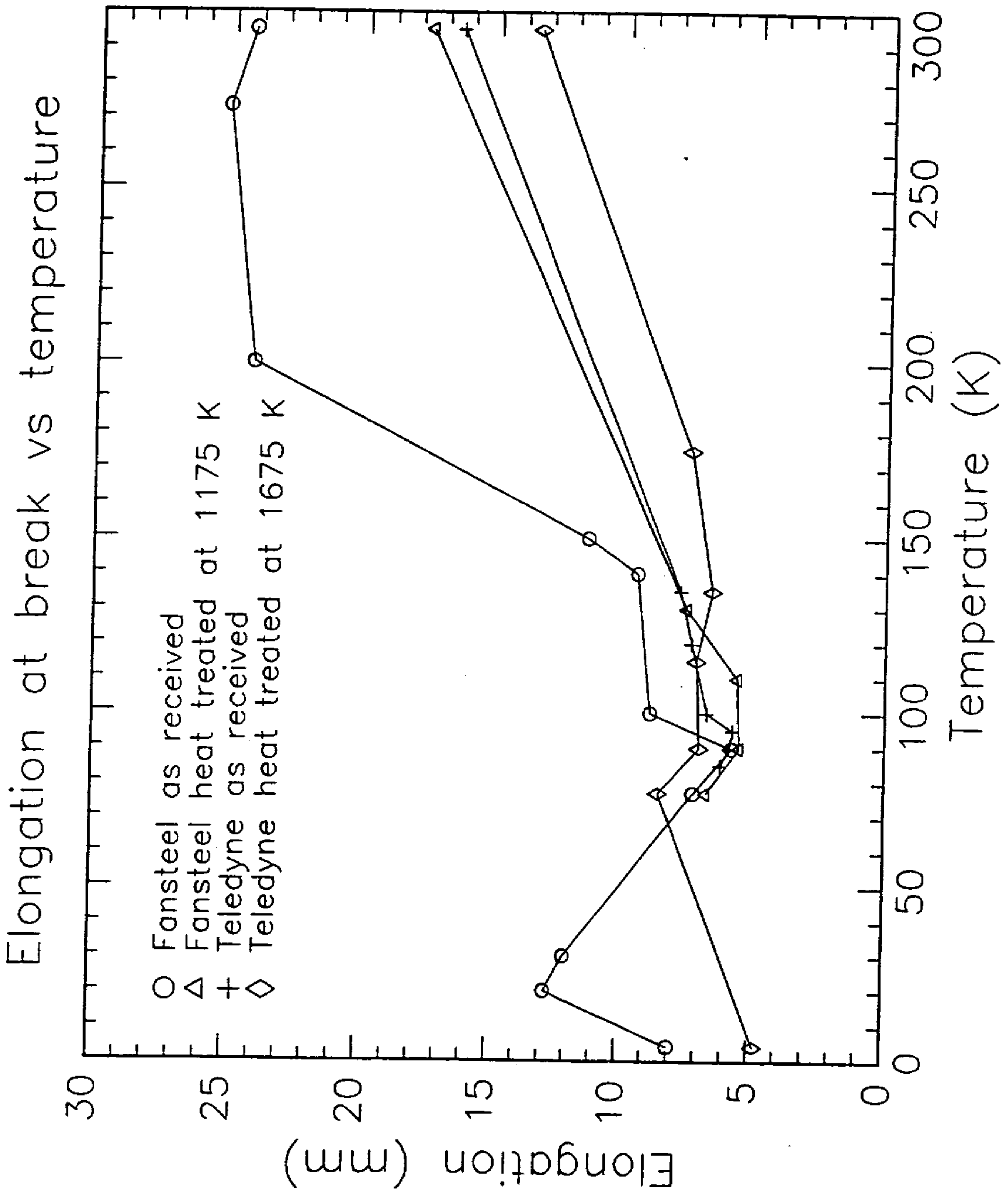
Elongation at break vs temperature
Fansteel as received
Fansteel heat treated at 1175 K
Teledyne as received
Teledyne heat treated at 1675 K
Temperature (K)
Elongation (mm)
0
50
100
150
200
250
300
0
5
10
15
20
25
30

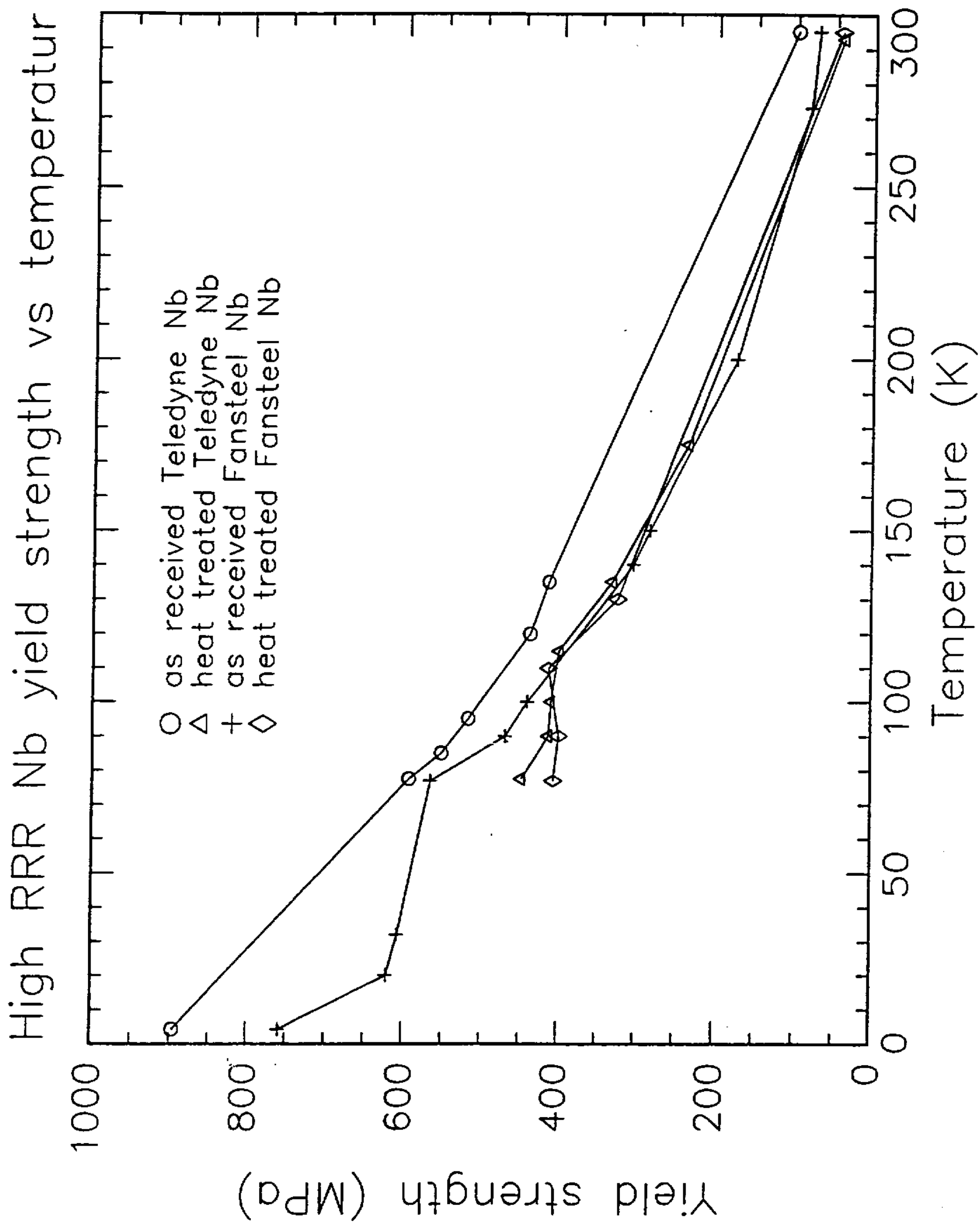
High RRR Nb yield strength vs temperatur
○ as received Teledyne Nb
△ heat treated Teledyne Nb
+ as received Fansteel Nb
◇ heat treated Fansteel Nb
Yield strength (MPa)
1000
800
600
400
200
0
Temperature (K)
0
50
100
150
200
250
300

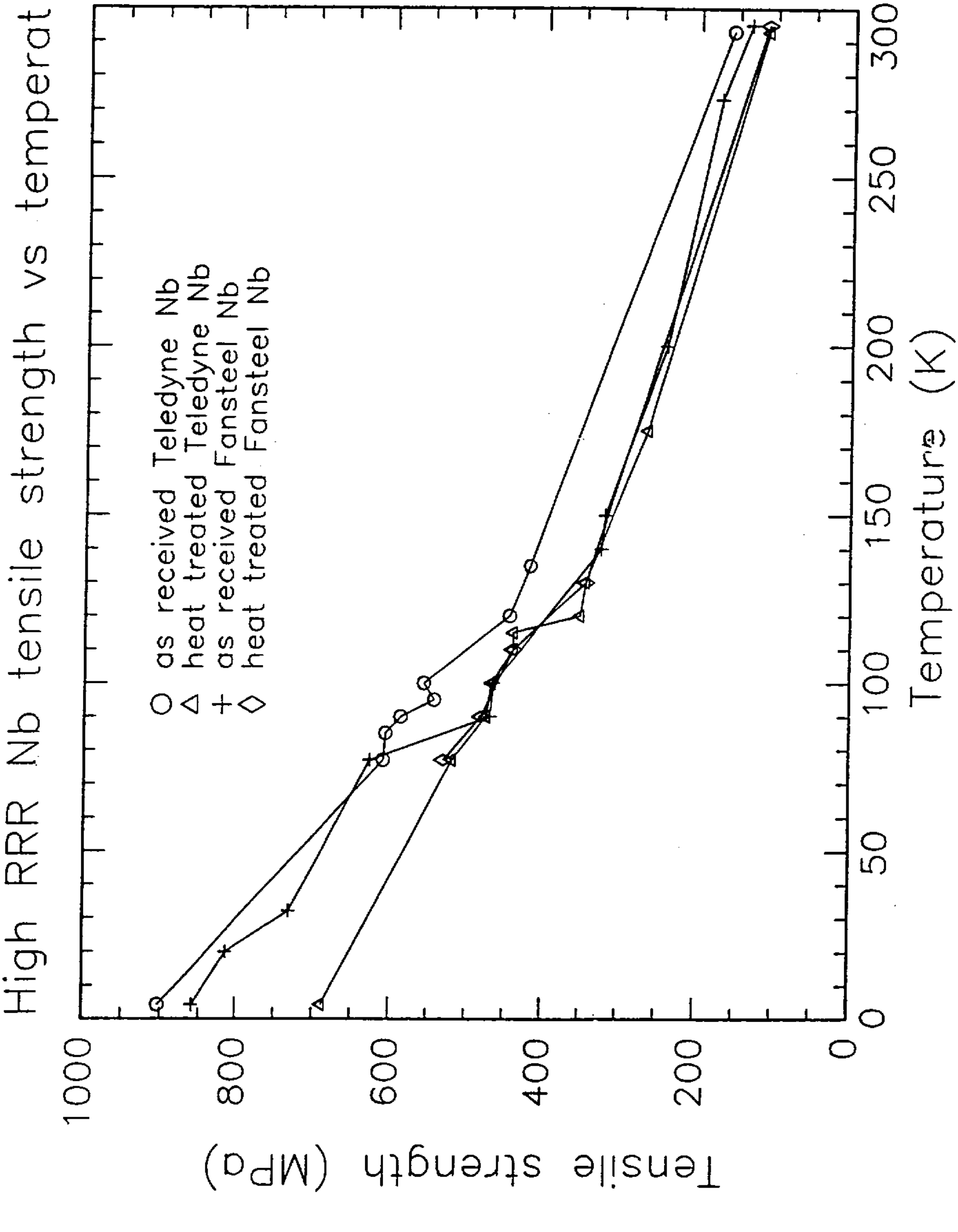
High RRR Nb tensile strength vs temperat
O as received Teledyne Nb
△ heat treated Teledyne Nb
+ as received Fansteel Nb
◇ heat treated Fansteel Nb
Temperature (K)
Tensile strength (MPa)
0
50
100
150
200
250
300
0
200
400
600
800
1000

Summary of USA Nb Tensile Properties

Sample	RRR	Grain Size	295 K			77.4 K			4.2 K		
			YS (KSI)	TS (KSI)	Elongation %	YS (KSI)	TS (KSI)	Elongation %	YS (KSI)	TS (KSI)	Elongation %
Cabot	40	7	21	31	46	92.5	94.2	16.8	_*	165	0.4
Teledyne	>250	8	14.5	23	42	86	88.4	12.1	130	131	>1
Fansteel	>300	6	10.6	19.5	34	82	91	14	110	124.6	>1

*The sample fractured prior to reaching to 0.2% offset

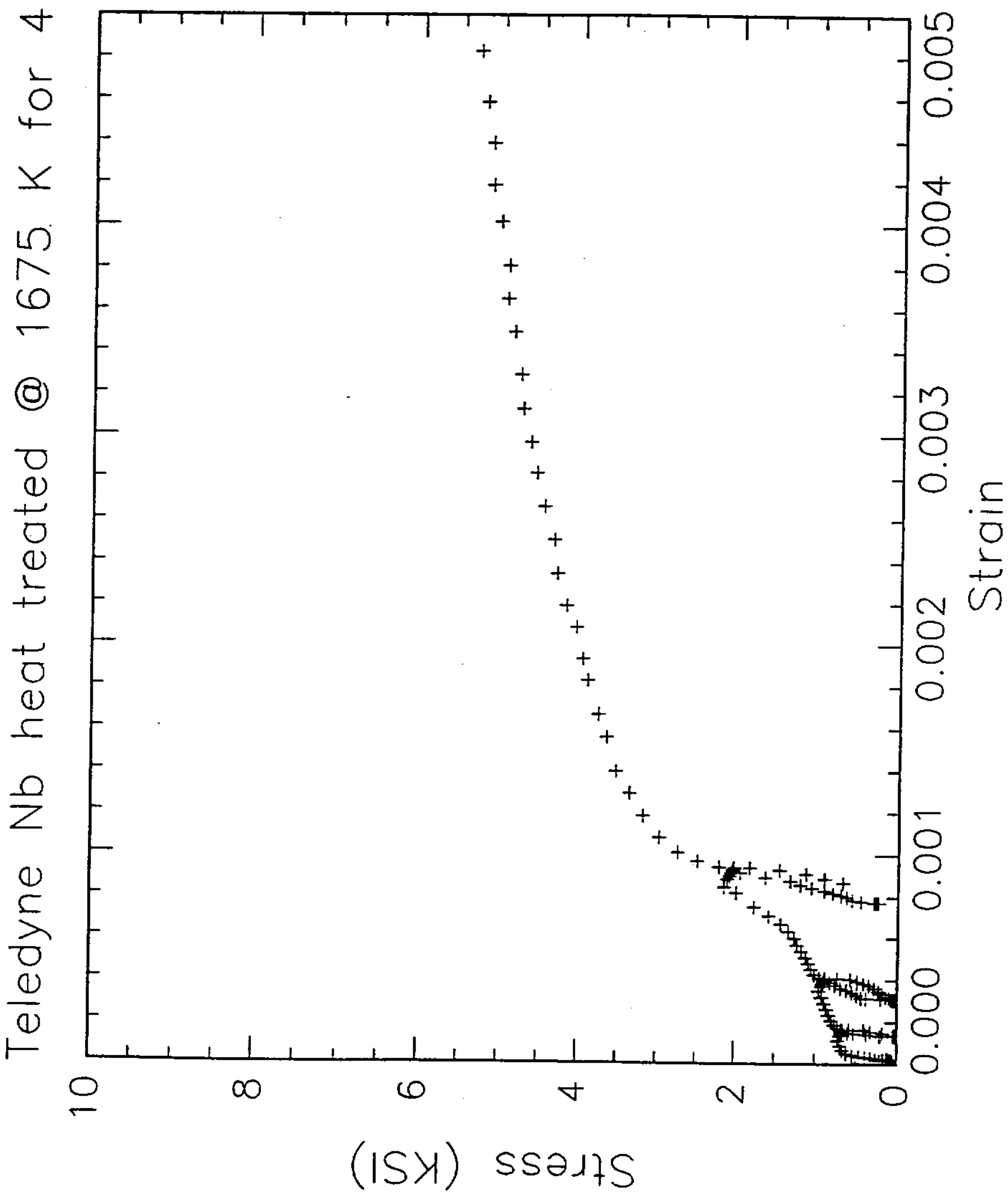
Teledyne Nb heat treated @ 1675 K for 4
Stress (KSI)
10
8
6
4
2
0
0.000
0.001
0.002
0.003
0.004
0.005
Strain

Comparison of Teledyne Nb Tests

Property	As Received		Heat Treated (1400 C)	
	CEBAF	Los Alamos	CEBAF	Los Alamos
YS (KSI)	14.5	6.3	5.3	6.4
TS (KSI)	23.1	23	16.3	15
% Elongation	42	50	46	40

SUMMARY

- Sharp yield point is observed with Nb, heated to 1075K. Pinning of dislocations by the interstitial impurities seems to be responsible for this

- The ductility of Nb gets worse with heat treatments at 1675 K

- The cavity manufacturing processes viz bcp, pressing (or deep drawing) appear to reduce the ductility of Nb
- Recrystallisation seems to be completed with heat treatments at 1275 K.

Work in Progress:

1) The effect of purity of Nb on the recrystallisation process

2) The effect of heat treatment time & temperatures on the ductility

3) The size of the crystals variations on the above parameters.

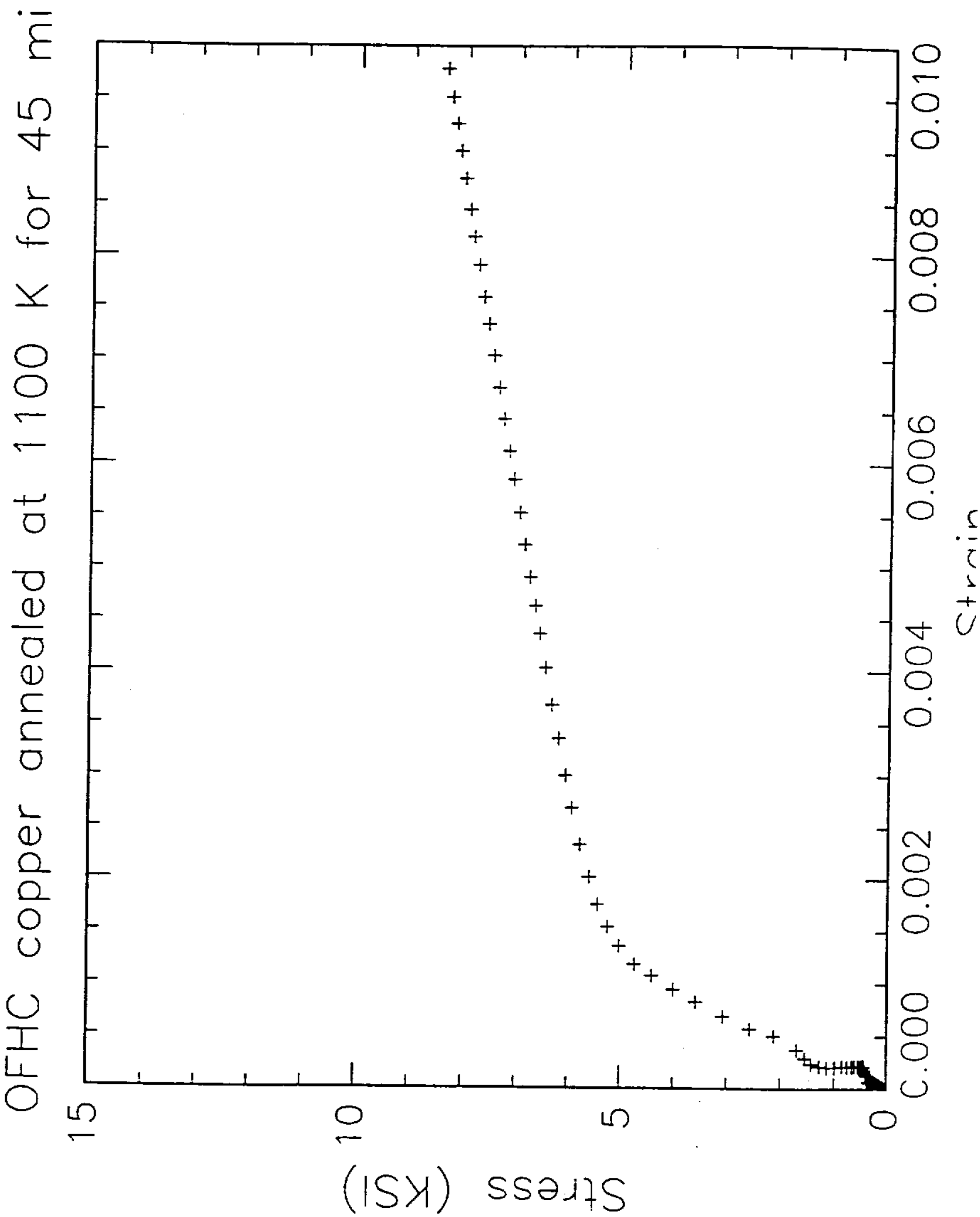
OFHC copper annealed at 1100 K for 45 mi
Stress (KSI)
0
5
10
15
0.000
0.002
0.004
0.006
0.008
0.010

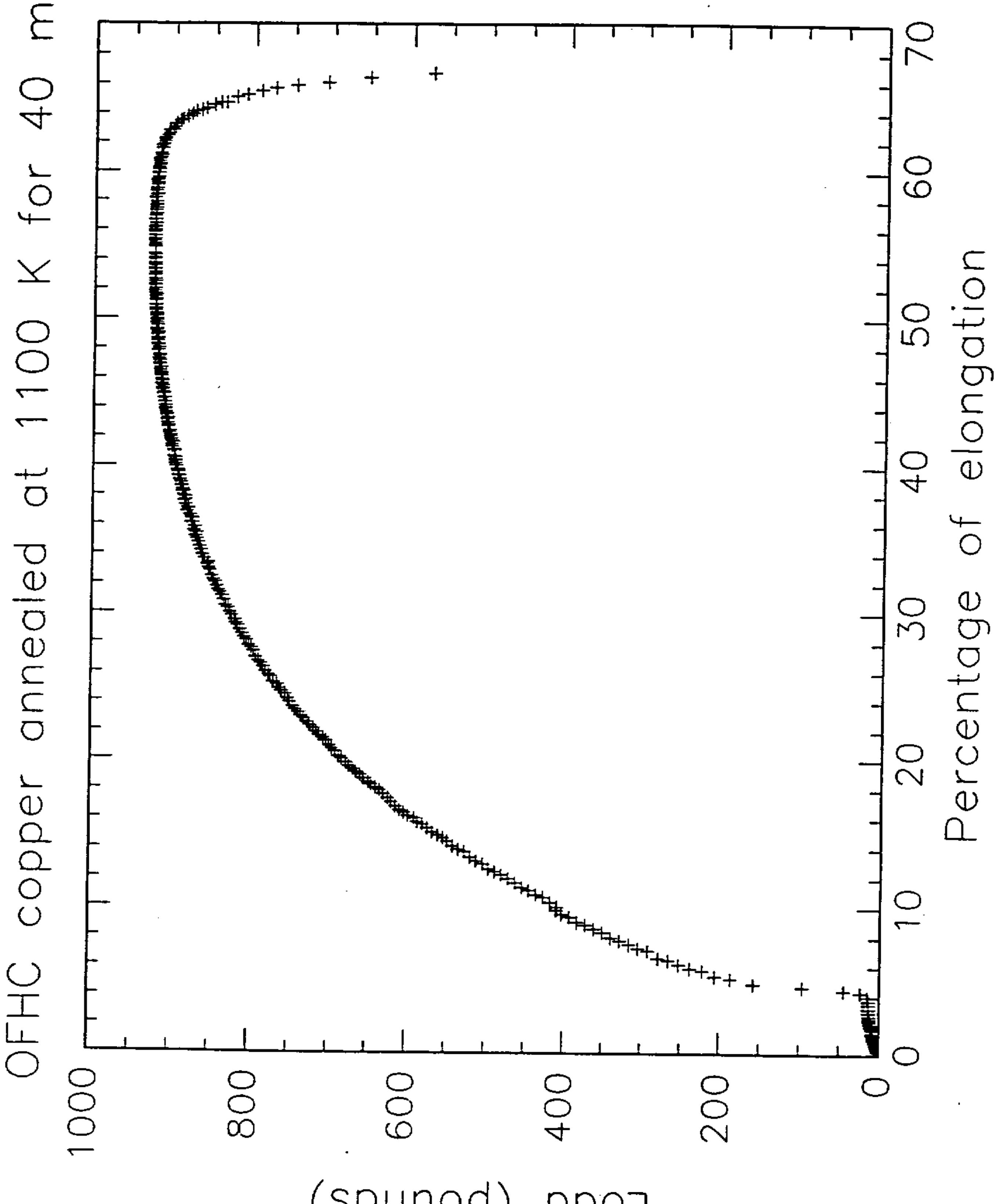
OFHC copper annealed at 1100 K for 40 mi
Load (pounds)
1000
800
600
400
200
0
Percentage of elongation
0
10
20
30
40
50
60
70

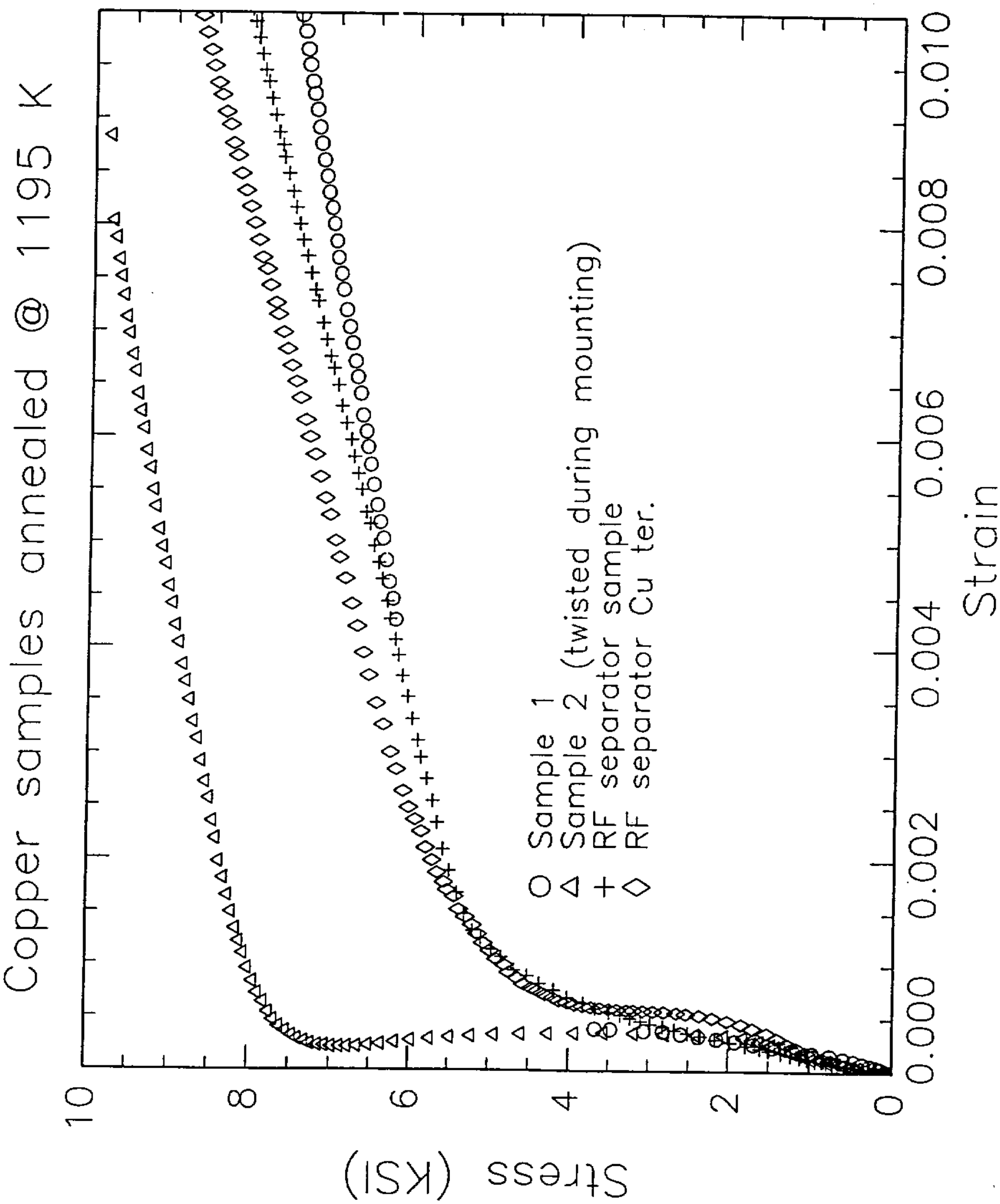
Copper samples annealed @ 1195 K
Sample 1
Sample 2 (twisted during mounting)
RF separator sample
RF separator Cu ter.
Stress (KSI)
Strain
0
2
4
6
8
10
0.000
0.002
0.004
0.006
0.008
0.010

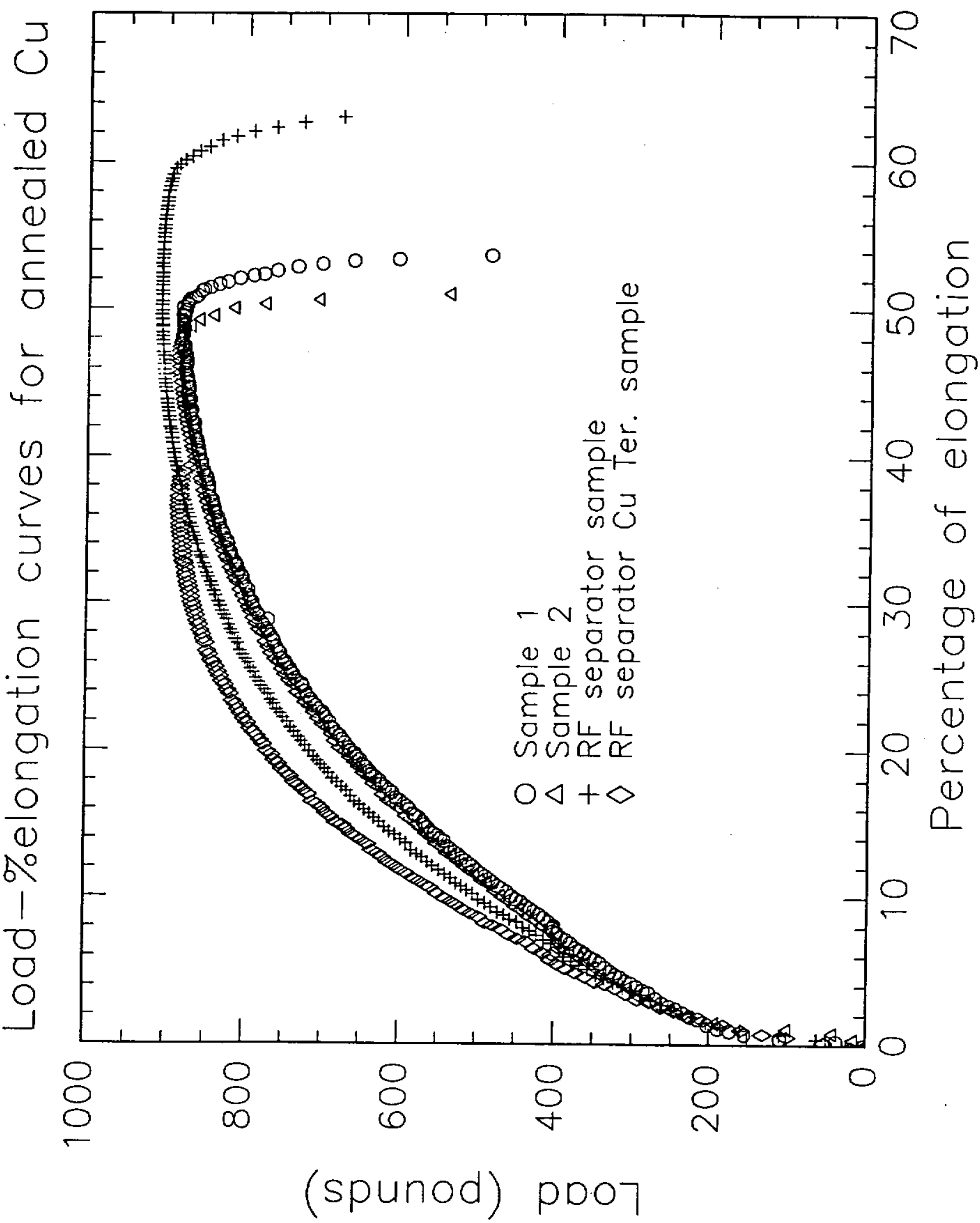
Load-%elongation curves for annealed Cu
Load (pounds)
Percentage of elongation
0
200
400
600
800
1000
0
10
20
30
40
50
60
70
○ Sample 1
△ Sample 2
+ RF separator sample
◇ RF separator Cu Ter. sample

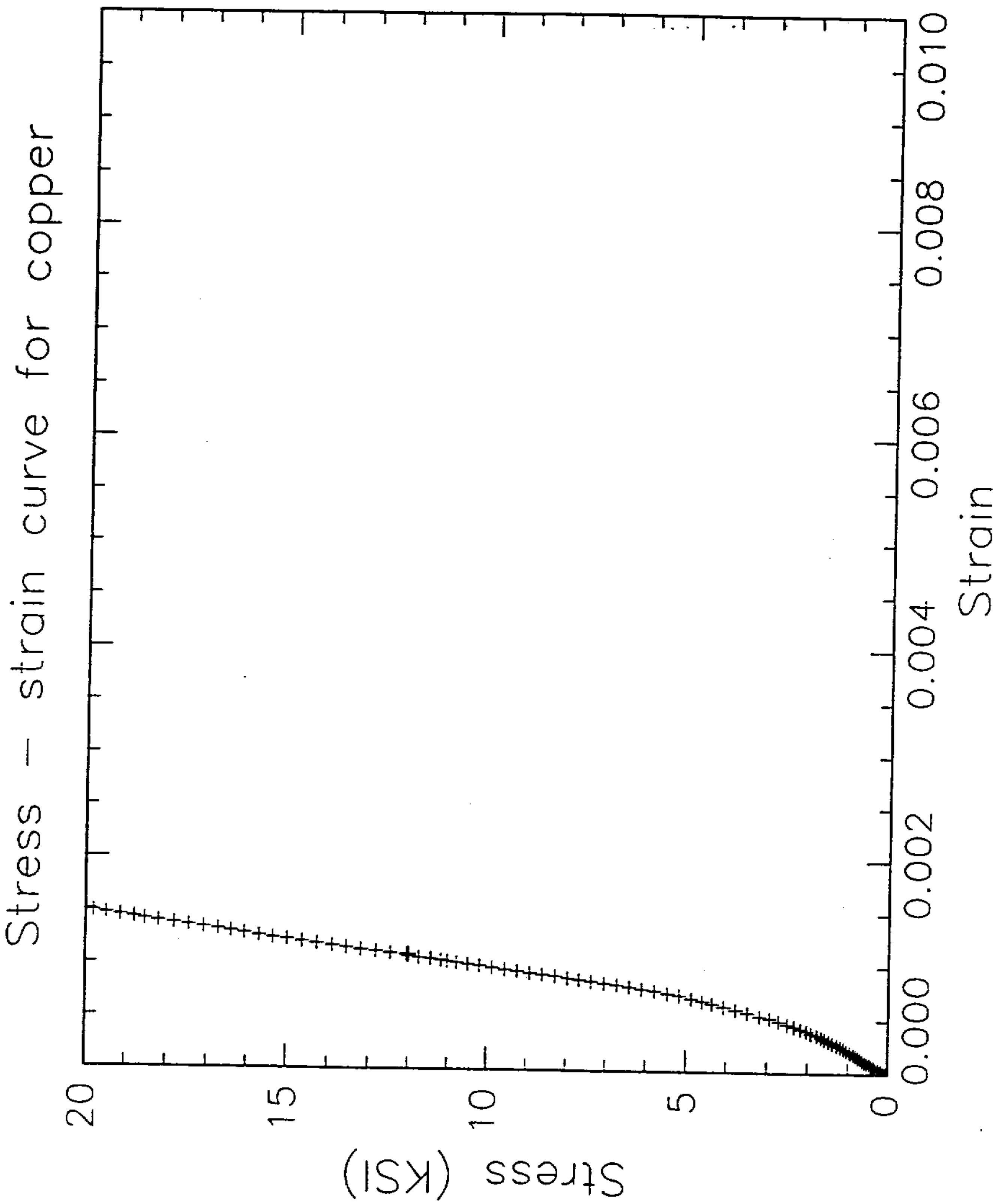
Stress - strain curve for copper
Strain
0.000
0.002
0.004
0.006
0.008
0.010
Stress (KSI)
0
5
10
15
20

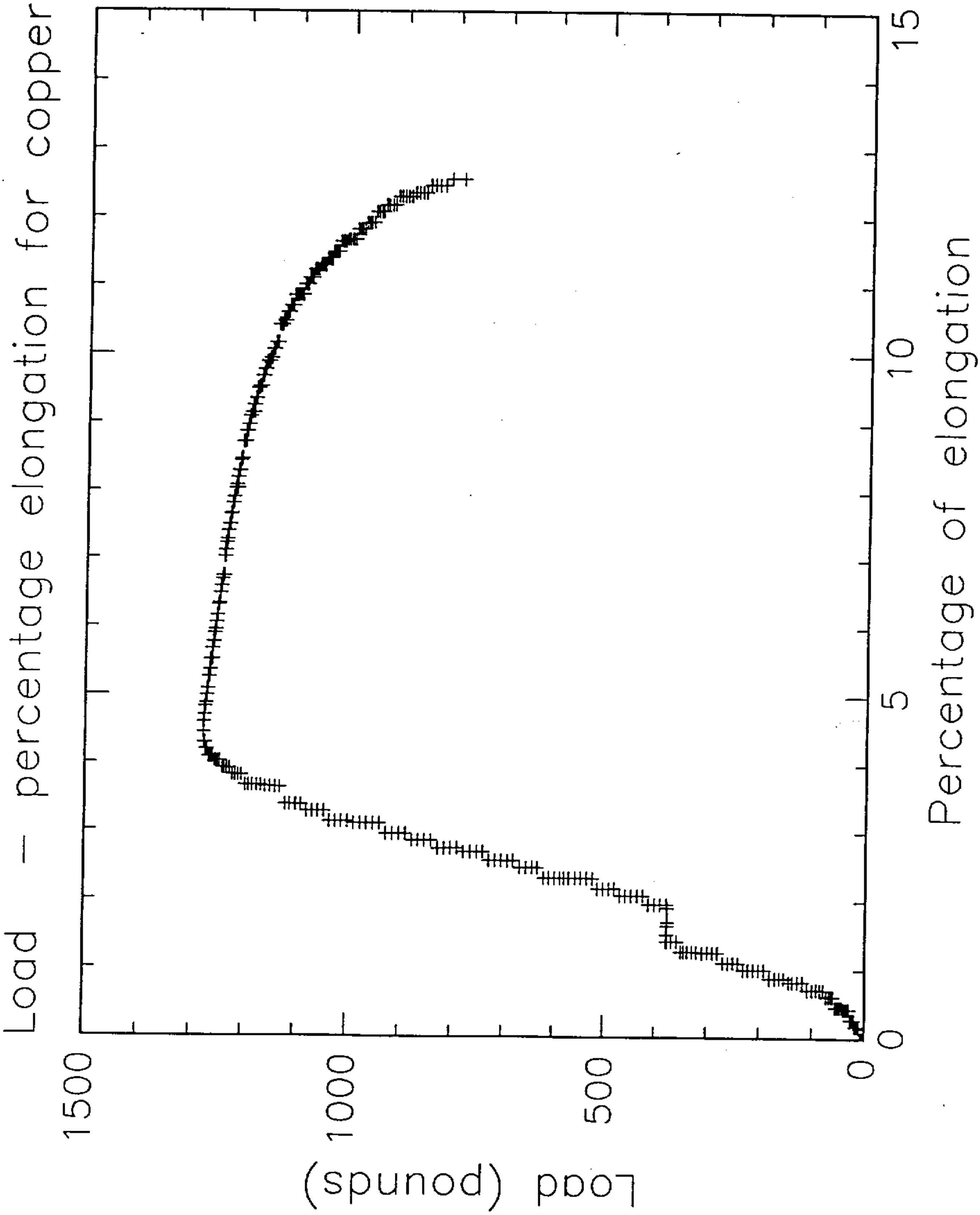

Load – percentage elongation for copper
Percentage of elongation
Load (pounds)
0
5
10
15
0
500
1000
1500

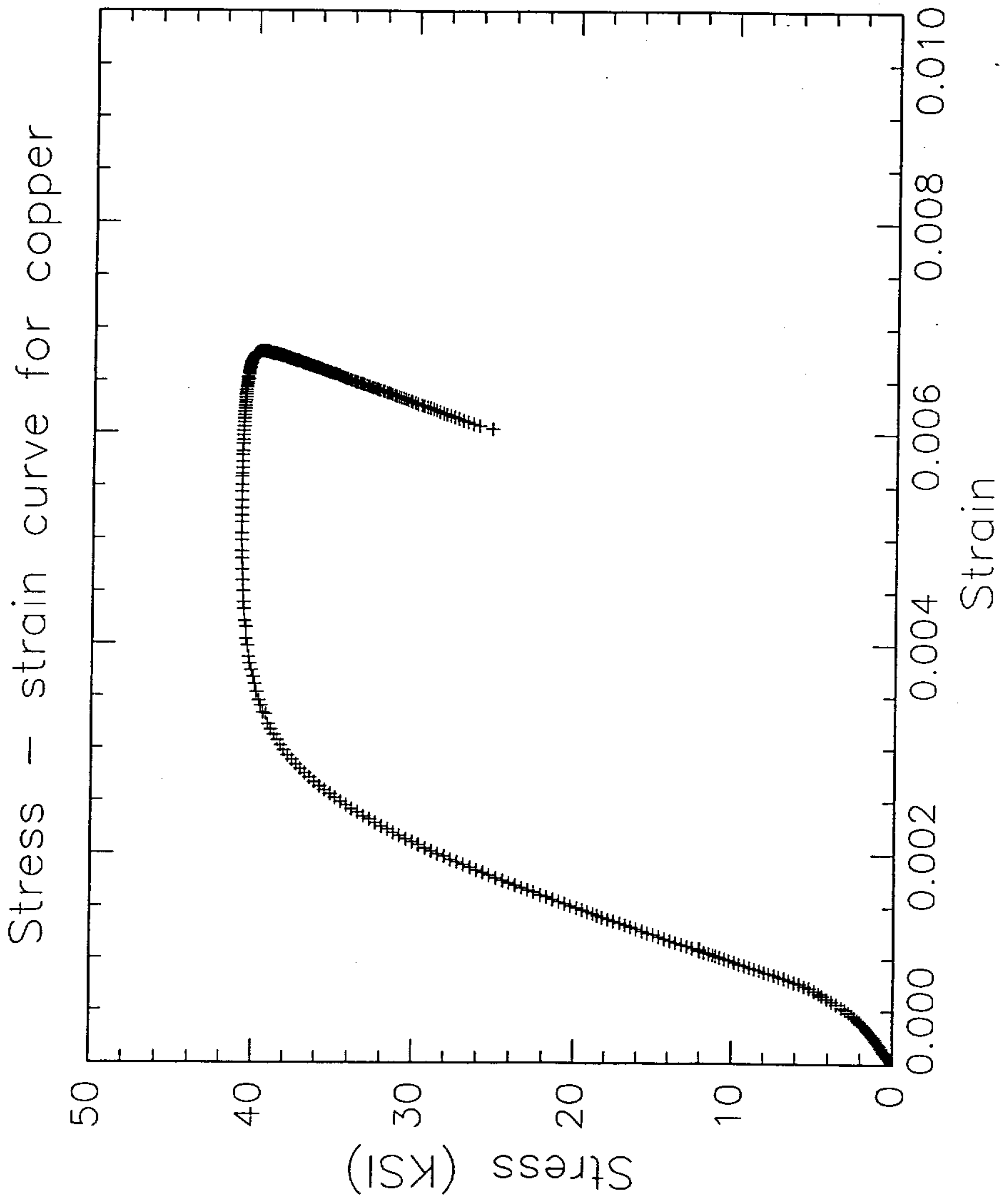
Stress - strain curve for copper
Stress (KSI)
Strain
0
10
20
30
40
50
0.000
0.002
0.004
0.006
0.008
0.010

Summary of OFHC Copper Properties

Status of the Material	Yield Strength KSI	Tensile Strength KSI	% of Elongation
As received	40	40.8	13
Annealed at 1175 K for 1 h	6	29	63
Annealed at 1100 K for 40 min.	6.4	29.5	66.8

A.Matheisen
march 95

Electrical Data of Niobium

typical data to qualify a s.c. resonator made from Niobium

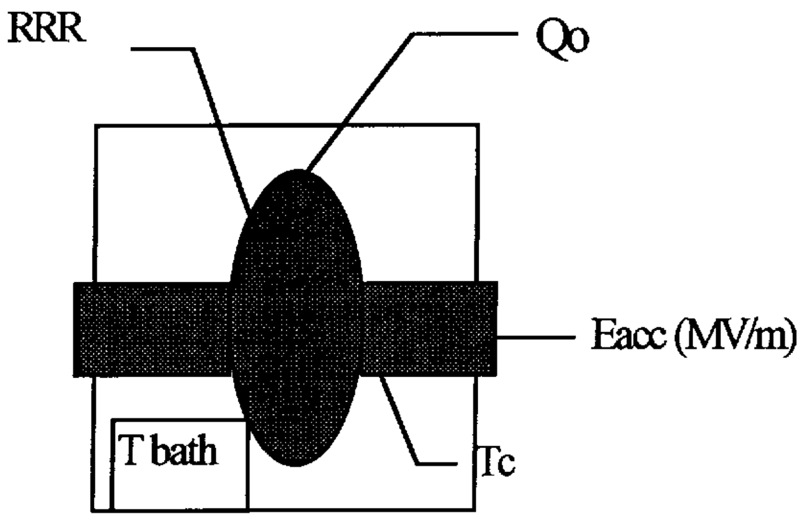

Qo = Quality factor
Eacc = acceleration voltage in MV/ m acceleration structure
RRR = residual resistance ratio
Tc = critical temperature of the superconductor
T bath = temperature of the cooling liquide
(working temperature of the structure)

But what do this data mean for manufacturing of a structure?

What´s behind Qo?

$$Q_o = \frac{W}{P_o}$$

Po= power dissipated on the cavity wall
Po ∝ surface resistance of the cavity wall

This losses are measured after the removal of the „Demage layer„ *(with state of the art of technology 100 µm)*

W = stored energy in a accelerator cavity (resonator)

The storred energy is depending on the geometry of the cavity and is calculated by computer codes.

o This geometry is fixed in technical drawings.

Deviation from this will lead to misleading data and to wrong interpretation of data taken during the measurements of the cavity!

=> follow the drawings !

A.Matheisen MRZ 95

with some additional mathematics you will find

$$Qo = \frac{G}{R(\omega,T)}$$

G = geometrical factor defined by the frequency and the integration of the magnetical field over the resonator volume

R (ω,T)= losses of the resonator wall depending on the frequency, the temperature and the integration of the magnetic field over the cavity surface

$$R(\omega,T)=R(BCS)+R(res)$$

R(BCS)= natural surface resistance of a superconductor in electromagnetic fields, depending on the frequency and temperature

R(res) = all residue resistances that are not due to the pure superconductor. This R (res) is depending on remains of fabrication and preparation technology of Niobium and cavity

Typical Data published

Q or R versus Tc/ T

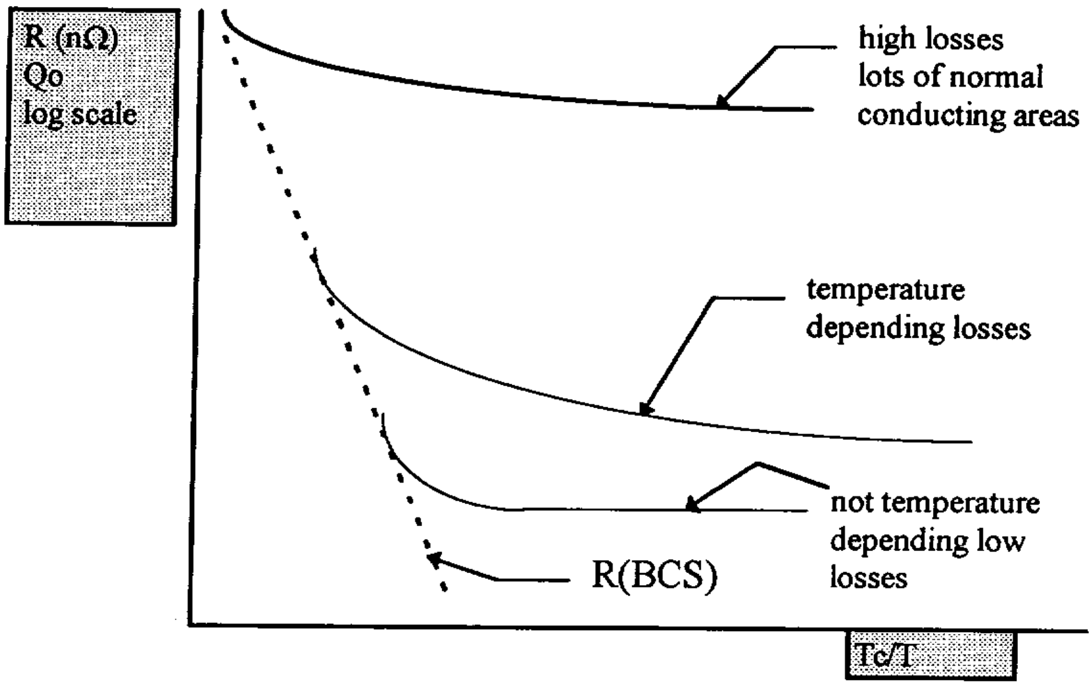

Q/E curve

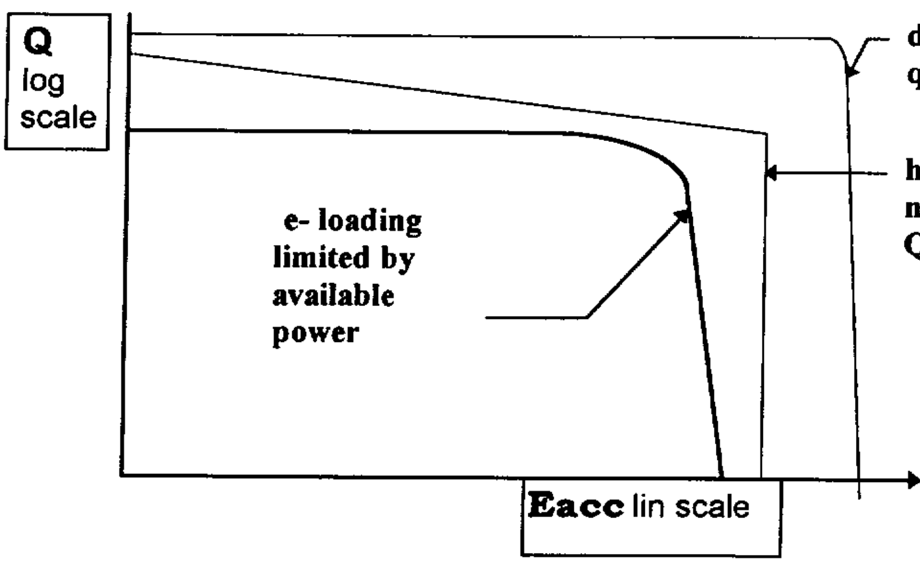

A.Matheisen MRZ 95

R(res)= residue impurities can origin from

$$R(res)= R(n.c)+ R(impurities)+R(grid)+R(.....)$$

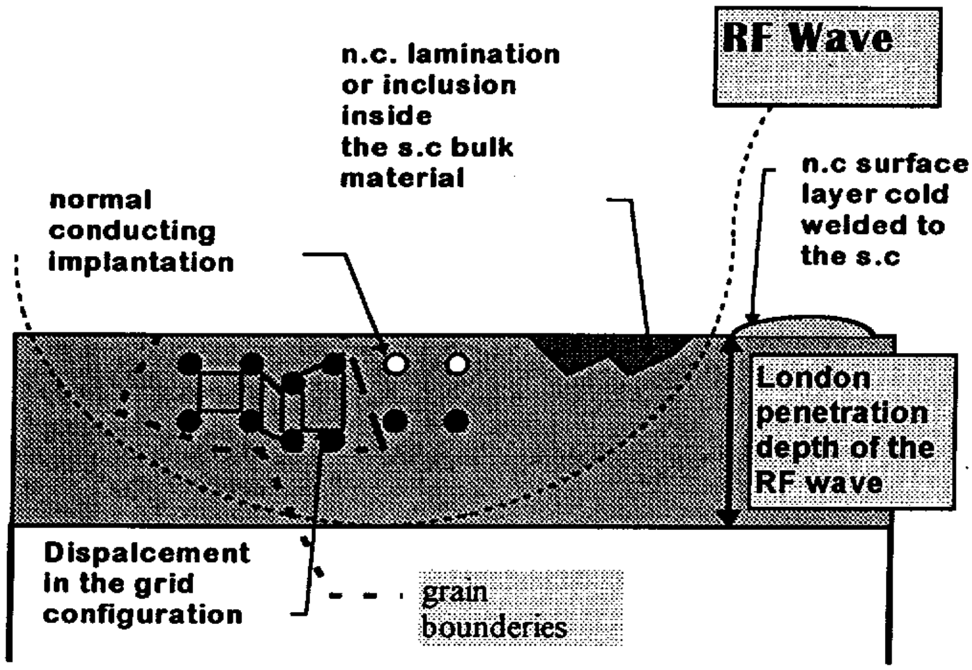

crossseection of a Nb sheet

fabrication=>

- o inclusion of material by pressing
  = cleanliness of tools
- o lamination of Niobium
  = spinning,deep drawing
- o chemical reactions of the Niobium
  = heat / cleanser/grease
- o mechanical deformation
  = deformation of grid
- o residual n.c.material in grain bounderies
  = chemical reaction / implantation
  during heat up of material
- o cold welded acide resistant material
  = plastic coverages for storrage

preparation and treatment

- o Chemistry and rinsing of the surface
- o heattreatment on cavity

A.Matheisen MRZ 95

Whats behind Eacc (acceleration voltage)

Po=U*I=U*U/R=>

$$(Eacc)^2 = \frac{R*Qo*P}{Q}$$

[Units MV/m =nominalized voltage per unit length of one meter]

->
E acc = The Voltage a charged particle sees during it passes the accelerating structure on the center axis

->
E acc (Hc;Tc;e-)=limited by critical magnetic field (Hc)
critical temperature (Tc)
electron loading of the cavity (e-)

The acceleration voltage

- o is build up from 3 dimensional electro- magnetic waves in a cavity which are defined as modes of the resontor
- o Each mode has a well defined current and voltage distribution on the resonator walls
- o is sensitive for ....

Eacc= 25 MV/m as goal for TESLA

A.Matheisen MRZ 95

Field distribution in accelerator cavities

->
E = field parallel to the surface

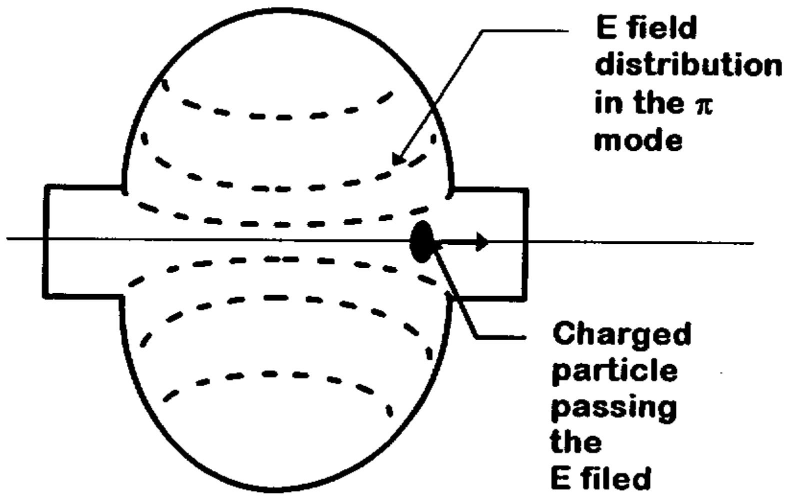

->
H = magnetic field perpendicular to the surface

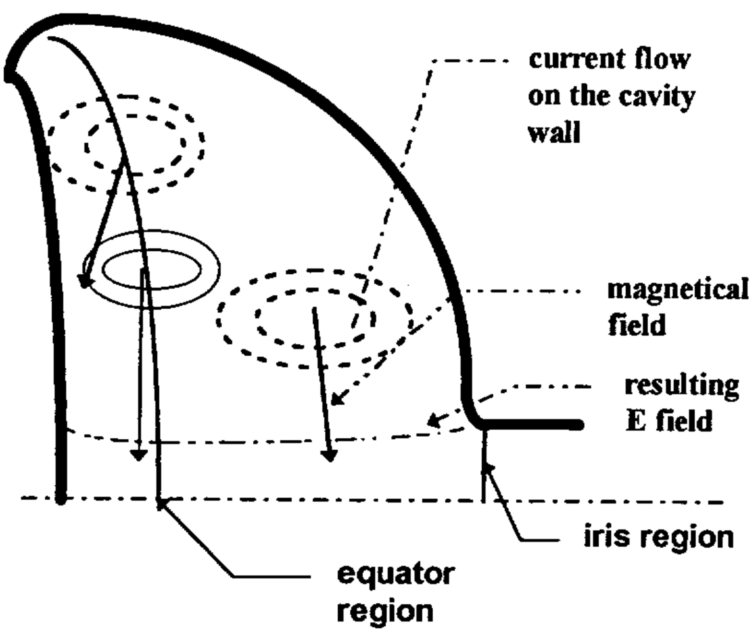

A.Matheisen MRZ 95

Limitations of the E acc in superconduting structures

\# E´acc (Hc) = maximum theoretical acceleration voltage
=> crossing Hc on the wall

ORIGIN of Eacc (Hc):
basic physics law

\# E´acc (Tc) = real limitation up to now
=> local hot spots (defect) on the surface
result in local heating and rise of
temperature above Tc

=> The normal conducting areas of the s.c.
surface dissipate additional power from
the cavity and drive more and more areas
normal conducting

RESULT : „Quench" of a s.c. Resonator

ORIGIN of E´acc (Tc) :
dust,lamination of s.c.material,
clusters of n.c. material
lossy spots of the s.c. wall (oxides)
frozen in magnetic flux (iron bolts)

\# E´acc (e-) :
electron loading of a resonator
=> power consumtion from the storred
energy by non resonant electrons

RESULT : power limitation by consumption in field emission

ORIGIN of E´acc (e-):
local surface irregularities; needles,grooves,
oxides
metal particles (dust)
glow discharge (dust)

A.Matheisen MRZ 95

Powerdisipation in a resonator parallel to the beam

R tot= R (bcs)
R tot= R (bcs) + R (res)
R tot= R (bcs) + R (res) + R (hot spot)
R tot= R (bcs) + R (res) + R (hot spot) + R (e-)
R tot= R (bcs) + R (res) + R (hot spot) + R (e-) + R(n.c.)

result in heating of the wall

Statistics shows:

Losses	result		appearing from
R(bcs)	Q 10E11	E=max theory	nature
R(res)	Q 10E10	E=reality	impurties in the Niobium
R (hot spot)	Q 10E 8	??	n.c. particles in/on the wall
R (e-)	Q 10E 6	??	geometrical deviation;dust
R (n.c)	Q 10E 4	some MV/m	lossy region on the wall drive the s.c. surface normal conducting

How to fight against the limitations ?

o cleanliness during fabrication
(avoide inclusion of n.c. material)
o ceanliness during handling and treatment
(ovoide dust -> „cleanroom")
o high peak power processing/ high pressure rinse
(disturb particles and emitters)

o high thermals conducting Niobium (RRR)
(cool away the losses and keep the wall below Tc)

A.Matheisen MZR 95

Whats behind RRR?

$$RRR = C * \lambda$$

RRR= residual resitivity ratio
C = empirical constant about 4
λ = thermal conductivity (W/mK)

$$RRR = \frac{R(300\ K)}{R\ (4,2K\ )}$$

o RRR depends on impurities inside the niobium bulk o
(Remember: Eacc and Qo depend on irregularities on the surface or inside the London penetration depth and are surface effects)

RRR is a bulk effect

<u>ORIGIN:</u>

dislocations
grain bounderies
intertitials
soluble gas most effect on O2
(see table 1)

history of resonators

RRR	Eacc limited at
10-60	2- 7 MV/m
100-200	5-15 MV/m
200-600 (1000)	12-27 MV/m

A.Matheisen MRZ 95

Effect of improved thermal conductiviy

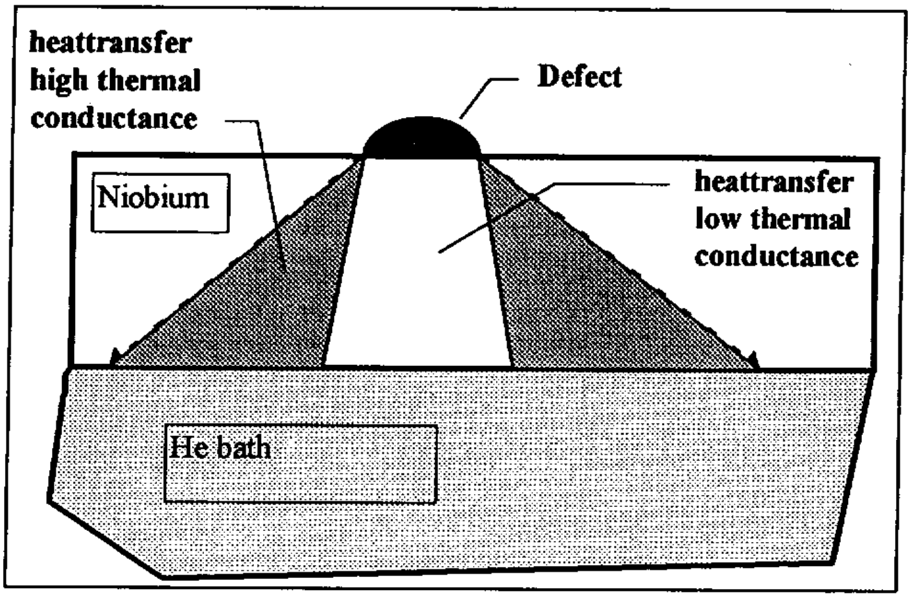

To reach and keep high RRR

o manufacturing of ultra pure niobium

o prevent heat during forming and machining
(absobtion of gas starts at 200 C)

o annealing in ultra high vacuum (800-900 C)

o postpurification by getter material in UHV oven

o minimize mechanical stress ?

A.Matheisen MRZ 95

Conclusion:

if you apply new forming and processing techniques to make cavities

o machine the Niobium like other ductile metall. o

but keep in mind it is different .It is a getter-material that needs to be kept pure for high RRR and has to be used as a s.c.resonator with 25 MV/m acceleration voltage

some remarks for fabrication of resonators

- avoid impurities penetrate more than 100 µm into the surface
- avoide laminations of the Niobium
- avoide implantation and cold welding of material
- cross check chemical reactions
- qualify production steps by cold tests
- avoide heat and keep RRR high
- cross check RRR on samples during different maching steps
- hard working of Nb leads to cracks

- ????

A.Matheisen MRZ 95

Q.S. SHU
D. Renken
8/3/95

Consideration of the three-in-one option

Technical Items	Sensors in parallel	Sensors in series
T-R board	use existed	redesign and fabr.
Cabling	use existed	redesign and fabr.
Feedthrough	use existed	redesign and fabr.
Internal E-box	not needed	optional
U-bar	new design	new design
Top/bottom flanges	need modify	need modify
Moving adapting Device (pancake)	need a reliable design (box, holder, protector guide, positioner etc.)	need a reliable design (holder, protector guide, positioner etc.)
Special cables	need order	need order
Special connnectors	need order	need order
Advantages	less assembling time - for pancake	less assembling time - for pancake, less wires for T, same for R
Disadvantages	difficult to repair	difficult to repair, any wire broken will influence each other

TESLA 1995-09

DESY Workshop
March 4, 1995

HYDROFORMING OF MONOLITHIC PARTS TO PRODUCE RF CAVITIES FOR PARTICLE ACCELERATORS

C. HAUVILLER

CERN
European Laboratory for Particle Physics

136

Hydroforming is a common manufacturing procedure, ex. production of bellows (axisymmetry).

The principle is to push the part against a rigid die by applying a large pressure through a liquid or polymer.

Production of monolithic pieces , no need for welding.
Better mechanical behaviour than welded parts.
Reproducible parts obtained in a straightforward way.
Expensive tooling for small series.

137

Cavities produced from a copper tube.
Very large deformations, typically up to about 200%.

Ultimate elongation of annealed copper is only of the order of 50%
Multistage process: swaging and several expansions (room temperature) with intermediate annealing.

Circular / elliptical cavities in the decimetric range (300 MHz to 3 GHz)
- 2.1 GHz as a first demonstration model,
- 1.5 GHz for CEA Saclay and CERN teams,
- 352 MHz for the LEP 200 project

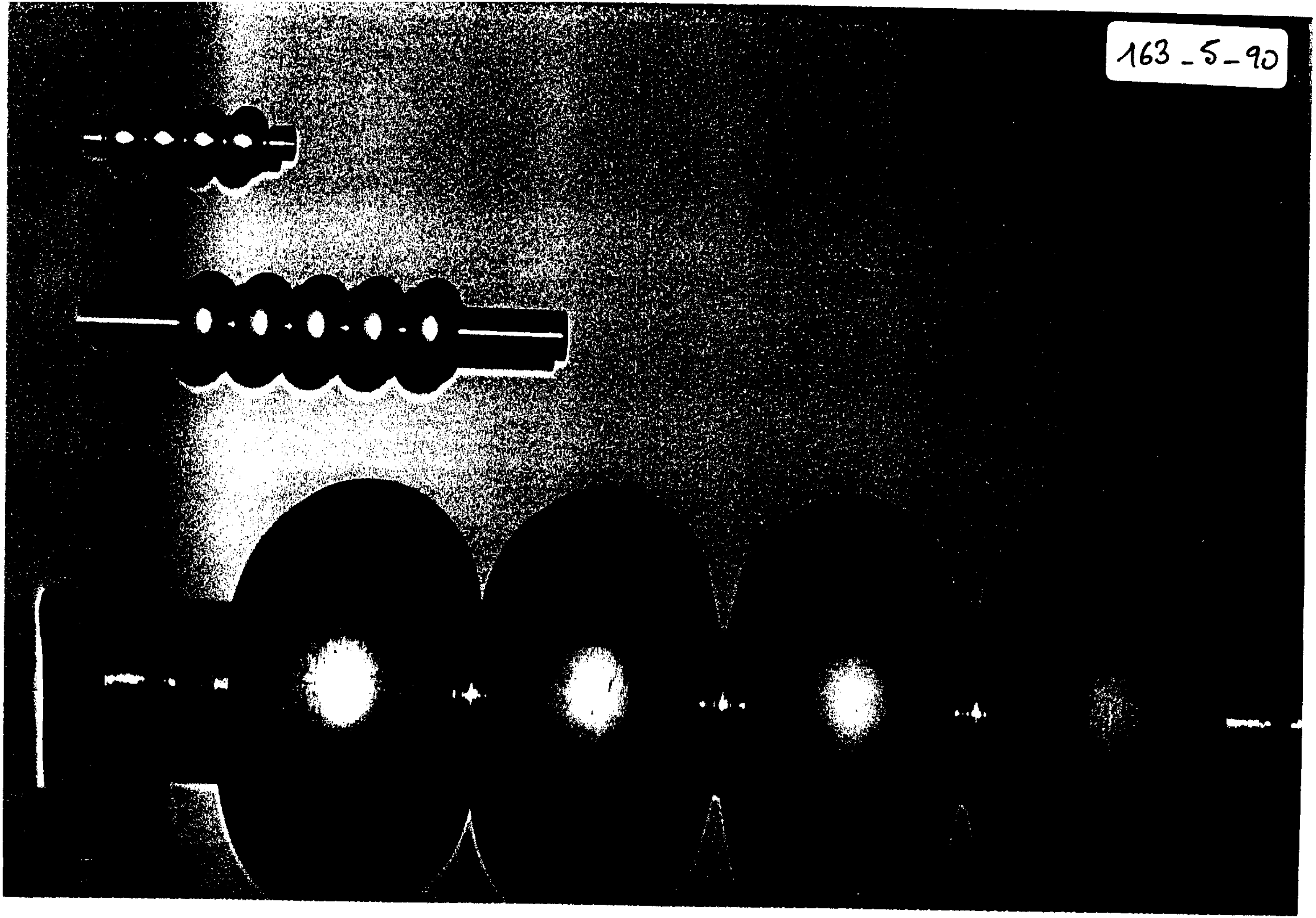
163-5-90

Frequency	Diameters (external value) (mm)			D/d	Thickness (mm)	
	Tube	Maximum (D)	Minimum (d)		Tube	Minimum
2.1 GHz	59.3	126.1	39.6	3.18	2.15	1.04
1.5 GHz	86	184.1	75	2.45	3.0	1.36
352 MHz	304	759.9	259	2.93	9.0	3.67

139

Swaging

A oil-pressurised membrane pushes the annealed copper tube onto the internal core creating a toroidal groove.

Problem: to prevent plastic buckling due to high compressive stresses, creating ripples.

Modelled using the BOSOR5 software and checked experimentally.

Good correlation for the critical buckling values in the case of uniform thickness but divergence appears in the case of a local thinning, probably because local defects greatly influence the buckling mode (mode 20).

Reduction up to 35% of the diameter achieved in only one stage with a pressure up to 650 bars.

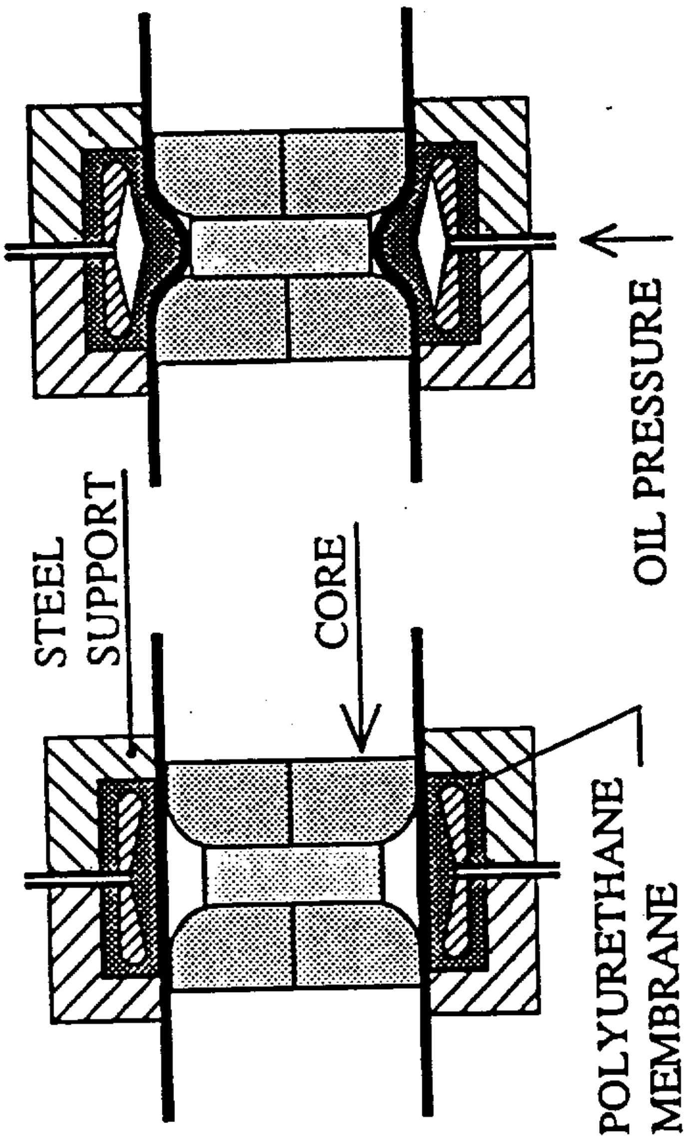
STEEL
SUPPORT
CORE
OIL PRESSURE
POLYURETHANE
MEMBRANE

Expansion

Multi-part die initially open and closed progressively during expansion.

Virtually no axial elongation .
The closed die has the exact external shape of the final cavity.
Progressive internal hydraulic pressure up to 200 bars.
Number of expansion steps depends on the radial deformation needed and on the behaviour of the annealed copper (multi-variable optimisation process).

Modelled using CASTEM software.

Complex phenomena of hydroforming:
plasticity, large deformations and displacements, variable boundary conditions and contacts.

Axisymmetric shell elements (thicknesses updated after each expansion step)
Updated Lagrangian formulation.

Precise prediction of the behaviour during all stages:
measured values agree to better than 5% with the measured ones.
actual thicknesses larger than predicted ones.

141

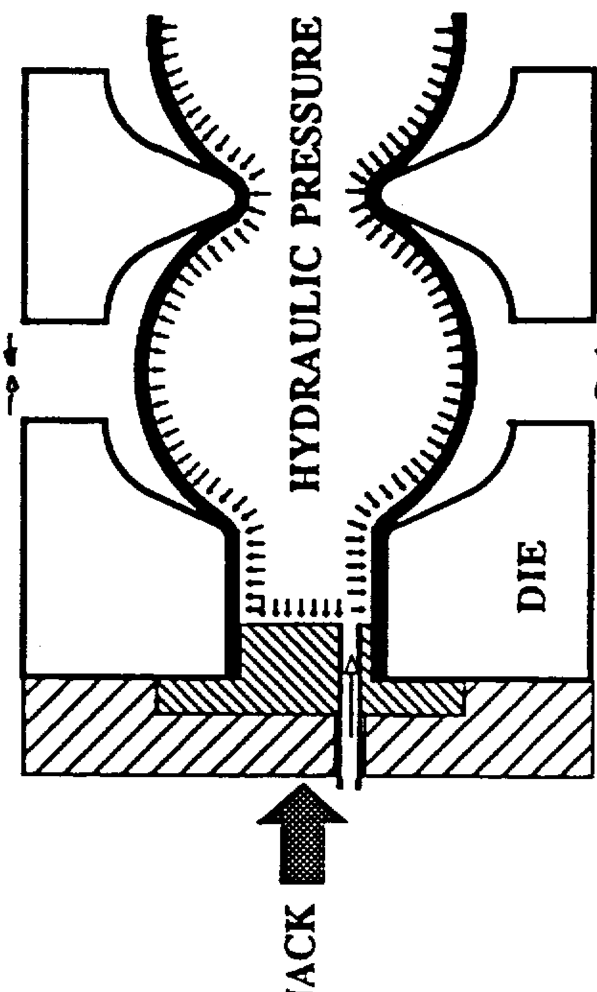
HYDRAULIC PRESSURE
DIE
JACK

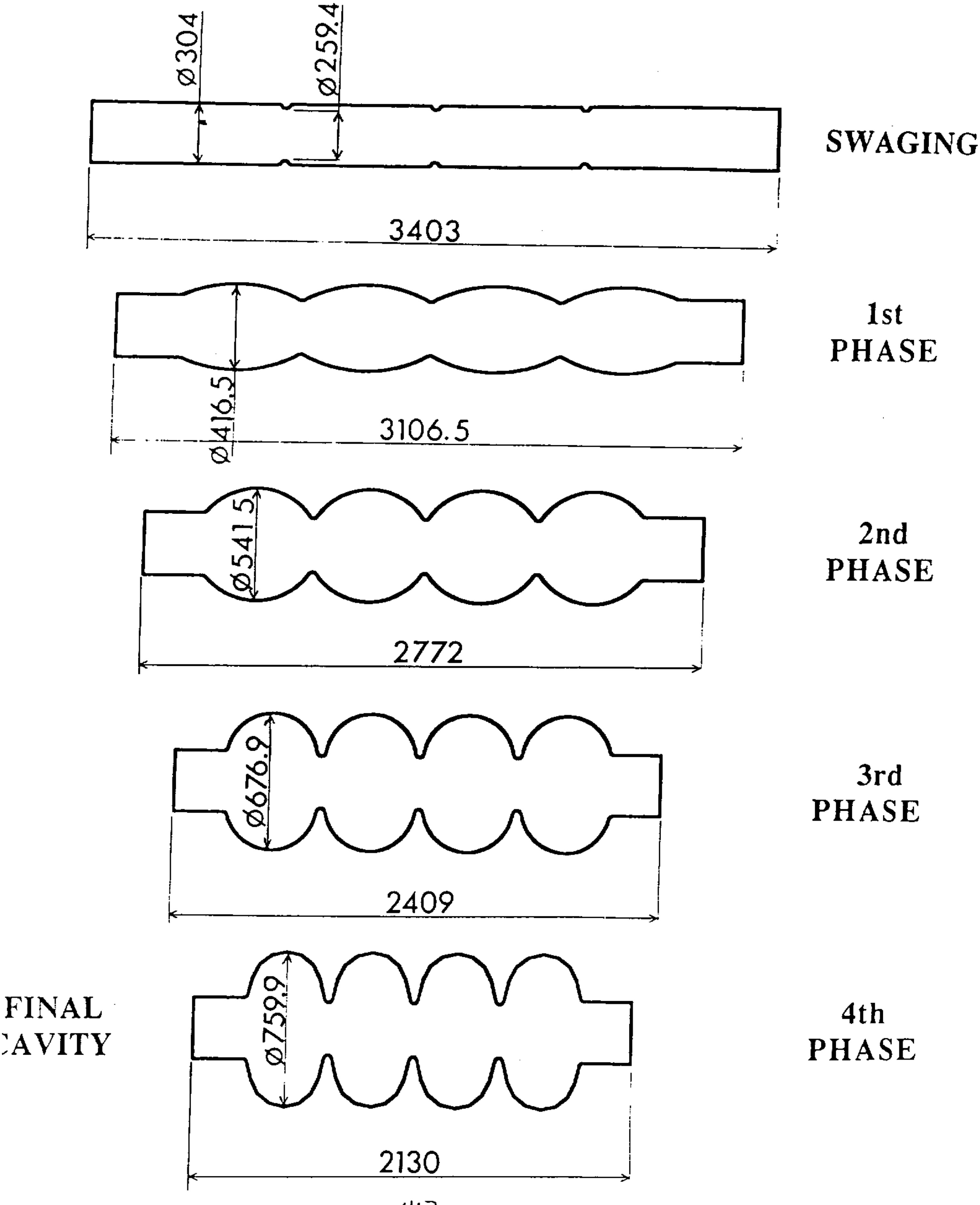
Ø304
Ø259.4
3403
SWAGING
Ø416.5
3106.5
1st PHASE
Ø541.5
2772
2nd PHASE
Ø676.9
2409
3rd PHASE
Ø759.9
2130
FINAL CAVITY
4th PHASE

C. HAUVILLER
March 4, 1995

OFE COPPER AND HEAT TREATMENT

OFE (Oxygen Free Electrolytic) : purity and high conductivity at cryogenic temperatures.

Annealed under vacuum.
Drastic influence of temperature and time on metallurgical and mechanical behaviour.
Determination of heat treatment using standard tensile tests.

1st step: single traction

Search for maximum elongation avoiding grain growth

Heat treatment starts to influence material properties only at 400 °C : ultimate elongation, hardness, but also surface roughness of prime importance for coating quality.

No direct relation between roughness and grain size.

2nd step: hydroforming phases simulated on test samples

initial (as received + annealed), phase 1 (elongation (32%) + annealed), phase 2 (elongation (32%) + annealed),...

- impossible to recover entirely from the "damage"(cracks, voids) generated by the previous steps

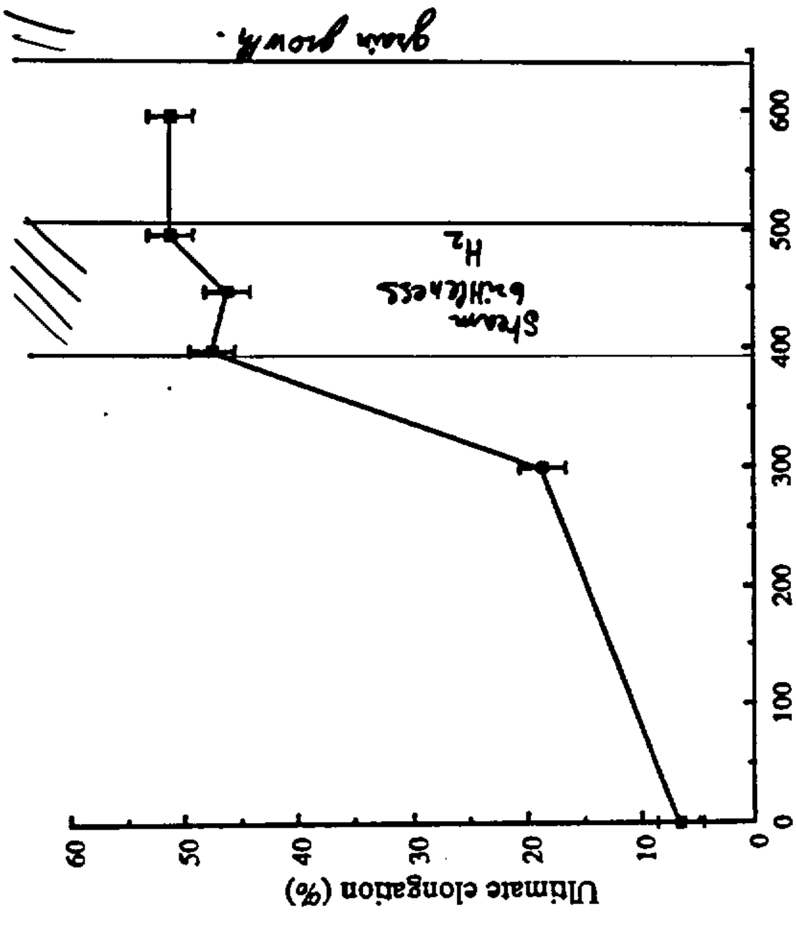

Figure 5. Ultimate elongation after 30 mn annealing

Ultimate elongation
(simulation of the multistep forming)

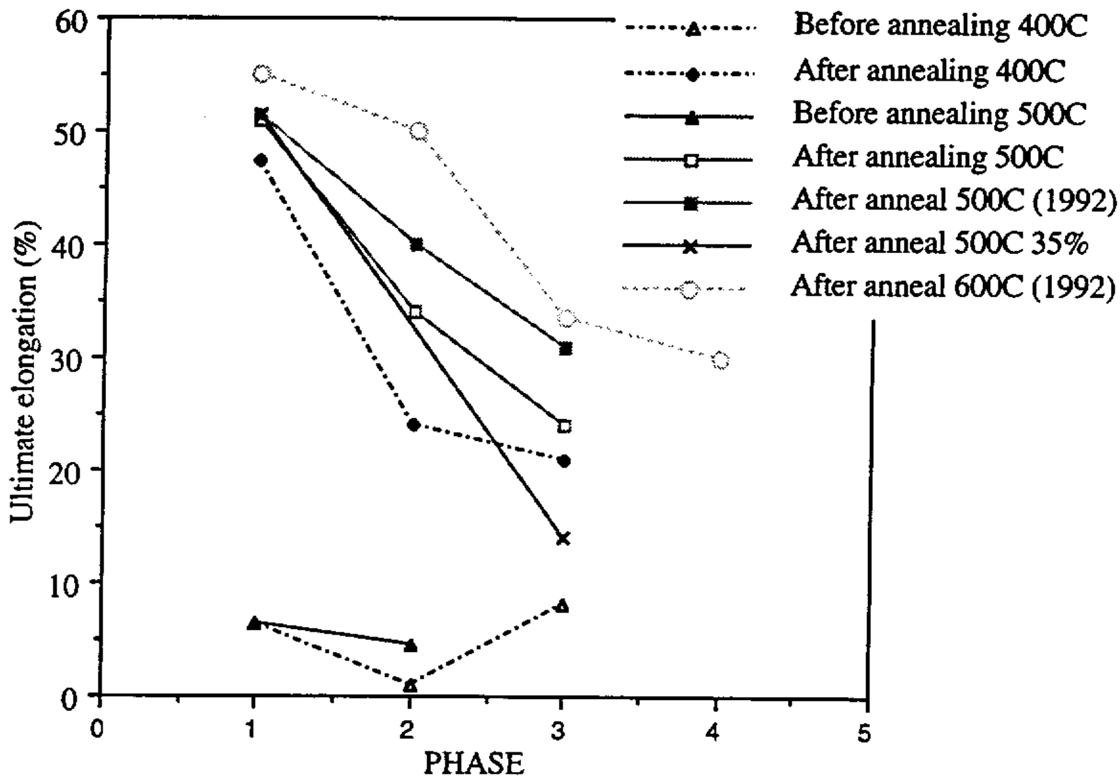

C. HAUVILLER
March 4, 1995

QUALITY OF THE MANUFACTURED PARTS

Geometrical dimensions (no adjustment after forming):
The most critical one is the diameter

Single cell cavities:	± 0.1% on 38 parts
5-cell cavities:	± 0.1% on 10 parts (2 different batches)

Roughness corrected by chemical process

Frequency measurements on four 5-cell cavities

147

**Diametres extérieurs mesurés sur
38 cavités 1.5GHz monocellulaires (1992)**

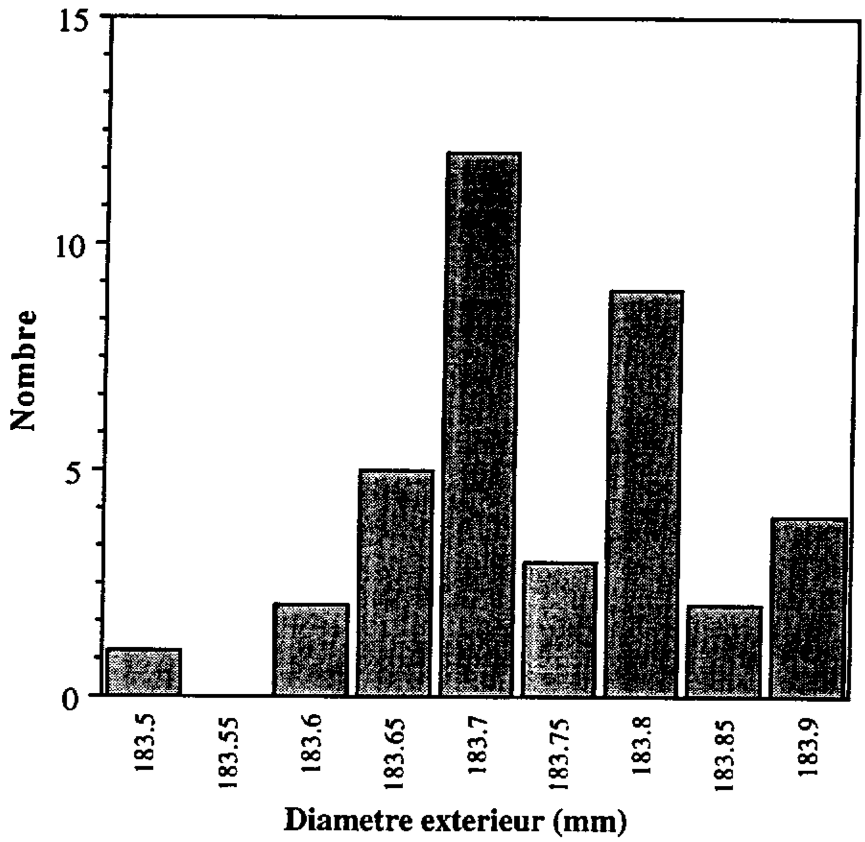

Diametres extérieurs mesurés sur cavités 1,5 GHz (38 mono- et 5 pentacellulaires) (1992)

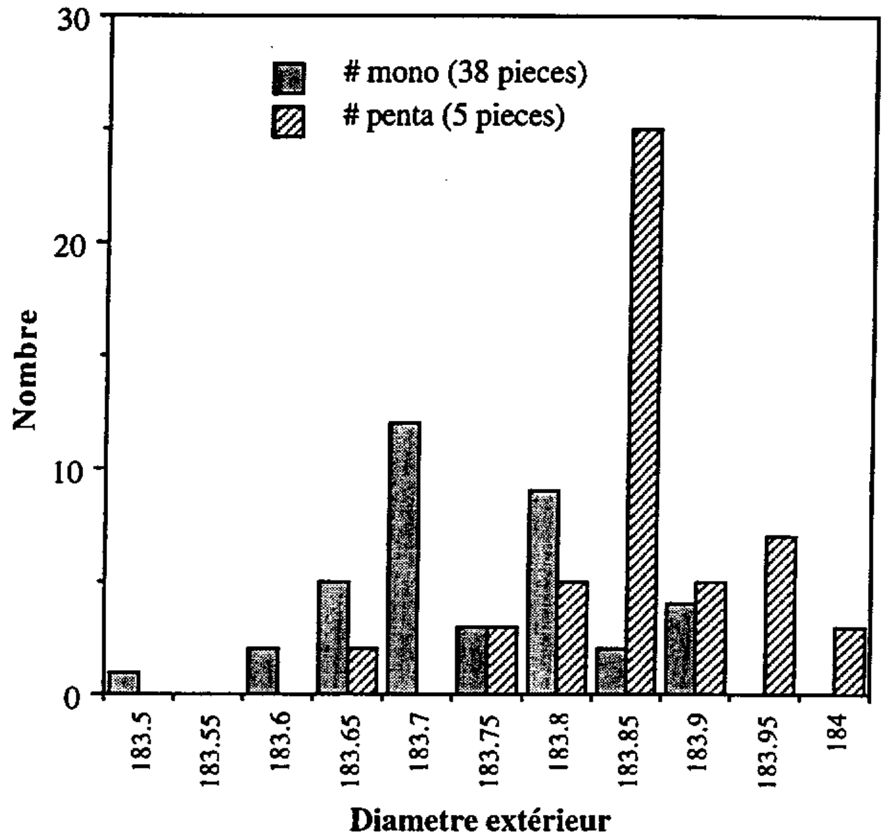

MULTI5 DIAFREQ 940620

	DIA 1	DIA 2	DIA 3	DIA 4	DIA 5	MAX DIA	MEAN DIA	MEAN DIA 2+3+	FREQ 1	FREQ1/MAXDIA	FREQ1/MEANDIA	FREQ1/MEANDI
CAV 1	183.95	183.825	183.875	183.85	183.825	183.95	183.865	183.85	1447.39	7.86838815	7.87202567	7.87266794
CAV2	183.75	183.975	184	183.95	183.85	184	183.905	183.933333	1445.85	7.85788043	7.86193959	7.86072852
CAV3	183.875	183.825	183.825	183.75	183.85	183.875	183.825	183.808333	1447.43	7.87181509	7.87395621	7.87467017
CAV4	183.825	183.9	183.9	183.9	183.85	183.9	183.875	183.883333	1447.8	7.87275693	7.87382733	7.8734705
						183.93125	183.8675					
						0.06875	0.0375					
						-0.05625	-0.0425					

150

C. HAUVILLER
March 4, 1995

HYDROFORMING GIVES GOOD RESULTS FOR COPPER CAVITIES. WHAT ABOUT NIOBIUM?

Annealed niobium has some mechanical properties similar to copper ones:
- maximum elongation up to 50%
- Young's modulus 104 MPa

Unsuccessful trial with extruded tubes obtained from CEBAF, but poor metallurgical quality (anisotropy)!

Annealing 1400°C.1h.

TIME (mn)	0	1	2	3	4	5	6	7	
PRESSURE (bar)	0	80	100	116	123	125	125	125	
DIES'GAP (mm)	57	57.5	59.2	60.6	61.8	62.7	62.8	63.9	RUPTURE
RADIUS (mm)	76	76.5	77.3	78.2	79.3	80.1	80.5	81.1	13.40%

Table 3
Values of pressure, gap and radius during experiment

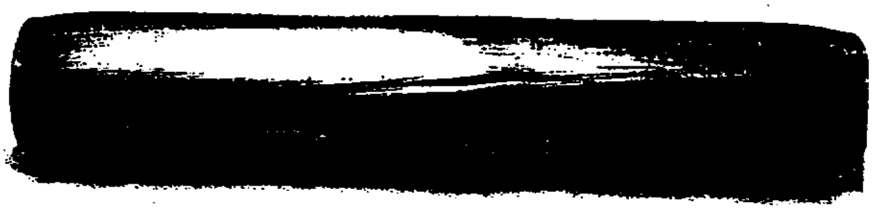

Figure 4
Photograph of the cracked tube

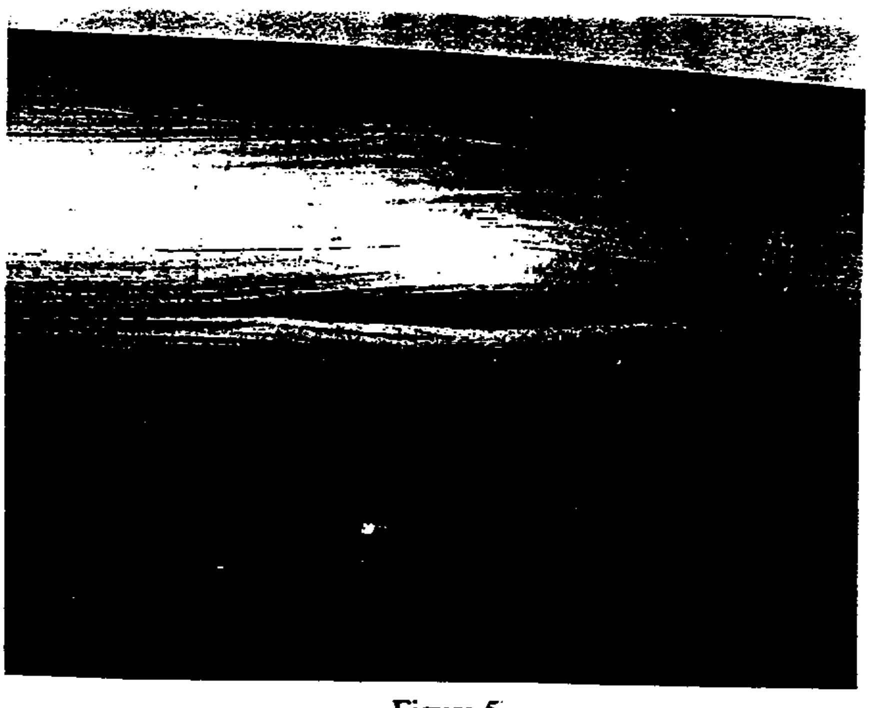

Figure 5
Photograph of the crack

WHAT ARE THE MANUFACTURING STEPS ?

	COPPER	NIOBIUM
TUBE		
Procurement	Easy (above 500MHz) Cheap	Difficult to get the required quality Expansive (not for large series ?)
Machining (turning)	Easy (if necessary)	
FORMING		
Tooling	The largest investment (becomes negligeable for large series)	
Swaging	Not necessary needed (depends upon of the cavity shape)	
Hydroforming		
CLEANING		
HEAT TREATMENT	600C , 1 hour	Around 1400C, 1 hour

C. HAUVILLER
March 4, 1995

PROCUREMENT OF THE HIGH QUALITY NIOBIUM TUBES IS PRESENTLY THE MAJOR DRAWBACK.

TWO POSSIBLE WAYS EXISTS:

- Seamless tubes: new processing method proposed by HEREAUS
- Rotary swaged longitudinally welded tubes proposed by CEA.

154

THE OTHER STEPS SHOULD BE FEASIBLE WITH NO MAJOR DIFFICULTIES............

Publications on Hydroforming

C. Hauviller- Fully Hydroformed RF Cavities - IEEE 1989 Particle Accelerator Conference (March 1989)

S. Dujardin, J. Genest, C. Hauviller, R. Jaggi, B. Jean-Prost- Hydroforming monolithic cavities in the 300 MHz range - 1990 European Particle Accelerator Conference (June 1990)

G. Cavallari et al.- Status report on SC RF cavities at CERN - 5th Workshop on RF Superconductivity - DESY - (August 1991)

C. Hauviller - Hydroforming of monolithic parts to produce RF cavities for particle accelerators - Plasticity '91: Third International Symposium on Plasticity and its current Applications (August 1991)

Ph. Bernard et al.- Superconducting Niobium Sputter-Coated Copper Cavities at 1500 MHz - 1992 European Particle Accelerator Conference (March 1992)

Ph. Bernard et al.- Superconducting Hydroformed Niobium Sputter Coated Copper Cavities at 1.5 GHz - 6th Workshop on RF Superconductivity - CEBAF, Newport News (October 1993)

D. Bloess et al.- Superconducting, Hydroformed, Niobium Sputter Coated Copper Cavities at 1.5 GHz -1994 European Particle Accelerator Conference (June 1994)

A NEW METHOD FOR FORMING SEAMLESS 1.5 GHZ MULTICELL CAVITIES STARTING FROM PLANAR DISKS.

V. Palmieri, R. Preciso, V.L. Ruzinov*, S.Yu. Stark*, I.I. Kulik^

ISTITUTO NAZIONALE DI FISICA NUCLEARE

Laboratori Nazionali di Legnaro,

I-35020 Legnaro (Padua), Italy

* On leave from Moscow Institute of Steel and Alloys, Moscow, Russia.
^ On leave from the Institute for the Low Temperature Physics and Engineering, Kharkov, Ukraine.

Work performed in the framework of the CERN-INFN collaboration on superconducting cavities.

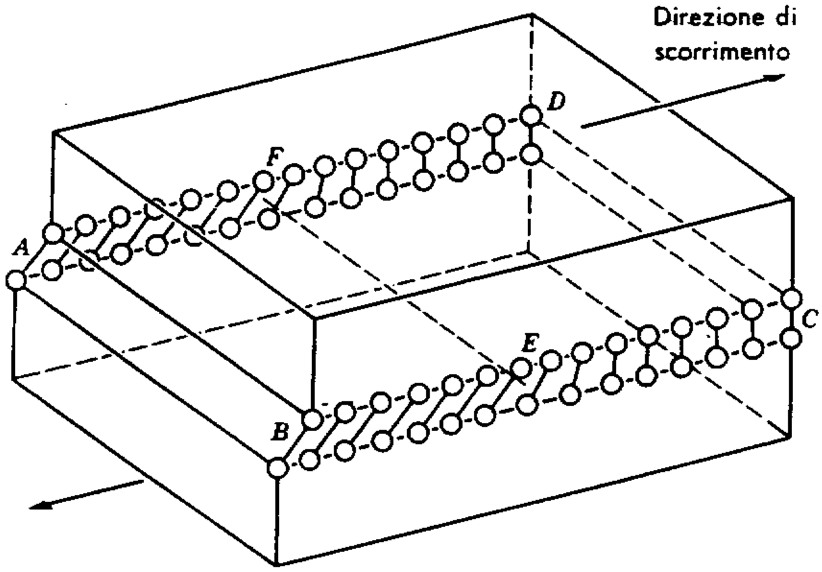

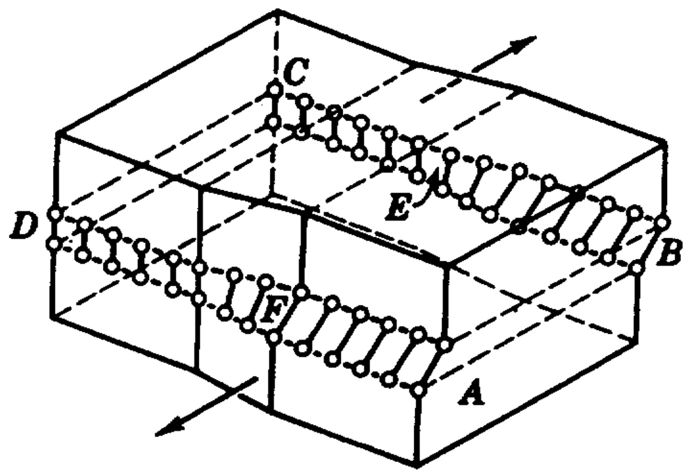

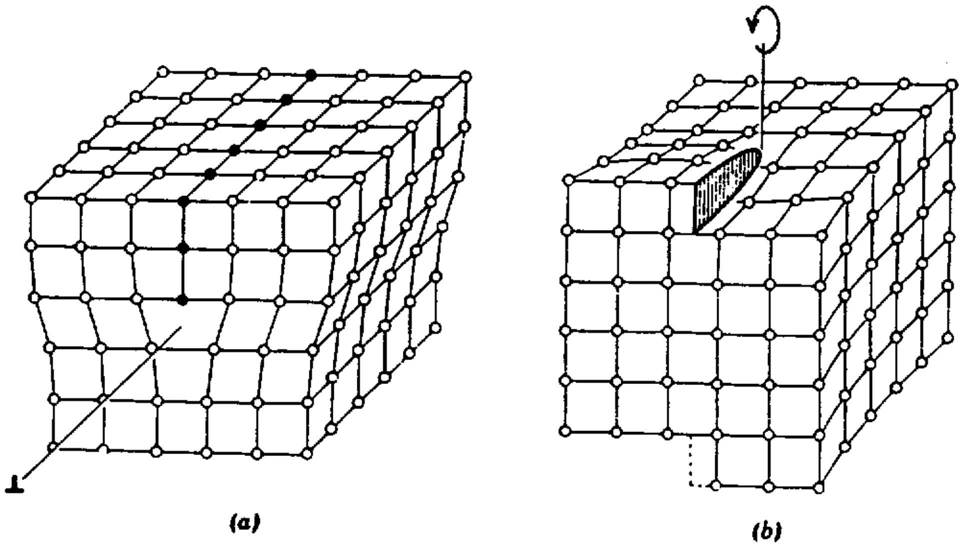

Fig. 4.2 Geometria di dislocazioni semplici: (*a*) lineari (*b*) elicoidali. Sono indicate pure le linee normalmente usate per rappresentare le dislocazioni e i loro simboli, ⊥ e ⊙.

The application of load to the workpiece, if generating shape distortions, generates plastic deformations

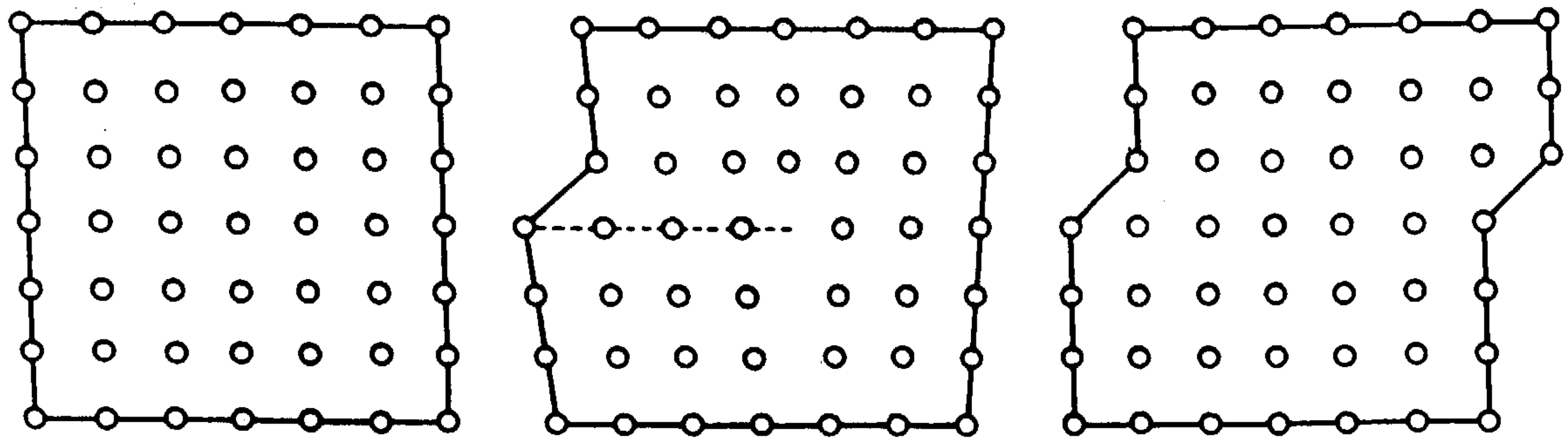

Moto di una dislocazione sotto l'azione di uno scorrimento che tende a muovere la superficie più alta del campione verso destra. (Secondo Taylor).

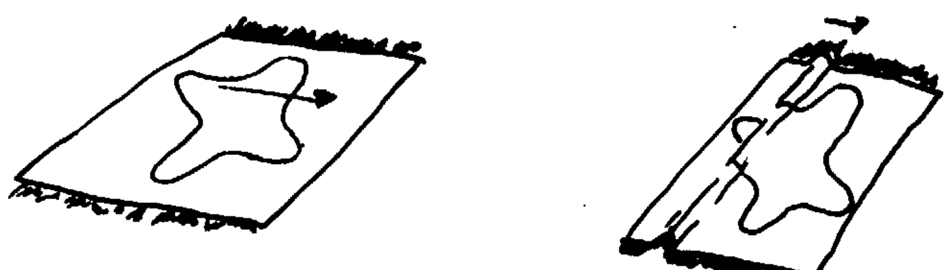

plastic deformations do not involve volumetric changes

A perfect plastic material does not harden

Sistemi di scorrimento osservati in cristalli

STRUTTURA	PIANO DI SCORRIMENTO	DIREZIONE DI SCORRIMENTO	NUMERO DI SISTEMI DI SCORRIMENTO	
CFC Cu, Al, Ni, Pb, Au, Ag, γFe, ...	{111}	$\langle 1\bar{1}0\rangle$	4 × 3 = 12	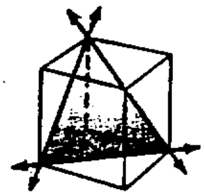
CCC αFe, W, Mo, ottone β	{110}	$\langle \bar{1}11\rangle$	6 × 2 = 12	
αFe, Mo, W, Na	{211}	$\langle \bar{1}11\rangle$	12 × 1 = 12	
αFe, K	{321}	$\langle \bar{1}11\rangle$	24 × 1 = 24	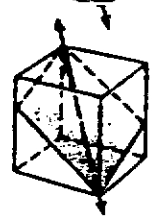
EC Cd, Zn, Mg, Ti, Be, ...	(0001)	$\langle 11\bar{2}0\rangle$	1 × 3 = 3	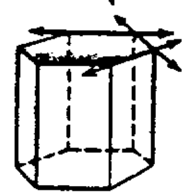
Ti	$\{10\bar{1}0\}$	$\langle 11\bar{2}0\rangle$	3 × 1 = 3	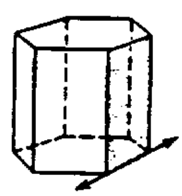
Ti, Mg	$\{10\bar{1}1\}$	$\langle 11\bar{2}0\rangle$	6 × 1 = 6	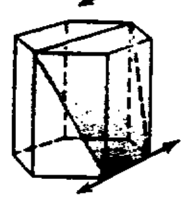
NaCl, AgCl	{110}	$\langle 1\bar{1}0\rangle$	6 × 1 = 6	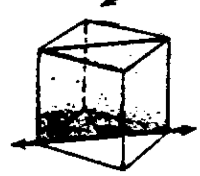

Tab. IV.2. ***Energia e sforzo di Peierls di alcuni metalli fcc e bcc, calcolati secondo vari modelli.***

Elemento	Sistema di slittamento Piano	Direzione	A: E_p erg/cm	A: σ_p dyn/cm²	B: E_p erg/cm	B: σ_p dyn/cm²	C: E_p erg/cm	C: σ_p dyn/cm²
Al	(001)	[010]	3.8×10^{-9}	7.2×10^{7}	8.0×10^{-9}	1.5×10^{9}	1.1×10^{-8}	2.1×10^{9}
	(001)	[110]	2.5×10^{-10}	9.7×10^{5}	2.8×10^{-9}	1.1×10^{7}	2.4×10^{-8}	9.0×10^{7}
	(111)	[01̄1]					4.2×10^{-9}	1.6×10^{7}
Cu	(001)	[010]	7.5×10^{-7}	1.8×10^{9}	8.0×10^{-7}	1.9×10^{9}	6.7×10^{-7}	1.6×10^{9}
	(001)	[110]	1.8×10^{-9}	8.5×10^{6}	1.3×10^{-9}	6.3×10^{7}	1.2×10^{-9}	5.7×10^{7}
	(111)	[01̄1]					1.9×10^{-9}	9.2×10^{6}
Ni	(001)	[010]	8.6×10^{-7}	2.1×10^{9}	1.2×10^{-6}	3.1×10^{9}	1.7×10^{-6}	4.4×10^{9}
	(001)	[110]	1.4×10^{-9}	7.3×10^{6}	2.2×10^{-9}	1.1×10^{8}	3.6×10^{-8}	1.8×10^{8}
	(111)	[01̄1]					6.2×10^{-9}	3.1×10^{7}
Fe	(001)	[010]	2.2×10^{-6}	8.5×10^{9}	9.3×10^{-7}	3.6×10^{9}	1.1×10^{-6}	4.1×10^{9}
	(001)	[110]	1.1×10^{-5}	2.1×10^{10}	3.7×10^{-6}	7.1×10^{9}	1.7×10^{-5}	$3{\cdot}2\times10^{10}$
	(101)	[010]	1.4×10^{-7}	5.3×10^{6}	2.3×10^{-7}	8.9×10^{8}	4.3×10^{-9}	1.7×10^{6}
	(101)	[101̄]	9.7×10^{-9}	1.9×10^{7}	1.1×10^{-8}	2.2×10^{7}	2.1×10^{-6}	4.1×10^{9}
	(101)	[111̄]					1.5×10^{-8}	2.9×10^{7}
W	(001)	[010]	2.4×10^{-7}	7.5×10^{9}	1.7×10^{-7}	5.5×10^{9}	6.8×10^{-6}	2.1×10^{10}
	(001)	[110]	7.7×10^{-6}	1.2×10^{10}	2.6×10^{-6}	4.1×10^{9}	8.9×10^{-5}	1.4×10^{11}
	(101)	[010]	1.2×10^{-8}	3.7×10^{7}	7.1×10^{-9}	2.2×10^{9}	3.6×10^{-7}	1.1×10^{9}
	(101)	[101̄]	1.1×10^{-6}	1.7×10^{9}	1.5×10^{-6}	2.4×10^{9}	1.4×10^{-5}	2.1×10^{10}
	(101)	[111̄]	3.2×10^{-11}	1.3×10^{5}	2.2×10^{-8}	9.4×10^{7}	1.4×10^{-7}	2.2×10^{6}
Ta	(001)	[010]	3.1×10^{-7}	9.1×10^{8}	2.9×10^{-7}	8.6×10^{8}	1.5×10^{-6}	4.5×10^{9}
	(001)	[110]	1.7×10^{-5}	2.5×10^{10}	2.3×10^{-6}	3.3×10^{9}	2.4×10^{-5}	3.5×10^{10}
	(101)	[010]	2.2×10^{-8}	6.4×10^{7}	1.4×10^{-7}	4.2×10^{8}	6.2×10^{-9}	1.8×10^{9}
	(101)	[101̄]	4.6×10^{-7}	6.7×10^{9}	2.5×10^{-8}	3.6×10^{7}	3.1×10^{-6}	4.5×10^{9}
	(101)	[111̄]					2.2×10^{-9}	3.2×10^{7}
Nb	(001)	[010]	1.7×10^{-9}	5.8×10^{6}	1.3×10^{-8}	4.4×10^{7}	1.6×10^{-8}	5.4×10^{9}
	(001)	[110]	5.3×10^{-6}	9.0×10^{9}	4.3×10^{-7}	7.4×10^{9}	2.4×10^{-5}	4.1×10^{10}
	(101)	[010]	9.3×10^{-12}	3.2×10^{4}	2.4×10^{-9}	8.2×10^{6}	7.0×10^{-9}	2.4×10^{8}
	(101)	[101̄]	4.5×10^{-7}	7.6×10^{8}	9.5×10^{-9}	1.6×10^{9}	3.2×10^{-8}	5.4×10^{9}
	(101)	[111̄]					2.5×10^{-8}	4.3×10^{7}

160

ABDE (010)
DB [$\bar{1}01$]

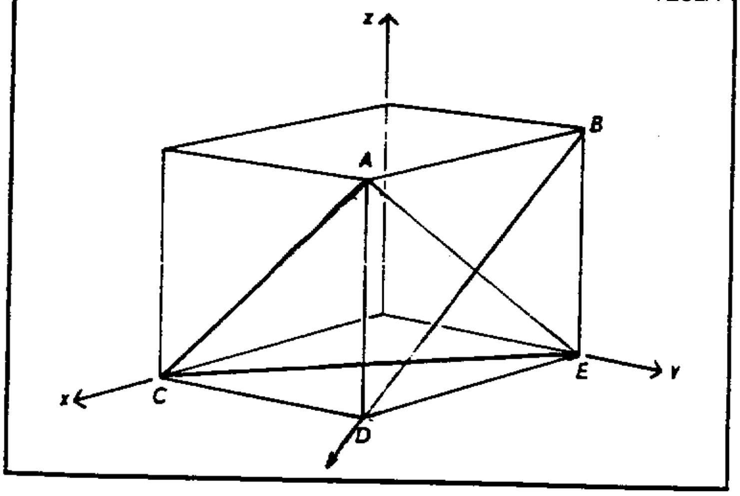

Struttura cubica nella quale sono individuati piani e direzioni.

(101)
[101]

Fe (110) [$\bar{1}11$]
Nb (101) [010]

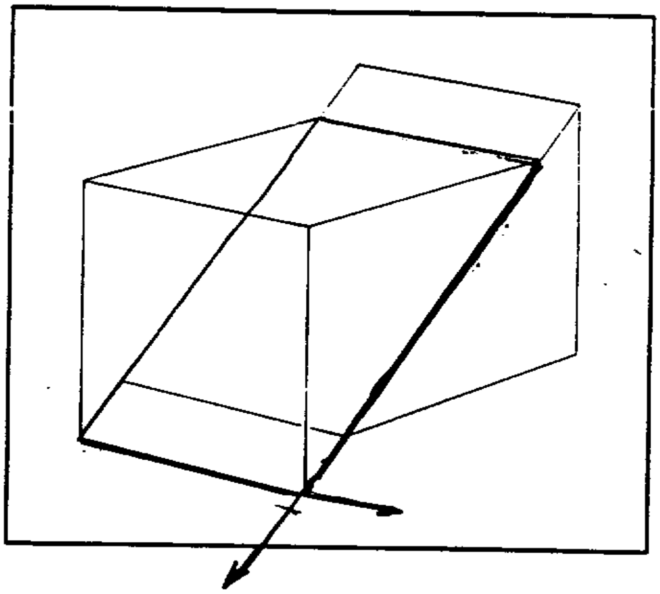

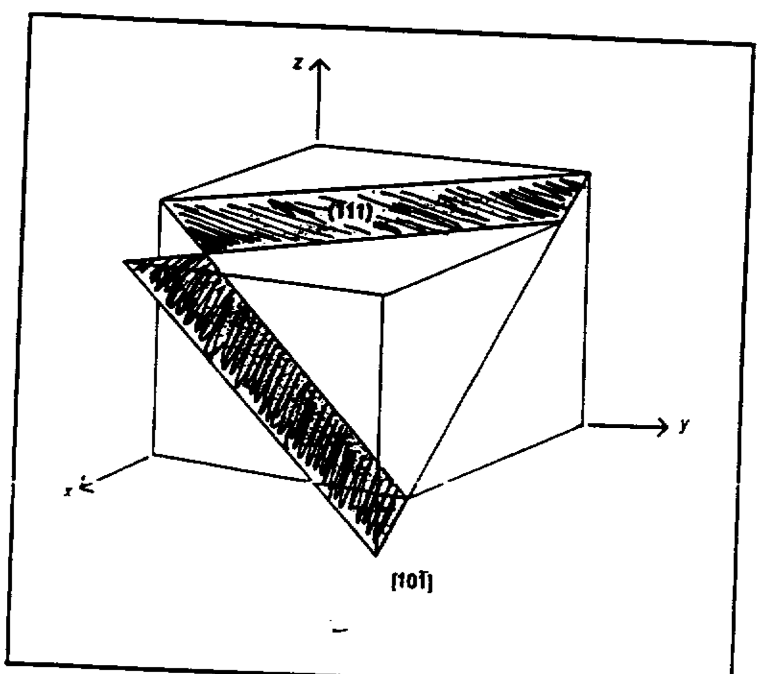

Sistema di slittamento (111) [10$\bar{1}$] in un cristallo con struttura cubica a facce centrate. La parte superiore del cristallo slitta sul piano (111) nella direzione [10$\bar{1}$].

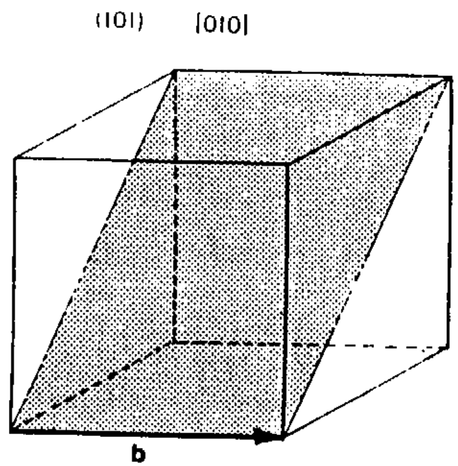

Fig. IV.11. Il sistema di slittamento caratteristico del niobio.

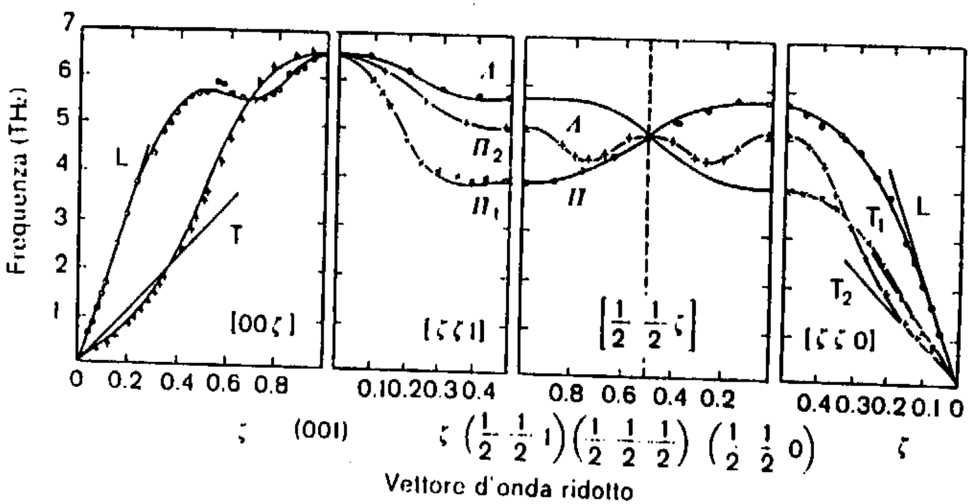

Le relazioni di dispersione per i modi normali di vibrazione del niobio. Si notino la marcata rigidità della branca [001]L e il comportamento singolarmente soffice della branca [110]T_2. Questa ultima, per piccoli valori del vettore d'onda, presenta addirittura la concavità verso l'alto. Queste anomalie nelle relazioni di dispersione determinano l'eccezionale configurazione del sistema di slittamento del niobio.

(da Y. Nakagawa and A. D. B. Woods, Lattice Dynamics of Niobium, Phys, Rev. Lett. *11* (6) 271. (1963)).

162

TENSILE PROPERTIES

Effect of Temperature on Tensile Properties of Annealed Niobium (after T. J. Heal[3])

Test temp. °C	Ultimate strength ton/in.^{2}	Limit of proportionality ton/in.^{2}	Elongation (on 1·25 in.) per cent	Young's modulus lb./in.^{2} × 10^6
20	22·1	18·6	19·2	15·2
200	23·9	15·5	14·2	14·7
300	20·0	13·1	13·2	14·5
400	21·9	14·3	13·3	14·6
500	22·0	12·6	9·6	14·2
600	20·8	8·0	17·5	--
660	20·8	7·1	22·4	—
800	20·1	5·8	20·7	—
970	12·3	5·2	37·5	—
1050	7·2	4·4	42·5	—

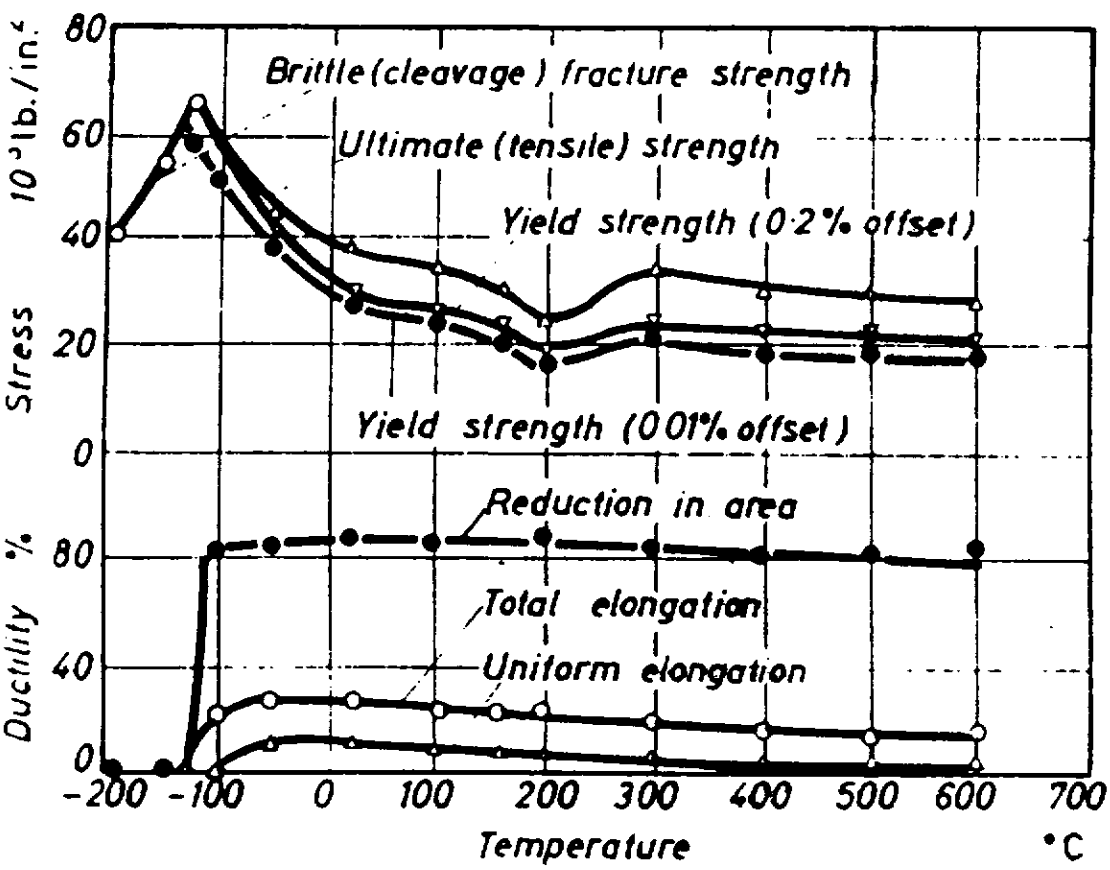

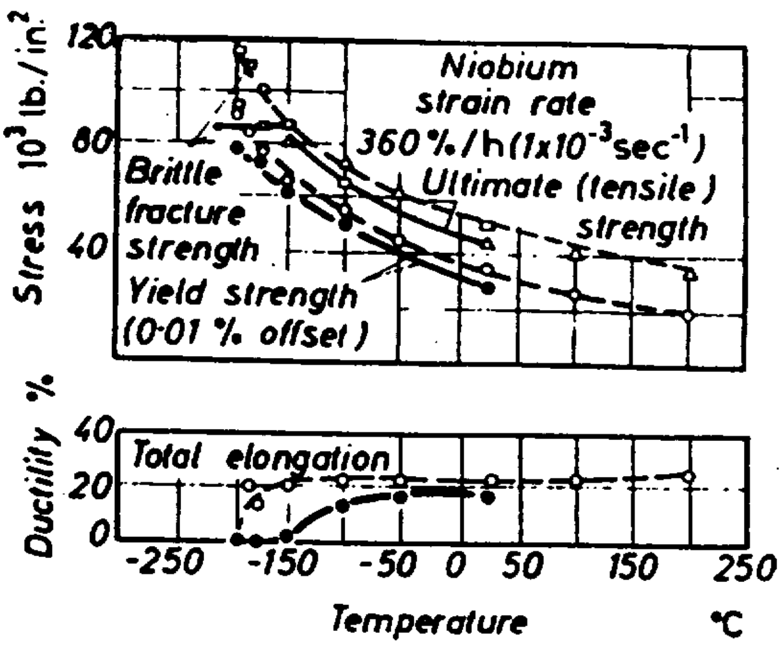

Figure 9.16. Effect of recrystallization temperature on brittle behaviour in niobium. ●—●— *Recrystallized, 2 h at 2000°C;* ○--○— *recrystallized, 2 h at 1475°C. after* E. T. WESSEL *and* D. D. LAWTHERS[12])

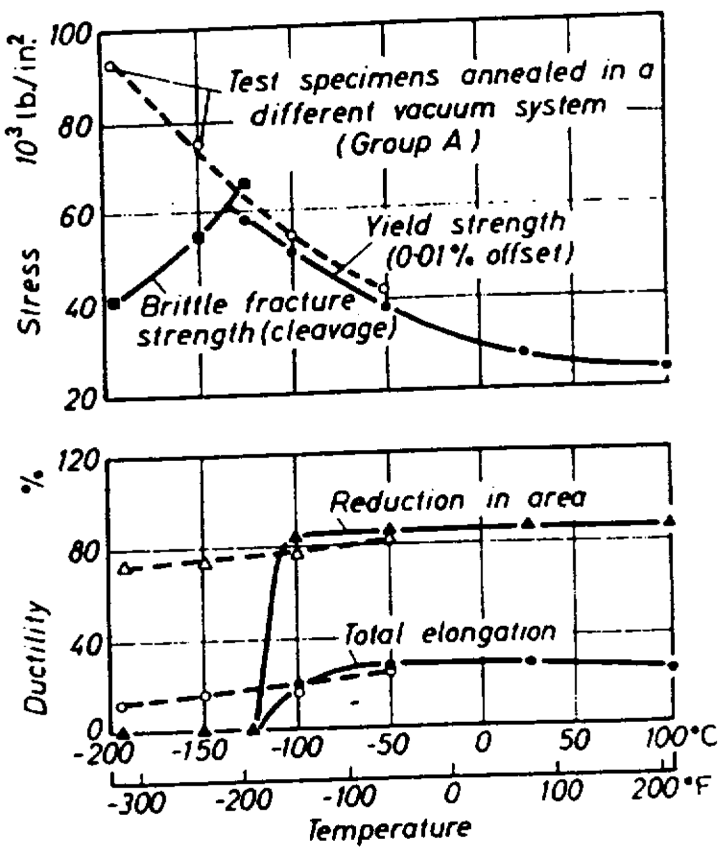

Figure 9.21. Effect of strain rate and annealing temperature on the ductile-to-brittle transition of niobium. —●—● *Strain rate* 360%/h (1 × 10⁻³ sec⁻¹); ···○—○ *Strain rate* 4000%/h (1·11 × 10⁻² sec⁻¹) (*after* E. T. WESSEL *and* D. D. LAWTHERS[12])

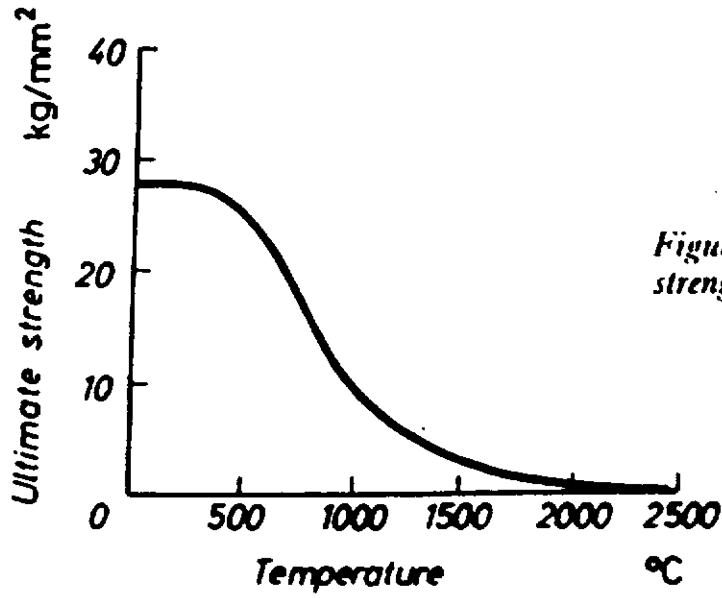

Figure 9.5. Effect of temperature on t strength of niobium (after B. L. MOR *and* L. M. FITZGERALD[8])

402

TENSILE PROPERTIES

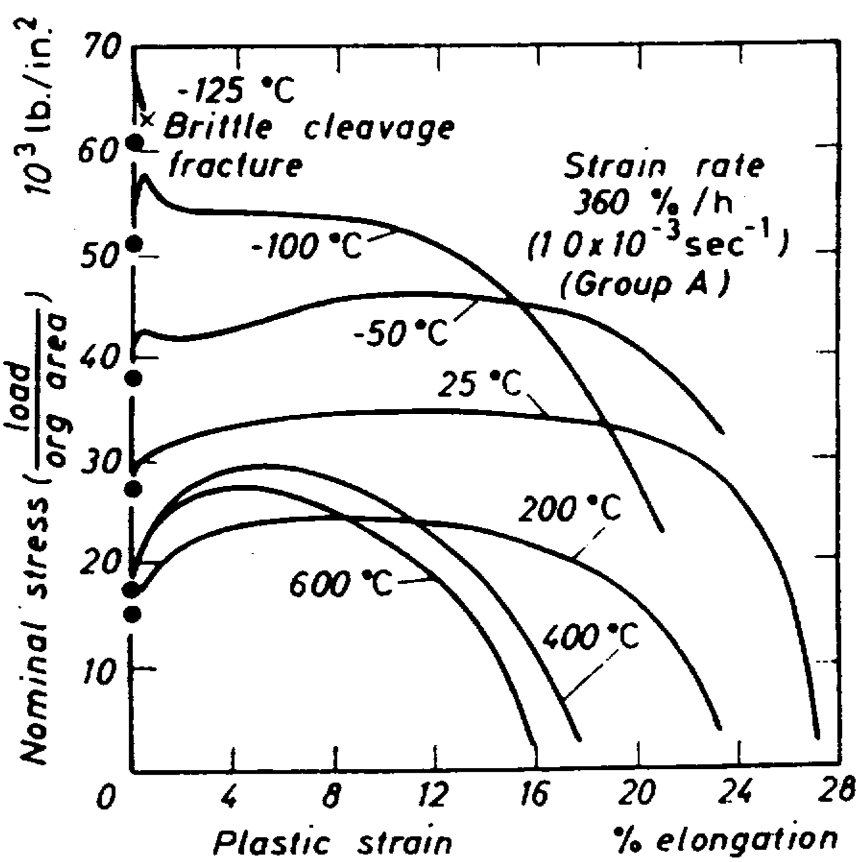

Figure 9.6. Effect of temperature on stress strain curves of annealed niobium (after E. T. WESSEL *and* D. D. LAWTHERS[12])

165

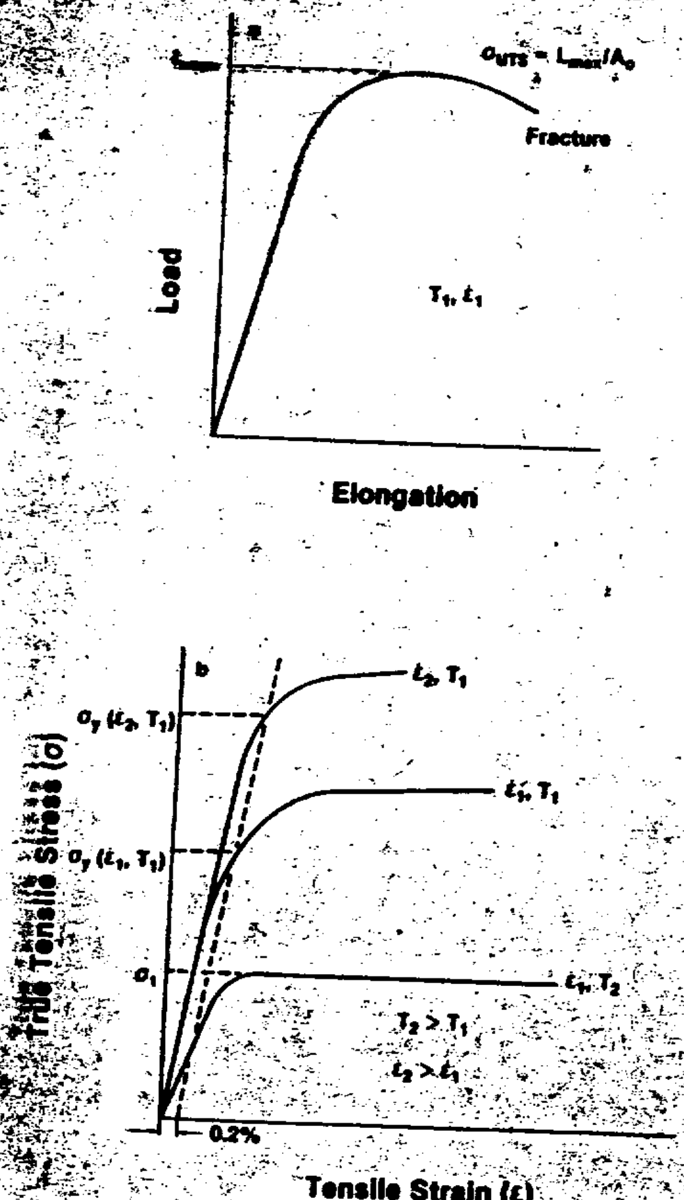

(a) Typical load–elongation curve for a polycrystalline metal. (b) Results of the load–elongation data of (a) converted to true tensile stress and tensile strain. Also shown is the effect of increasing temperature from T_1 to T_2 and strain rate from $\dot{\varepsilon}_1$ to $\dot{\varepsilon}_2$. The schematic data are for a test performed at elevated temperatures.

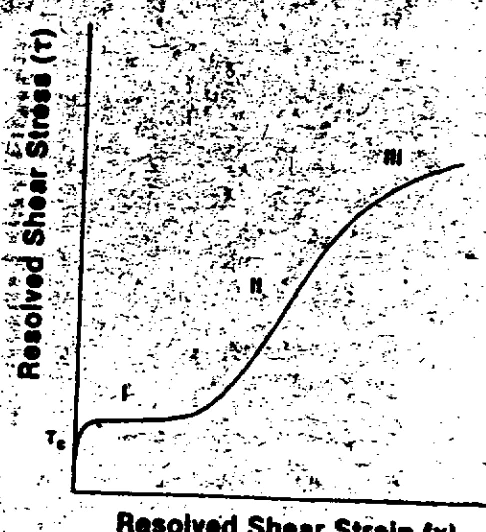

Typical tensile stress–strain curve for an fc single crystal measured at room temperature.

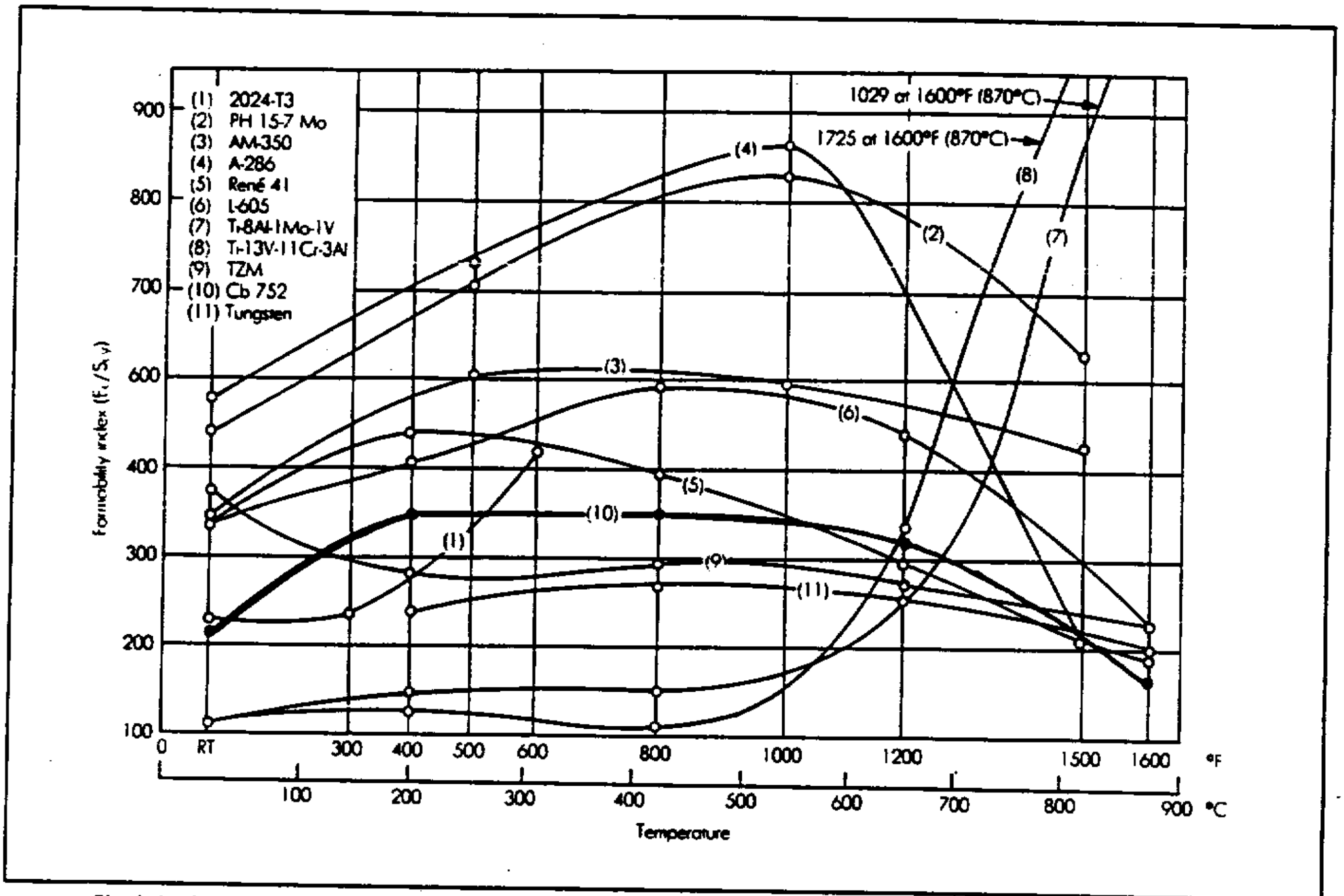

Elastic-buckling formability index vs. temperature for manual spinning, where E_c is the compressive modulus and S_{cy} is the compressive yield strength of the workpiece material.

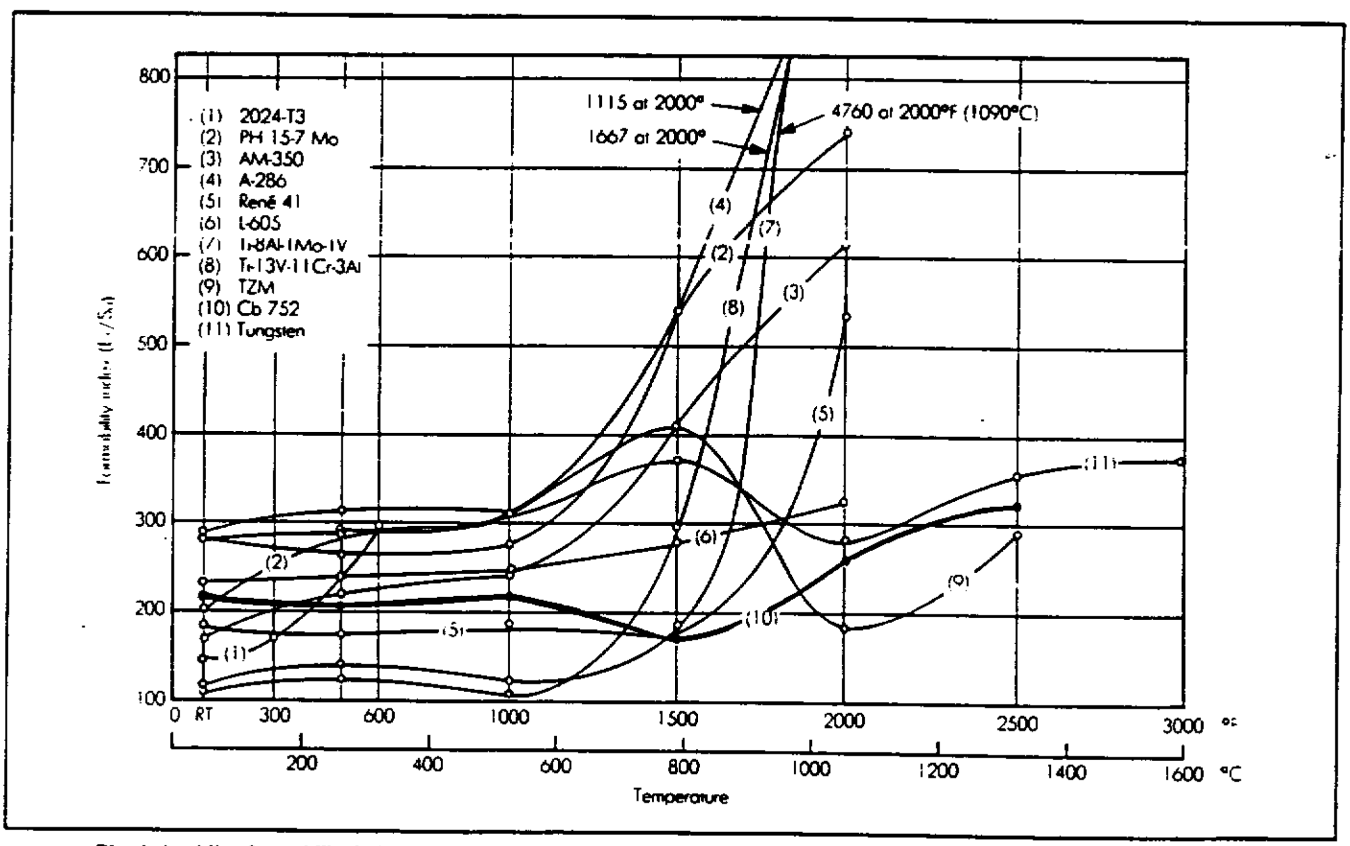

Plastic-buckling formability index vs. temperature for manual spinning, where E_t is the tensile modulus and S_u is the ultimate modulus of the workpiece material.

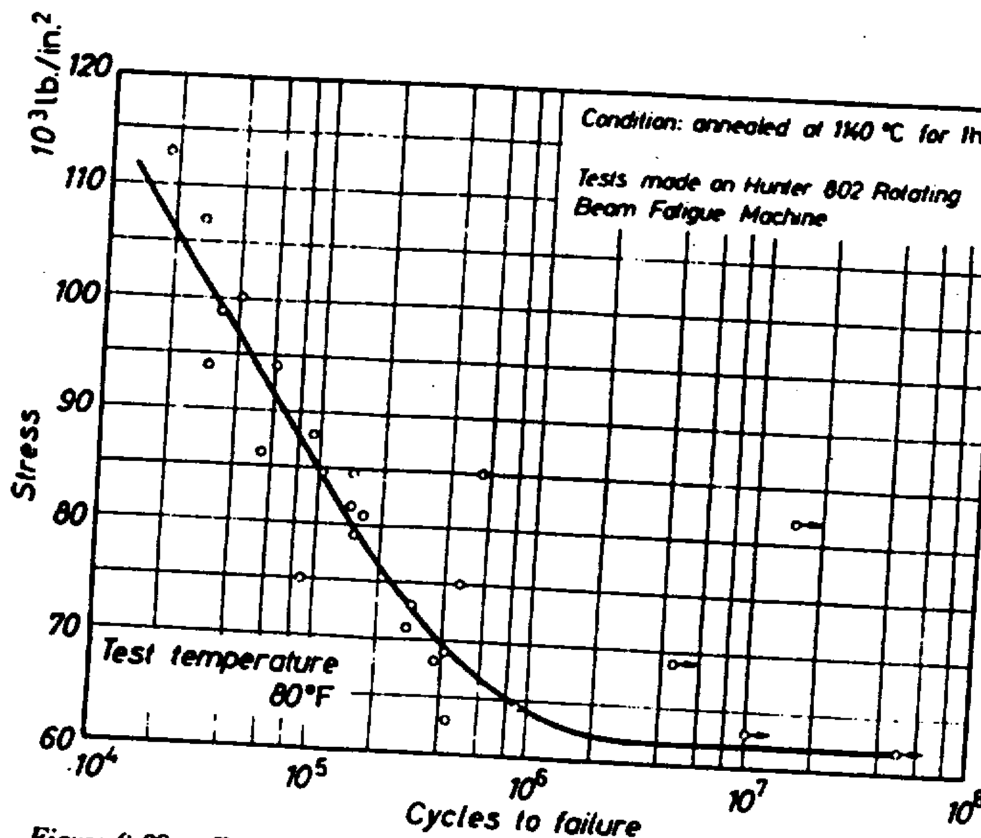

Figure 9.29. Fatigue characteristics of 0·004 in. *diam. tantalum wire* (*after* A. BORNEMANN *et al.*[14])

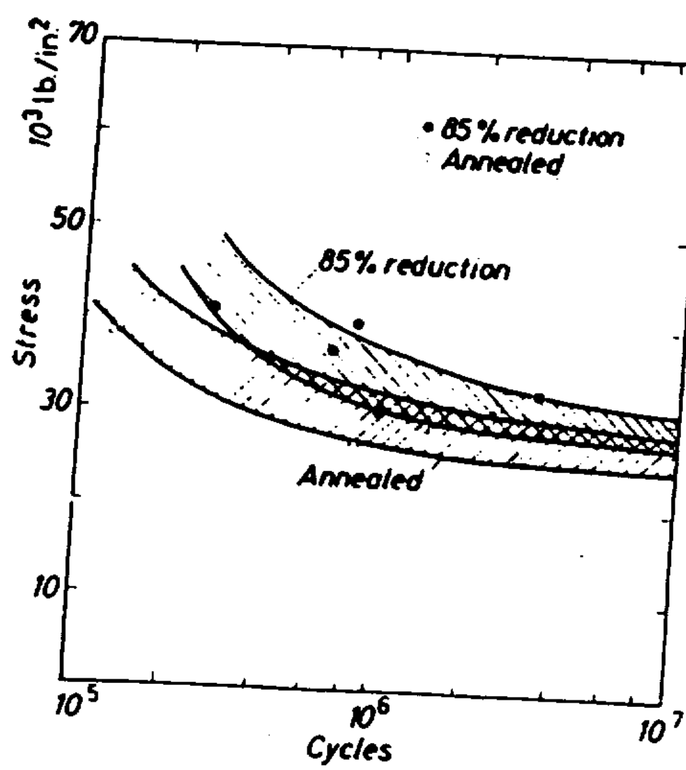

Figure 9.30. Flexure fatigue S–N curve for annealed and cold worked powder metallurgy niobium (*after* R. T. BEGLEY[20])

Process Comparisons

Criteria	Mode			
	Hot	Cold	Warm	Isothermal
Ductility	Good	Poor to Good	Moderate	Ideal
Forming Loads	Moderate	High	Moderate	Low
Forming Rate	Fast	Fast	Fast	Low
Dimensional Precision	Poor	Good	Moderate to Good	Good
Surface Finish	Poor	Good	Moderate	Good
Material Conservation	Poor	Moderate	Good	Good
Die Cost	Moderate	Moderate	High	High
Die Life	Poor	Good	Moderate	Poor

Forming operations achieve the desired shape of the workpiece by imparting plastic deformations

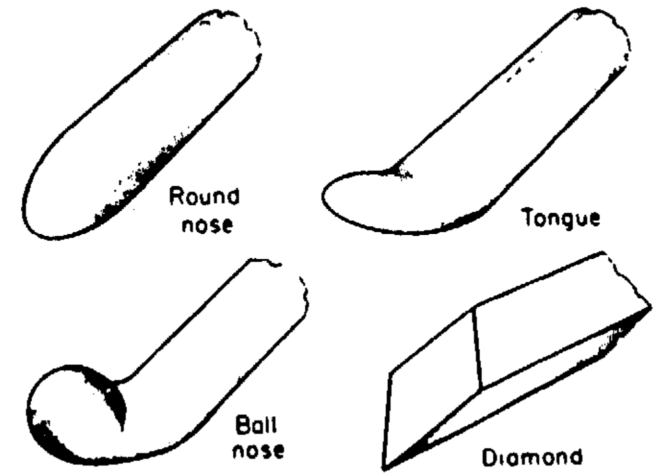

Round-nose, tongue and ball-nose tools are used for spinning; diamond tool, for trimming.

Typical shapes of working ends of tools used in manual spinning

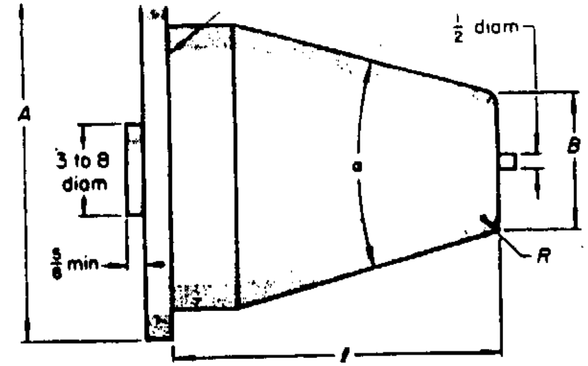

Fig. 11. Typical profile of a mandrel for power spinning of cones

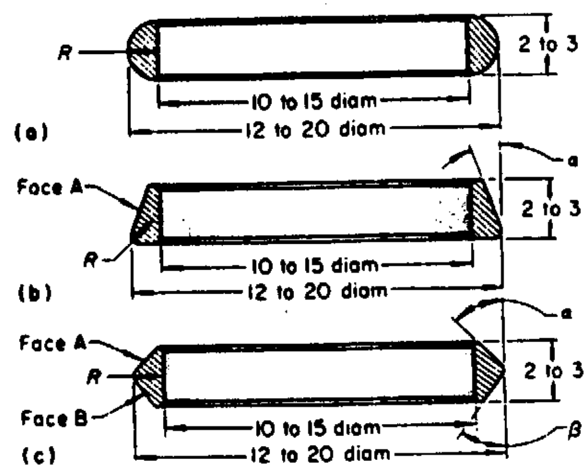

Fig. 12. Typical rollers used in spinning of cones and hemispheres

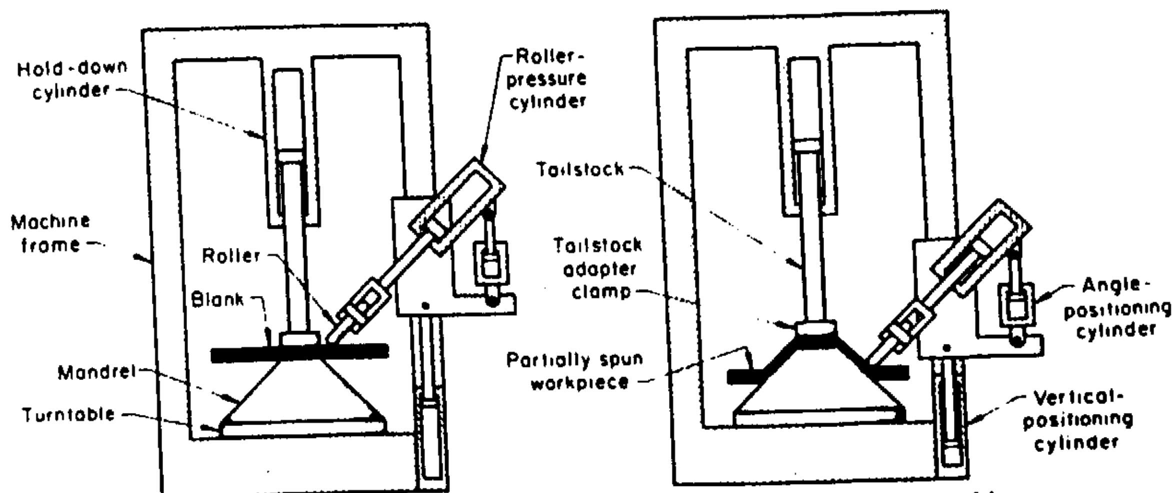

Schematic illustration of power spinning in a vertical machine

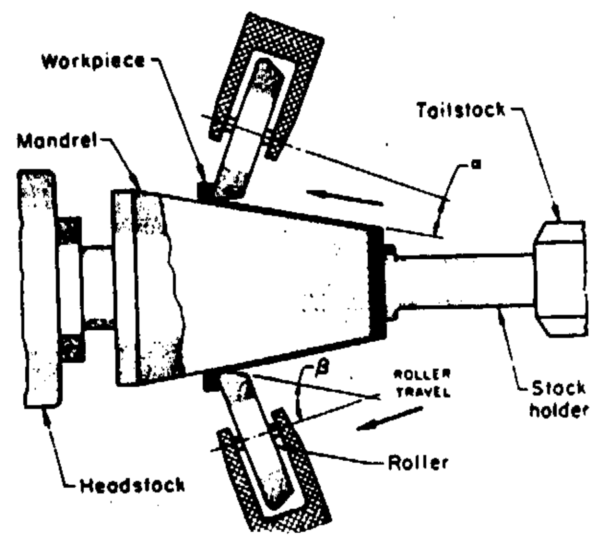

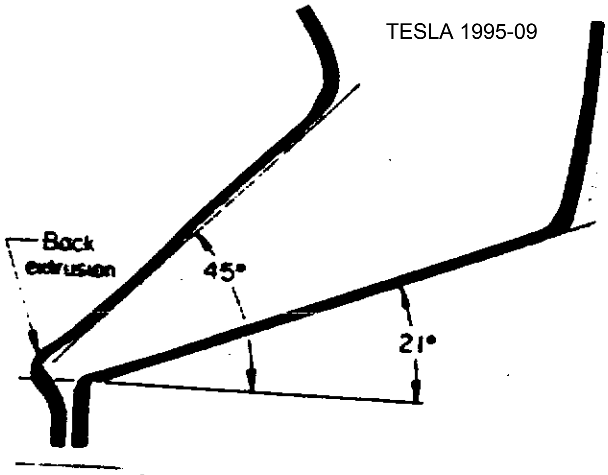

Back extrusion as a result of overreduction in power spinning of low-carbon steel

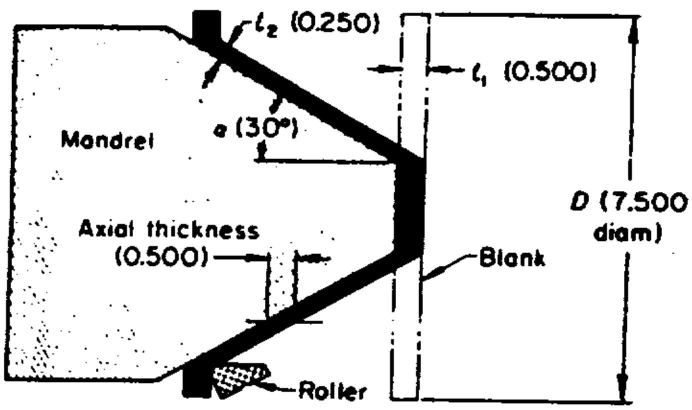

Fig. 7. Setup and dimensional relations for one-operation power spinning of a cone. See text for application of sine law in relation to this illustration.

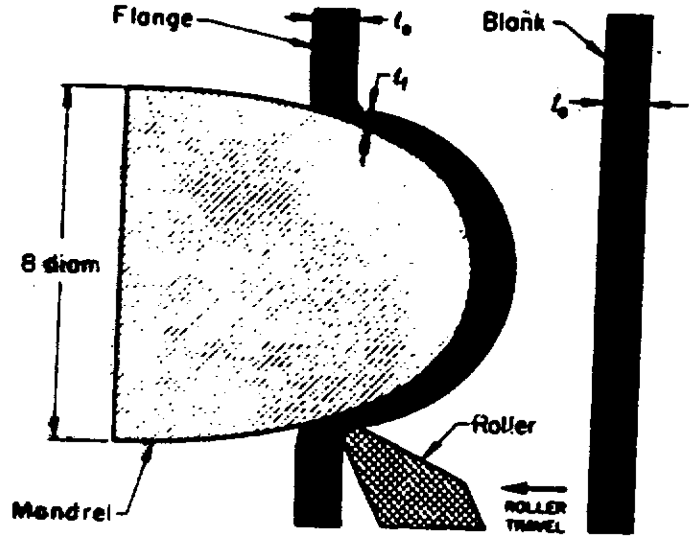

Setup for testing shear spinnability

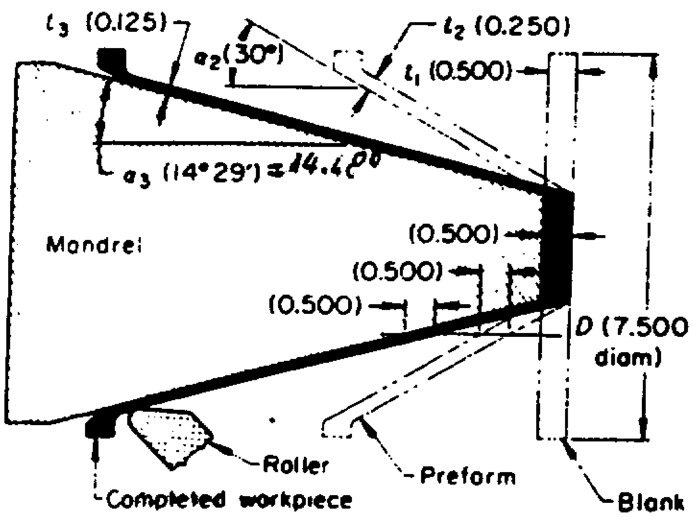

Setup and dimensional relations for two-operation spinning of a cone to a small angle (less than 35° included angle)

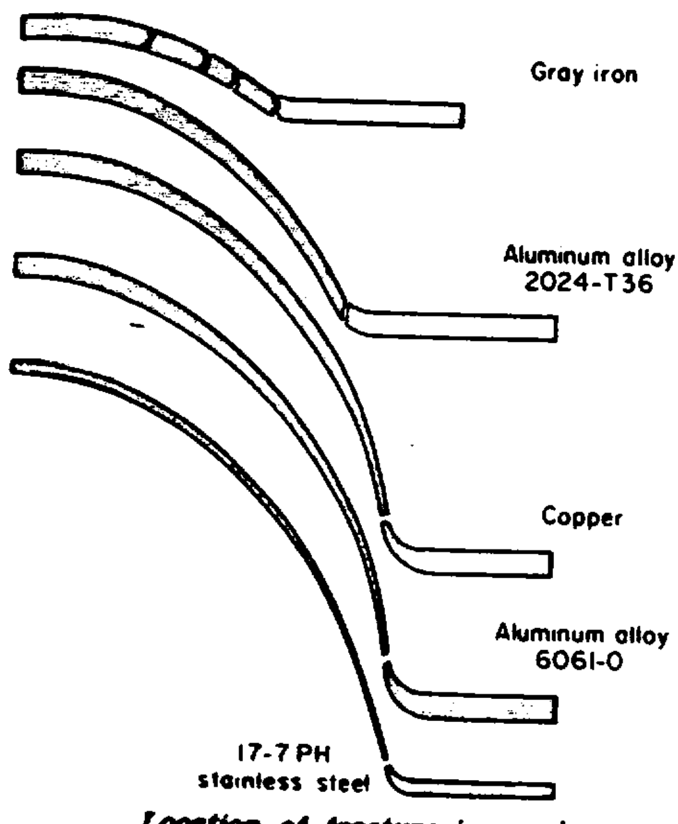

Location of fracture in specimens of five different metals that were tested for shear spinnability

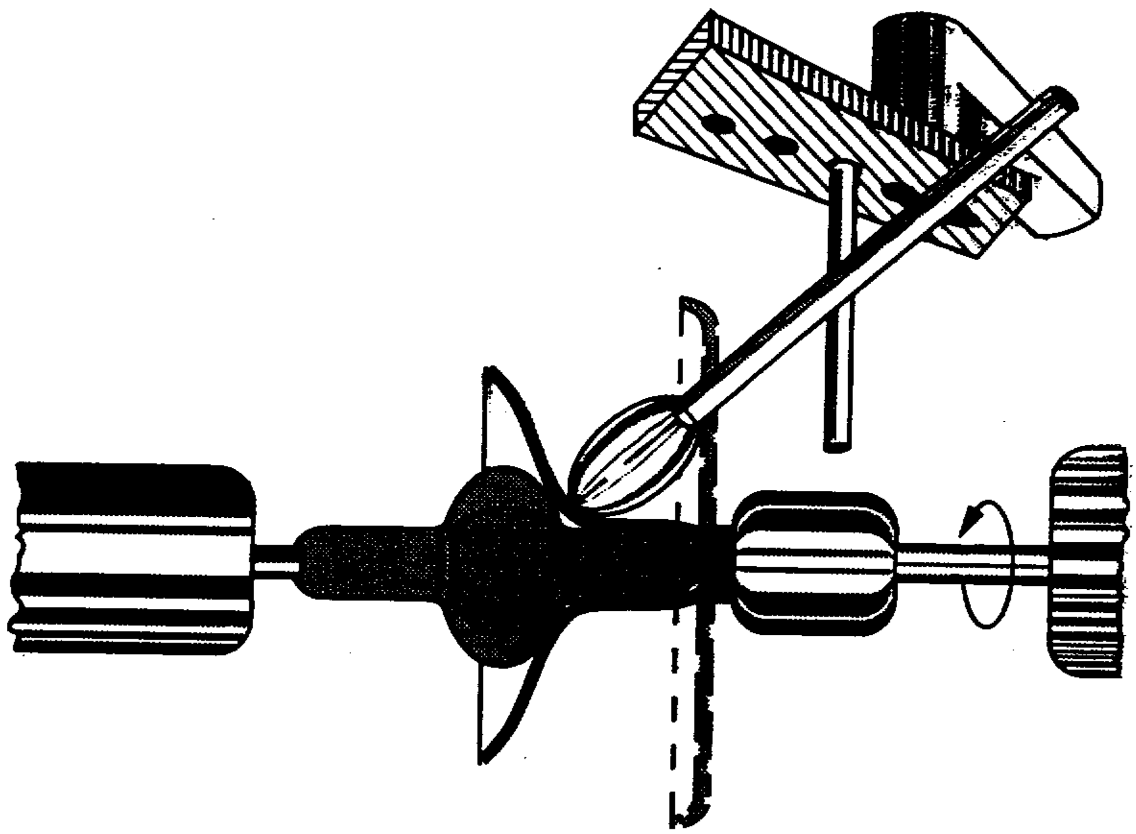

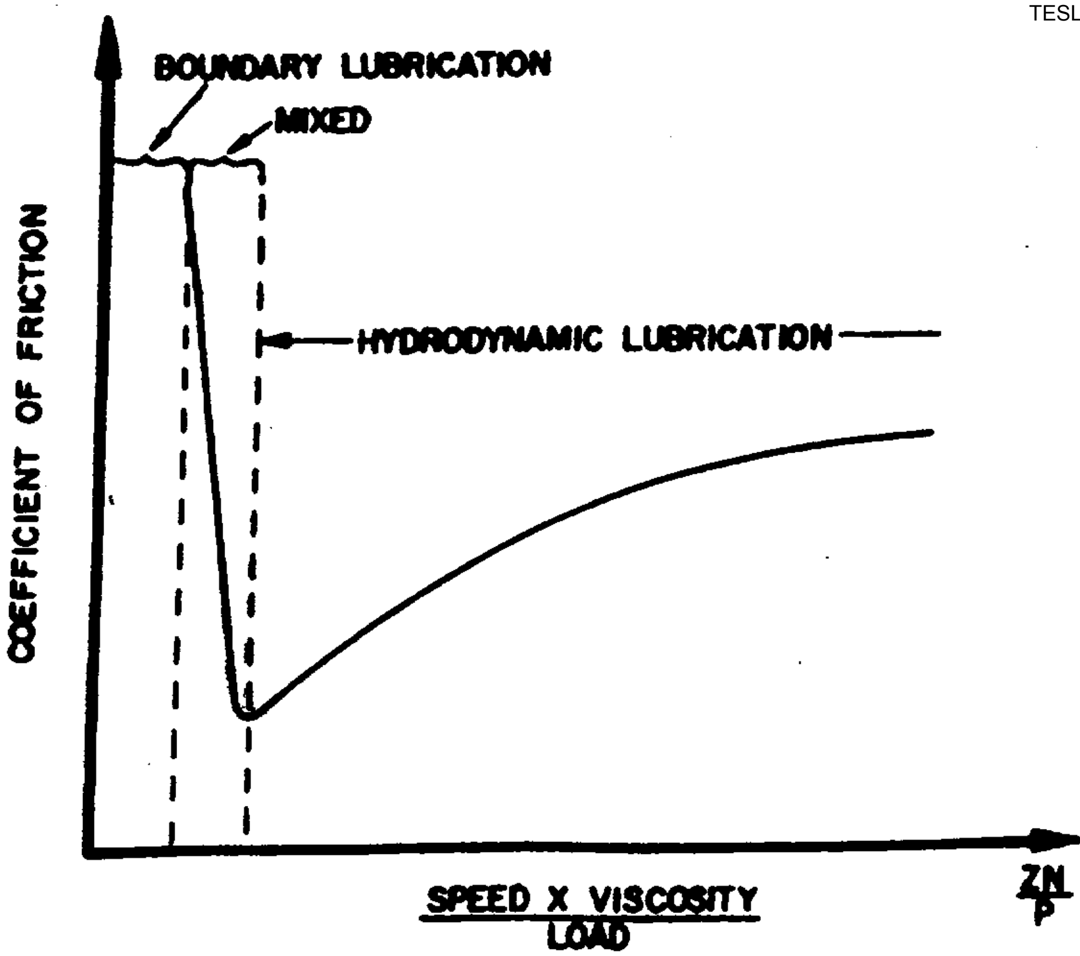

Friction value versus speed.

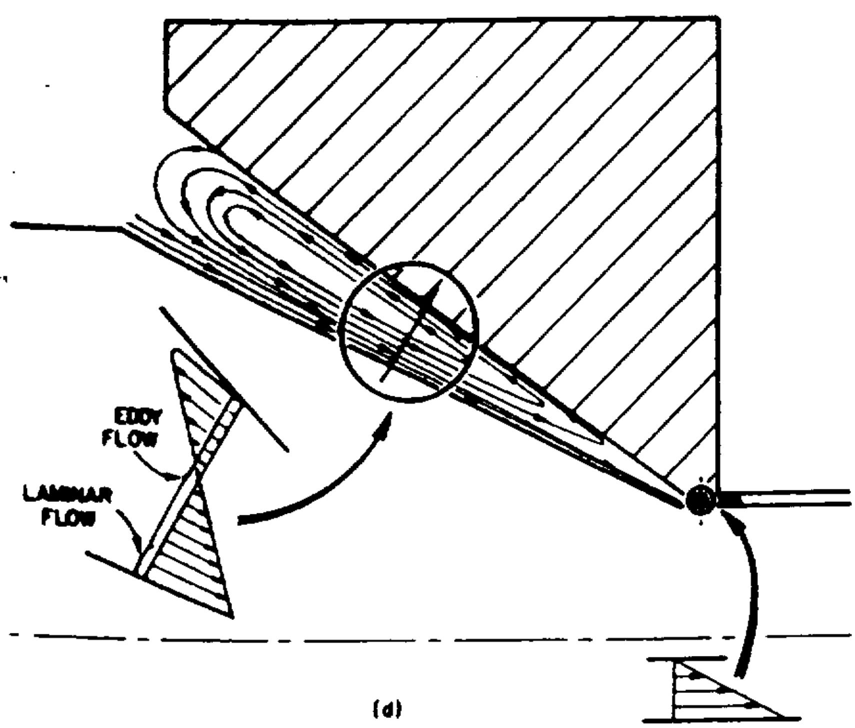

. Lubricant film: (a) entry zone, (b) velocity profile of lubricant, (c) eddy flow in entry zone, and (d)

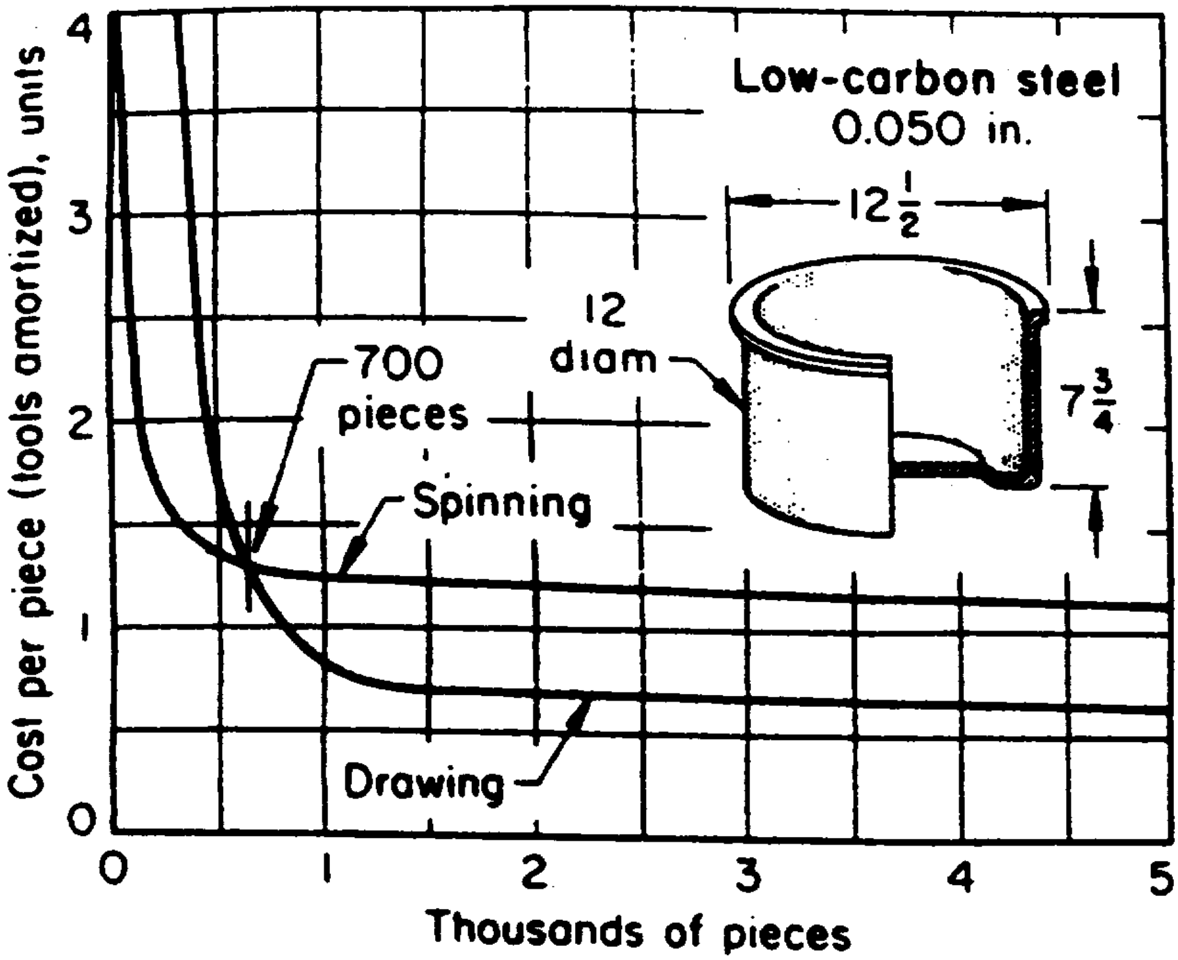

Relation of quantity and cost for producing a flanged cylindrical part by manual spinning vs drawing in a press

Typical Dimensional Tolerances for Manual Spinning

Diameter of blank, in.	Tolerance, in. Commercial	Tolerance, in. Aerospace
Up to 12	±1/64	±0.008
13 to 36	±1/32	±0.015
37 to 54	±1/16	±0.020
55 to 96	±1/8	±0.030
97 to 144	±1/4	±0.040

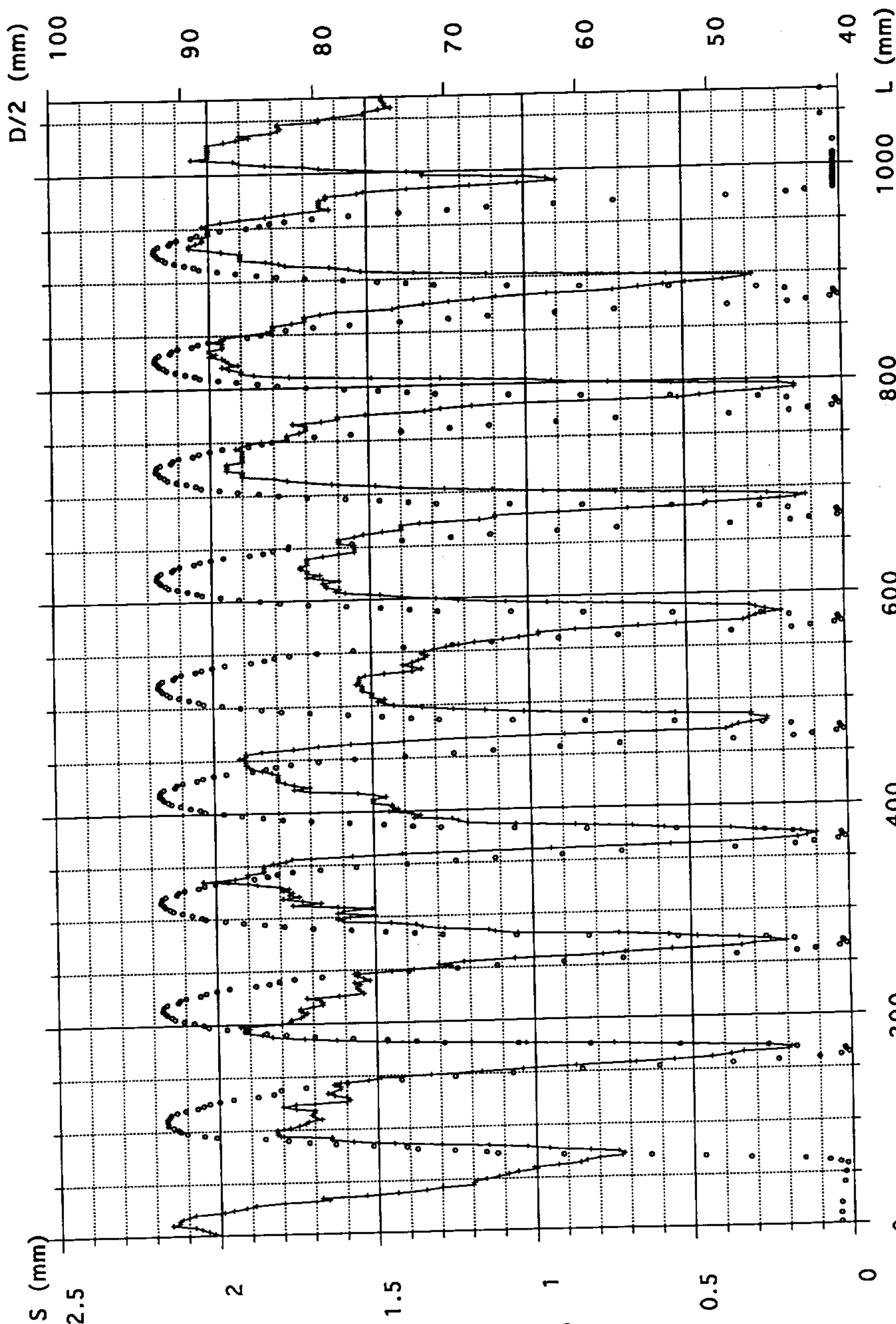
D/2 (mm)
100
90
80
70
60
50
40
L (mm)
0
200
400
600
800
1000
S (mm)
2.5
2
1.5
1
0.5
0

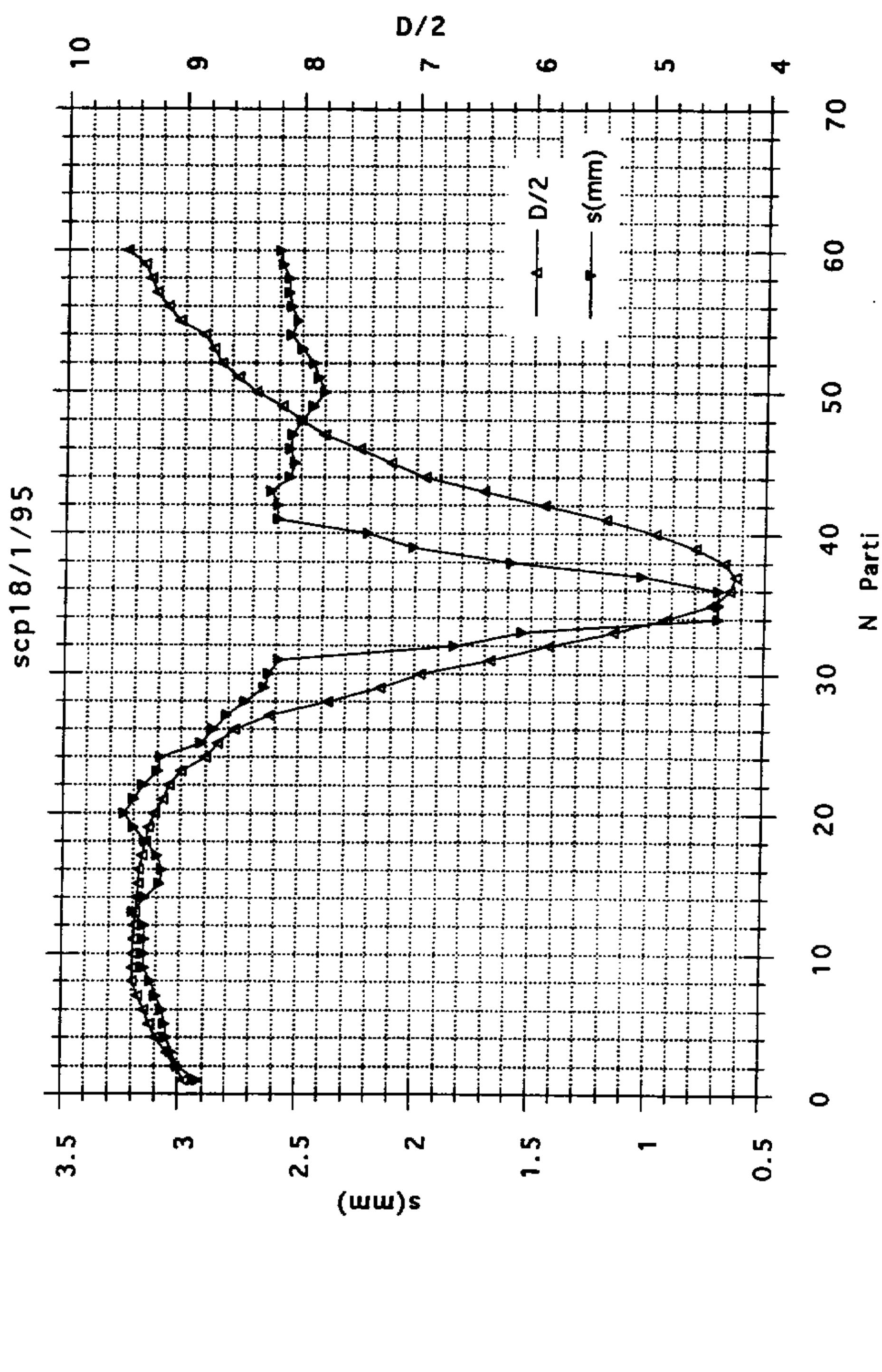
scp18/1/95
D/2
s(mm)
N Parti
D/2
s(mm)
0
10
20
30
40
50
60
70
3.5
3
2.5
2
1.5
1
0.5
10
9
8
7
6
5
4

Coupe métallographique Secteur E

x 500

x 1000

Secteur D

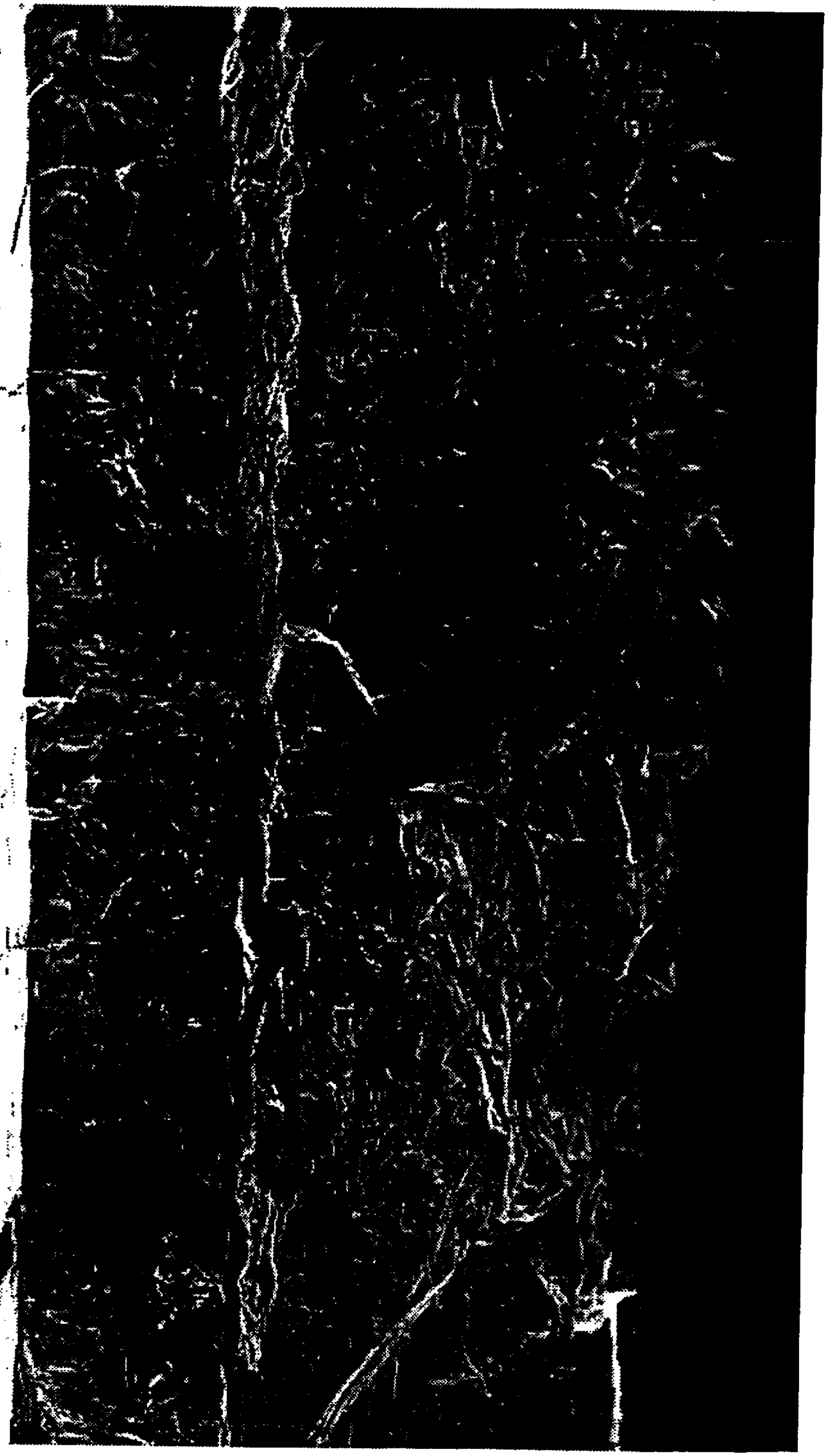

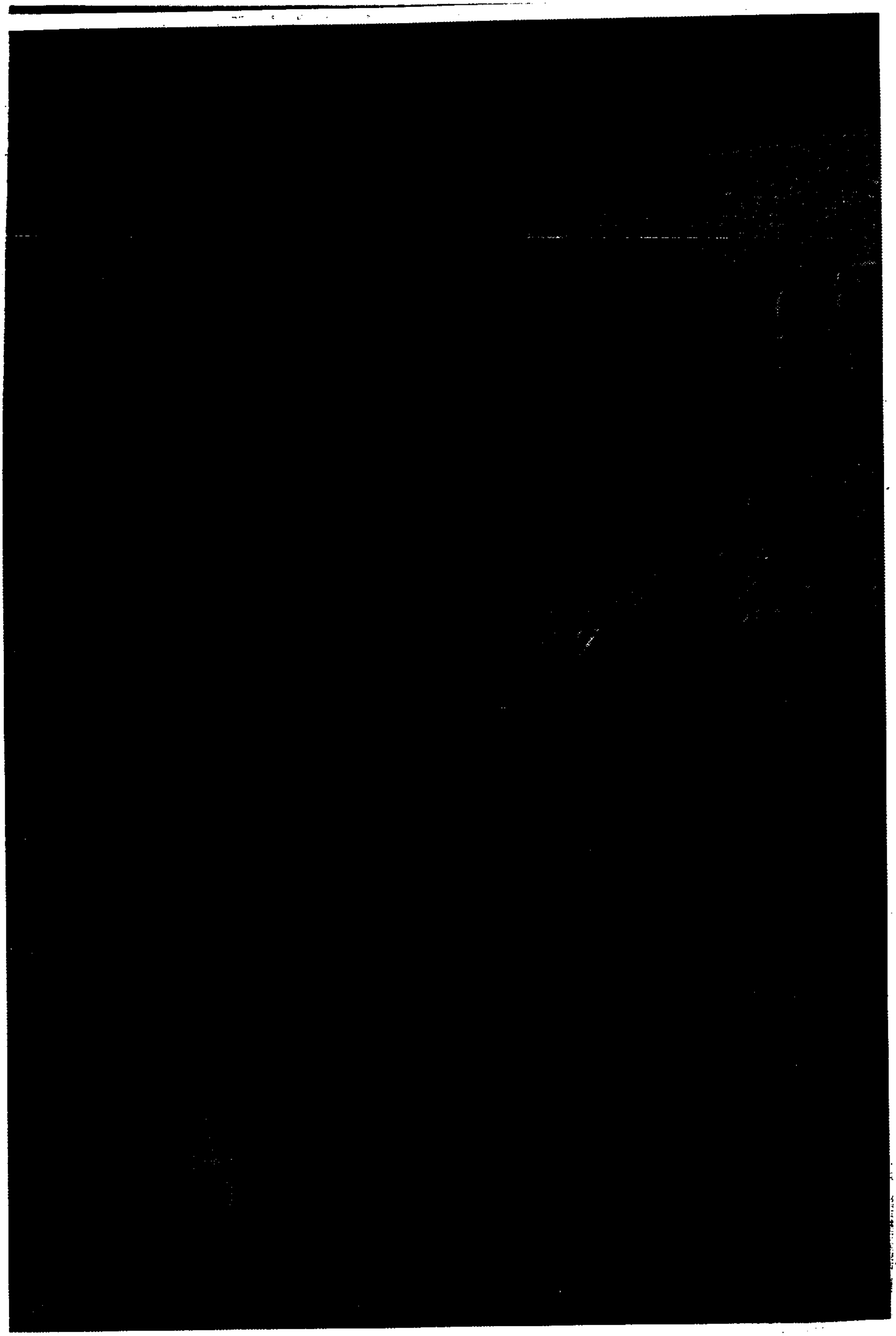

Secteur E

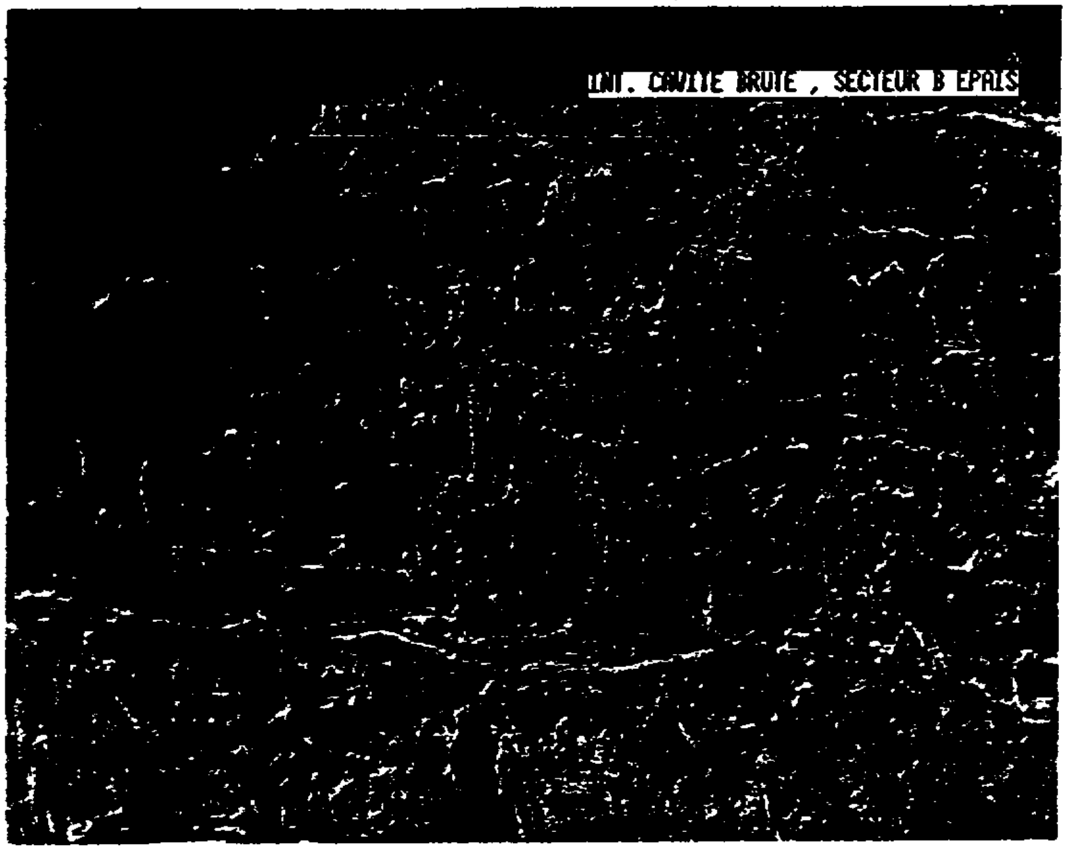
INT. CAVITE BRUTE , SECTEUR B EPAIS

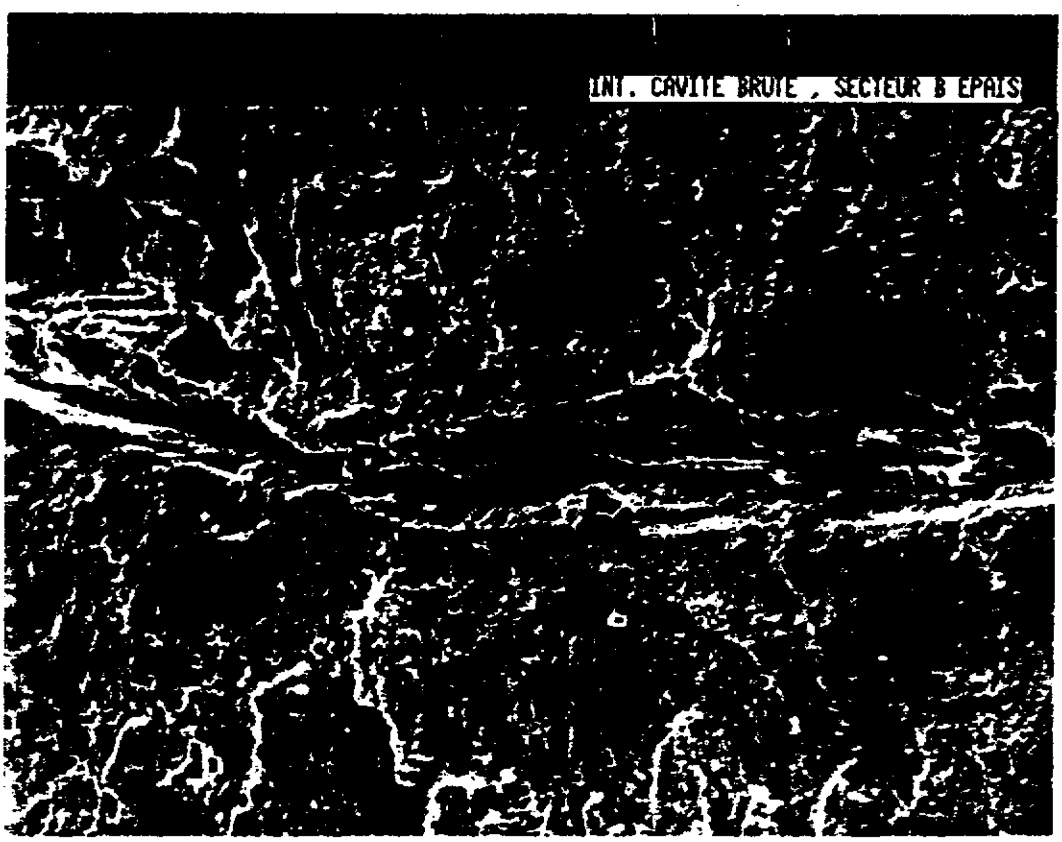
INT. CAVITE BRUTE , SECTEUR B EPAIS

Coupe métallographique Secteur E

Intérieur de la cavité

x 500

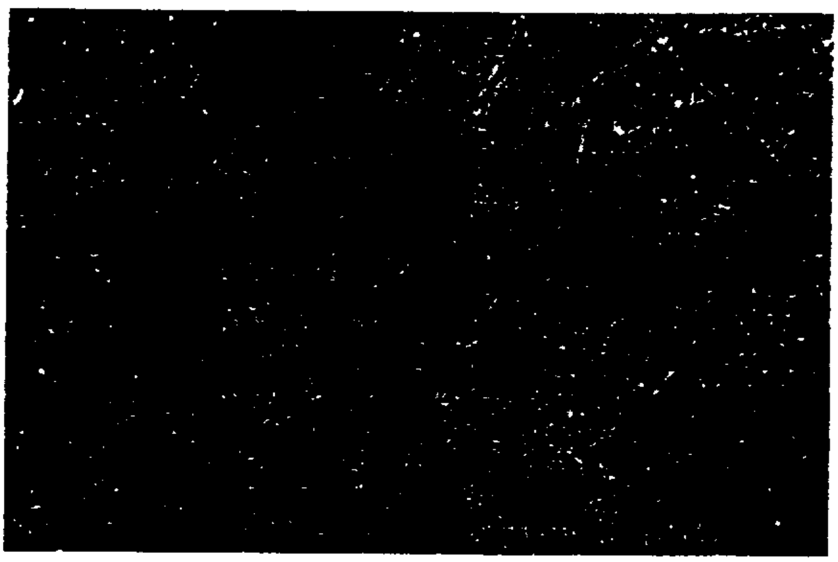

Centre de la section

x 500

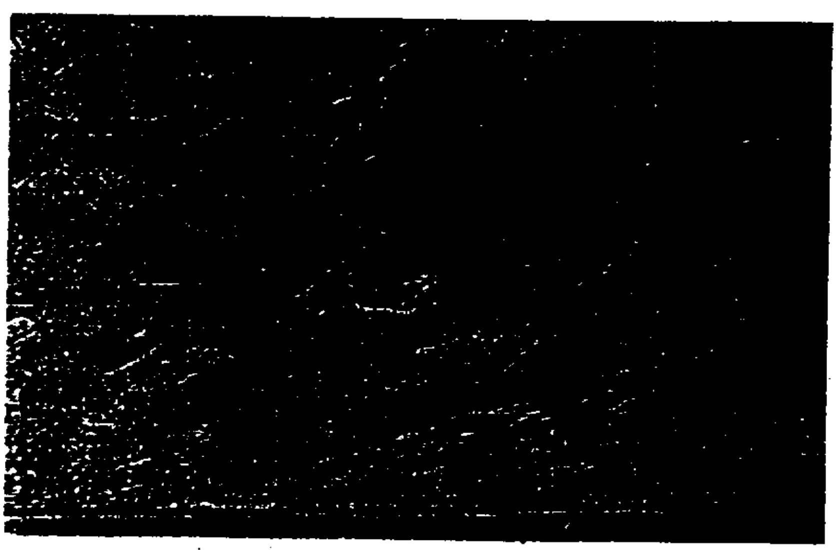

Extérieur de la cavité

x 500

Coupe métallographique Secteur C

x 500

Pour éviter les problèmes de polissage de la zone proche de la surface interne, les échantillons ont été nickelés (20 µm de nickel : partie blanche au-dessus du cuivre).

x 1000

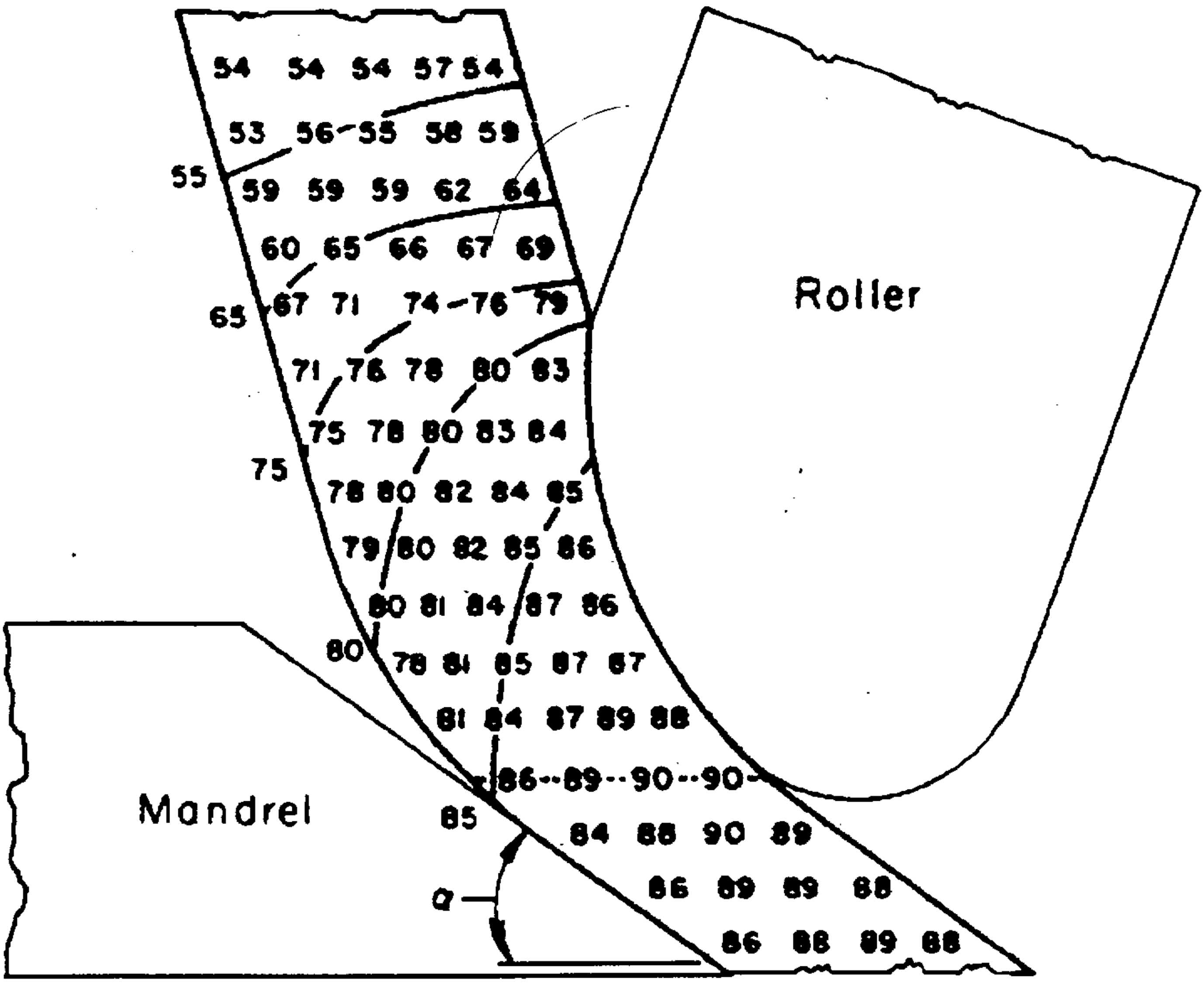

Fig. 3. Hardness distribution in a Copper workpiece reduced 43% by spinning (After ref.3).

HERF processes

1. Uniform application of pressure.
2. High degree of repeatability.
3. Reduced springback.
4. Improved surface finish.
5. Improved tolerances with sheet metal.
6. Ductility marginally improved in some metals when sheet metal is being formed.
7. Reduced tooling costs.
8. Relatively low energy costs.
9. Reduced production costs for small-to-large production runs (except in explosive forming, which is labor intensive).

Characteristics of High-Energy-Rate Forming Processes

	Electrohydraulic: Exploding Bridge Wire	Electrohydraulic: Spark Discharge	High-Explosive Standoff	High-Explosive Direct Contact	Explosive Propellant Closed Die
Metalworking operations	Tube bulging, sizing, drawing, flanging, coining, blanking, stretching	Tube bulging, drawing, sizing, expanding, flanging, coining, embossing, blanking, stretching	Draw forming, stretch forming, flanging, coining, blanking, embossing, sizing, heading, cutting, expanding, powder compacting, stretching, joining	Hardening, welding, cutting, perforating, cladding, powder compacting	Tube bulging, powder compacting, sizing, perforating, stud driving, machining, flanging
Size limitations	0.25-60" (6-1524 mm) diam or larger	0.25-60" (6-1524 mm) diam or larger	Limited only by available blank size; presently, 144-180" (3658-4572 mm)	Part size not limiting	Limited by equipment
Shape complexity	Complex surfaces and shapes, especially tubular	Complex surfaces and shapes, especially tubular	Small and intricate, large and simple	Simple shapes	Compound surfaces, non-symmetrical shapes
Principal advantage	Controllability and repeatability	Controllability and repeatability	Neither pressure nor energy limited, i.e., large parts	Extremely high pressures	Reduces number of operations to produce complex parts
Capital investment	Moderate	Moderate	Low	Low	Low
Tooling costs	Low	Low	Low	None to low	Moderate
Labor costs	Moderate	Moderate	Moderate	Moderate	Low to moderate
Production rate	360 parts per hr depending on part complexity and equipment	Up to 360 parts per hr depending on part complexity and equipment	0.5-4 parts per hr or less depending on part and facility	0.5-4 parts per hr depending on part and facility	2-12 parts per hr depending on part and facility
Cycle time	Long	Medium	Medium	Medium	Medium
Energy costs	Low	Low	High	High	High
Lead time required to place facility in operation	Moderate to long	Moderate	Short	Short	Short
Safety considerations	Equipment interlocks, high-voltage safety practices, trained personnel	Equipment interlocks, high-voltage safety practices, trained personnel	Trained personnel	Trained personnel	Trained personnel
Facility location	In-plant	In-plant	Field or plant	Field or plant	In-plant or separate facility
Method of energy release	Vaporization of wire	Vaporization of medium	Chemical detonation	Chemical detonation	Chemical burning
Pressure-wave velocity, fps (m/s)	20,000 (6096)	20,000 (6096)	4000-25,000 (1219-7620)	4000-25,000 (1219-7620)	1000-8000 (305-2438)
Pressure-wave duration	Microseconds	Microseconds	Microseconds	Microseconds	Milliseconds
Energy range, ft - lb (kJ)	20,000-175,000 (27-237)	10,000-110,000 (13.5-150)	100,000-2,000,000 (136-2712) per lb of explosive; up to 100 lb (45 kg) detonator	0.5-8 psf high explosive	Low to moderate (detonation wave in gas)
Workpiece-deformation velocity, fps (m/s)	50-700 (15-213)	50-700 (15-213)	60-400 (18-122)	Not applicable	50-200 (15-61)
Energy transfer medium	Water or other suitable liquid	Water or other suitable liquid	Water, elastomers, sand, molten salts	Direct contact or buffer material	Air or water; high-velocity projectile or ram

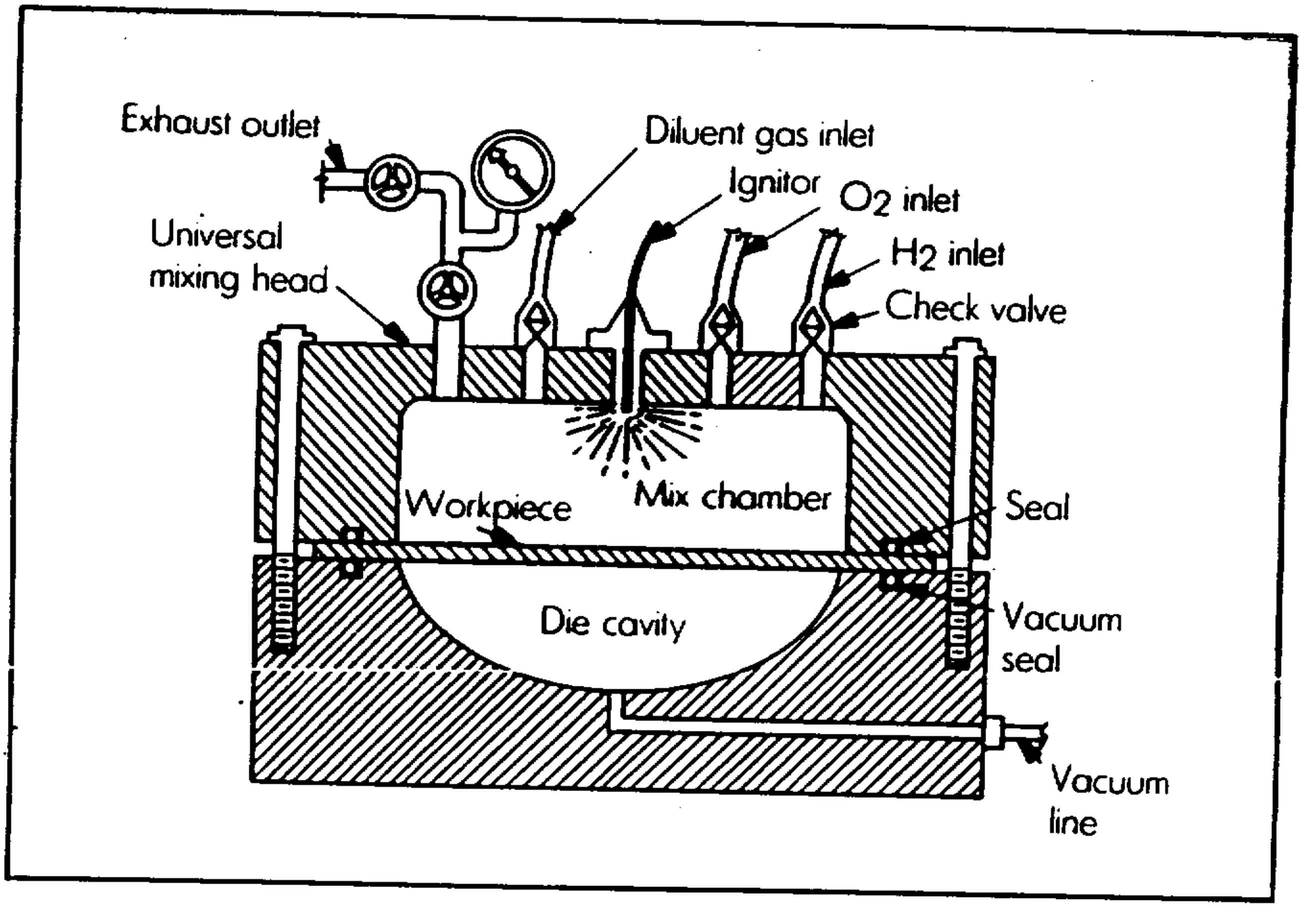

Schematic view of typical combustible gas forming operation employing a spark igniter to initiate uniform shock front.

Types of Gases Used in Combustible Gas Forming

Fuels	Oxidizers	Diluents
Hydrogen	Oxygen	Helium
Ethane	Air	Nitrogen
Methane	Ozone 13	Carbon dioxide
Natural gas		Argon

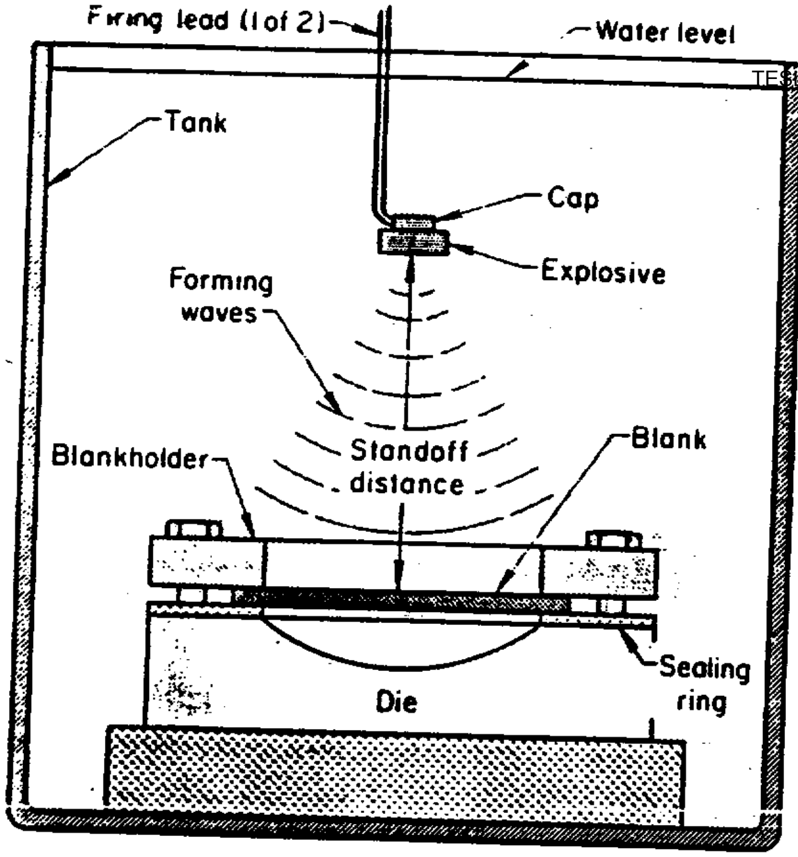

Unconfined system for explosive forming

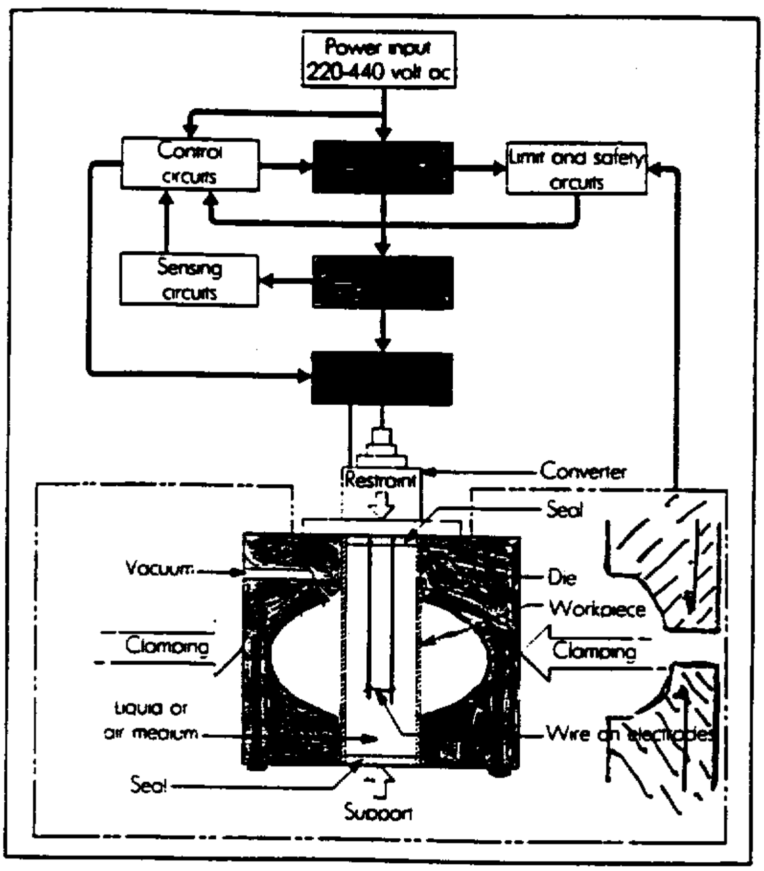

Components of an electrohydraulic forming system.

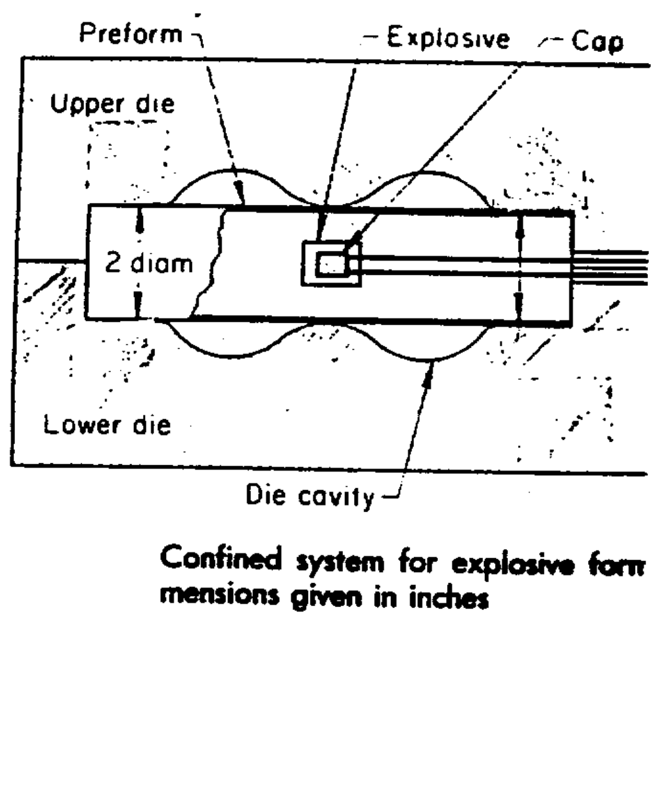

Confined system for explosive form mensions given in inches

Properties of Selected High Explosives

Explosive	Relative Power, % TNT	Form of Charge	Detonation Velocity, fps (m/s)	Energy, ft · lb/lb (kJ/kg)	Detonator Required	Storage Life	Maximum Pressure, ksi (MPa)
Trinitrotoluene (TNT)	100	Cast	23,000 (7010)	262,000 (780)	J-2*	Moderate	2400 (16 548)
Cyclotrimethylene trinitramine (RDX)	170	Pressed granules	27,500 (8380)	425,000 (1270)	No. 6	Very good	3400 (23 443)
Pentaerythritol tetranitrate (PETN)	170	Pressed granules	27,200 (8290)	435,000 (1300)	No. 6	Excellent	3200 (22 064)
Pentolite (50/50)	140	Cast	25,000 (7620)	317,000 (950)	No. 8	Good	2800 (19 306)
Tetryl	129	Pressed granules	25,700 (7835)		Special**	Excellent	
Composition C-3	115	Hand-shaped putty	26,400 (8045)		No. 6	Good	
40% straight dynamite	94	Cartridge granules	15,500 (4725)	202,000 (605)	No. 8	Fair	970 (6688)
50% straight ditching dynamite	103	Cartridge granules	17,400 (5305)	220,000 (660)	No. 6	Fair	
60% extra dynamite	109	Cartridge granules	12,500 (3810)	240,000 (715)	No. 6	Fair	620 (4275)
Blasting gelatin	99	Cartridge plastic	26,200 (7985)	408,000 (1220)	J-2	Fair	2600 (17 927)
Bituminous coal D permissible explosive		Cartridge granules	4600 (1400)		No. 8	Fair	
Primacord, 40 g/ft		Plastic or cotton cord	20,800 (6340)		No. 6	Excellent	
Mild detonating cord, 10 g PETN/ft		Metal-coated cord	24,000 (7315)		Special†	Excellent	
Detasheet†		Cut to shape	23,700 (7225)		No. 8	Very good	
Cyadyn 3‡	90	Cartridge granules	7000 (2135)		No. 6	Fair-good	
IRECO DBA-10HV§	20	Slurry (two parts)	11,500 (3505)		Special	Excellent (unmixed components)	

* With booster.
** Special engineer's blasting cap.
† Registered trademark, E. I. du Pont de Nemours & Company, Inc.
‡ Registered trademark, American Cyanamid Company.
§ Intermountain Research and Engineering Corp.

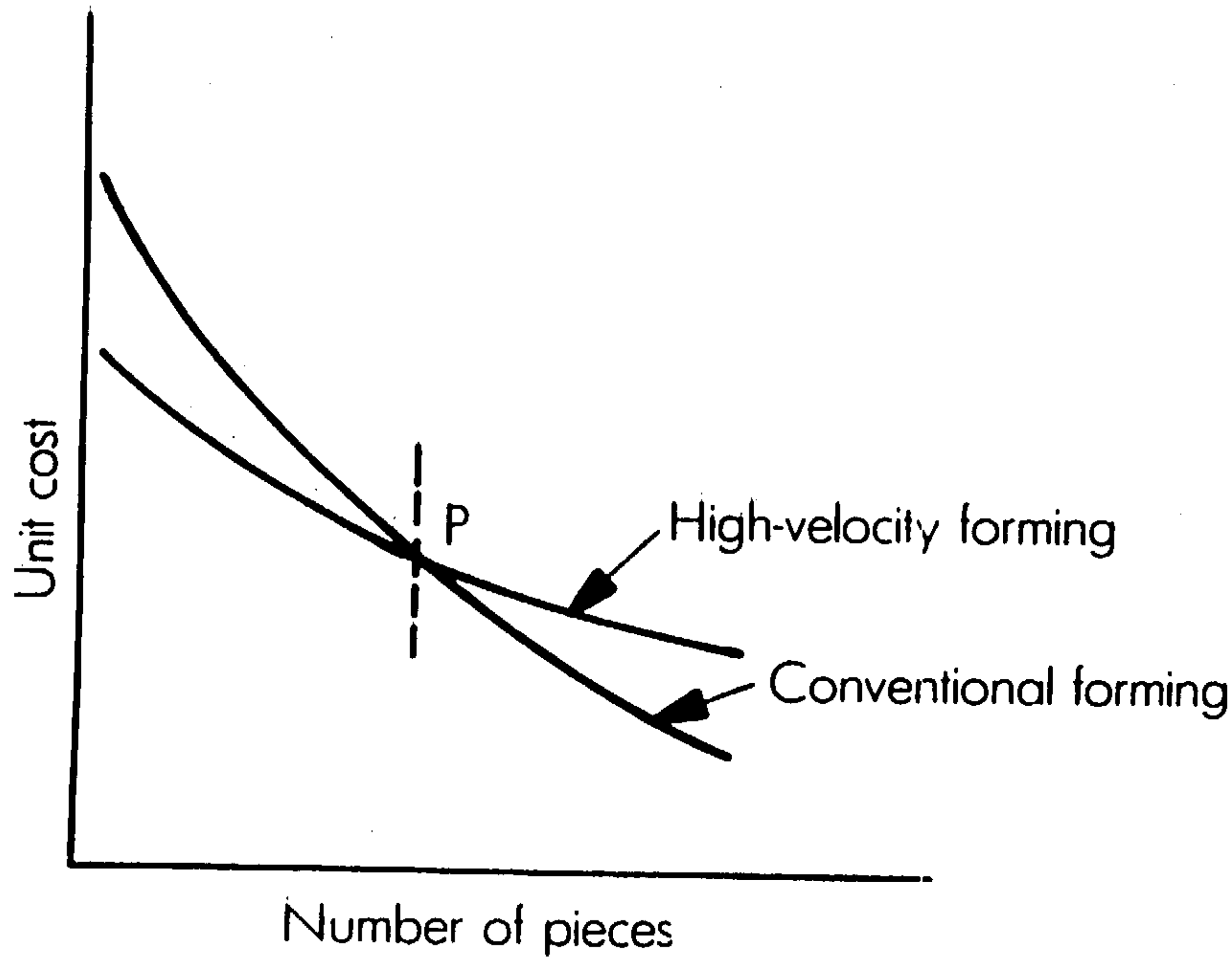

Fig. 19-1 Cost comparison between conventional forming and high-energy-rate forming.

S.c. properties of a material in terms of three fundamental (rather easely measurable) quantities

$T_c \longleftrightarrow \Delta$ $\qquad$ $\Delta = \frac{5}{2} K \underline{T_c}$

$\gamma \longleftrightarrow N(E_F)$ $\qquad$ $\gamma = \frac{1}{3} \pi^2 K^2 \underline{N(E_F)}$

$\rho_0 \longleftrightarrow l_0$ $\qquad$ $\rho_0 = \dfrac{1}{\frac{2}{3} e^2 \underline{N(E_F)} v_F \underline{l}}$

if $\quad l_0 \ll \xi_0 \quad , \quad T < T_c/2 \quad , \quad \nu \ll \Delta/h$

$H_{c1} = 1.90 \times 10^2 \left(T_c/\rho_0\right) \ln\left(.90 \times 10^{-2} \gamma^{\frac{1}{2}} \rho_0\right)$

$H_c = 2.43 \, \gamma^{\frac{1}{2}} T_c$

$H_{sh} = .75 \, H_c$

$H_{c2} \propto \gamma \rho_0 T_c$

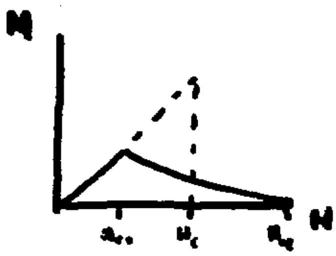

ρ_0 - $\mu\Omega \cdot cm$
γ - $erg \, cm^{-3} K^{-2}$
H - Oe

$\lambda_L[\text{Å}] = 1050 \left[\rho_0/T_c\right]^{\frac{1}{2}}$

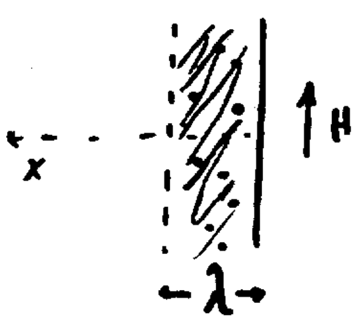

$R_s \propto \lambda \cdot \frac{m_n}{m}$

$R_s \propto \rho_0^{\frac{1}{2}} e^{-\frac{5}{2} \frac{T_c}{T}}$

The s.c material needs to be a reasonable metal too

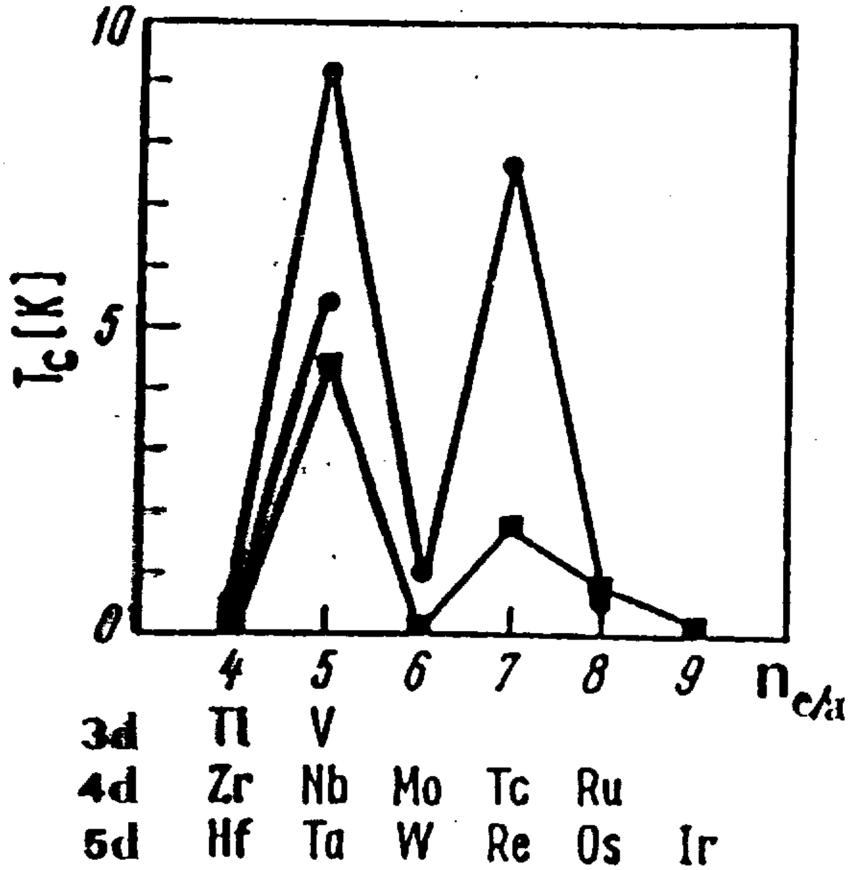
10
5
0
Tc [K]
4
5
6
7
8
9
ne/a
3d
Tl
V
4d
Zr
Nb
Mo
Tc
Ru
5d
Hf
Ta
W
Re
Os
Ir

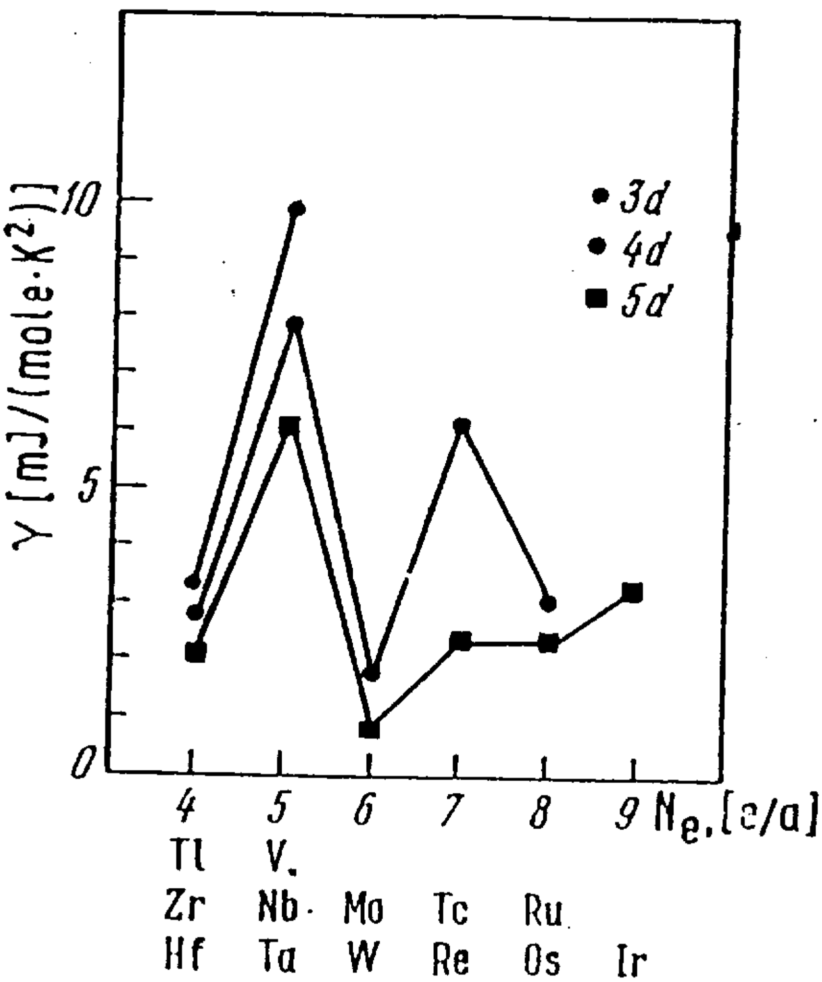
• 3d
• 4d
■ 5d
10
5
0
γ [mJ/(mole·K²)]
4
5
6
7
8
9
Ne, [e/a]
Tl
V
Zr
Nb
Mo
Tc
Ru
Hf
Ta
W
Re
Os
Ir

for solid solutions AB

$$E_F^{3/2} = n_{e/a}(AB) = C_A\, n_{e/a}(A) + C_B\, n_{e/a}(B$$

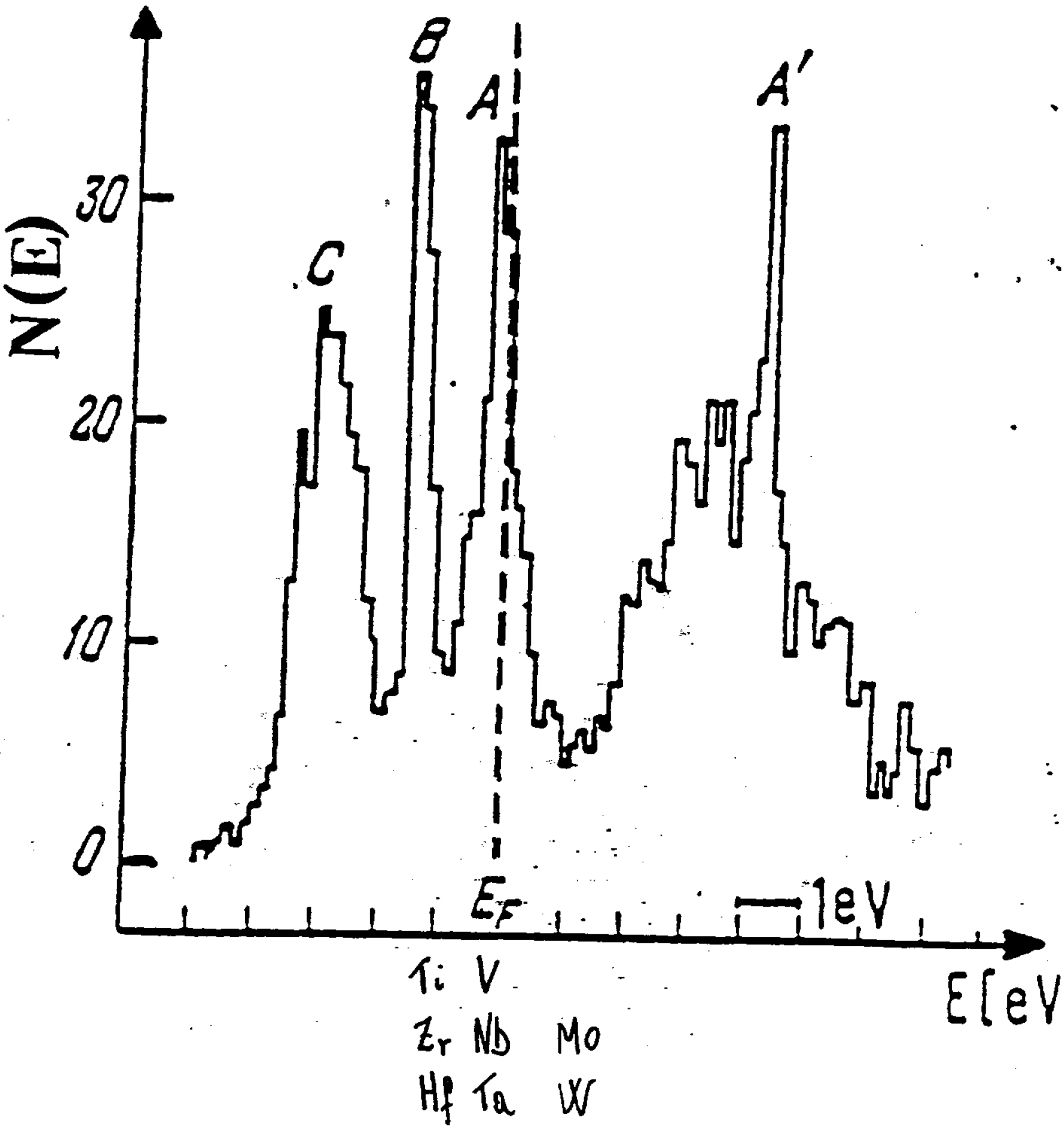

EFFECT OF PLASTIC DEFORMATION OF V, Nb AND Ta ON THE SUPERCONDUCTING TRANSITION TEMPERATURE AND THE SPECIFIC HEAT COEFFICIENTS

R. KUENTZLER

Laboratoire de Magnétisme et de Structure Electronique des Solides. L.A. 306 du C.N.R.S., Institut de Physique, 67084 Strasbourg, France

Received 9 April 1984

Specific heat measurements performed between 1.4 and 20 K on bulk and cold-worked V, Nb and Ta superconducting materials are presented. The plastic deformation produces an increase in the superconducting transition temperature T_c, an increase which is relatively less important for Ta than for Nb and less for Nb than for V. An increase is registered for the normal linear coefficient of specific heat γ whereas the Debye temperature decreases slightly. The apparent relation between the increase of T_c and γ suggests qualitatively that the vibrating mobile dislocation contribution is not the only origin of the increase of γ but that a band structure contribution is also to be taken into account.

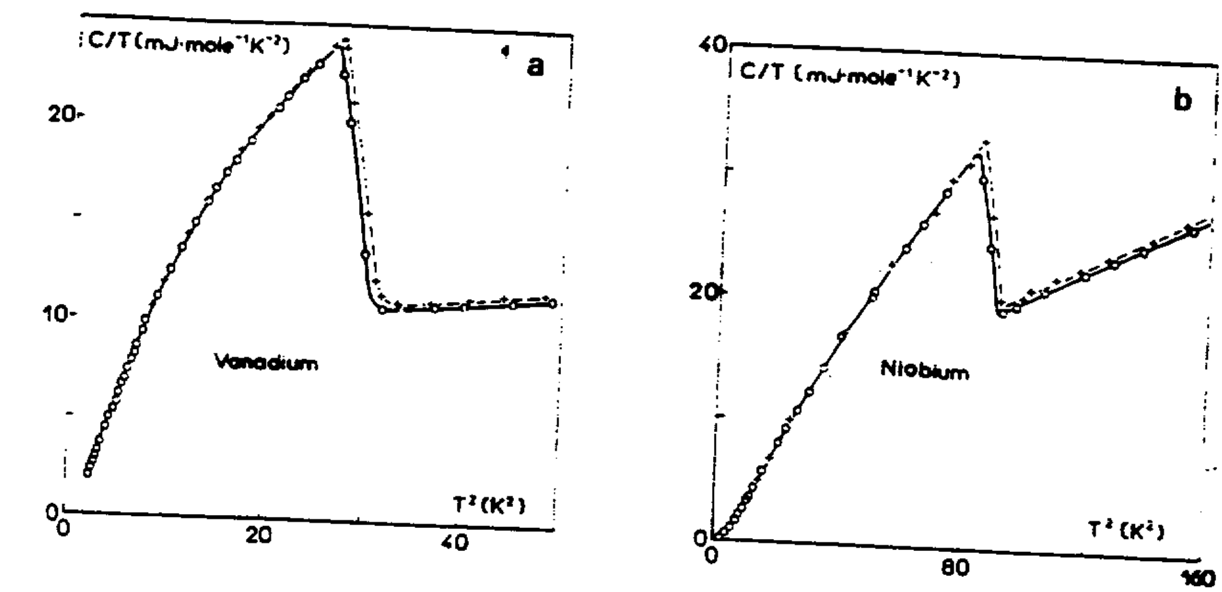

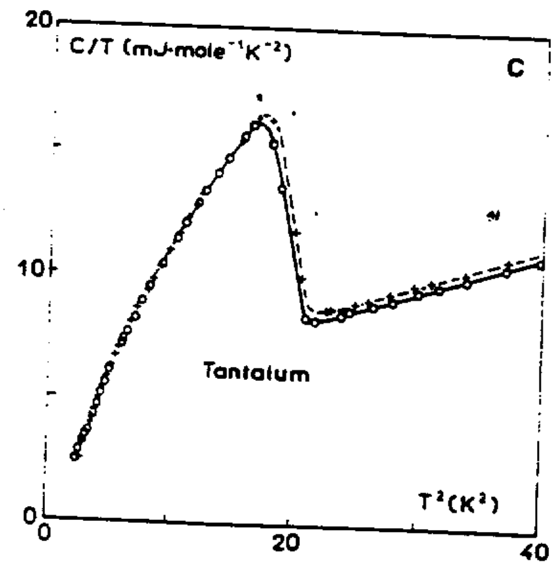

Fig. 1. Specific heat of (a) vanadium, (b) niobium, (c) tantalum in bulk state (o) and after deformation by cold work (+) in the C/T versus T^2 representation.

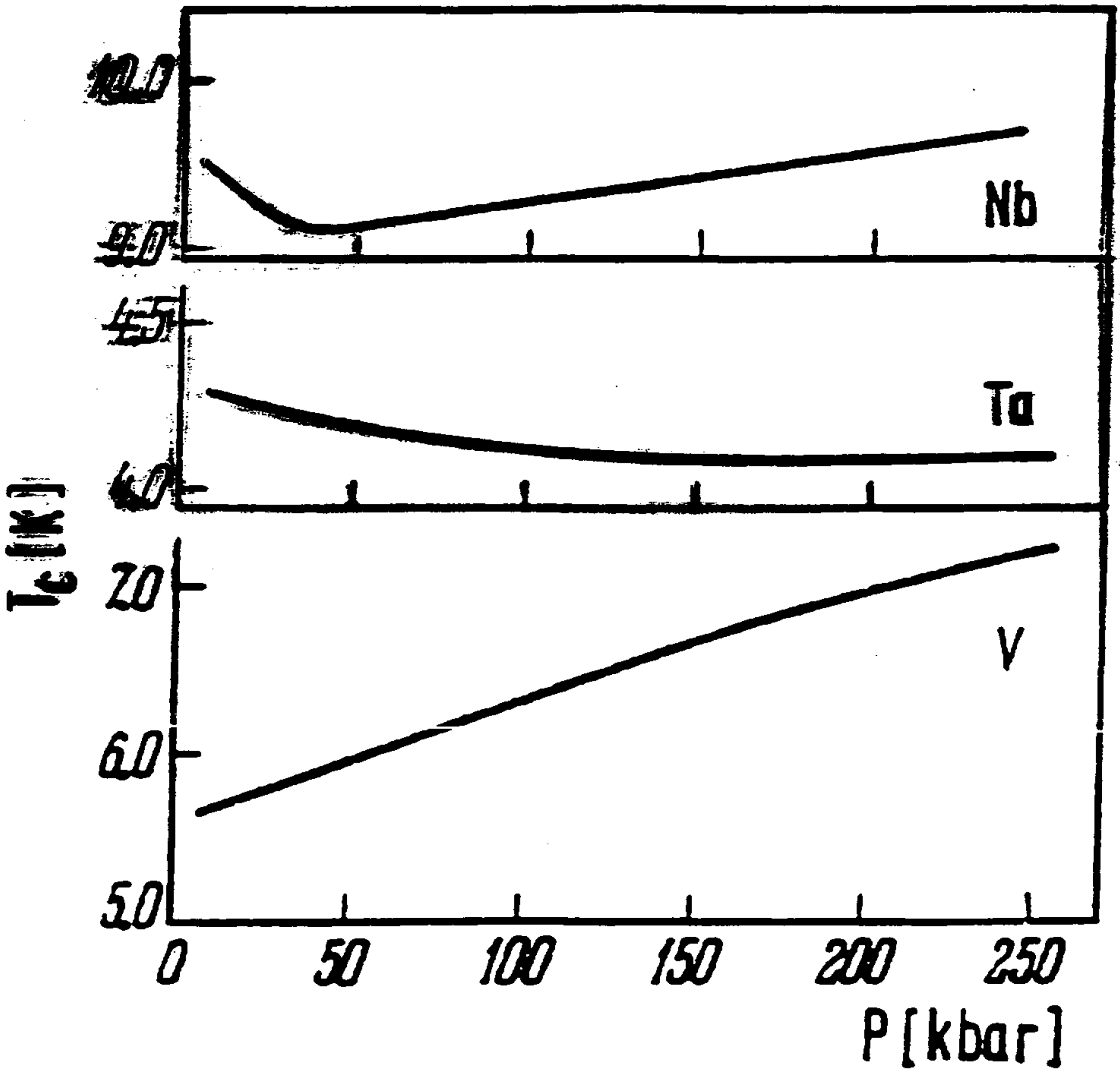
10.0
9.0
Nb
4.5
4.0
Ta
T_c [K]
7.0
6.0
5.0
V
0
50
100
150
200
250
P [kbar]

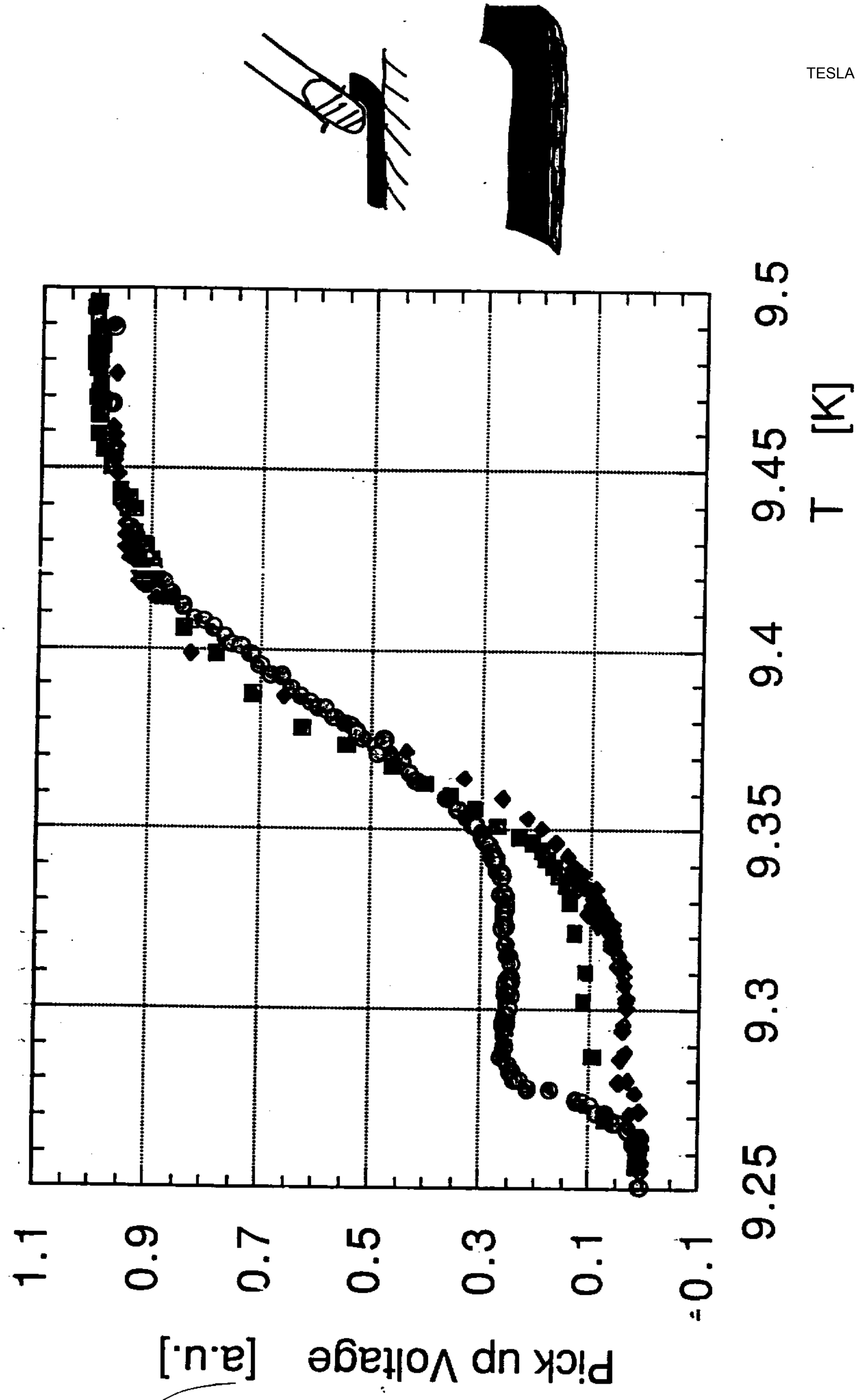
Pick up Voltage [a.u.]
1.1
0.9
0.7
0.5
0.3
0.1
-0.1
9.25
9.3
9.35
9.4
9.45
9.5
T [K]

Successes and Failures in alternative methods

(H. Padamsee)

For

Joe Kirchgessner

Cornell

1) Explosive Forming
2) Hot Working
3) Multistage hydroforming

---

4) Making tubes (RRR) From sheet

Explosive Forming (1982)

Joe Kirchgessner

Idea:

In rapid cold working of niobium
%elongation may be stress rate dependent

Explosively form niobium tube into a 7075 Aluminum die.

Tube = 3 mm wall, 25 mm inner diameter
reactor grade niobium
annealed

Spherical cavity about 60 mm

Many explosive tests made

Varied amount of explosive charge
detonation at one end, both ends
full length of charge and charge only in middle

4% diamter expansion successfuly
> 20% expansion, ruptured

Conclusions

%change in tube radius before rupture is actually much less than change achieved with a slowly applied force
rapid cold working is worse!

Explosion Forming

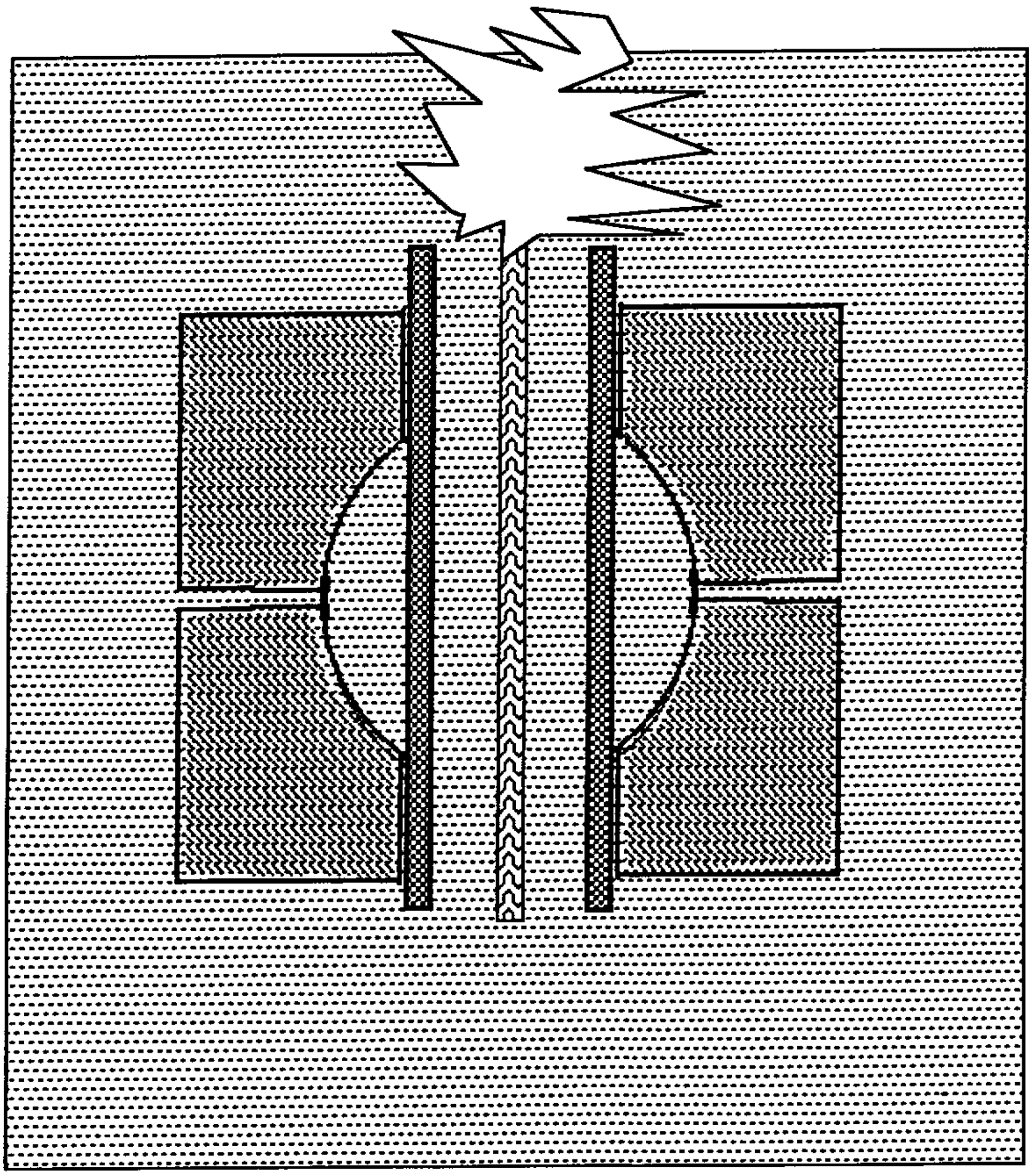

TESLA 1995-09

9-23-8
J. Kirchgess

Explosion forming of Nb cavity cells

With the hope that Nb were sufficiently stress rate sensitive a test was made of explosively forming Nb tubing into a 7075 alum. fo

the Nb tube was full annealed Wa Chang matl. 1.250" OD × 1.00" ID × .125" wall.

The shape cut in the alum. form was a spherical shape 2.312" OD, flattened in such a way that the shape would fit within an eliptical shape 2.72

The aluminium forms had provisions for a vacuum between the Nb tubing and the alum. form. The alum forms were manufactured by us guided by drawings provided by NTI (North West Technical Industries)

Four Nb tubes along with the alum forms were sent to NTI where the tests were performed 9-21-82. We witnessed the tests.

The tests were done in a 55 gal drum full of water with the alum form suspended in the center.

The explosives used were "primer cord" rated at various grains per foot. Electric detonators were used. The inside of the Nb Tube (where the explosives were placed) was full of water.

The results were as follows:

Tube #	Shot #	Charge	Result
1	1	25 grain full length det. at one end	1.250"OD → 1.300"OD no split
1	2	100 grain full length det. at one end	1.3"OD → 2.250"O. split in 7 places
2	1	100 grain 1" long in center only	1.250"OD → 1.50"OD split in 2 places
3	1	25 grain full length det both ends	1.250" → 1.300"OD no split
3	2	50 grain full length det both ends	1.3"OD → 1.55"OD split 2 places
4	1	400 grain full length det one end	1.25"OD → 2.3"O tube ruptured both ends, mult splits alum form damag

Conclusion: The stress rate characteristics of Nb are such that Nb does not lend itself to this type of forming. The people at NTI agreed with this conclusion and had no ideas on how to improve the technique.

Multi-Stage Hydroforming (1982)

Joe Kirchgessner/John Walters

Compressive force along axis is needed to prevent excessive thinning

Hydraulic force: 7000 psi
Ram force : 20,000 psi

extrusion marks or flaws in starting material are regions of excessive thinning and fracture start in later stages

30% elongation before annealing necessary

32 mm OD, 2.3 mm thick tubing

3:1 expansion in diamter acheived using 7 forms and two anneals

Total 35% thinning
about a few% at each stage

Conclusions

Successful, but too many stages and too many anneals
Probably more expensive than forming and welding
Also tubing is more expensive than sheet.

13

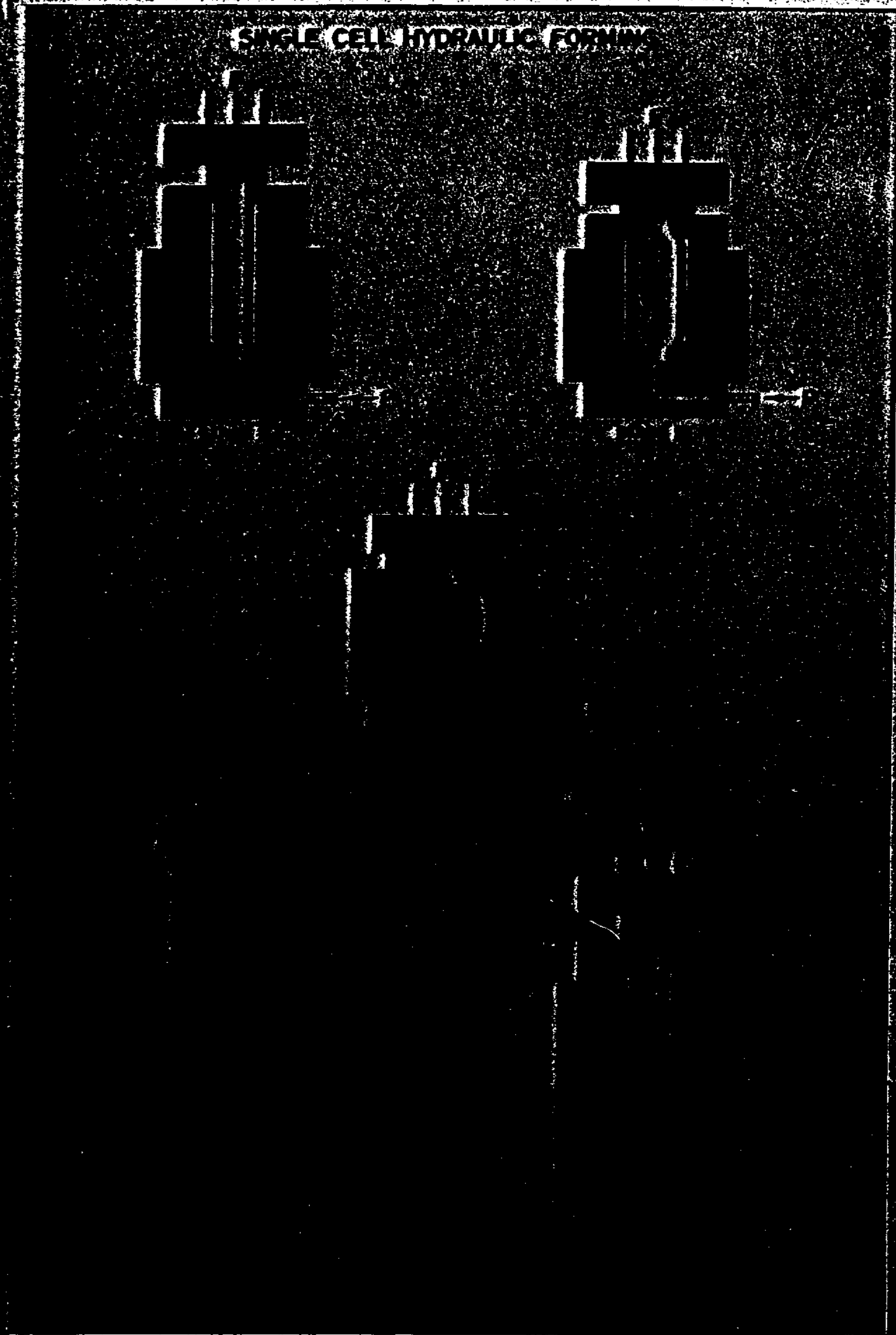

Hot Working (1983)

Joe Kirchgessner/Chuck Henderson

Motiviation: Welds used to be full of defects when done with a focussed beam

Idea:

Blow bubbles out of niobium tubing at high temperature

13 mm OD, 0.5 mm thick tubing, 16 cm long
Reactor grade niobium

Vacuum outside
high pressure argon (3 Kpsi max) inside

20 tests done between 400 C and 1500 C

Below 1200 C
All failed longitudinally before 50% diameter increase
much orange peeling
Increase in pressure needed as diameter increased
Because work hardening was not being sufficiently annealed out at T< 1200 C

Above 1200 C, tubes expanded continuously
Nb flowed better
but

problems sustaining temperatures long enough with simple arrangement

At 1500 C achieved near 100% diameter expansion
no orange peeling

Conclusion:
3:1 expansion desired may be possible
but need good furnace design
& dies (not even addresed yet)
Temp may be less for high RRR Nb because of lower yield point

Maybe worth trying again.

Stopped because new defocused beam welding technique eliminated defects.

Also : Tubing is more expensive than sheet

C. Henderson

Feb 3 198

SRF
830201

Pressure Forming of Niobium Tubing at Elavated Temperatures

I recently performed a series of tests to see the effects of temperature on pressure forming niobium cavities.

A niobium tube $6\frac{1}{4}$" x $\frac{1}{2}$" O.D. x 0.020" wall thickness was swagelocked into a fixture that supplied argon gas to pressurize the tube and an axial compressive force by means of a threaded rod running through the length of the tube. (see diagram)

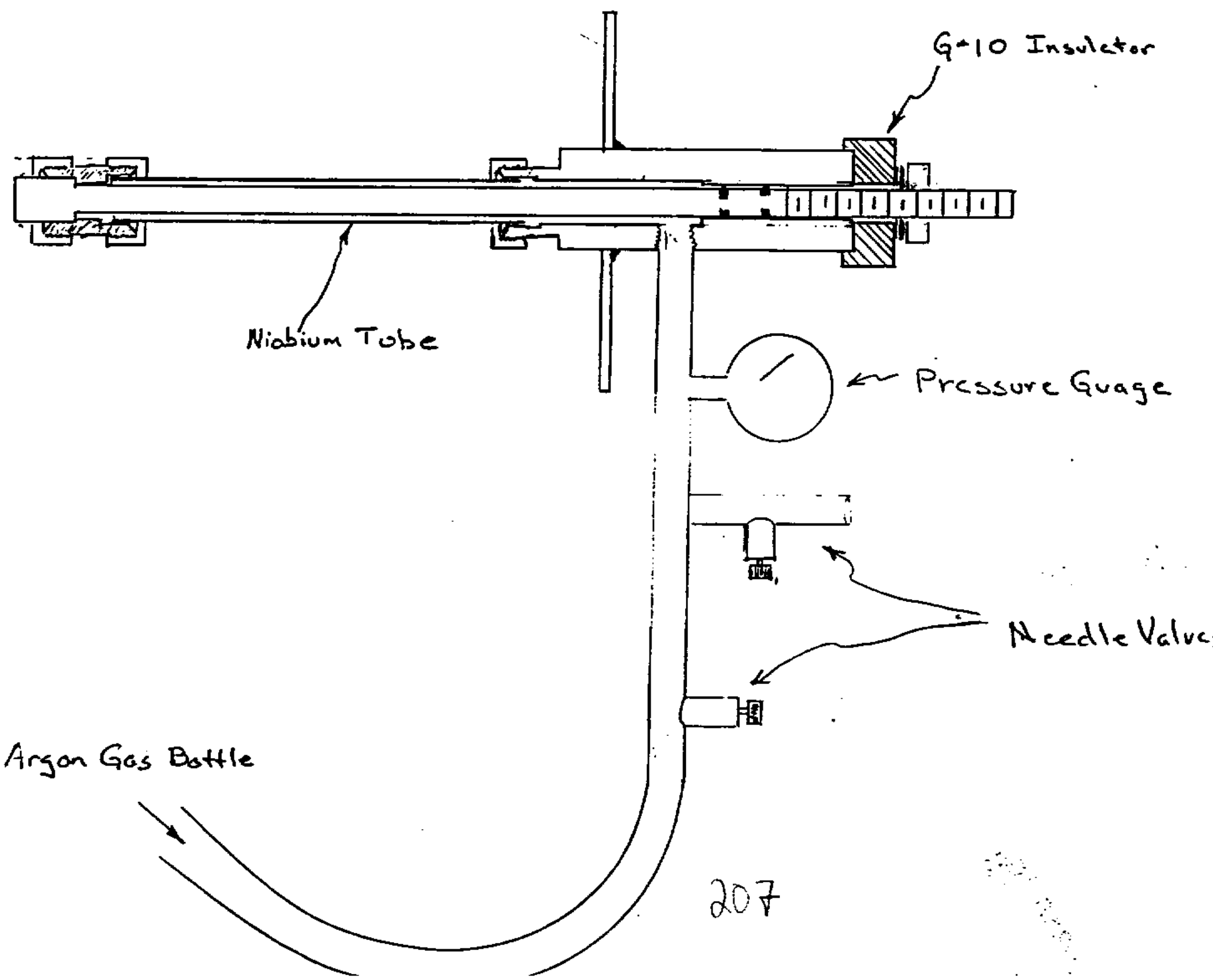

Two tests were performed at room temperature using a hydraulic cylinder to pressurize the tube as the bursting pressure was higher than the argon bottle. The fixture was fastened to a vacuum chamber. A Hobart 1000 amp power supply was connected by 1/4" water cooled tubing, through a vacuum feed through, to blocks on either end of the niobium tube. Two cromel-alumel thermocouple wires were held on to the tube under a stainless steel band which was in turn held by a spring. This was done to allow for the expansion of the tube. It was found that above 400-500 °c the swagelock fittings leaked argon into the vacuum. Loctite PST teflon pipe sealant was put on the fittings to forestall the leakage.

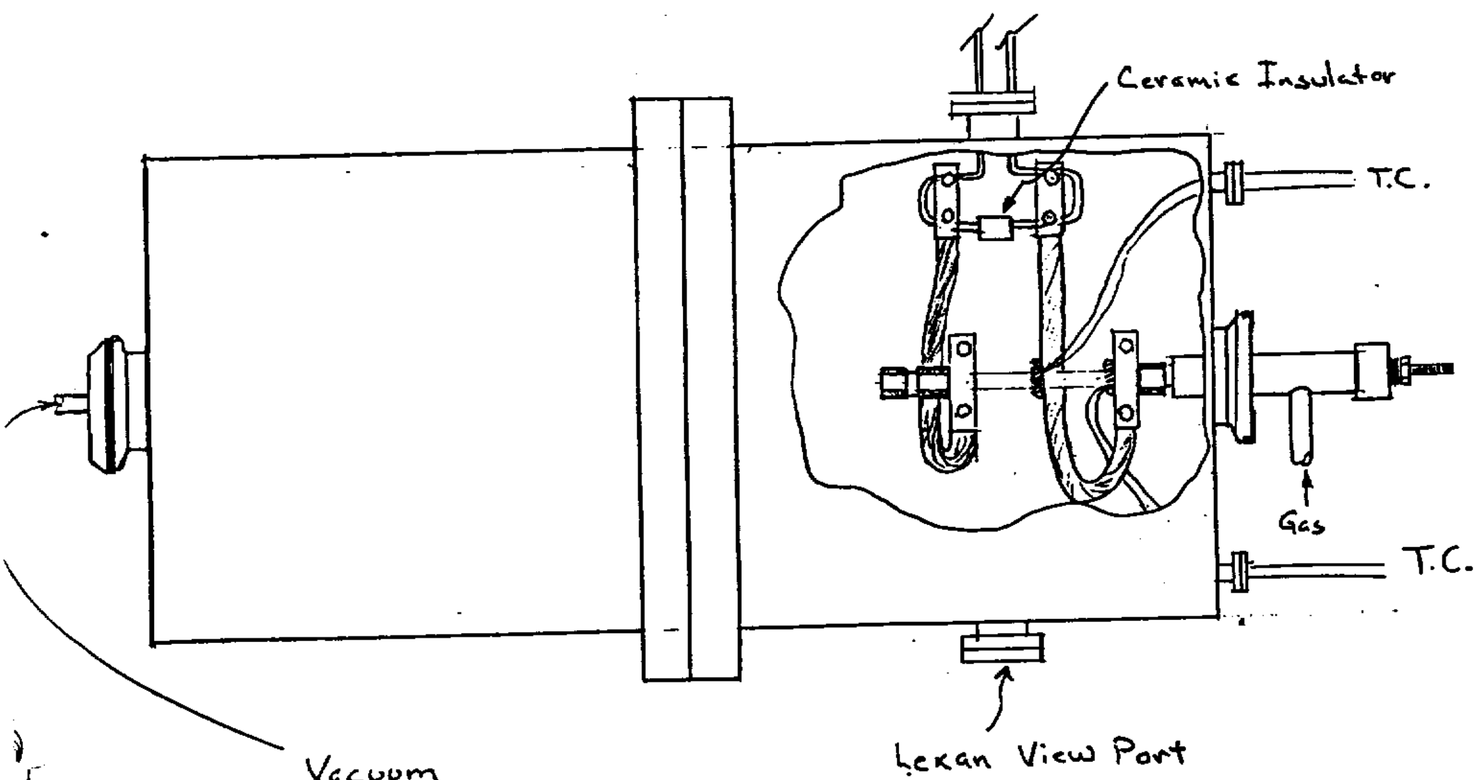

As John Walters stated in his paper (7-27-82) the critical stress in an internally pressurized tube is the Hoop Stress

$$\sigma_H = \frac{Pr}{t}$$

P= Internal Pressure
r= radius
t= thickness

Once the Hoop Stress becomes greater than the yield stress of the niobium the tube will deform until the ultimate stress of the material is exceded. Both the yield stress and the Ultimate Tensile Stress are dependent on the temperature of the material. Both stresses can be expected to decrease with an increase in temperature but this is not as important to the sucessful forming of a cavity as is how the increased temperature improves the plasticity of the deforming material.

The yield stress of the annealed niobium increases as the niobium deforms. because the material work hardens. Inconsistancies in grain size and direction increase when the material deforms increasing the internal stresses created. It is hoped that if enough thermal energy is added the additional mobility of atoms will relieve the stresses created. Under those conditions the yield point of the niobium will not increase and since the Hoop Stress increases proportionaly to the radius the tube will deform continuously without an increase in the internal pressure.

Test no	Center °C Temp	Side °C Temp	PSIG Burst Pressure	% of Increase of Diam	Surface Appearance
a	23	N.A.	3100	24	All exposed surface expanded and rough
b	23	N.A.	3150	28	All exposed surface expanded and rough
1	500	N.A.	1950	36	Center 3/4 in expanded and rough
2	550	N.A.	1500	43	Center 1 1/4 in expanded and rough
3	600	N.A.	1000	38	Center 1 1/2 in expanded and rough
4	750	NA	1350	44	Orange peel 1 1/2 in along length of tube
5	670	N.A.	950	21	Orange peel 2 1/4 along length of tube
6	945	N.A.	700	33	Some orange peel not as pronounced a tests 4 & 5
7	1100	N.A.	900	38	1 in length orange peel
8	1150	880	600	47	tube bent in the middle bent stainless steel rod
9	730	NA	900	36	2 in of orange peel
10	1110	785	700	40	Orange Peel along all exposed surface
* 12	1200	870	*600	45	Peice did not burst, minimal orange peel, SS. band fused to center
13	1400	NA	500	114	Peice buckeled to one side
14	1400	NA	*700	82	Excessive axial force buckeled piece in several places
15	1400	900	700	45	Tube lengthened to 7 1/2" to keep heat from fittings
16	1500	NA	*600	35	Electrical connection melted Reheating failed
17	1500	NA	*600	94	No orange peel, forming flowed well, excessive axial force
18	800	NA	600	30	Band in center to avoid buckling insufficient heat
19	1400	NA	700	60	Reduced length to avoid buckling worked well,
20	1500	NA	700	82	5" starting length, symetric, good forming. would not re-heat

Twenty tests were done ranging in temperature from 400°c to 1500 °c. Those formed below 1200°c showed no improvement in forming. The group below 1200 °c all failed longitudinaly before even a 50% diametrical increase was seen. More important was the fact that any increase in diameter at these temperatures required an increase in the internal pressure. Orange Peel was also common to all of this group. It indicates the niobium was not in a stress relieved condition.

Those tubes formed at temperatures above 1200 °c expanded continuously, but unfortunately I wasn't able to sustain the higher temperatures long enough to achieve the desired 3 to 1 cavity dimensions.

Several problems developed during these tests that prevented me from gathering more specific information. The thermocouples used were erratic at lower temperatures and inadequate in the higher temperature ranges. All temperatures above 1200 °c were estimated visually. Argon leaks into the vacuum convected heat away in the lower temperature range and contaminated the surface of the higher range pieces.

Tests 16 and 20 were stopped and attempts were made to reheat, which were never successful. It could not be determined if the resistance of the pieces had decreased or if they had shorted to the axial force rod creating two parallel current paths.

It appears that no advantage could be gained forming niobium cavities at elevated temperatures, unless the annealing temperature range is reached.

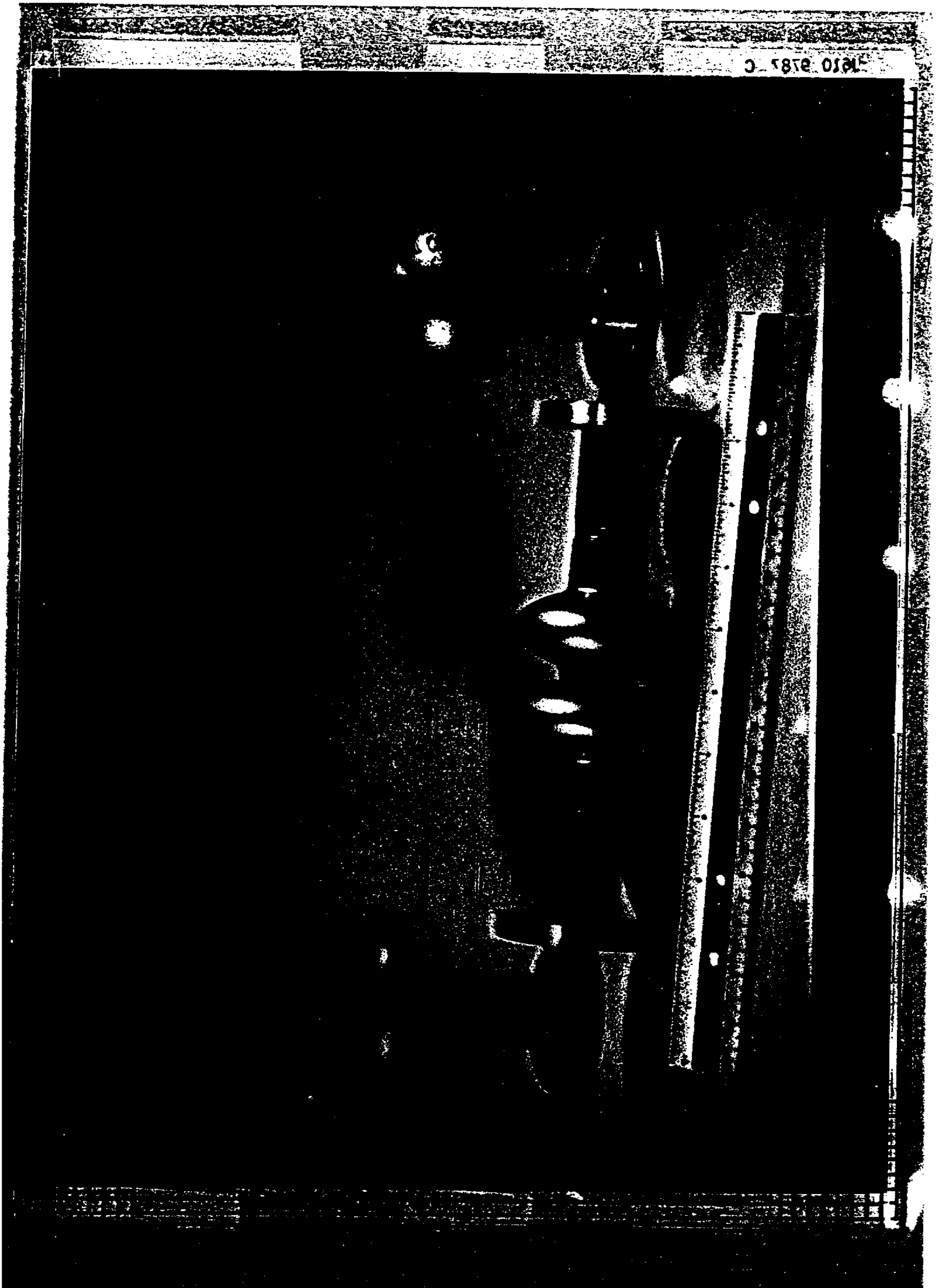

14

14

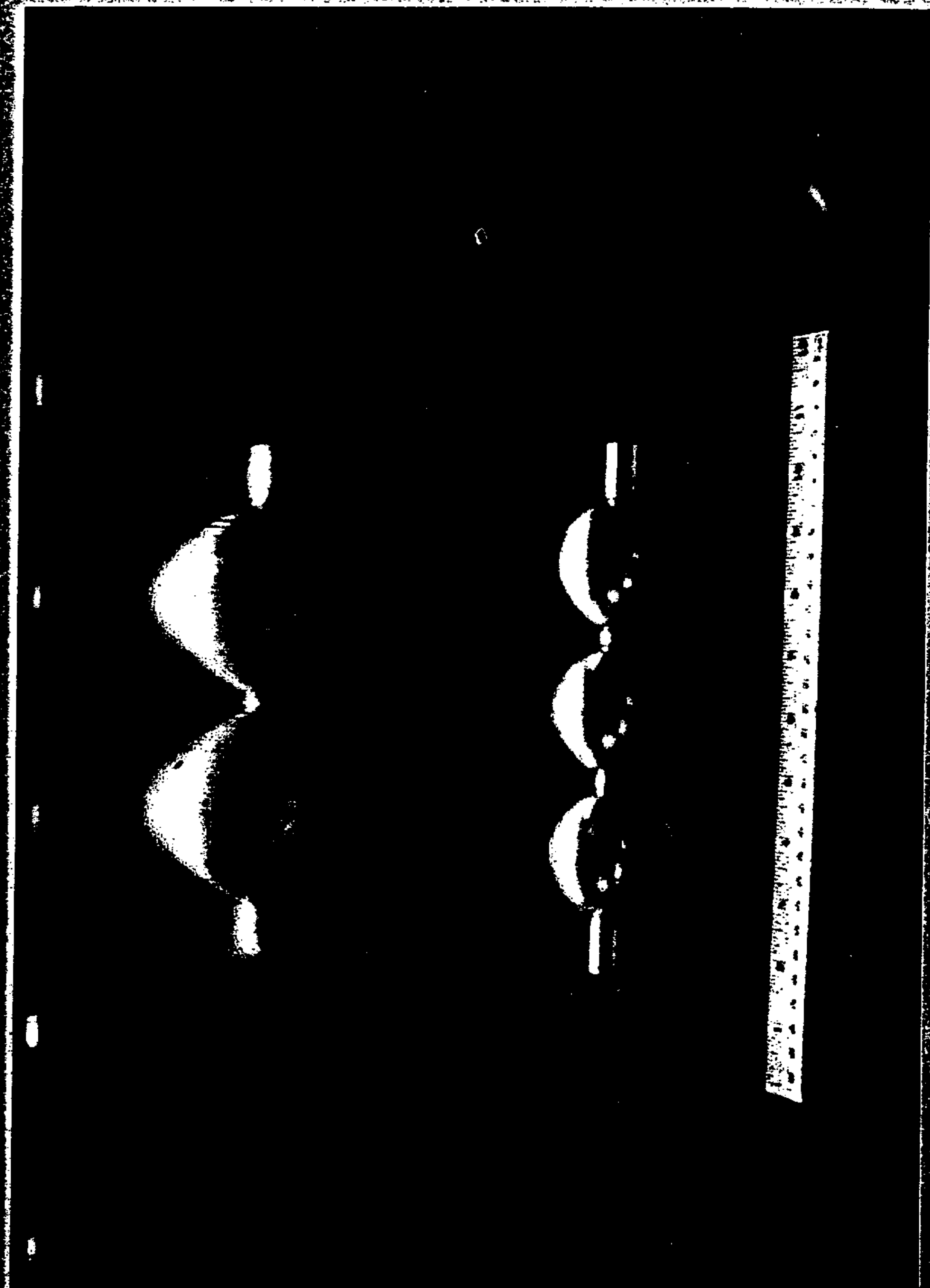

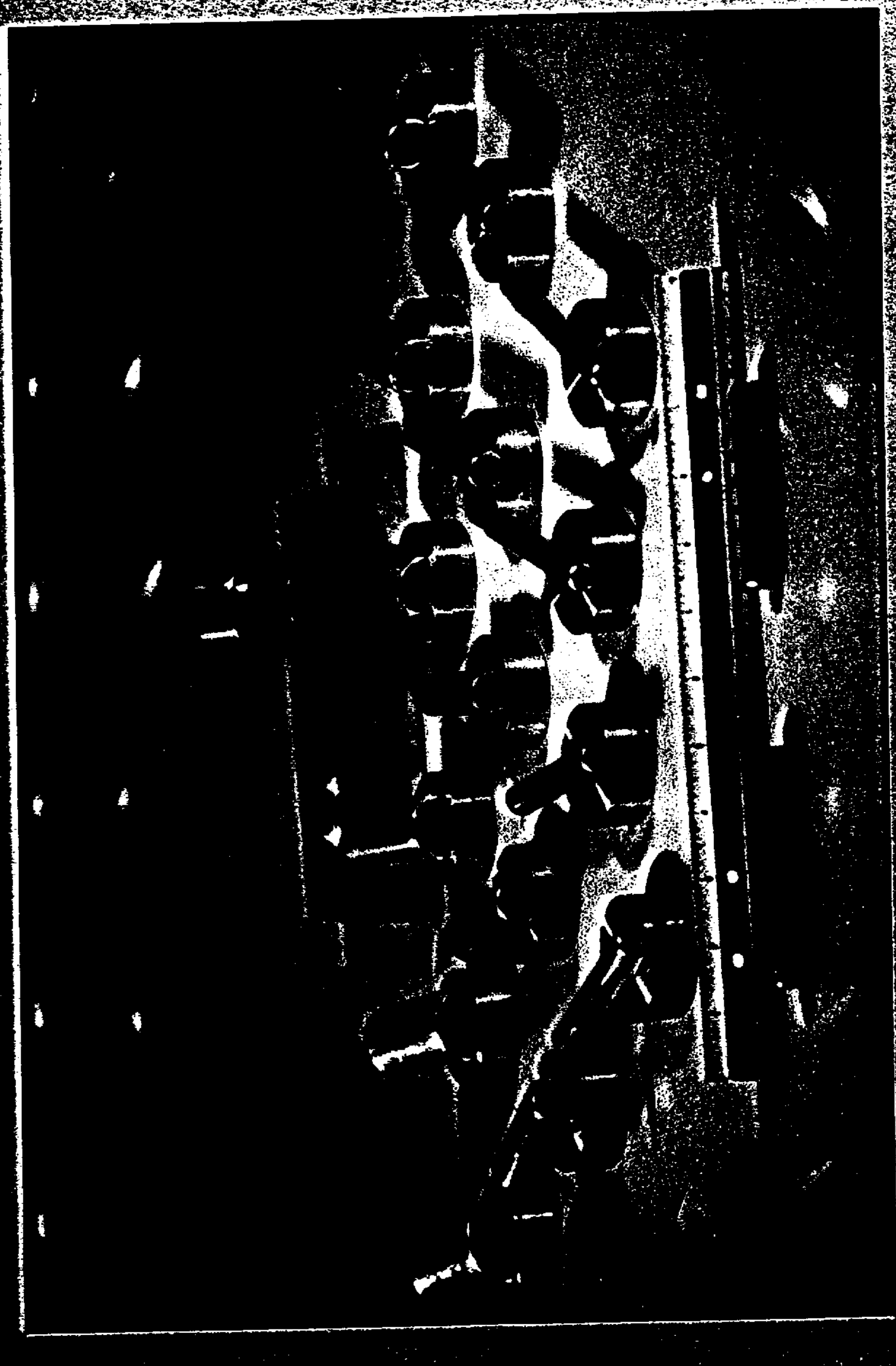

SRF 830503

To: SRF - group

From: P. Kneisel

Subject: Summary of rf tests on "bubble"-cavities

Date: May 19, '83

This note summarizes the tests, which have been carried out until now on hydroformed cavities.
(3 spherically shaped cavities SS1-1, SS1-2, SS1-3, f = 3430 MHz - large grain material;
1 elliptically shaped cavity SE1-1, f = 3896 MHz - fine grain material)

For comparison some recent tests done by "W. Krause, B. Hillenbrand, Y. Uzel, K. Schnitzke, Siemens Comp" on X-band-cavities made out of 1mm thick niobium sheet (thermal conductivity at 4°K = 4 $\frac{W}{mK}$ and niobium tubing are also listed. As can be seen from table 2, sheet metal cavities gave Q's of $\geq 9\times10^9$ and $H_p \sim 900$ Gauss, whereas with cavities out of seamless tubing fields were limited to <u>230 Gauss</u>. Only <u>high temperature firing at 1990°C for 5 hrs</u> improved the cavity performance to $Q_0 \sim 5\times10^9$, $H_p \sim 840$ Gauss

		low field	(high field)	[MV/m]	[Gauss]		
SS1-1	1	9.4×10^8	8×10^8	7	294	~80μm bcp	BD at equator
SS1-1	2	3.5×10^8	3.3×10^8	5.3	223	stress relief firing at 930°C for ~5hrs in "Anode"-furnace 25μm bcp	BD at equator in high magnetic field region
SS1-1	3	3×10^9	2.6×10^9	4.9	206	fired at 2100°C 2-3hrs ~5-10μm ccp	BD on upper cavity half
SS1-2	1	1×10^9	1.1×10^9	7.7	323	~75μm bcp	BD at equator
	2	1.9×10^9	1.6×10^9	2	82	fired at 2000°C 4hrs	Cavity shipped in N_2-filled bag; no treatment before assembly
	3	9.5×10^8	9×10^8	4.6	193	~5-10μm ccp	BD on lower cavity half
SS1-3	1	6.7×10^8	2.2×10^8	2.1	88	~75μm bcp	BD in upper half near surface crack
	2	1.1×10^9	3.7×10^8	2.8	117	fired at 1850°C for 3hrs 5-10μm ccp	BD not detected

Table 1 (bcp = buff. chem. polished ; ccp = cold polished)

Cavity	test #	Q_0 (low field)	Q_0 (high field)	E_{acc} [MV/m]	$H_{p,surf}$ [Gauß]	treatment	comment
SEI-1	1	6.9×10^8		5	392	~80μm bcp	

Siemens - results

cylindrical		8.4×10^9	2.4×10^9	22.6	890	TIG welded chem. polishing	sheet
spherical		10×10^9	1.1×10^9	19.7	880	ebw chem. polishing	sheet
cylindrical	1	—	—	5.8	230	chem. pol.	seamless tubing
	2	4.6×10^9	4×10^9	21.3	840	chem. pol. firing at 1930°C for 5 hrs	seamless tubing

Table 2 (Material thickness 1 mm, measuring temp. 1.3–1.5 K)

TESLA 1995-09

ANL-PHY-88-1

VOL. II

Physics Division

Physics Division
Physics Division
Physics Division
Physics Division
Physics Division
Physics Division
Physics Division
Physics Division
Physics Division
Physics Division
Physics Division
Physics Division
Physics Division
Physics Division
Physics Division
Physics Division
Physics Division
Physics Division
Physics Division
Physics Division
Physics Division
Physics Division
Physics Division
Physics Division
Physics Division
Physics Division
Physics Division
Physics Division
Physics Division
Physics Division
Physics Division
Physics Division
Physics Division

Proceedings of the Third Workshop on RF Superconductivity

Argonne National Laboratory, Argonne, Illinois 60439,
operated by The University of Chicago
for the United States Department of Energy under Contract W-31-109-Eng-38

Physics Division
Physics Division
Physics Division
Physics Division
Physics Division
Physics Division
Physics Division
Physics Division

219

/

FORMING AND WELDING OF NIOBIUM FOR SUPERCONDUCTING CAVITIES*

Joseph L. Kirchgessner

Laboratory of Nuclear Studies
Cornell University
Ithaca, New York 14853

Summary

Over the past two decades a variety of superconducting radio frequency structures have been designed, fabricated and tested, mostly in the pursuit of better and less costly particle accelerators. Over this period of time there has been an evolution in the fabrication processes as well as improvements in the test results. As in all technical endeavors, in the beginning fabrication was very difficult, but over the years developments in fabrication techniques have led to cheaper and improved structures in spite of the increases in the structures complexity.

This paper, which describes fabrication techniques, includes the description of work performed at many other laboratories as well as at Cornell. The author wishes to apologize to other laboratories for omissions, of which there are surely many. As far as disagreement on technical conclusions this paper describes those methods which have been found to be most satisfactory at Cornell as determined by our facilities and certainly does not claim that these findings would be the same in all other laboratories.

The author also wishes to thank all the other laboratories for sharing with Cornell the benefit of their experience over the years.

The types of forming which will be considered are:

Machining
Bending
Spinning
Deep Drawing
Hydro-forming
Hot Forming
Explosive Forming

The types of joining which will be considered are:

Explosive Bonding and Plating
Electron Beam Welding (EBW)
Tungsten Inert Gas Welding (TIG)
Laser Welding

Machining

The first Niobium structures which were fabricated and tested at Cornell were machined from solid Niobium material. Figure 1 shows an example of such an early structure. Half of a seven-cell, S-Band, "muffin-tin" structure is shown complete with machined filters at both ends which prevent RF leakage down the beam tube aperture.

The material cost and machining cost of such a structure were very high. However, a structure of this type was tested in the Cornell Electron Synchrotron and operated very well. [Ref. 1]

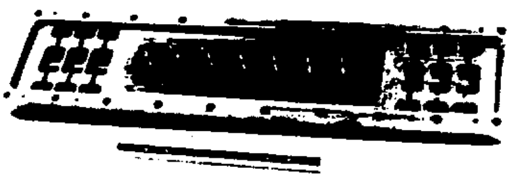

Figure 1.

The machining of Niobium has been described by some as having all the combined undesirable problems of stainless steel and soft copper. In spite of this, however, most shops have learned to machine the material with little or no difficulty. Several points make this required machining of Niobium possible and in some cases easier or more predictable than some other materials. These points are:

1. Flood cooling with Trichlorethane 1,1,1
2. Mill and lathe tools must have an extreme back rake angle (Aluminum cutting)
3. Cutting tools of high speed tool steel.
4. Cutting speeds of 80 SFM (25 m/min.) maximum.
5. Feed rates of 0.002 inches (0.05 mm) or less chip load, per revolution.

Internal tapping [especially blind tapping] remains difficult. External threading gives very nice results with roller dies. [Ref. 2],[Ref. 3]

There has been some Electrical Discharge Machining (EDM) done. Some of the Muffin Tin Shapes had a series of grooves (1.5 mm wide, 1.5 mm deep, and 3 mm spacing) cut in the bottom of the cups transverse to the beam direction. The grooves cut by EDM were used to prevent multipactoring in the cup bottoms. Ordinary EDM machines were used with highly filtered oil and copper electrodes. Currents of 10 amps average were used and material removal rates of 0.025 cu in per hour (400 mm^3 per hour) were experienced.

The need for material saving and the introduction of mass production called for advances in sheet metal techniques.

Bending

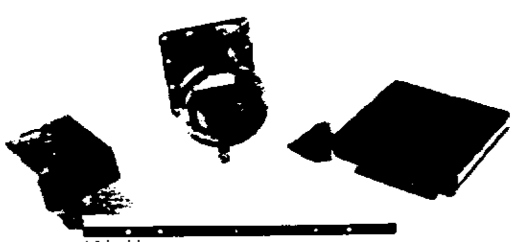

Figure 2

Shearing and bending of Niobium sheet metal poses no particular problems. A variety of wave guide shapes as well as wave guide T's and elbows have been made with these simple techniques. The use of proper back gauges on a press brake will yield bends accurate in position to ± 0.002" (0.05 mm). Figure 2 shows a transition beam tube and some wave guide sections made in this manner.

Spinning

While spinning has been used extensively at other laboratories, [Ref. 4],[Ref. 5] Cornell has had limited experience with this technique applied to Niobium. The disadvantages we have experienced are:

1. Need for intermediate anneals.
2. Lack of reproducibility.
3. Lack of in-house expertise

We realize that other laboratories do not share our experience and the technique has been applied with great success. Figure 3 shows a 4-cell cavity made with the spinning technique.

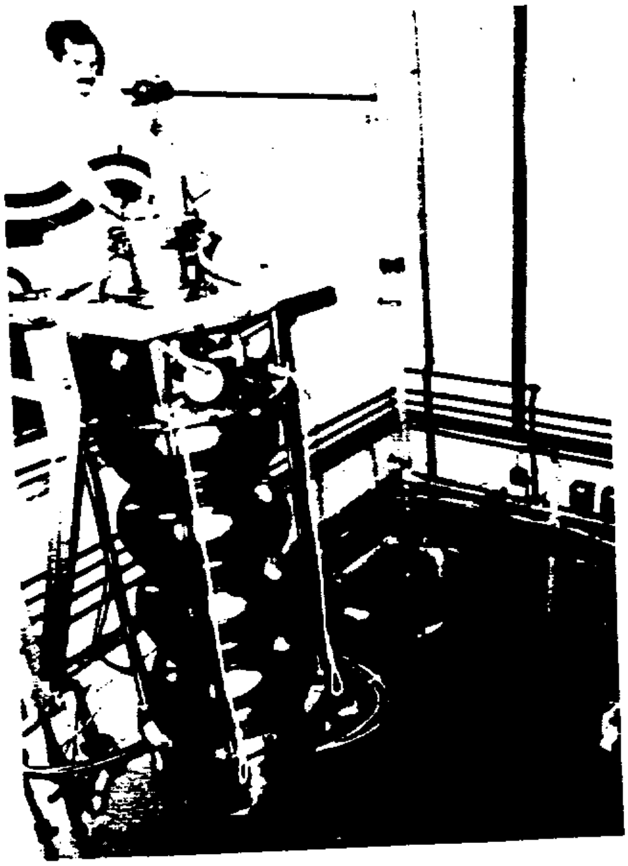

Figure 3

Deep Drawing

Our first attempts at deep drawing were made when we were manufacturing S-band, "muffin-tin" structures. In a very short time we also applied the technique to X-band and L-band cups. Figure 4 shows a series of cups made during this period. [Ref. 6], [Ref. 7]
The dies were made of Copper-Aluminum Alloy (AMPCO) and most were drawn in a 2-stage process without intermediate anneals.

When the effort at Cornell switched from "muffin-tins" to eliptical circular cavities, the deep drawing was accomplished with single stage dies made (in house) from 7075-T6 Aluminum alloy. These cups were made in a variety of frequencies and thicknesses as shown in Figure 5. [Ref. 8], [Ref. 9]

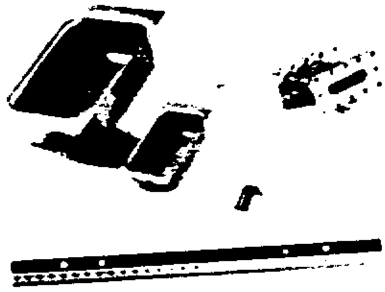

Figure 4

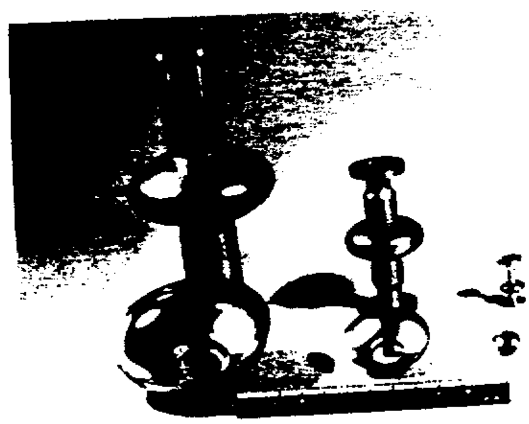

Figure 5

Most of the deep drawing was done using clean motor oil as a lubricant in order to avoid foreign inclusions. A typical L-band die is shown in Figure 6.

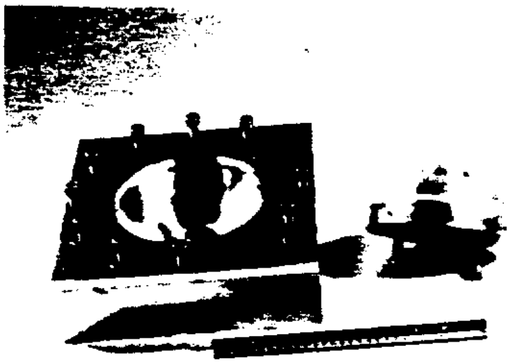

Figure 6

Figure 7

The die consists of three parts; a female die, a male die, and a bolted-on material hold down plate.

A variety of parts have been made by this process, all using aluminum dies with great success. Figure 7 shows a wave guide shorting dome, an HOM coupler body, and a cavity side port all made by the deep drawing process.

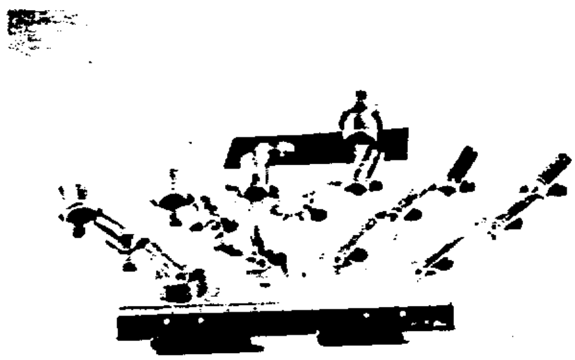

Several years ago an attempt was made in the laboratory to manufacture high purity tubing [high RRR] from flat Niobium sheet. A seven stage die set was made and used but the product showed excessive thinning and "orange peeling" even with two intermediate anneals. Another attempt was made with a very simple 16-stage die set and no intermediate anneals. To our surprise, the product showed no thinning or tendency to tear. Figure 8 shows the 16-stage die set as well as the product from the 7-stage and the 16-stage die set.

Our conclusion was that the metal deformation that could be achieved was a very strong function of the number of die stages that were used.

One disadvantage in the one stage deep drawing of the circular cavity cups has been a slight thinning of the material near the beam line nose. This thinning has made outside welding of the nose very difficult. Recently S-band cups have been made using a two-stage process. Figure 9 shows the contrast between the new 2-stage process and the old single stage process. Figure 10 is a picture of the dies used in the 2-stage process. The results of this effort will be discussed under Electron Beam Welding.

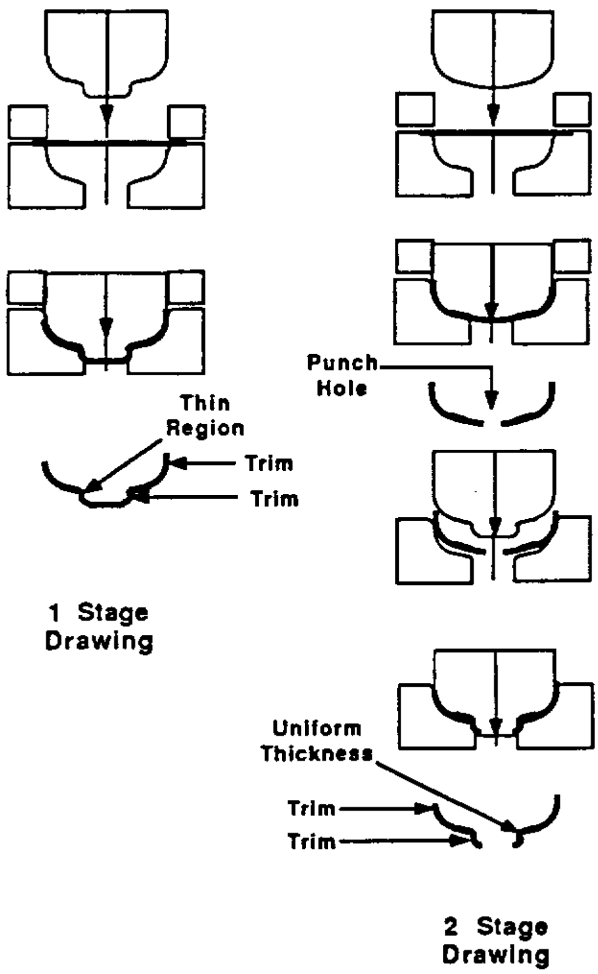

Figure 9

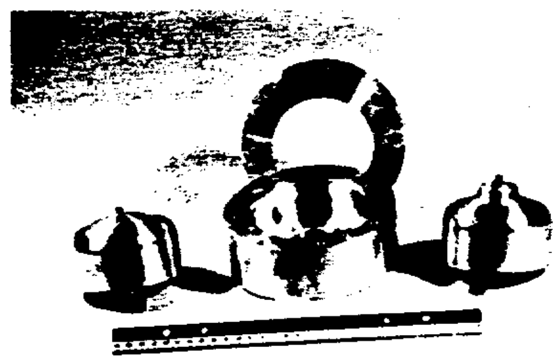

Figure 10

It should be mentioned that the interest in high RRR material in recent years has made more important the fact that intermediate anneals be eliminated in order to avoid decreases in the RRR. On the other hand, this high RRR material is much more difficult to produce with a small uniform grain size, so important in the deep drawing process. The final anneal must be controlled very closely in order to avoid excessive or non-uniform grain growth.

The general rules that may be followed for deep drawing are as follows:

1. Dies must be made of aluminum (7075-T6), AMPCO or Beryllium Copper. 7075 aluminum is by far the cheapest and easiest to machine, and has as high a yield strength as the other materials. Hundreds of pieces have made with such dies with no sign of die wear if adequate lubrication is used. Conventional die materials such as steel or Tungsten Carbide are not satisfactory as they tend to gall (friction weld) with the Niobium. This does not happen with the aluminum or copper base materials.

2. The die clearance which is used is equal to the material thickness. We have observed no excessive pinching or die wear.

3. A lubricant must be used. "Never Seez" works very well but can easily become contaminated with debris which will then be pressed into the Niobium surface. For this reason, clean, new motor oil is preferred.

4. Very simple "hold down" plates and hydraulic presses may be used. The use of a slow hydraulic press assures there will be no "stress rate" effects. Automatic hold down and stripping features would be significant only in very large production runs.

5. The ASTM metal grain size should be 4 or smaller in order to avoid orange peeling. This is sometimes difficult to achieve in the high RRR materials.

Hydroforming

The differences and distinctions between deep drawing and hydroforming become somewhat vague. Hydroforming will be defined to be when one side of the worked piece is forced only by a fluid, whether it be hydraulic fluid, gas, or polyurethane. Some of the earliest Niobium cups were hydroformed by HEPL at Stanford [Ref 10].

Several years ago in our development of circular L-band structures, there was a tendency to experience magnetic breakdown at the equator weld. In order to avoid any welds in the high magnetic field regions of the resonant structure, we pursued a technique of hydroforming a complete multicell cavity from a seamless tube. We have formed such shapes with an ID:OD ratio of 1:3. The essentials of the technique are shown in Figure 11.

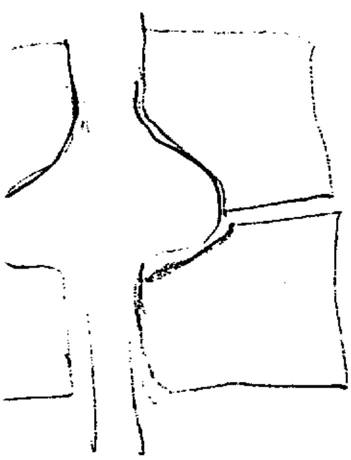

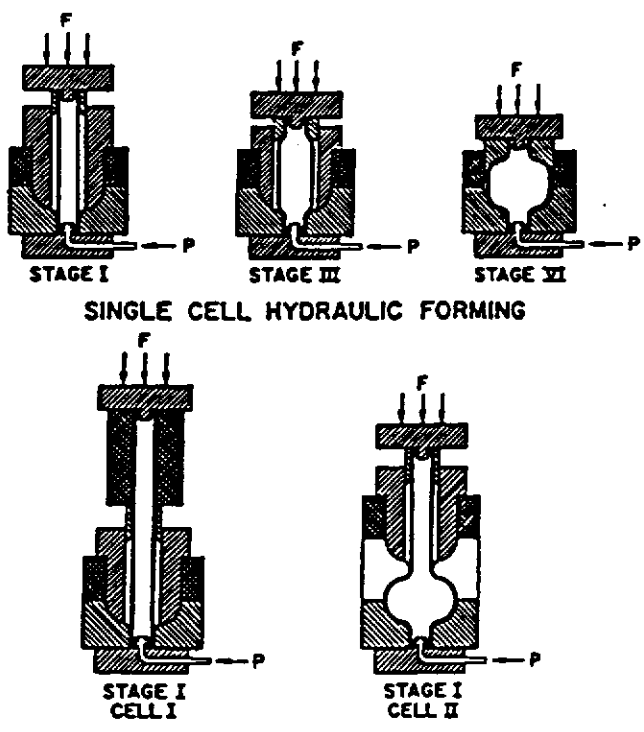

Figure 11

Multiple stages are required in order to avoid the lateral instability of the tube as axial force is applied. We found six stages to be satisfactory with an interstage anneal at every other stage. The chosen technique forms one cell complete at a time and imposes no limitations on the number of multiple cells which may be formed. While complete computer modeling of the process has not been done, calculations have been made which allow us to predict the thinning and buckling at each stage. Approximately 3% thinning per stage is our usual design goal. The development of a device to measure hydraulic fluid flow at 10 KPSI was necessary in order to monitor the process. The precision required on the fluid flow measurement was such that an analog computer was used to account for the compressability of the hydraulic fluid as a function of pressure. Figure 12 shows several S-band size structures manufactured in this manner.

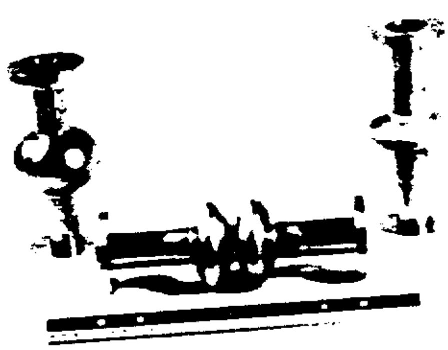

Figure 12

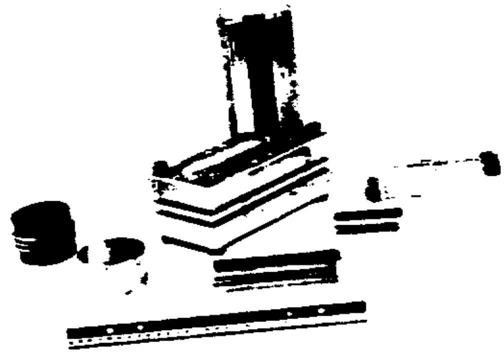

Figure 13

Cryogenic test results showed the typical cavity performance to be average even though the technique tended to give a very rough interior surface finish.

Our efforts were discontinued for the following reasons:

1. Improved welding techniques eliminated breakdown at the equator weld.
2. Seamless Niobium tubing of small, uniform grain size is expensive and difficult to acquire.
3. The cost of the dies, the labor of the process and the annealing cost were all much higher than the deep drawing, machining, and EBW costs of the present method.

Some other items have been made by hydroforming. Figure 13 shows a type of beam tube and wave guide bellows which have been made along with one of the typical die sets. A band of 0.015" thick Niobium is welded, then pressed axially as a polyurethane plug expands radially to form the convolutions. The die also collapses axially as this happens in order to avoid material being forced axially over the die convolution plates.

Hot Working

Some tests were performed in order to determine the advantage, if any, of trying to blow bubbles in Niobium tubing at an elevated temperature. This work was done in a vacuum with high pressure (3 KPSI) Argon gas inside the hot Niobium tube. Tests indicated that at 800 deg C the % change in radius before rupture was the same as at room temperature. At 1200 deg C there was some improvement, but the gain certainly was not enough to warrant the continuation of the effort.

Hot Isostatic Pressing (HIP) has been tried as a way to produce parts of Niobium from Niobium powder. Photo-micrographs indicate that there are voids in the material. Cryogenic tests bear this out, as the test results have not been very good.

Explosive Forming

Tests were also made to investigate any possible advantage in the very rapid cold working of Niobium due to a stress rate dependence of the % elongation. A small die was machined and primer cord explosive was used under water inside a 1.5" dia. Niobium tube. [Ref. 11] The results indicated that the % change in the tube radius before rupture was much less than the change achieved with a slowly applied force (hydraulic). The conclusion was that in the case of Niobium metal, the stress rate dependence is disadvantageous.

Bonding

For reason of increased thermal conductivity, considerable work has been done with Niobium bonded to copper. Vacuum furnace brazing can be used, as well as "melt on" techniques. [Ref. 12] Some cavities have been made at CERN using this method. At DESY, work is continuing to plate copper and/or silver on the outside of circular cavities for reason of tube cooling. [Ref. 13].

The explosive bonding of copper to Niobium on one or both surfaces has been used extensively at Argonne National Lab. [Ref. 14] This method has also been used at Argonne to manufacture Niobium-lined copper tubes.

All the copper clad Niobium structures, however, have the difficulty of requiring that all copper be removed from the regions where the Niobium must be welded. Very slight traces of copper which might be present will ruin the material in the welds.

Electron Beam Welding [EBW]

At the present time, most of the electron beam welding being done at Cornell is done in a full penetration, smooth underbead mode. [Ref. 15] This sort of weld parameter is used by many laboratories, achieved in a variety of ways. The method we use to "defocus" the beam is to deflect the beam in the shape of a rhombus with the beam deflection yoke. [See Figure 14]

This resulting reduction in the energy density gives a smooth underbead, but requires careful control of material thickness in order to achieve full penetration with no blow holes. Figure 15 depicts what is permissible in the way of material edge preparation for satisfactory welds. Material thickness uniformity is much more important than off-sets. This has led us to conclude that a square butt weld with no stepped edge machining is most desirable insofar as the material thickness remains uniform.

Figure 15 also shows the detail of the nose weld using 1-stage and 2-stage deep drawing. In the first case, we were forced to use an internal weld due to thinning on each side of the weld zone. With the 2-stage process this was not true, and satisfactory welds could be made from the outside. Figure 16 shows an S-band cavity with all welds made from the outside.

The only edge preparation after deep drawing was a facing of the cup. This technique should significantly decrease the cost of welding multicell structures.

The critical nature of material thickness when making the smooth underbead welds is unfortunate. Tests show the welds to be even more critical as the material thickness is increased. For this reason, the internal gun welding [as used at CERN] is desirable but cannot be used with the higher frequency structures.

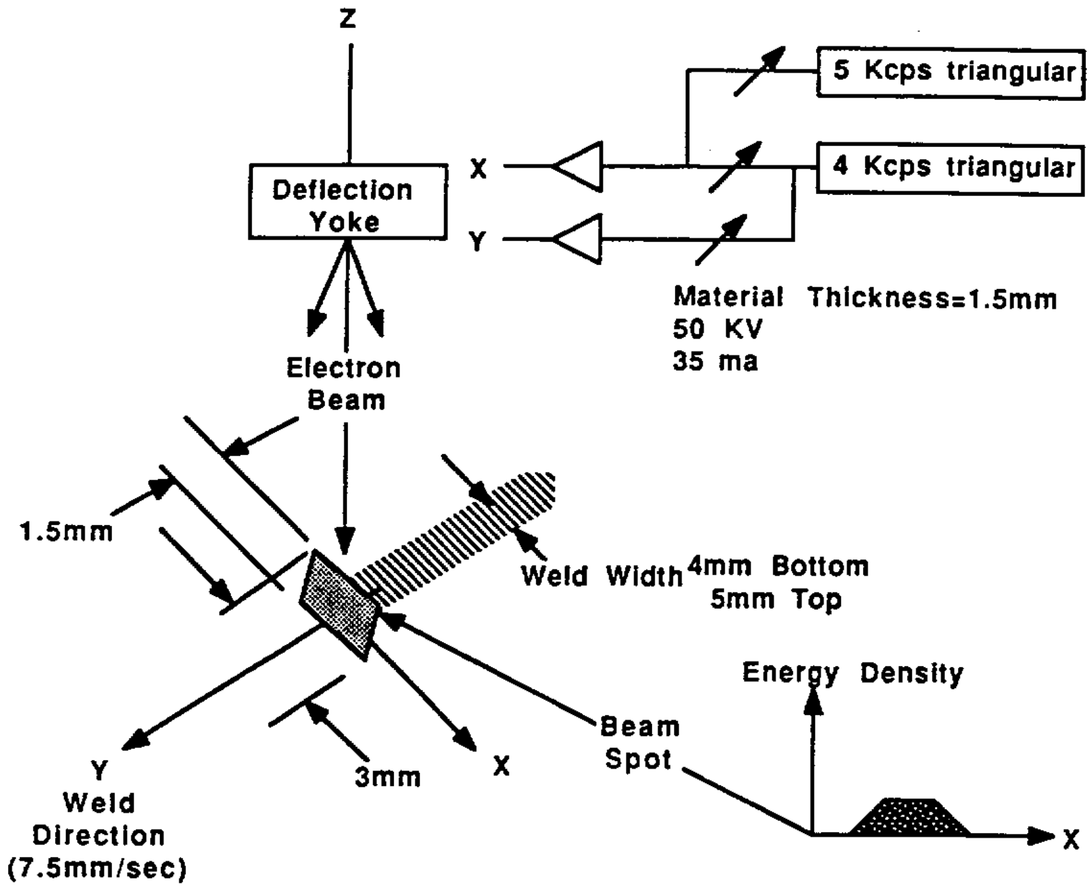

Figure 14

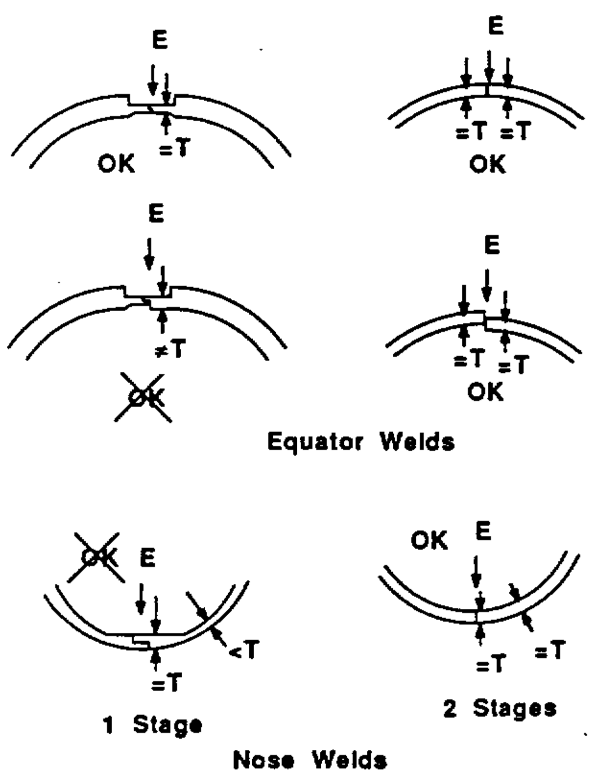

Figure 15

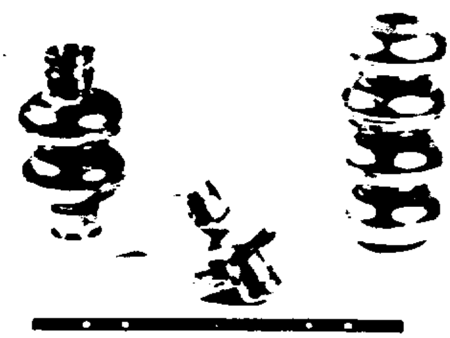

Figure 16

Some tests have been made using the "rhombic raster" weld in conjunction with negative weld current feedback from a weld temperature sensor placed on the underside of the weld. [Ref. 16] This technique shows great promise, but a large development effort would be required for final utilization.

TIG Welding

While at one time very popular, the use of TIG welding is rarely used because of the difficulty of excluding all air to a very high purity level from the hot weld in a reliable way. TIG welding does have the one advantage of giving a smooth underbead due to the lower energy density.

Laser Welding

Laser welding of Niobium structures has not been utilized to any great extent. This has probably been due to lack of penetration and difficulty with surface reflection. If these problems were solved the results should be as good as EBW but any advantages are not obvious. The lack of such welding facilities at the laboratories will probably also slow the development of this technique.

Conclusion

At the present time the utilization of RF Superconductivity is not limited by our ability to fabricate and weld the structures that are required. The required techniques are, however, sufficiently unique and specialized that it is difficult to find all the required facilities in one place other than at our own laboratories. Figure 17 shows some typical miscellaneous wave guide parts fabricated in our laboratory.

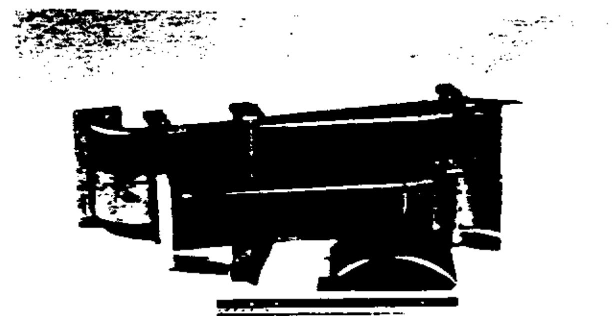

Figure 17

The fabrication of these parts required; machining, deep drawing, EBW, TIG welding, hydroforming, and bending as well as all the required intermediate chemical cleaning processes. This is typical of the complex structures and indicates the scope of the industrial involvement that will ultimately be required.

As one considers much larger accelerator projects involving superconducting RF there is no question but that the present designs must be altered to allow for much less expensive fabrication, both of the superconducting structures and of the auxiliary cryogenic and RF components. Such larger projects will require improvements in fabrication technology as much as they will require improvements in Q and voltage gradient.

Acknowledgements

The author wishes to thank the other laboratories around the world who have all been more than cooperative in the pursuit of our common goals. I wish to thank in particular the personnel at Cornell who have been doing all this fine work in an untiring manner.

References:

[1] J. Kirchgessner et al. IEEE Trans. Nucl. Sci. NS22 No.3 (1975) 1141

[2] W. Bauer, Proceedings of the Workshop on RF Superconductivity, Karlsruhe, (1980) 271

[3] J. Susta, Proceedings of the Workshop on RF Superconductivity, CERN (1984) 597.

[4] Y. Kojima, Proceedings of the Workshop on RF Superconductivity, CERN, (1984) 75.

[5] C. Benvenuti, et al., Proceedings of the Workshop on RF Superconductivity, CERN, (1984) 25.

[6] J. Kirchgessner, et al., IEEE Trans. Nucl. Sci. NS30 No.4 (1983) 3351

[7] R. Sundelin, et al., IEEE Trans. Nucl. Sci. NS30 No. 4 (1983) 3336

[8] P. Kneisel, et al., IEEE Trans. Nucl. Sci. NS30 No. 4 (1983) 3348

[9] R. Sundelin, et al., IEEE Trans. Nucl. Sci NS32 No. 5 (1985) 3570

[10] M.S. McAshan et al., Proceedings of the Ninth International Conference on High Energy Accelerators, SLAC, (1974), 123.

[11] North West Technical Associates, Port Angeles, Washington, Private Communication.

[12] H. Padamsee, IEEE Trans. Nucl. Sci. NS30 No. 4 (1983) 3354

[13] D. Proch, 1987 Particle Accelerator Conference Proceedings. (1987).

[14] K.W. Shepard, Proceedings of the Workshop on RF Superconductivity, CERN, (1984) 9.

[15] E. Chiaveri and H. Lengeler, Proceedings of the Workshop on RF Superconductivity, CERN, (1984) 611.

[16] J. Rothman, Cornell University, Private Communication.

*Work supported by the National Science Foundation and the U.S.-Japan Agreement.

DEVICE FOR FORMING OF THE SUPERCONDUCTIVE CAVITY FROM THE TUBE

INR (RUSSIA)
DESY (GERMANY)

I.Jelezov, G.Kliatchkov, L.Kravchuk, D.Proch, V.Singer, A.Stepanov

Presentation of W.Singer

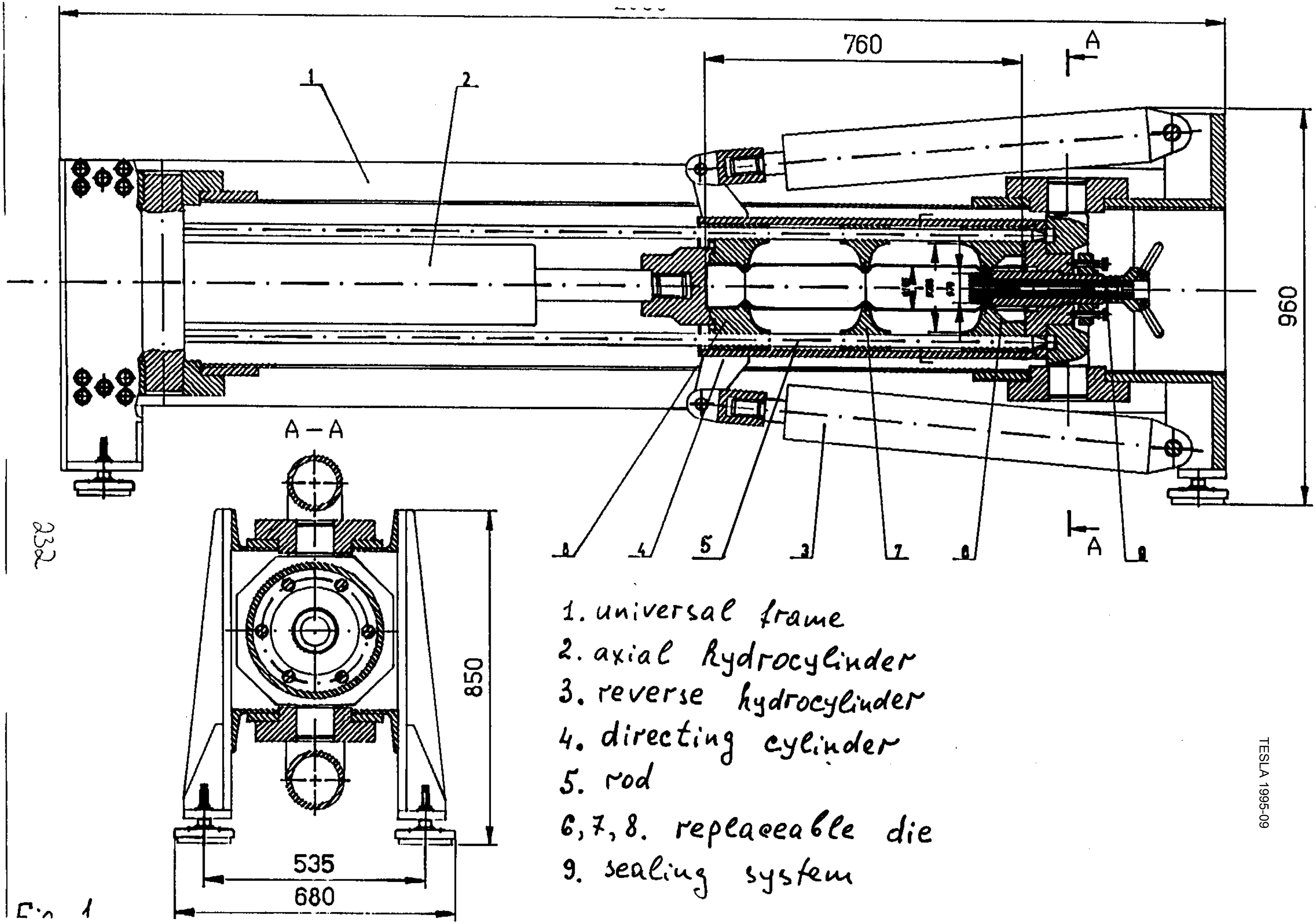

1. universal frame
2. axial hydrocylinder
3. reverse hydrocylinder
4. directing cylinder
5. rod
6, 7, 8. replaceable die
9. sealing system

Fig. 1

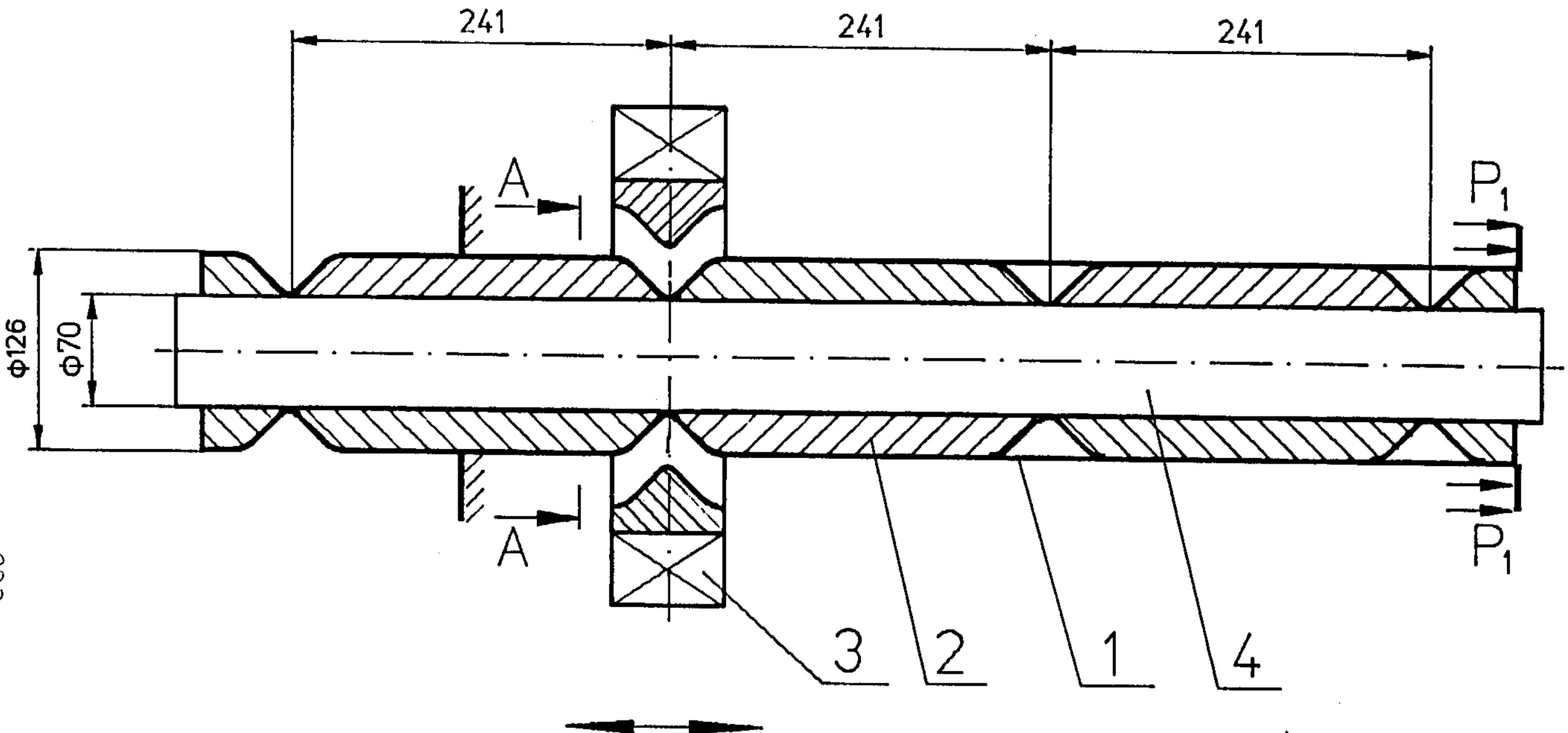

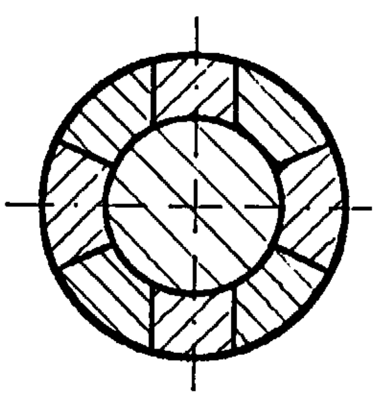

Magnetic pulsing device for forming of the iris shape

1. half-product (tube)
2. mandrel
3. magnetic inductor
4. rod

Fig. 2

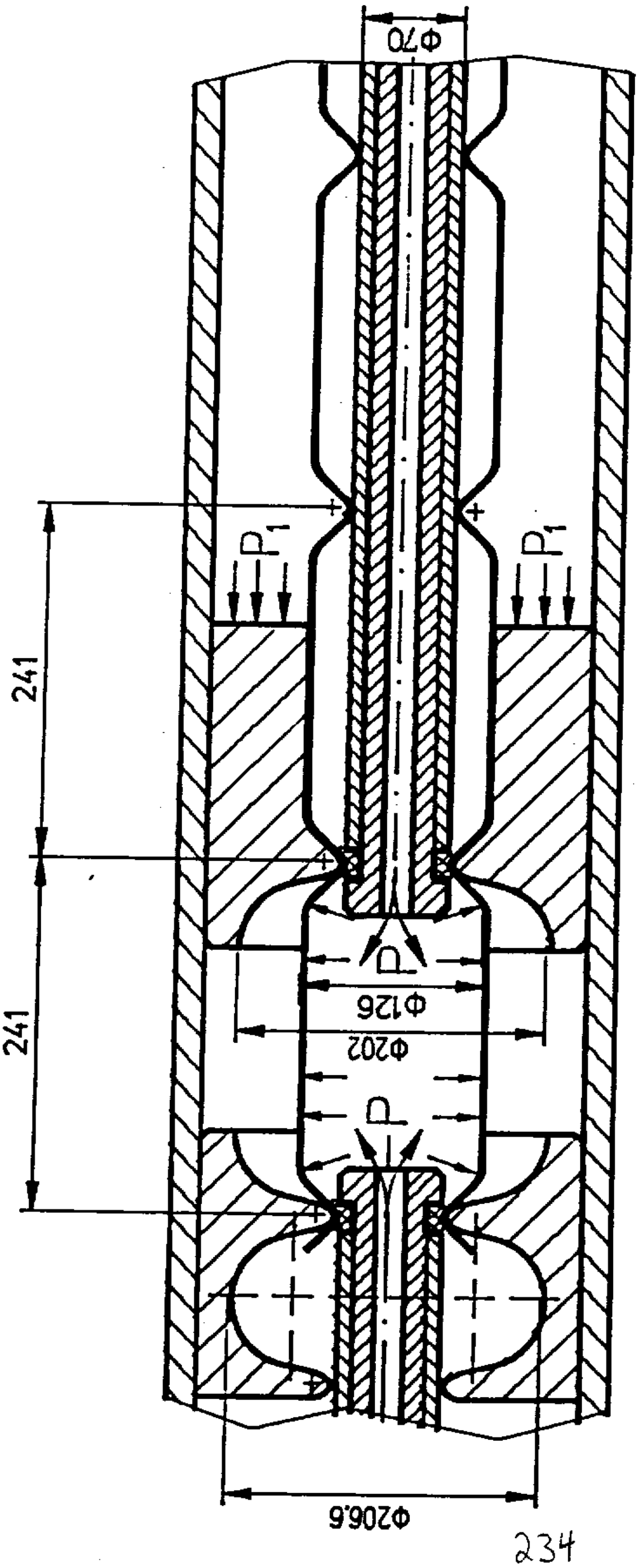

Principle of hydroforming
(stage one)

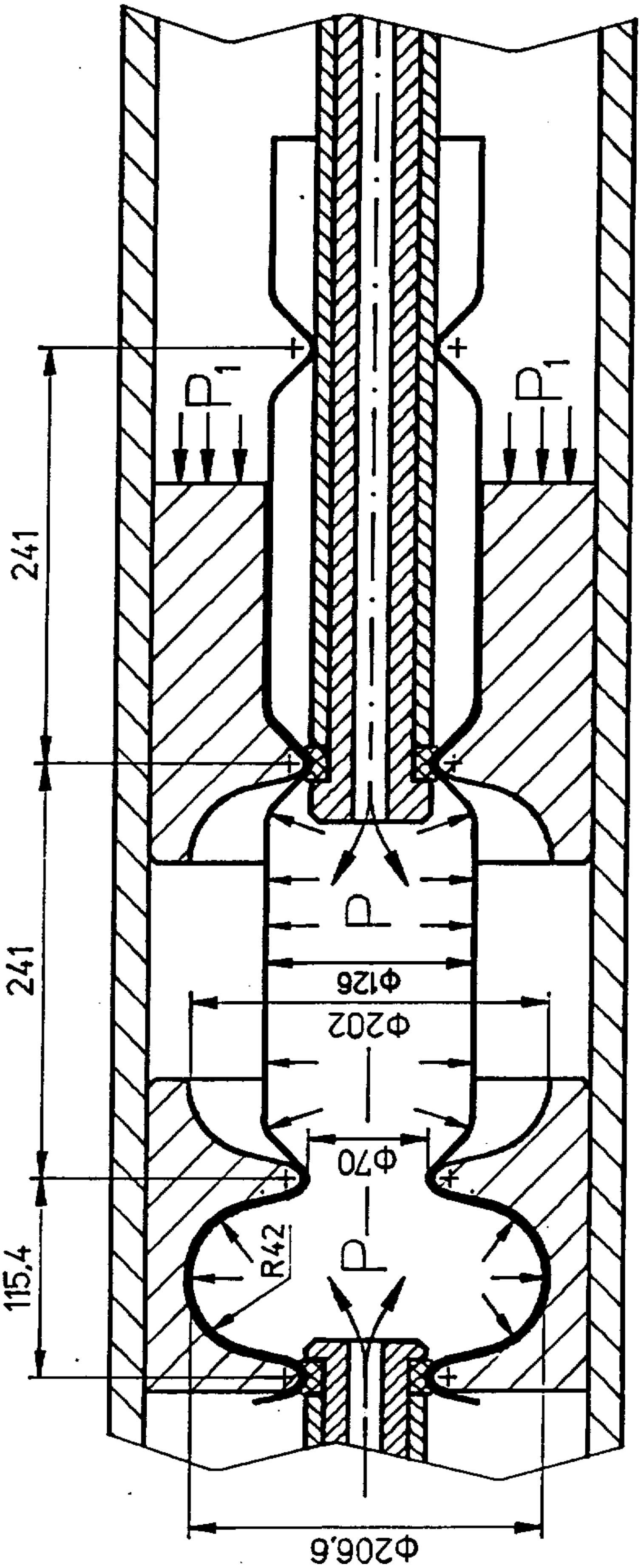

Principle of hydroforming (stage two)

ANALYZE OF NB PROPERTIES FROM POINT OF VIEW OF HYDROFORMING

TESLA 1995-09

W. Singer, A. Stepanov

Presentation of W.Singer

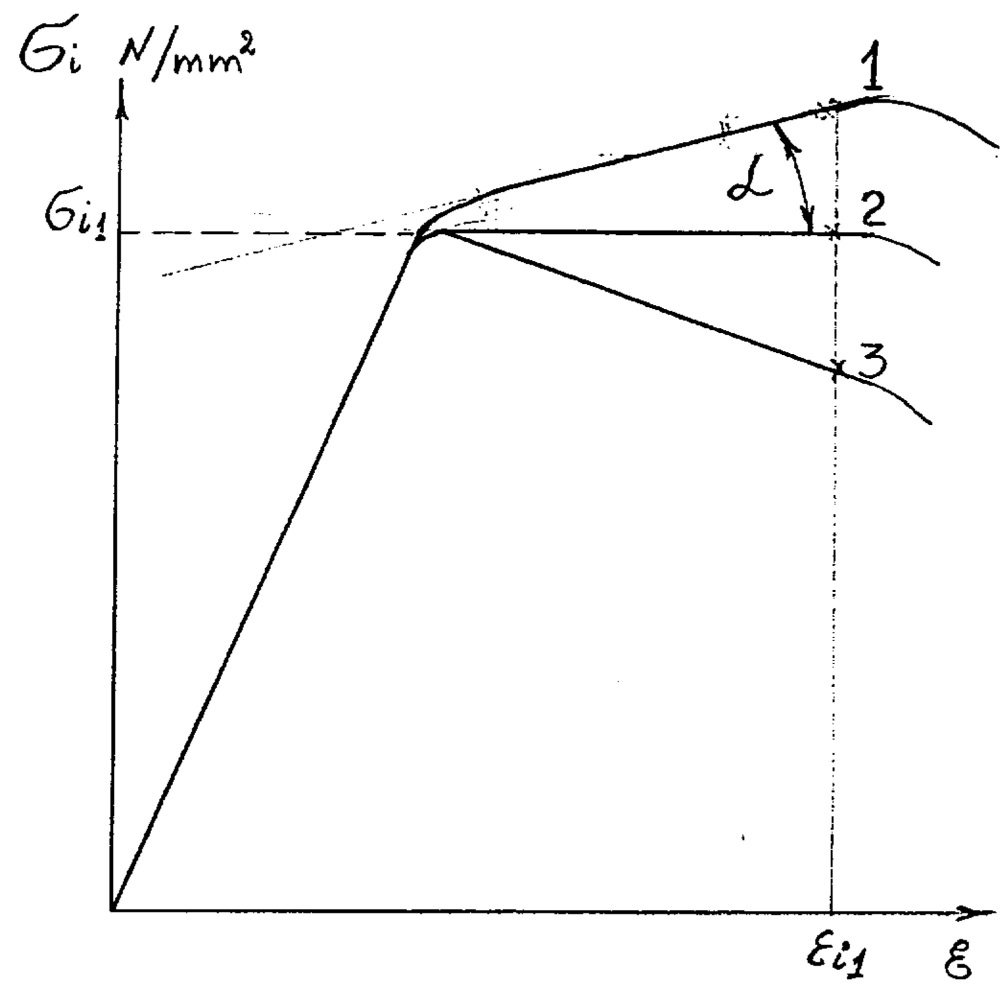

1. Materials with work-hardening by the plastic deformation (don't show localization of plastic deformation in rather big region)

2. Materials with small work-hardening (localization of deformation)

3. Materials with work-softening (localization of deformation)

Materials of first type are desirable for hydroforming

We need: maximum of ε_{i1}(reserve of plasticity)

minimum of σ_{i1}(technical reason)

high α (grade of work-hardening)

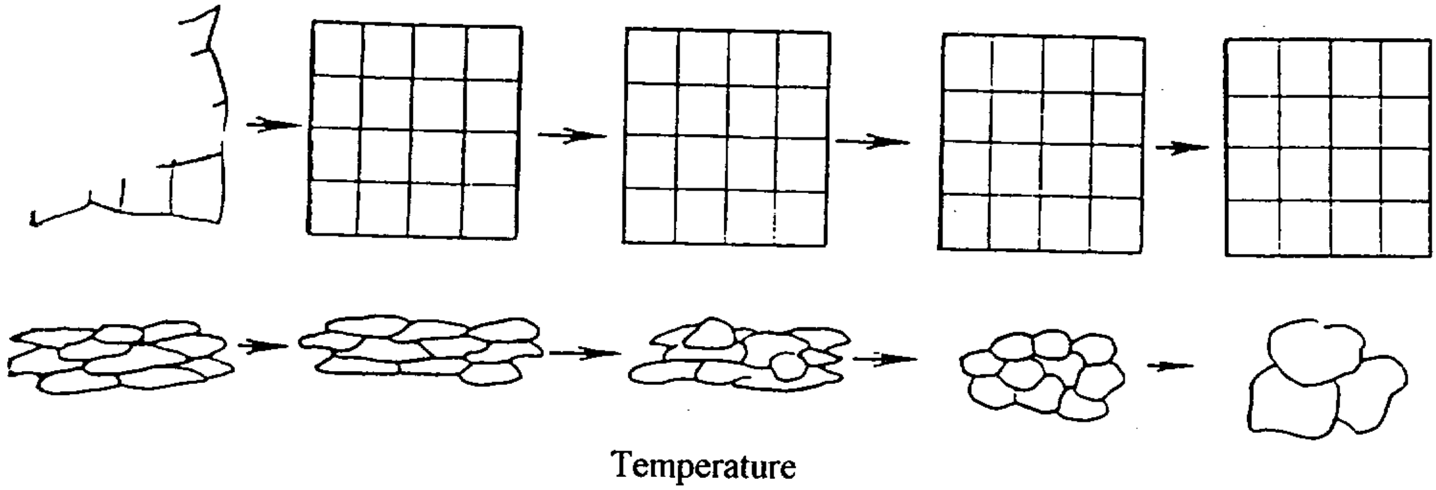

Scheme of the processes occurs by the annealing of the deformed metal

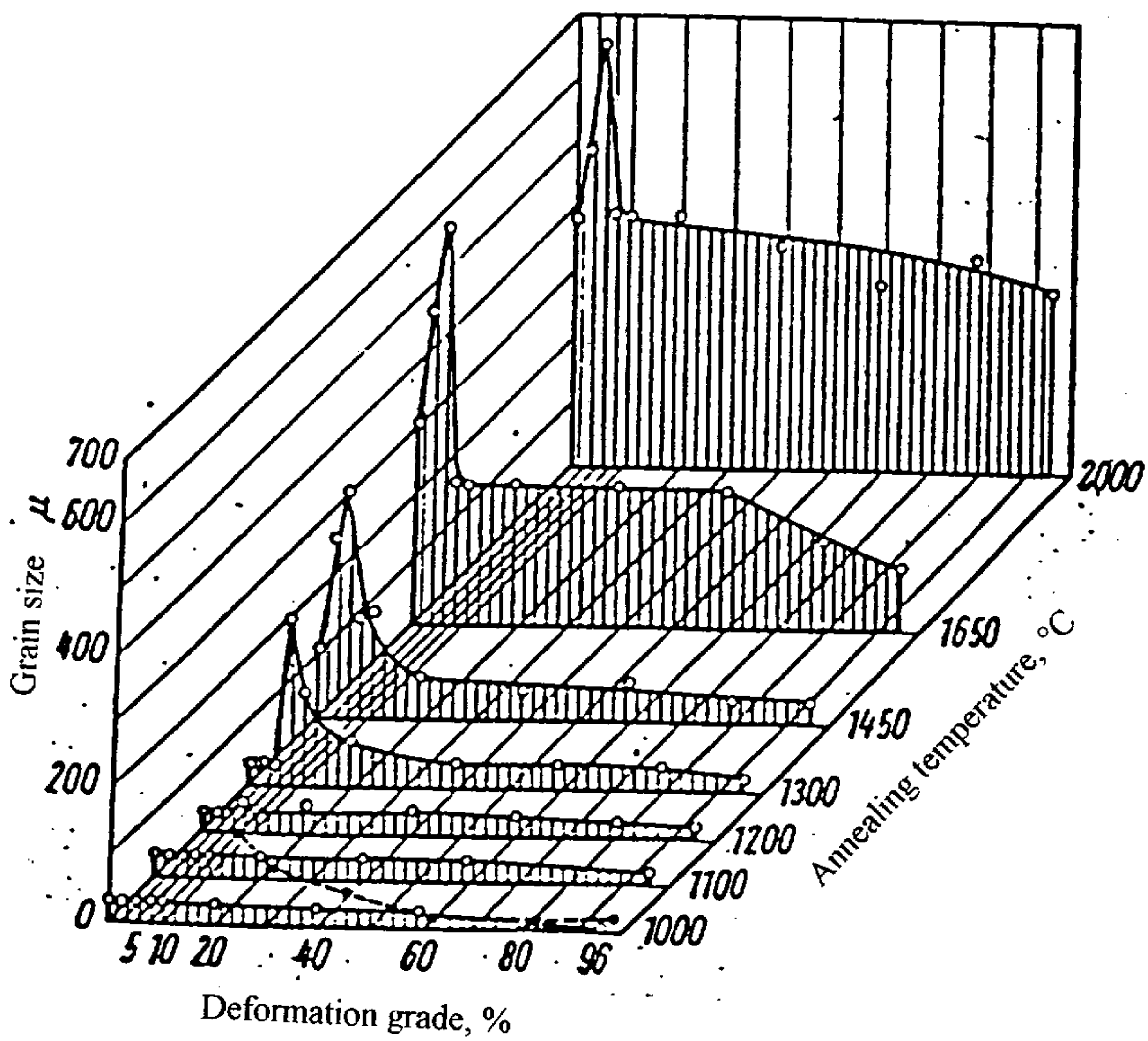

Situation of the samples on the Nb sheet

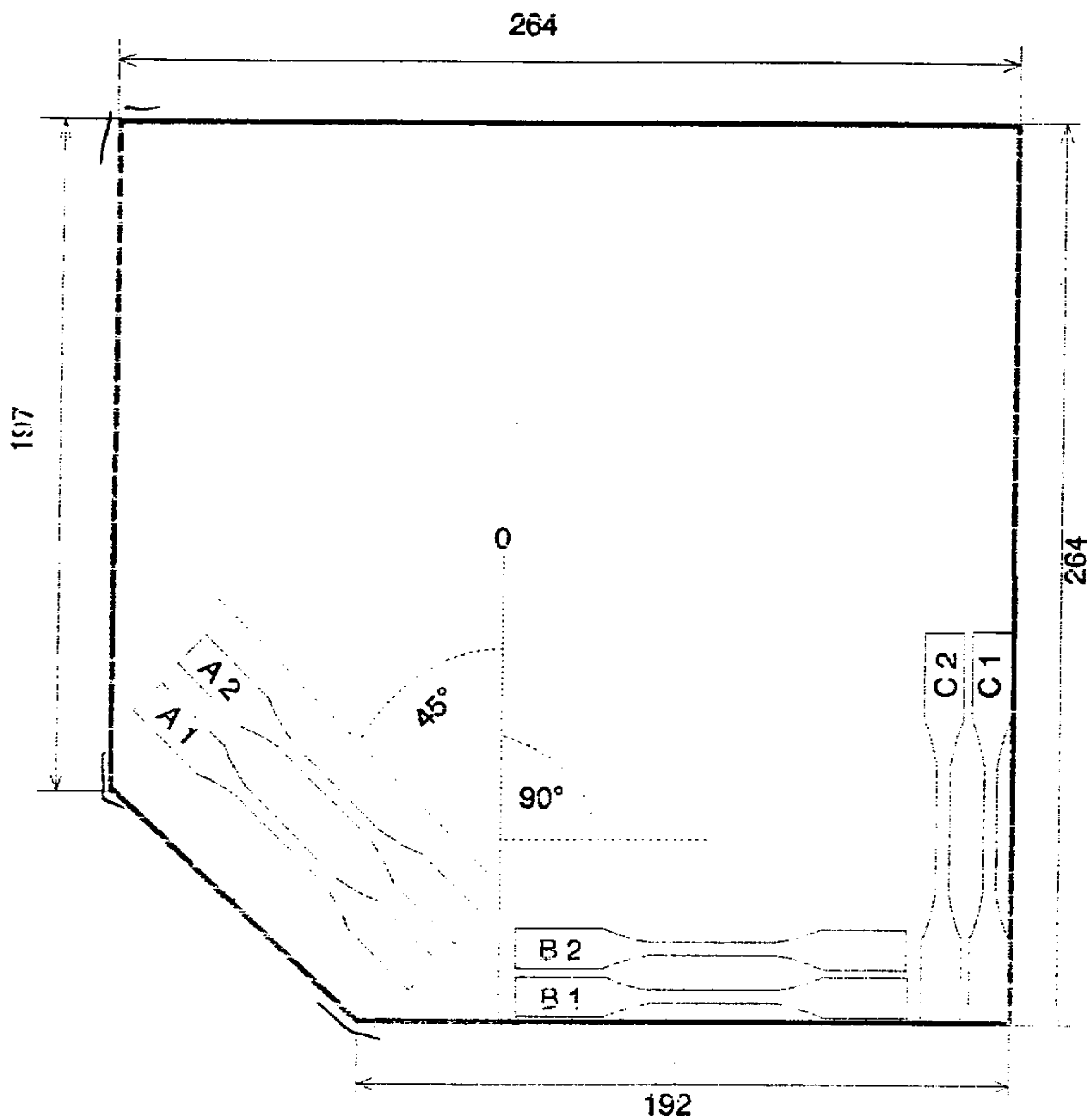

Anisotropy of mechanical properties of Nb 300

Sample	Tensile strength Rm, N/mm2	Yield strength Rp0,2, N/mm2	Elongation %	Remarke
A2	148	65	63	45° to roll. dir.
B2	170	69	37	90° to roll. dir.
C2	152	58	67	rolling direction

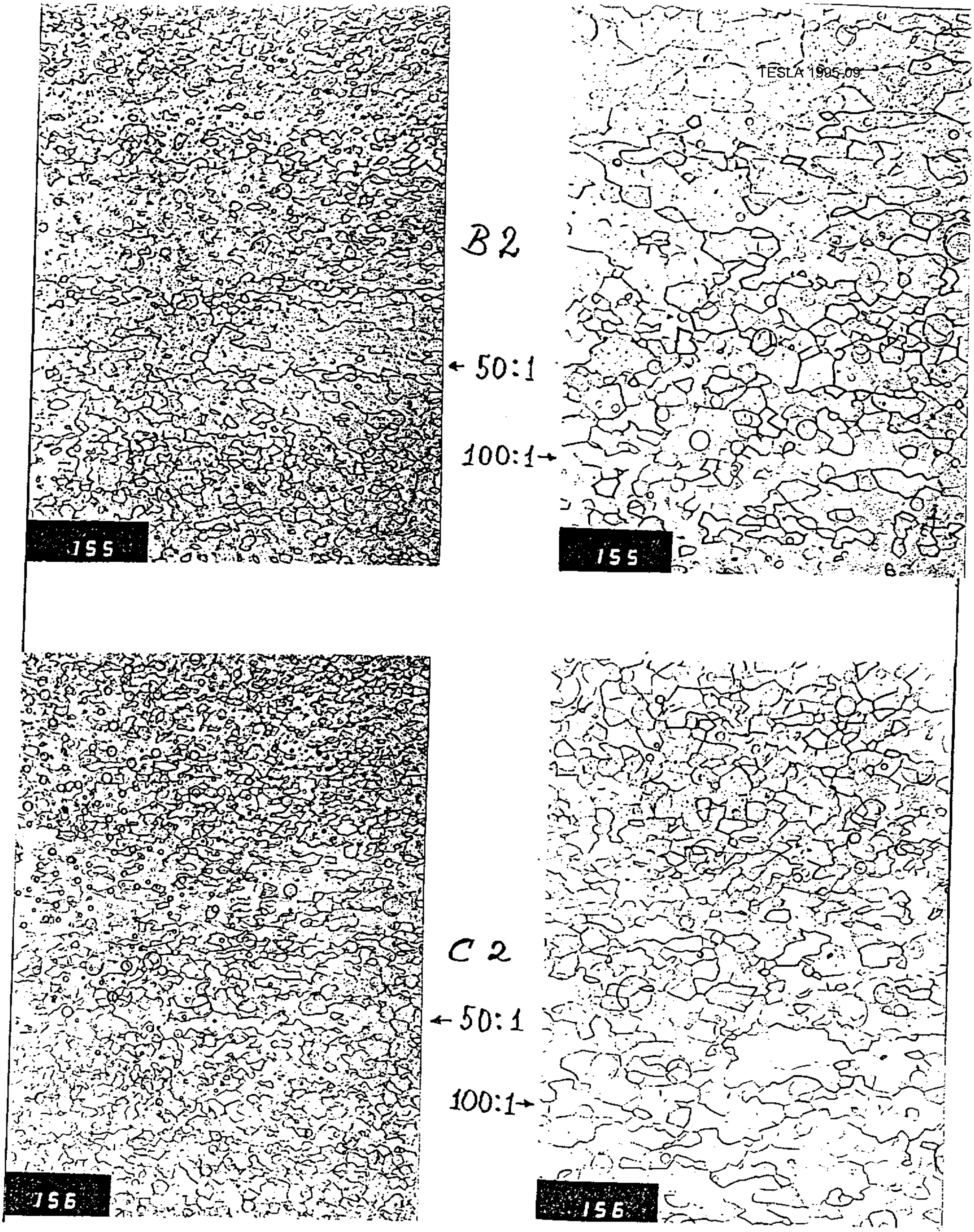

Microstructure of the samples B2 and C2. Grain size ASTM 7-8

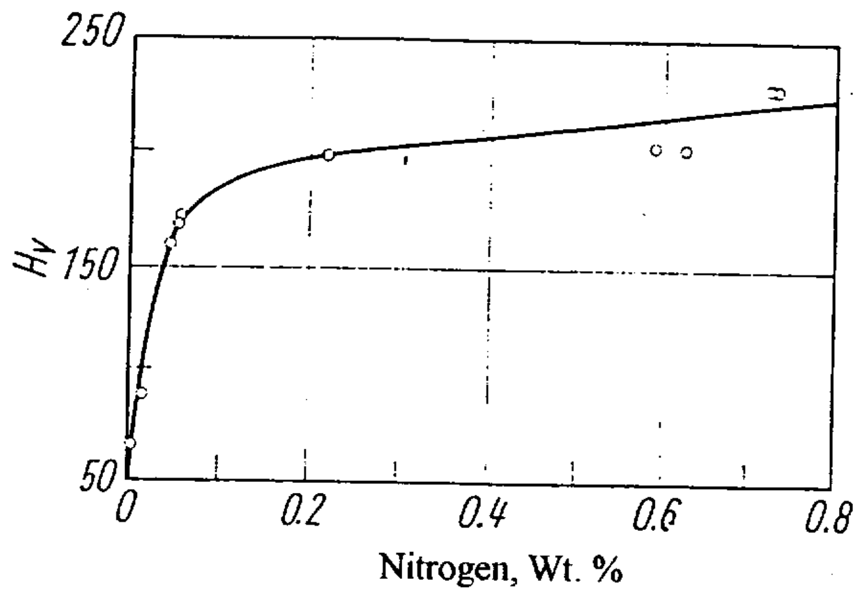

Dependence of hardness on content of nitrogen in Nb

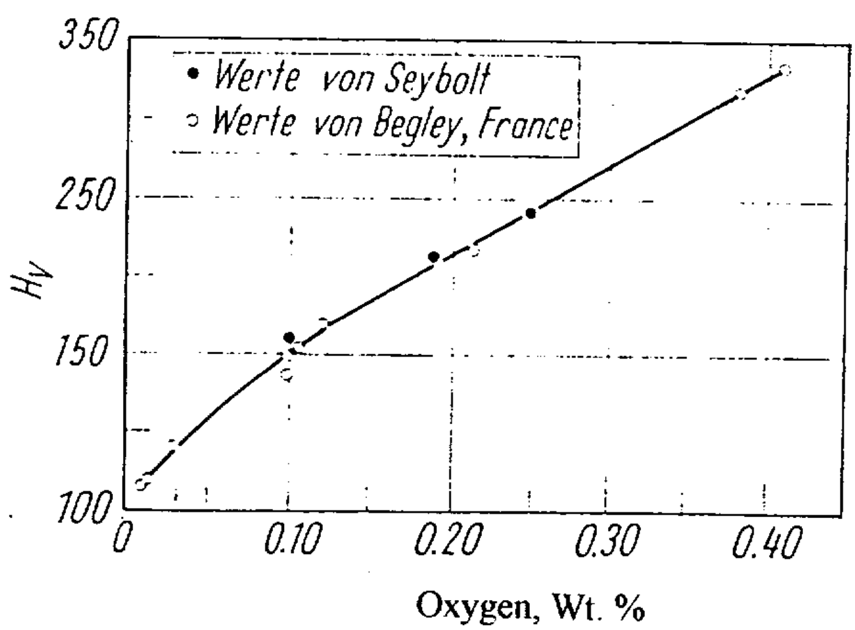

Dependence of hardness on content of oxygen in Nb

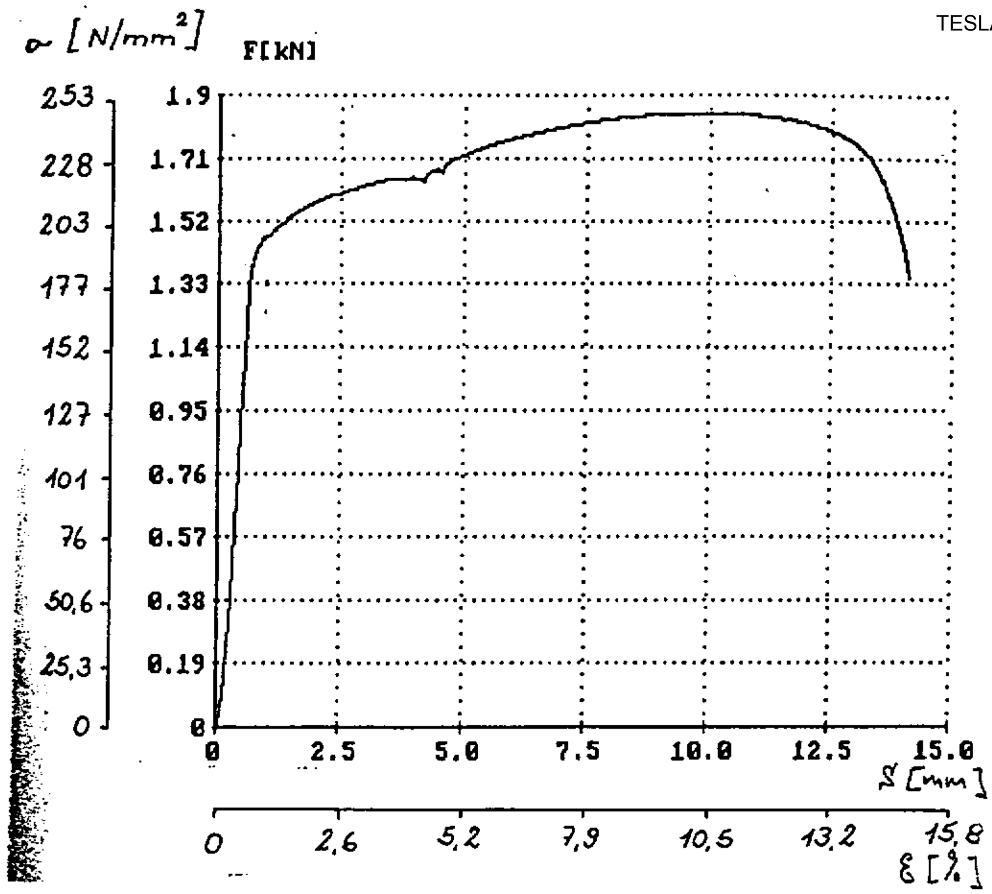

Stress - strain diagram of Nb (RRR=100)

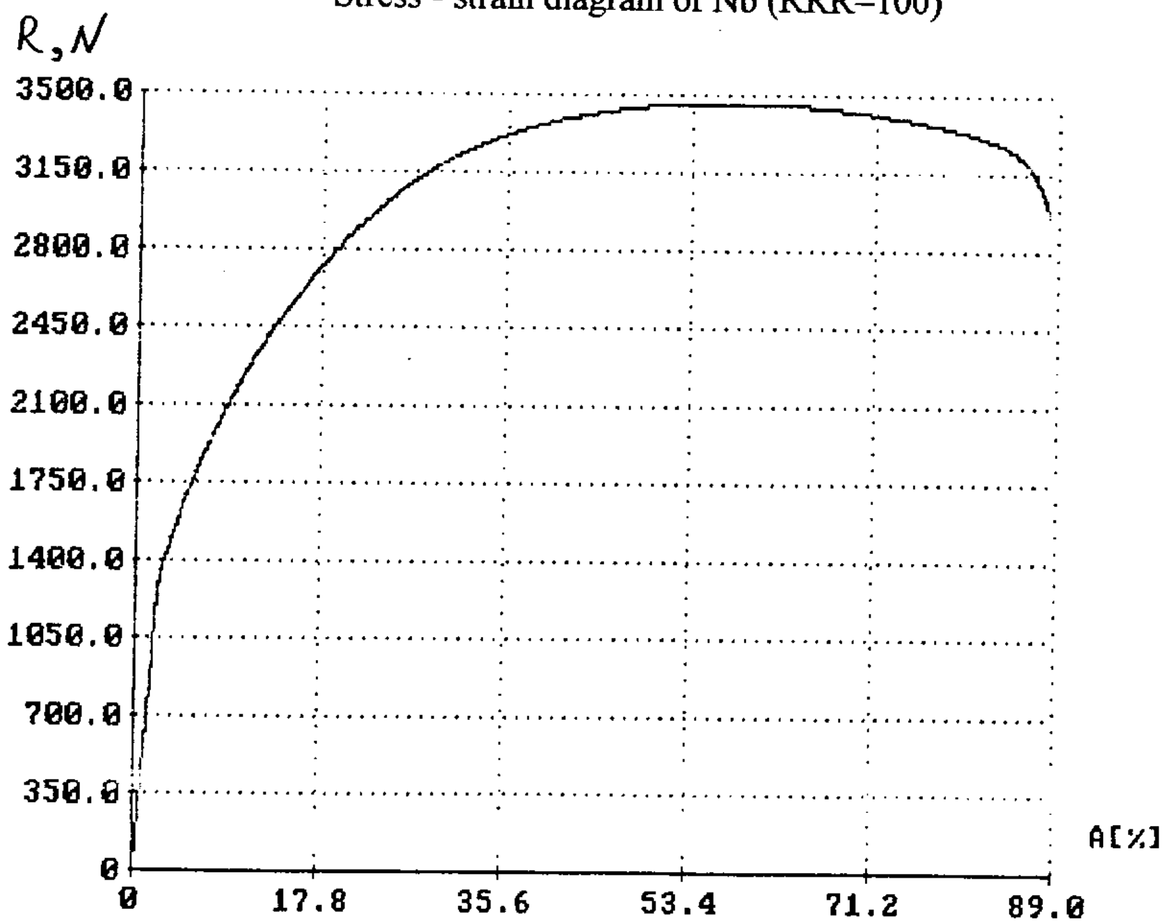

Versuch Nr.	R1 N/mm²	R2 N/mm²	Rm N/mm²	Ag %	A[illegible] %	E kN/mm²
2	54.24	56.25	144.52	49.8	83.3	2.57

Stress - strain diagram of Nb (RRR=300)

ERICHSEN TEST DIN 50101

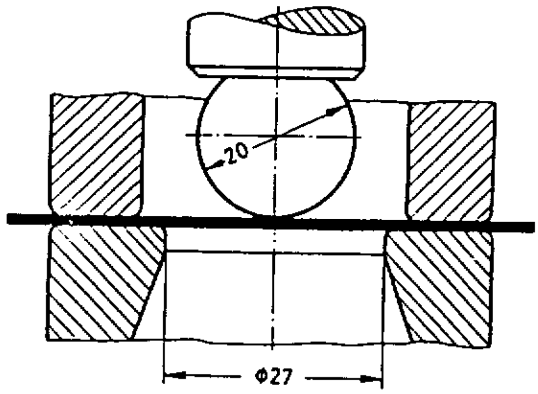

Material	Force, KN	Deepening, mm	Remarke
CARBOT Nb	38.00	16.50	
CARBOT Nb	38.00	16.90	smooth-rough
CARBOT Nb	38.00	16.20	
RRR 60	49.00	19.00	
RRR 60	52.00	18.80	very rough
RRR 60	51.50	18.70	
RRR 200	36.00	18.20	rather smooth
RRR 200	36.00	18.30	
RRR 300	37.00	19.30	relative smooth
RRR 300	37.00	18.60	

Data base (Nb sheet properties)

Manufacturer	W.C.HERAEUS GmbH	W.C.HERAEUS GmbH	W.C.HERAEUS GmbH	TELEDYNE WAH CHANG
Properties	Cavity -2,-1	Cavity D1...D6	S7-S12,A13-A18	
RRR	407-433	300 -380	278-350	400
Impurities content, %				
Ta	0,037	0,036	0,012	0,02
W	<0,005	<0,005	<0,005	<0,003
Ti	<0,001		<0,002	<0,004
Fe	<0,002	0,002	<0,002	<0,003
Si	<0,002	<0,002	<0,002	<0,002
Mo	<0,002	<0,002	<0,002	<0,003
Ni		<0,003	<0,002	
Zr		<0,003	<0,002	
H	<0,0005	<0,0005	<0,0005	<0,0003
N	<0,001	<0,001	<0,001	<0,002
O	<0,001-0,03	<0,001	<0,001	<0,004
C		<0,001	<0,001	
Mechanical properties				
Tensile strength,				
Rm, (N/mm2)	175	150 -180	152 - 160	157,6 - 161
Yield strength, Rp 0,2				
(N/mm2)	53	60 -97	79 - 81	90,8 - 94,9
Elongation,%	54	38 -70	48 - 68	51 - 52
Hardness, HV10		38 -45	40 - 46	49
Grain size, ASTM	6,5-8,5	6 - 8.	5 -8,5	7
Recristallisation heating.				
Temperature, °C	770	770	770 -800	
Time, h	1	1	1 -1,25	
Thickness, mm		2,69.....2,88	2,45.....2,85	2,67.... 2,90
Number of the sheet (2,8*262*262)	40	150	275	120
Delivery data		Feb 94	Jul 94	Jan 95

TREATMENT OF THE WELDING CONNECTION ON NB TUBE FOR HYDROFORMING DESY

H. Kaiser, D. Proch, W. Singer, A. Stepanov

Presentation of W.Singer

In principle the production of the seamless tube for hydroforming is possible now. But at the moment we are not available of the company, which can fabricate seam less tube from Nb with quality RRR>300 by requested length and diameter.

Therefore it is reasonable to fabricate a tube from the Nb sheet with welding connection along the tube. Welding connection is the area where the material was melted and heated.

In this case the microstructure and mechanical properties in the welding connection are different in comparison with the untreated metal.

We have investigated the possibility of the welding connection treatment with the aim to bring it microstructure and properties to the state close to the initial.

The idea is to distract the big grain in the welding area with deformation and then reconstruct the initial state by properly heating.

Nb reference sample

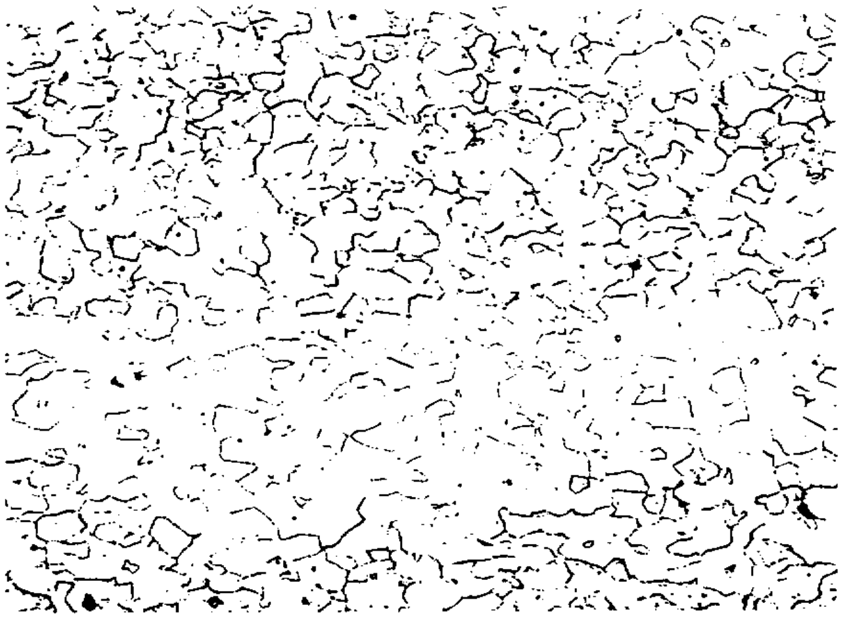

Basic material

50 : 1

II 21 513

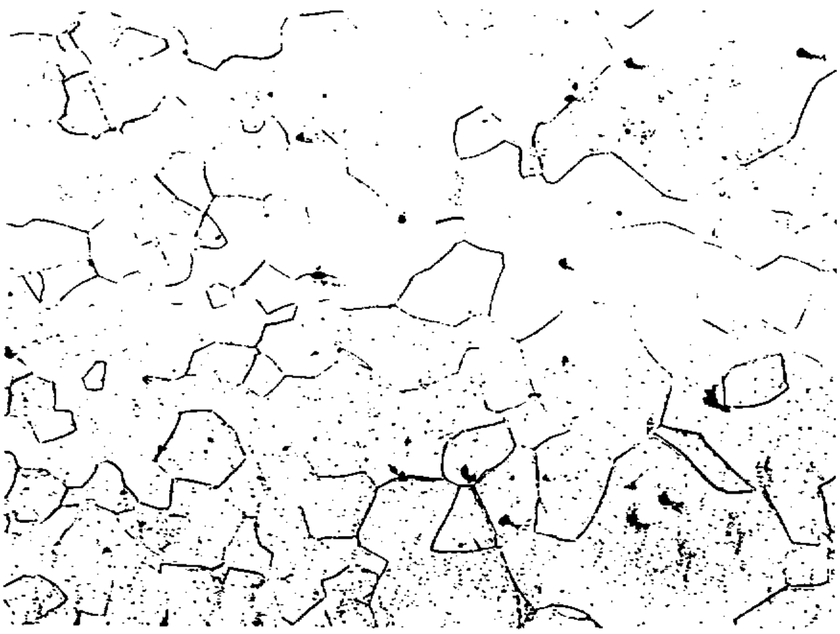

Edge of the welding connection

50 : 1

II 21 514

Center of the welding connection

50 : 1

II 21 515

1 - 0192

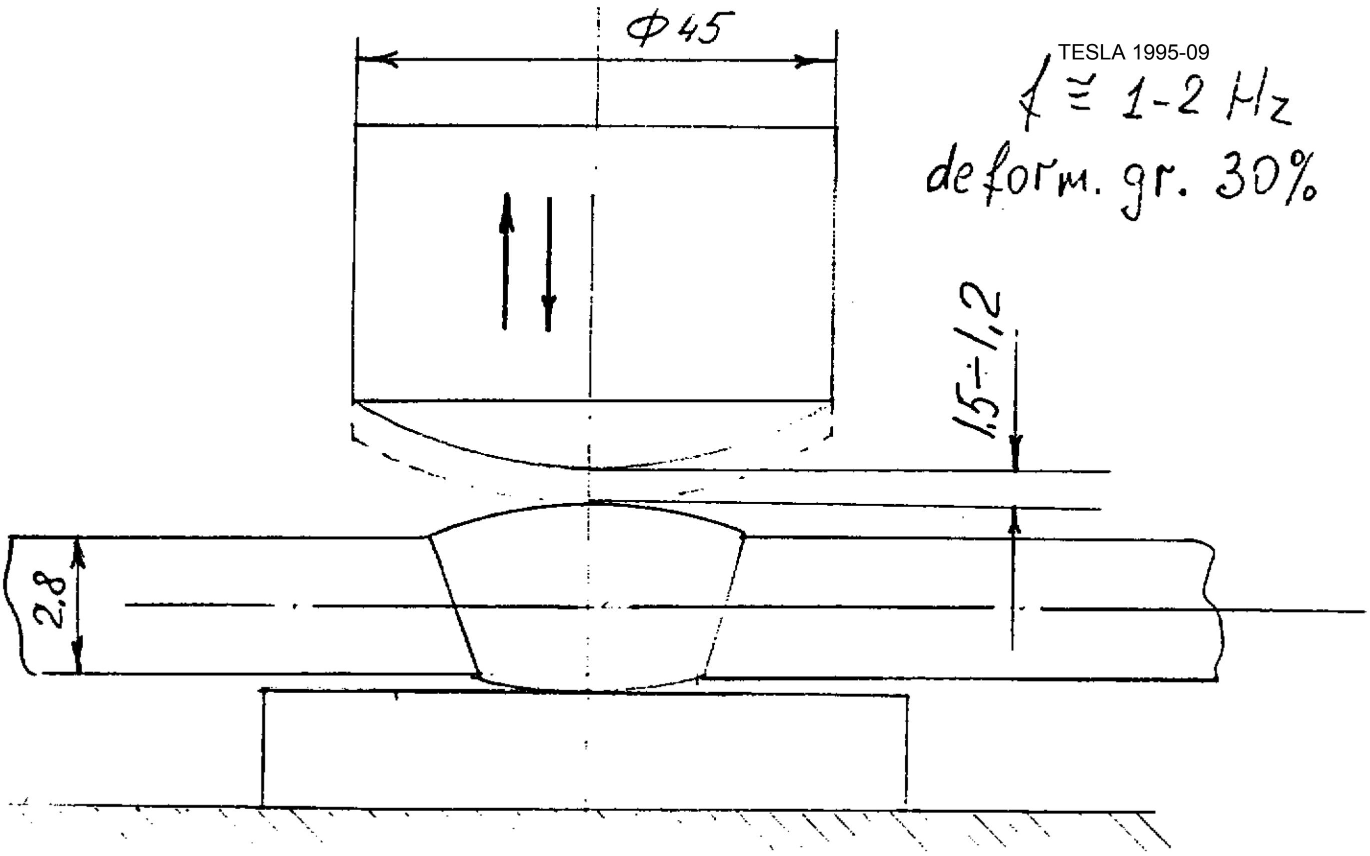

Hammering on the vibroforging lathe

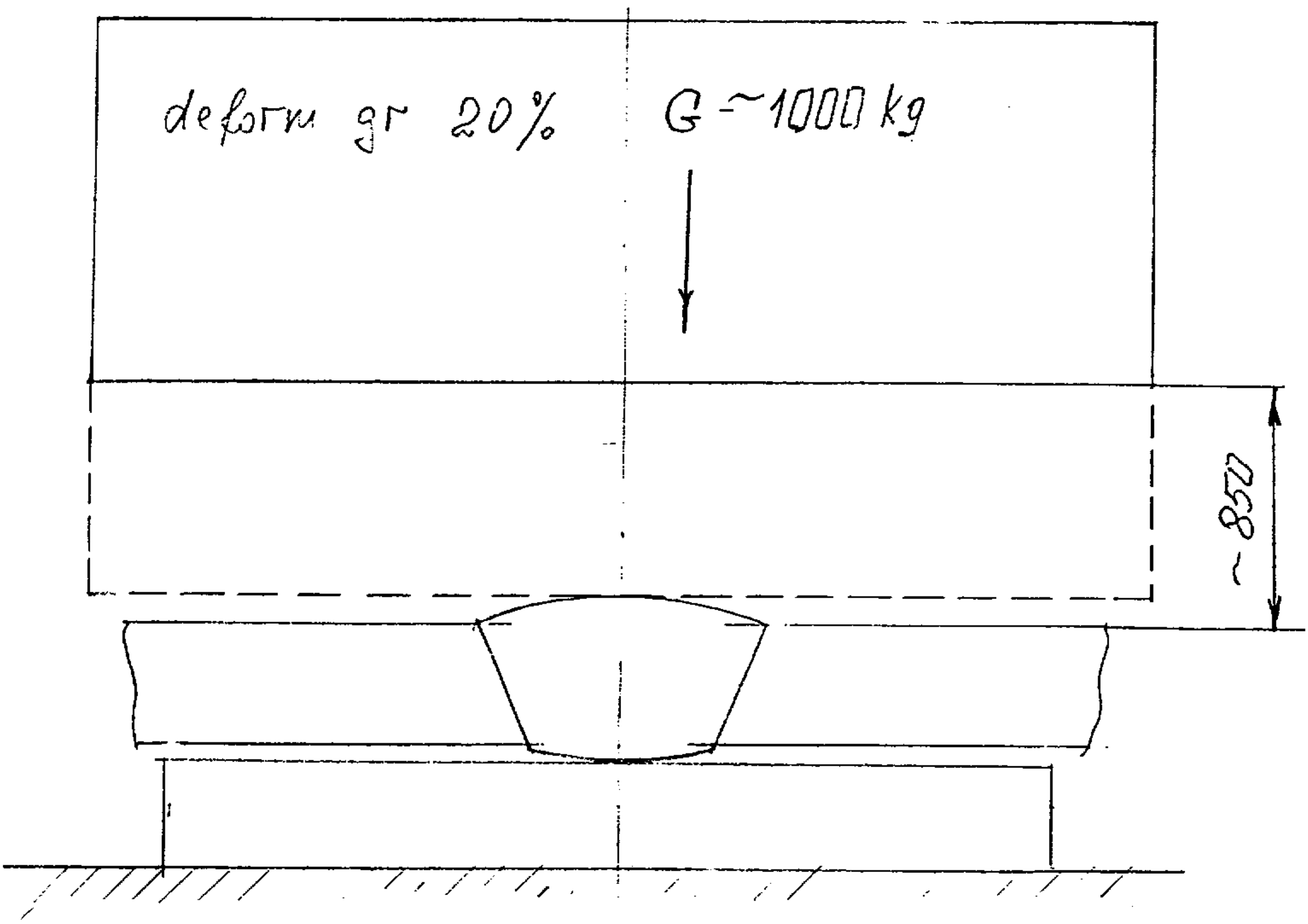

Hammering with the big hammer

Annealing program for treated welding connection

1. Charge the furnace. Pump up till ca. 10^{-6} mbar

2. Temperature increasing till 950°C with rate 200°C/h

3. Heating at 950°C, 1h

4. Switch off the furnace.

5. Pick up the samples by the temperature not higher, then 100-200°C

Position of the microstructure survey

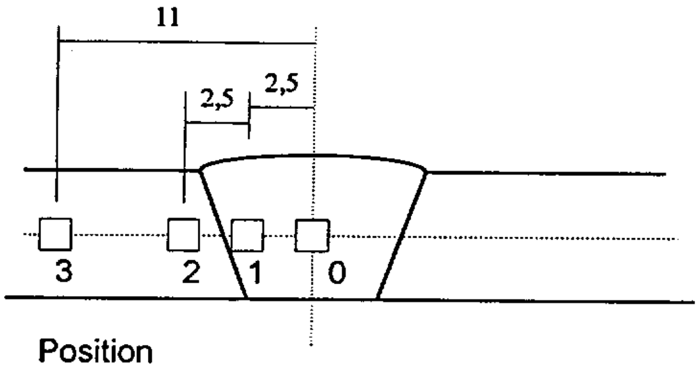

Position

Sample preparation

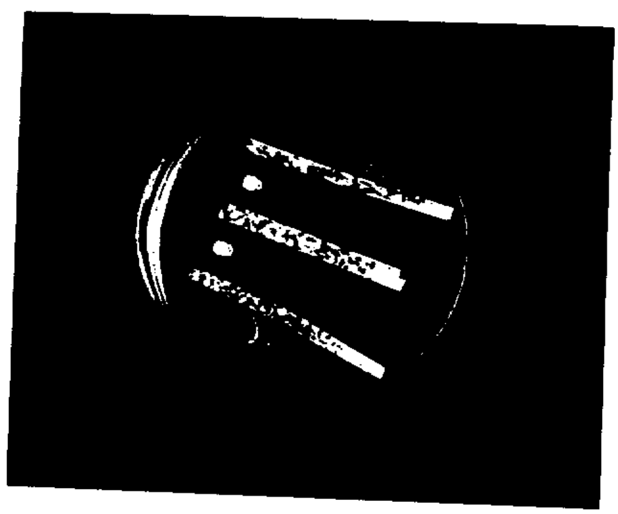

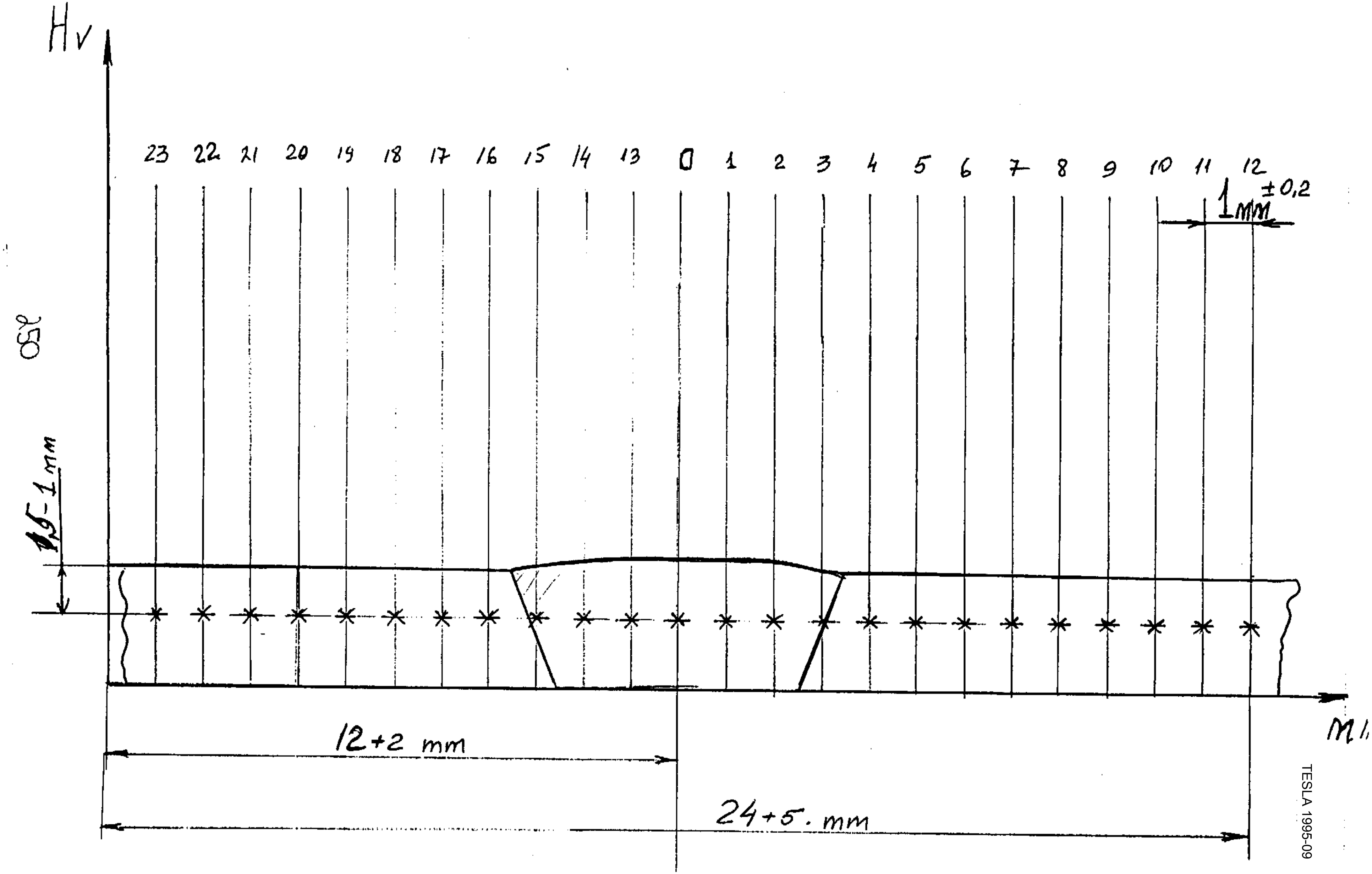

Scheme of the hardness measurement position

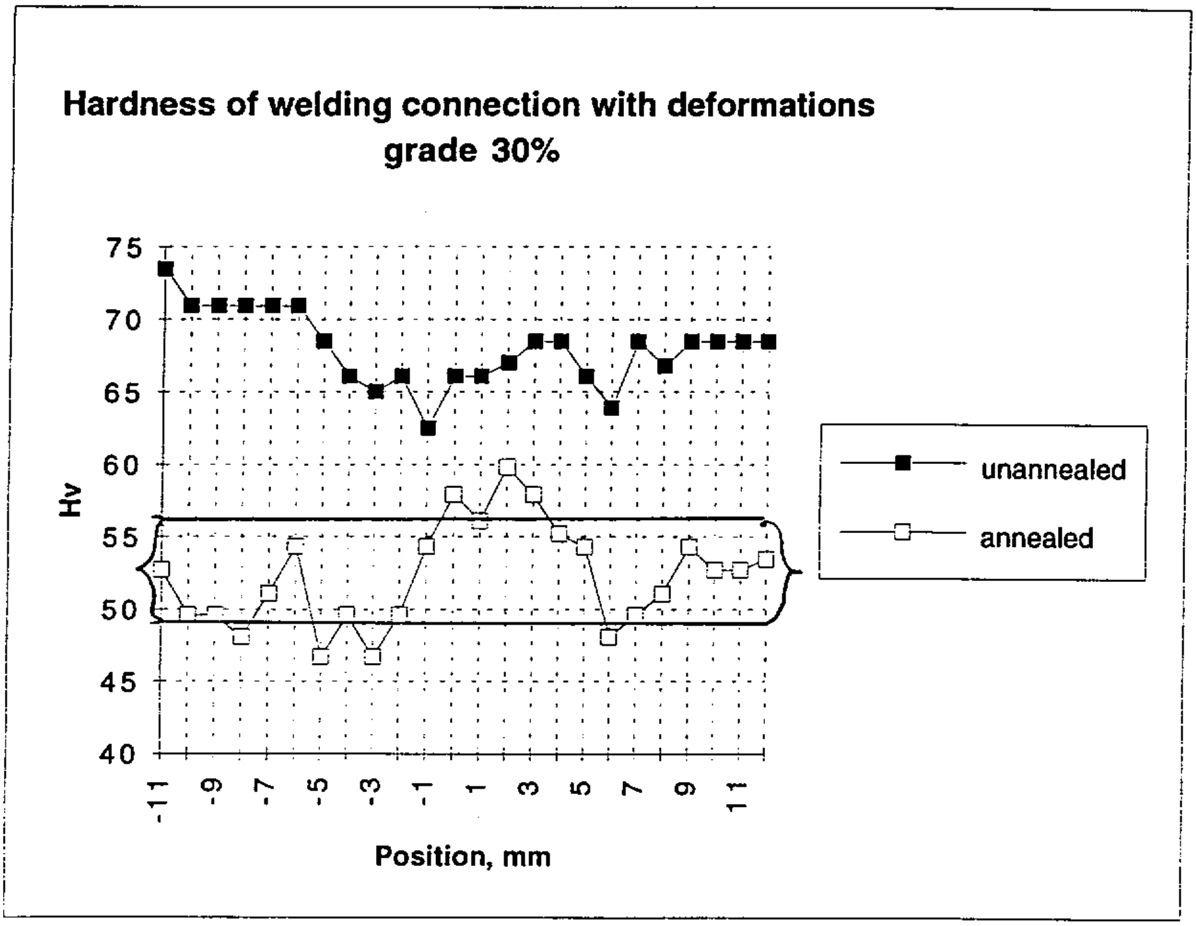

Range of the differencies of the hardness for the basic metal

Welding-Rolling
N2W

Deformation grade 30%

unannealed

Position 0

100 : 1

II 21536

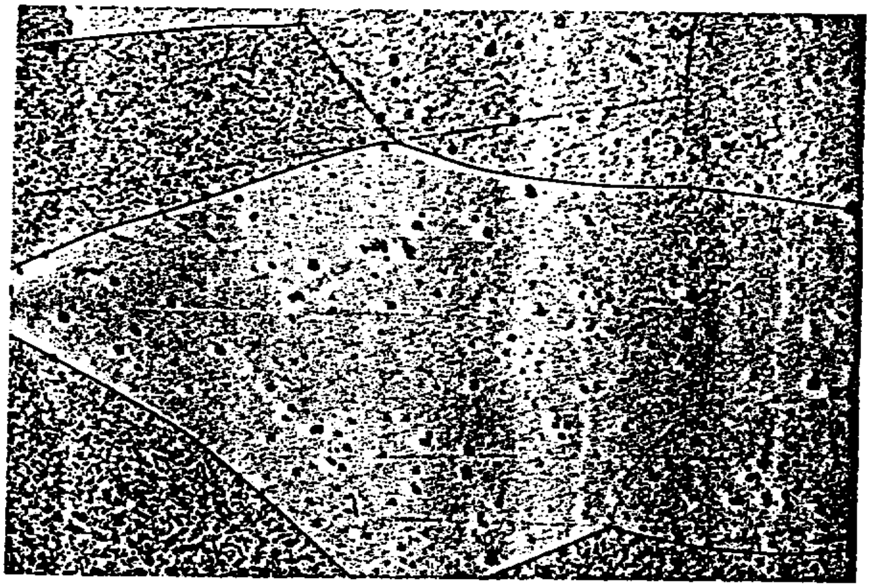

Position 1

100 : 1

II 21537

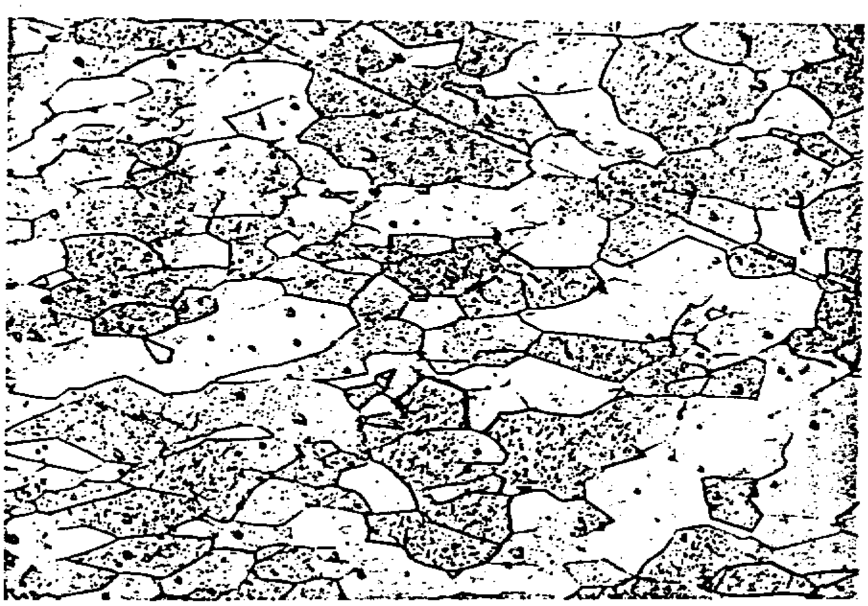

Position 3

100 : 1

II 21539

1-0192

N1W

Welding-Rolling

Deformation grade 30%

annealed

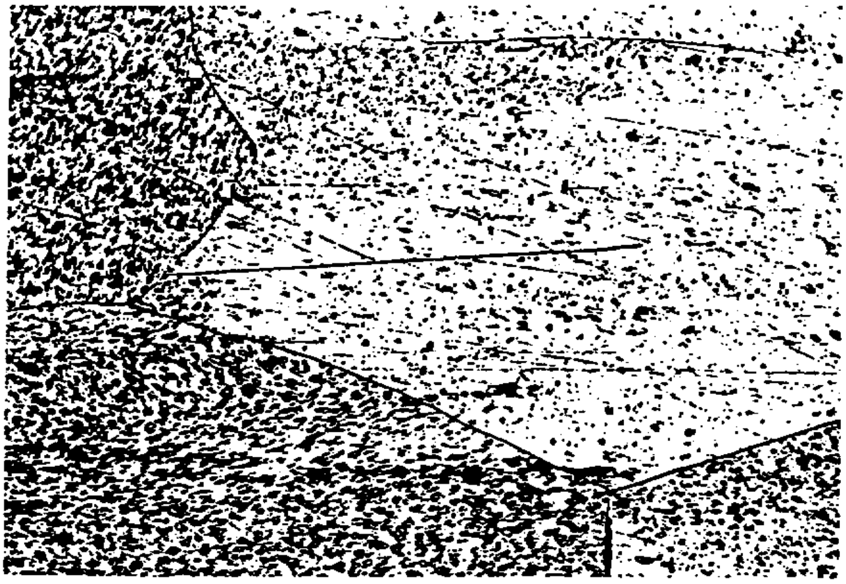

Position 0

100 : 1

II 21532

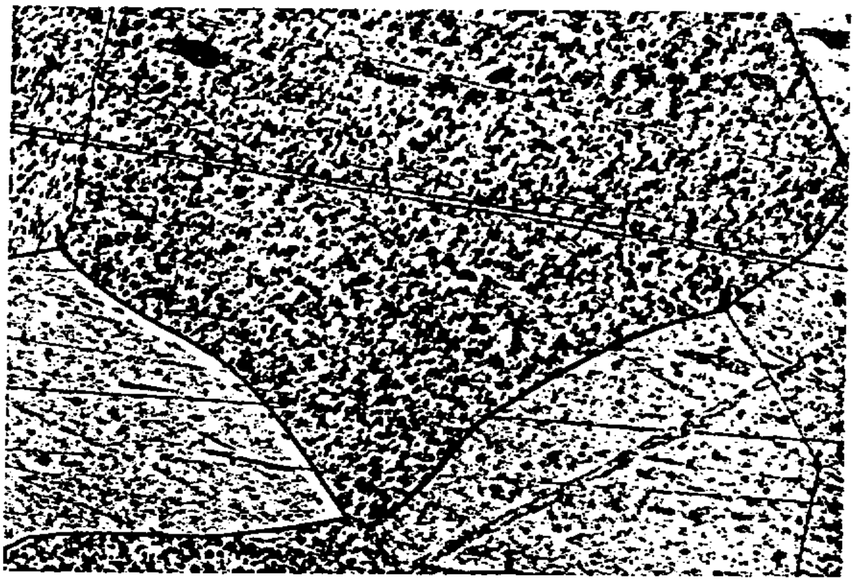

Position 1

100 : 1

II 21533

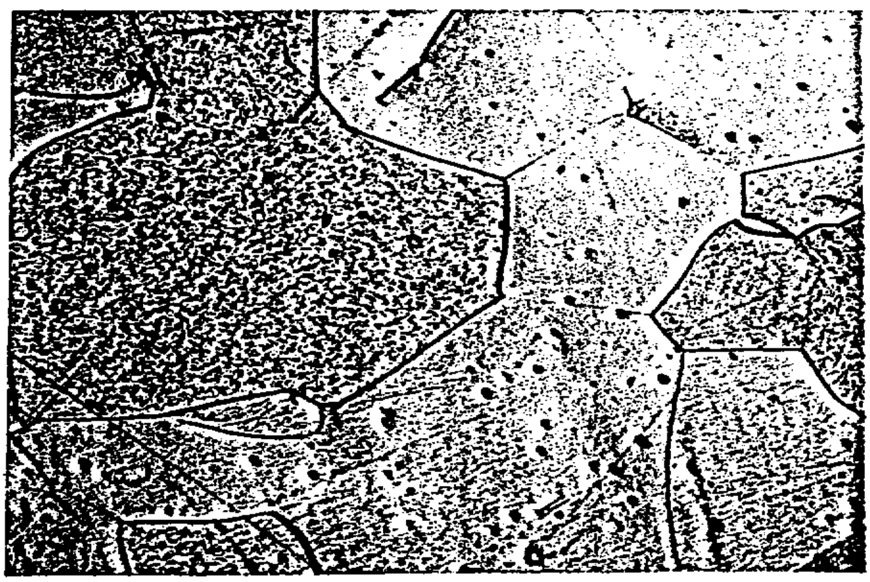

Position 3

100 : 1

II 21535

1-0192

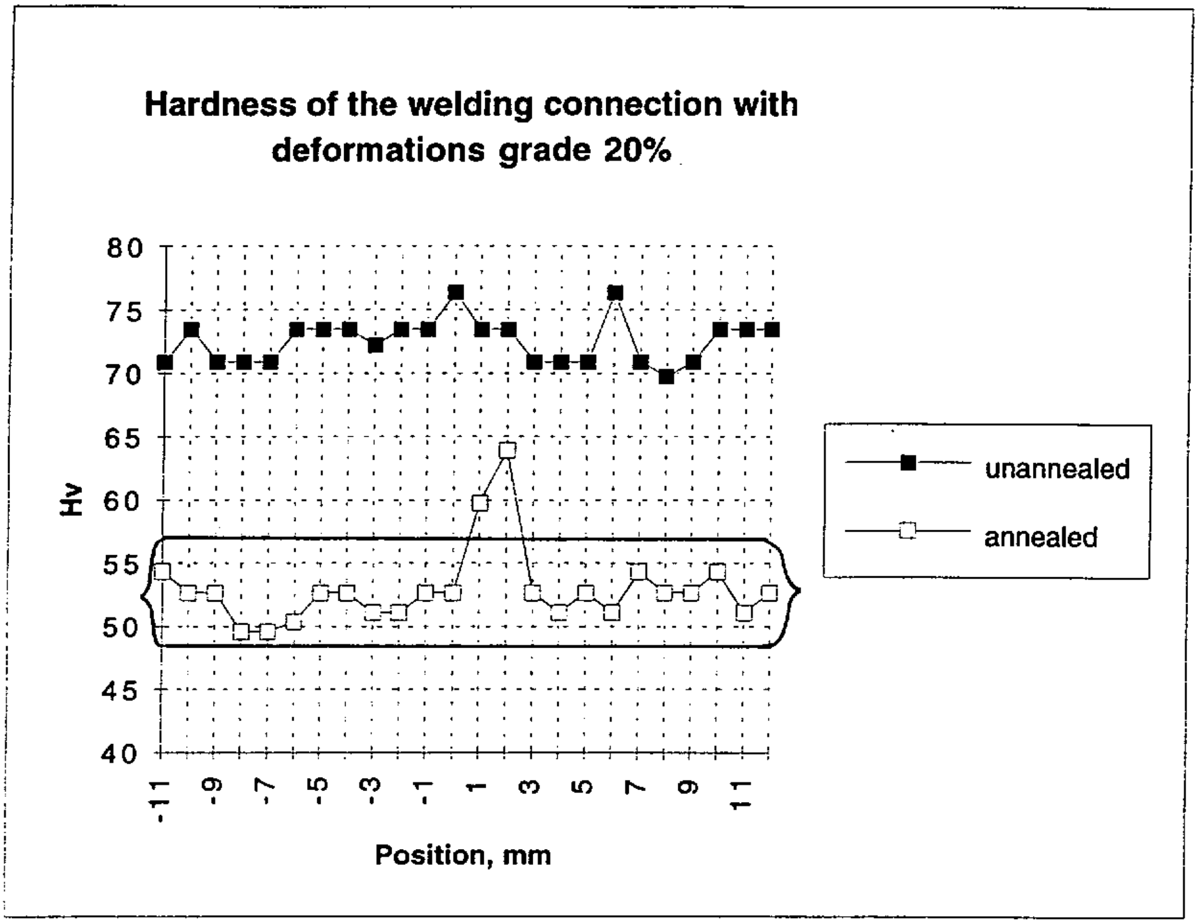


Range of the differences of the hardness for the basic metal

Welding-Rolling
N3W

Deformation grade 20%

unannealed

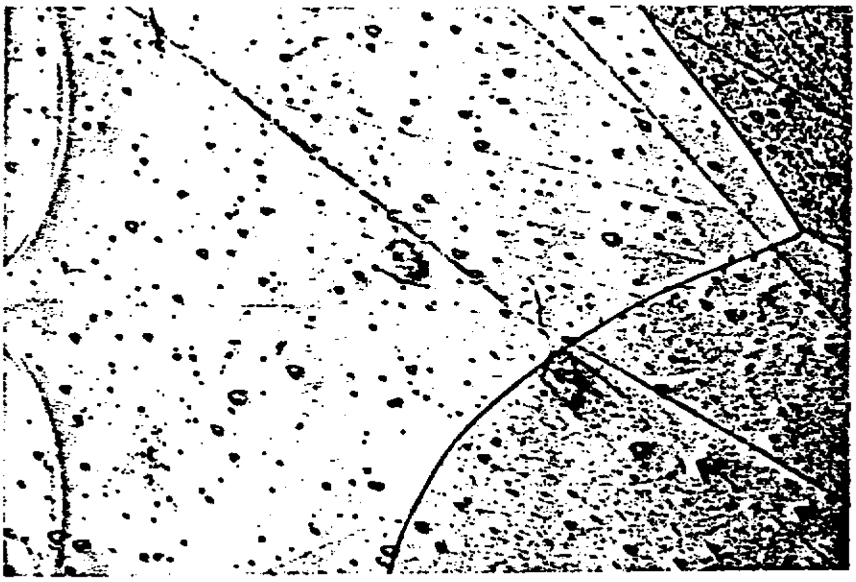

Position 0

100 : 1

II 21540

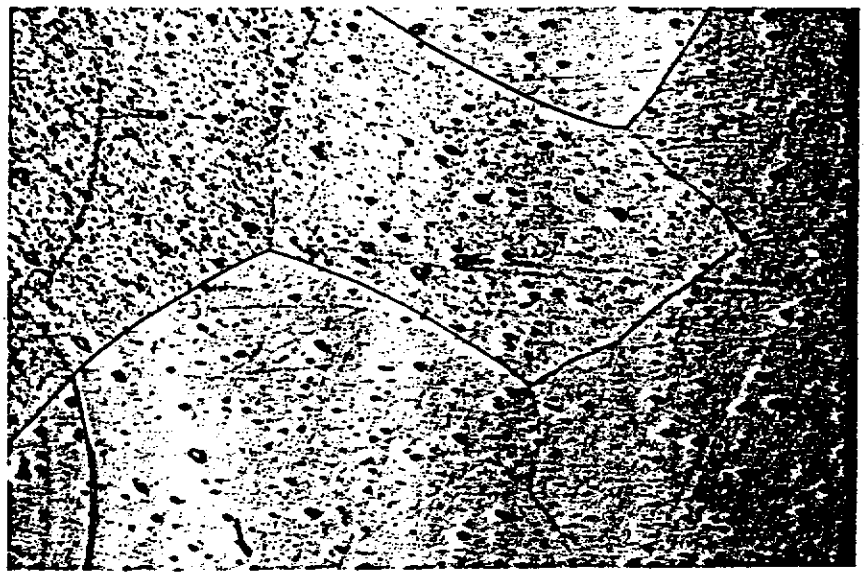

Position 1

100 : 1

II 21541

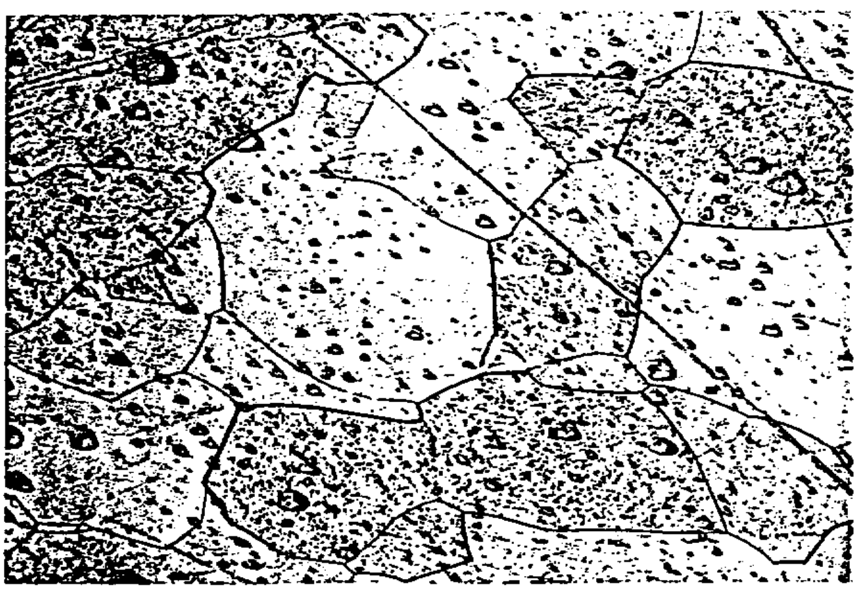

Position 3

100 : 1

II 21543

1-0192

Welding-Rolling
N4W

Deformation grade 20%

annealed

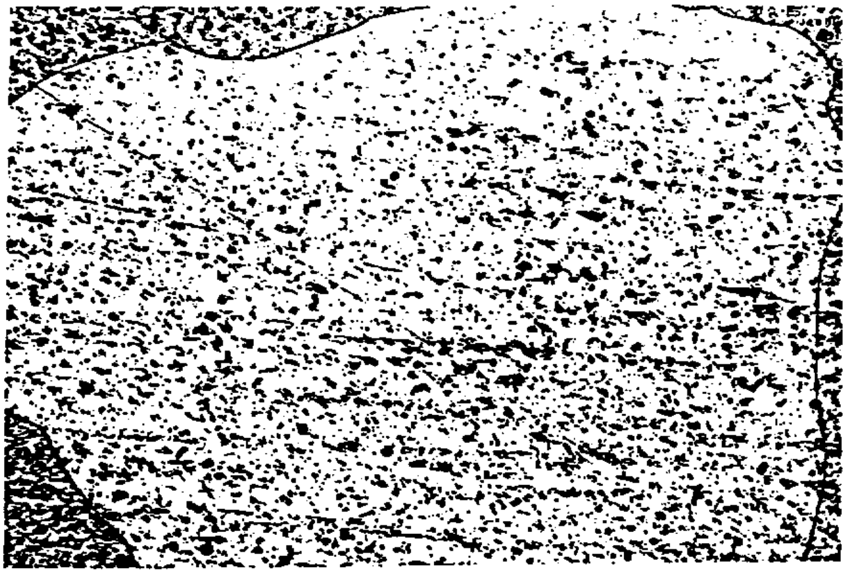

Position 0

100 : 1

II 21544

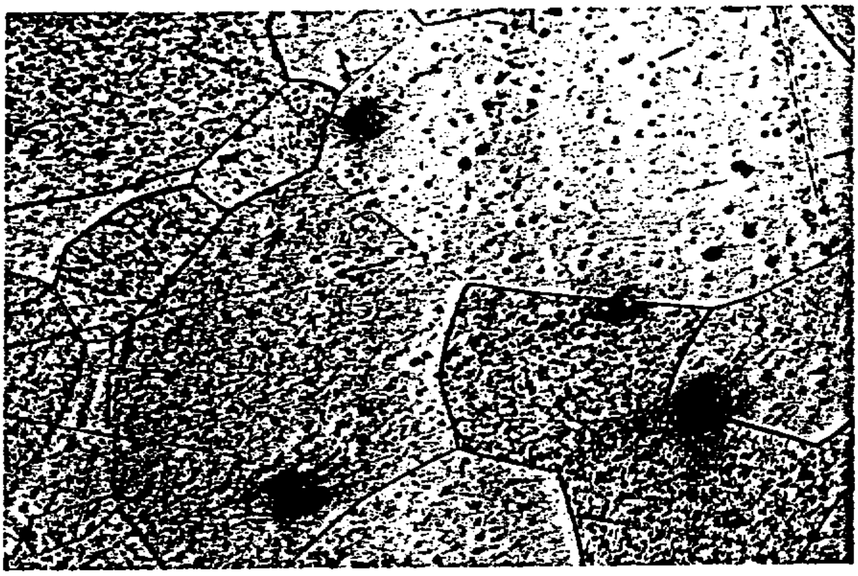

Position 1

100 : 1

II 21545

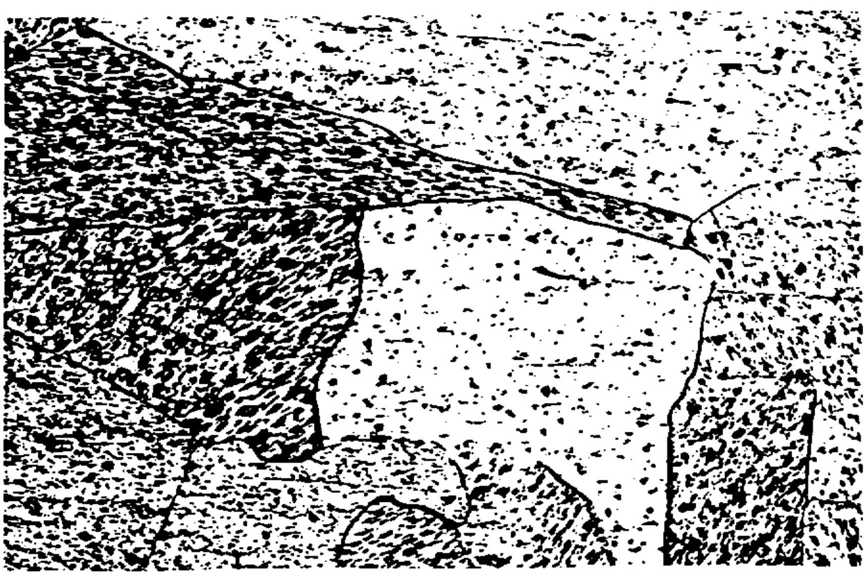

Position 3

100 : 1

II 21547

1-0192

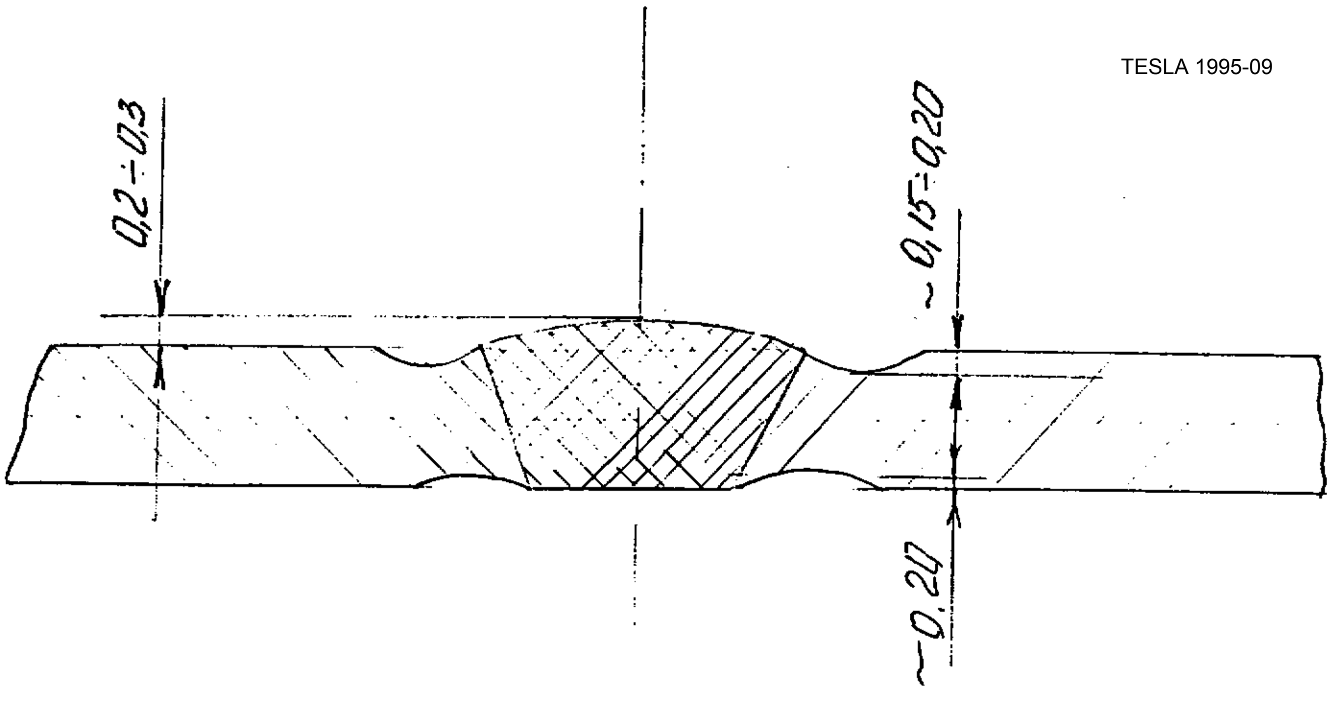

Used shape of the welding connection

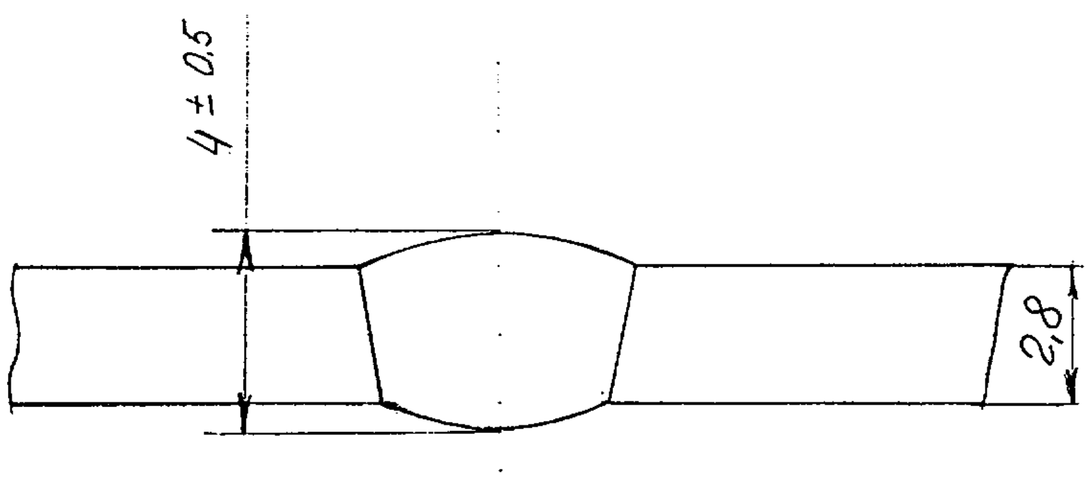

Proposing of the shape of the welding connection for hammering

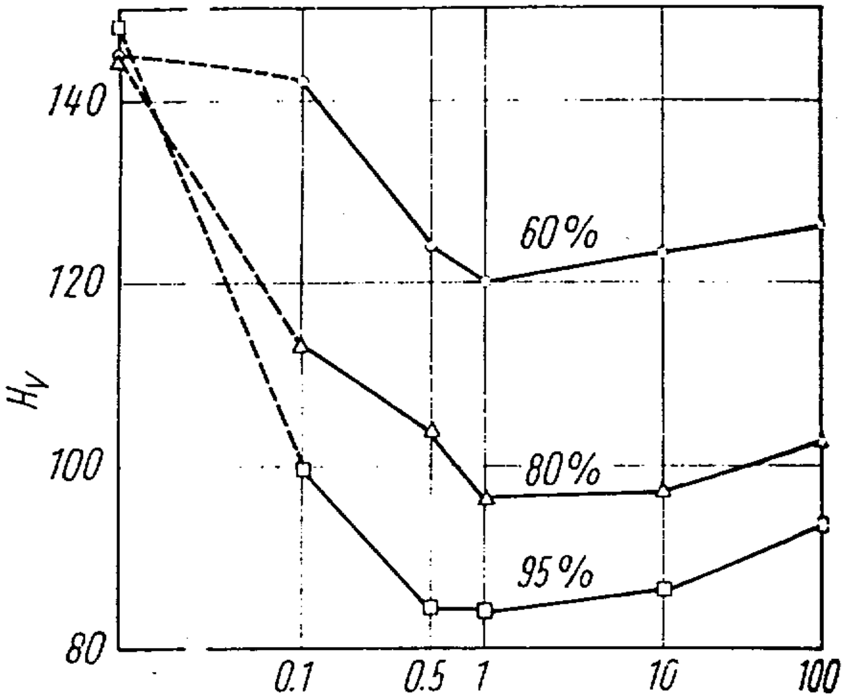

Annealing time, h (annealing temperature 1000°C)

Hardness of Nb with different deformation grade. Dependence on annealing time.

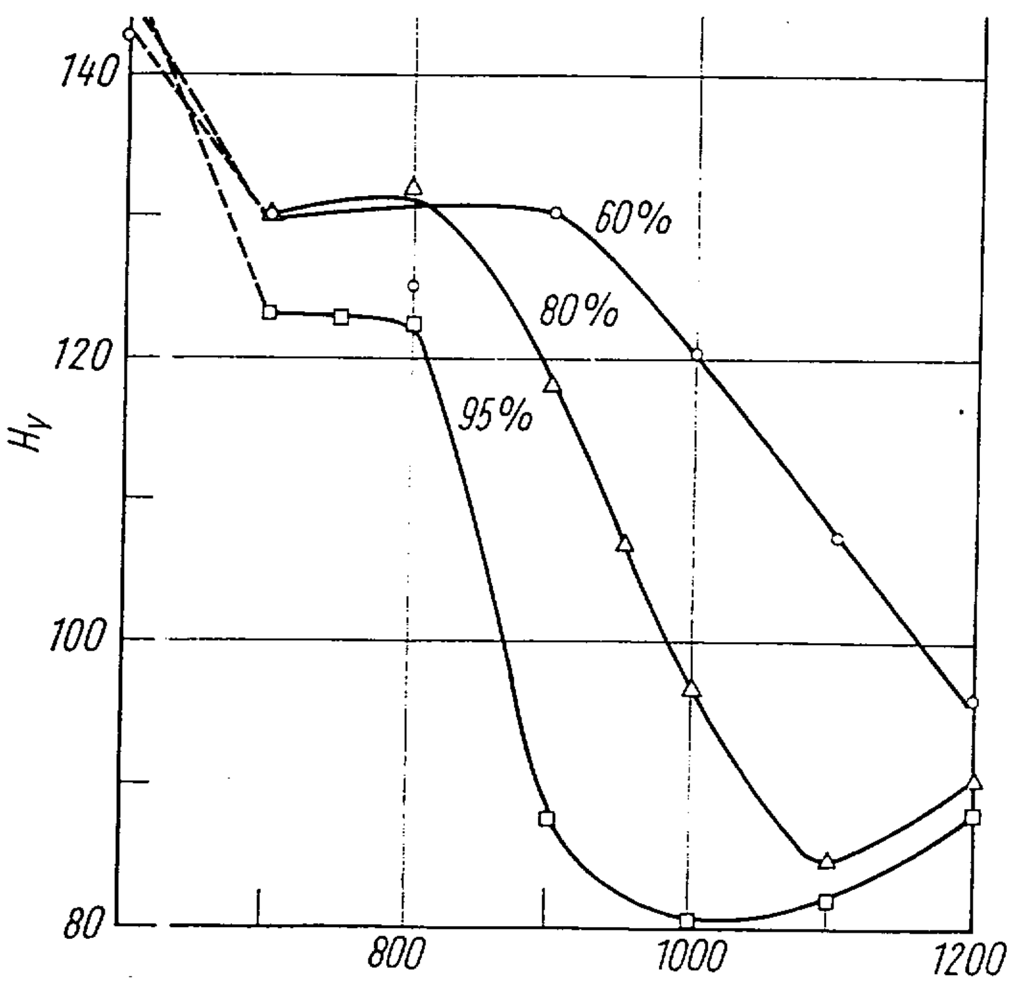

Annealing temperature, °C (annealing time 1h)

Hardness of Nb with different deformation grade. Dependence on annealing temperature.

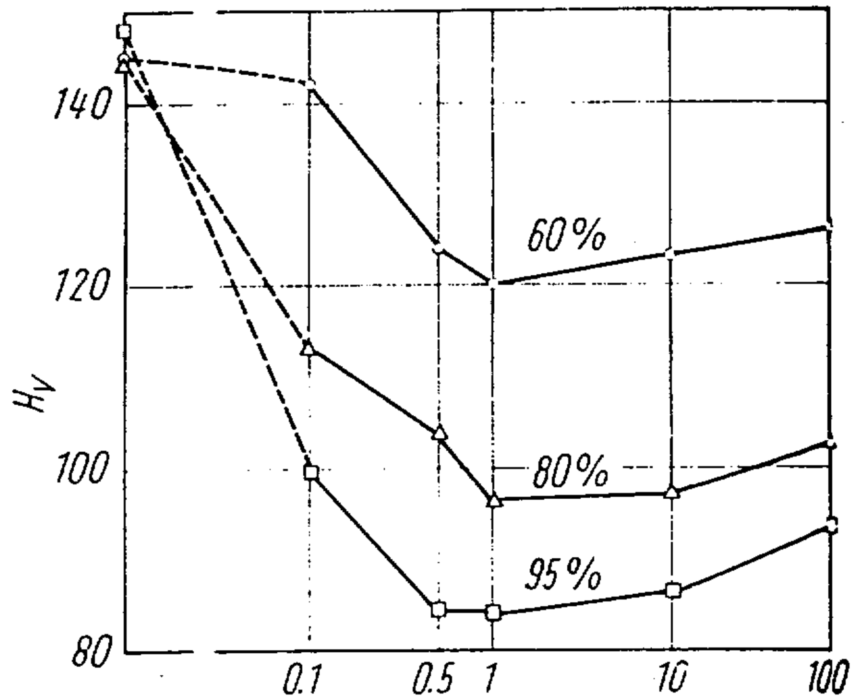

Annealing time, h (annealing temperature 1000°C)

Hardness of Nb with different deformation grade. Dependence on annealing time.

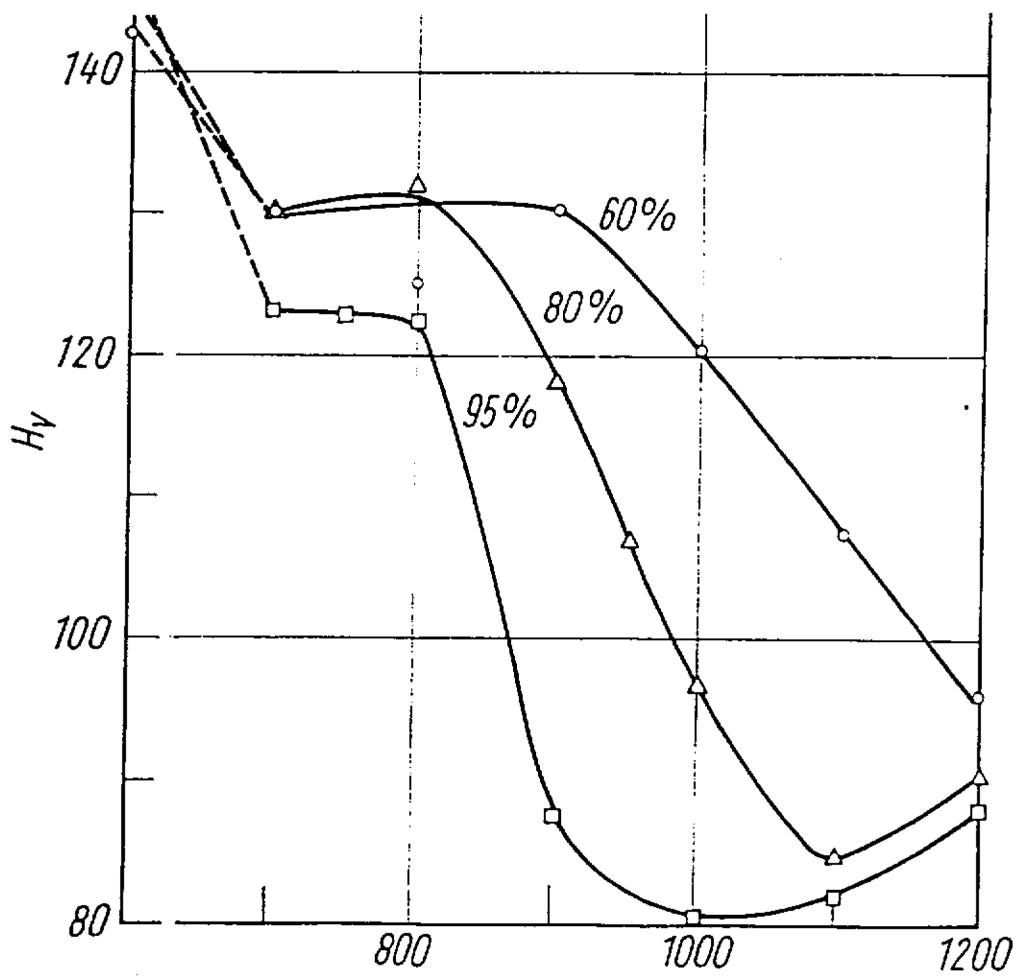

Annealing temperature, °C (annealing time 1h)

Hardness of Nb with different deformation grade. Dependence on annealing temperature.

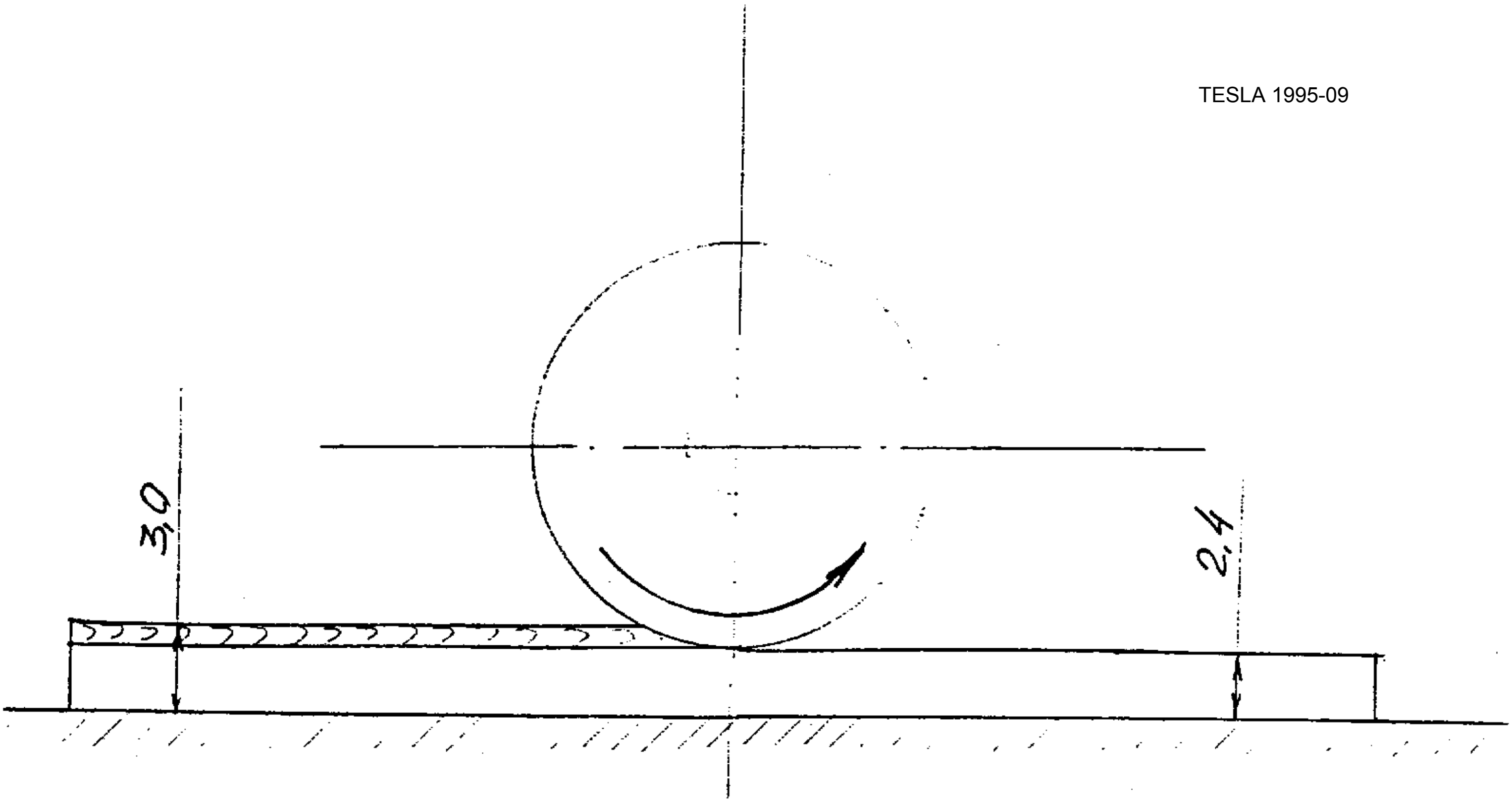

Scheme of rolling of the welding connection

Conclusions

1. Preliminary results approve the possibility of bringing the structure and properties of the welding connection to the state close to the based Nb. The welding connection's surface, grain size, hardness after hammering and heat treatment are closer to the basic Nb, then before treatment.

2. The procedure of the welding connection's treatment needs further improvement.

a) The shape of the welding connection must be optimized.

b) Parameters of the deformations grade and of the annealing must be optimized.

c) Technique of the plastic deformation of the welding connection must be optimized. Best results can be expected by the rolling procedure.

BUTTING
Edelstahlrohre

Statement: T. Schüller

Activities from an industrial company

Company
Butting GmbH, Knesebeck

The main job of the company is to produce longitudinal welded pipes, elbows and vessels out of stainless steel.
Other materials, like Al, Ti or Ni-basis - alloys, are used for production too.
The pipes, elbows and vessels are welded with different welding processes, e.g. TIG, PAW, SAW and Laser Beam Welding.

The contact with DESY (Mr. Kaiser) exists for a longer time. Butting works now on a future project:
They want to develop the 4-cell cavity structure without welding, in a hydroforming process.

Basis for the idea was the experience with hydroforming.

Butting uses a calibration press (see photo) to get good pipe tolerances (ovality, diameter).
Technical details of the press:

- Tools-force: 10 000 KN
- Side cylinder force: 25 000 KN
- Water pressure for hydroforming: 2500 bar

Based on the experience with the press, the idea was born to manufacture the cavity structures with a special tool by hydroforming.

Actual situation:

Butting is in the first stadium of development:

- the inside-tool was built and the first forming-experiments are done
- the forming was done with a copper pipe (diameter between iris and equator)
- the outside shape was done mechanically

The future will show, how succesful this work will be.

BUTTING
Edelstahlrohre
1777
H. Butting GmbH & Co. KG
29377 Wittingen-Knesebeck
Telefon (0 58 34) 50-0
Telex 91 714
Fax (0 58 34) 5 03 20

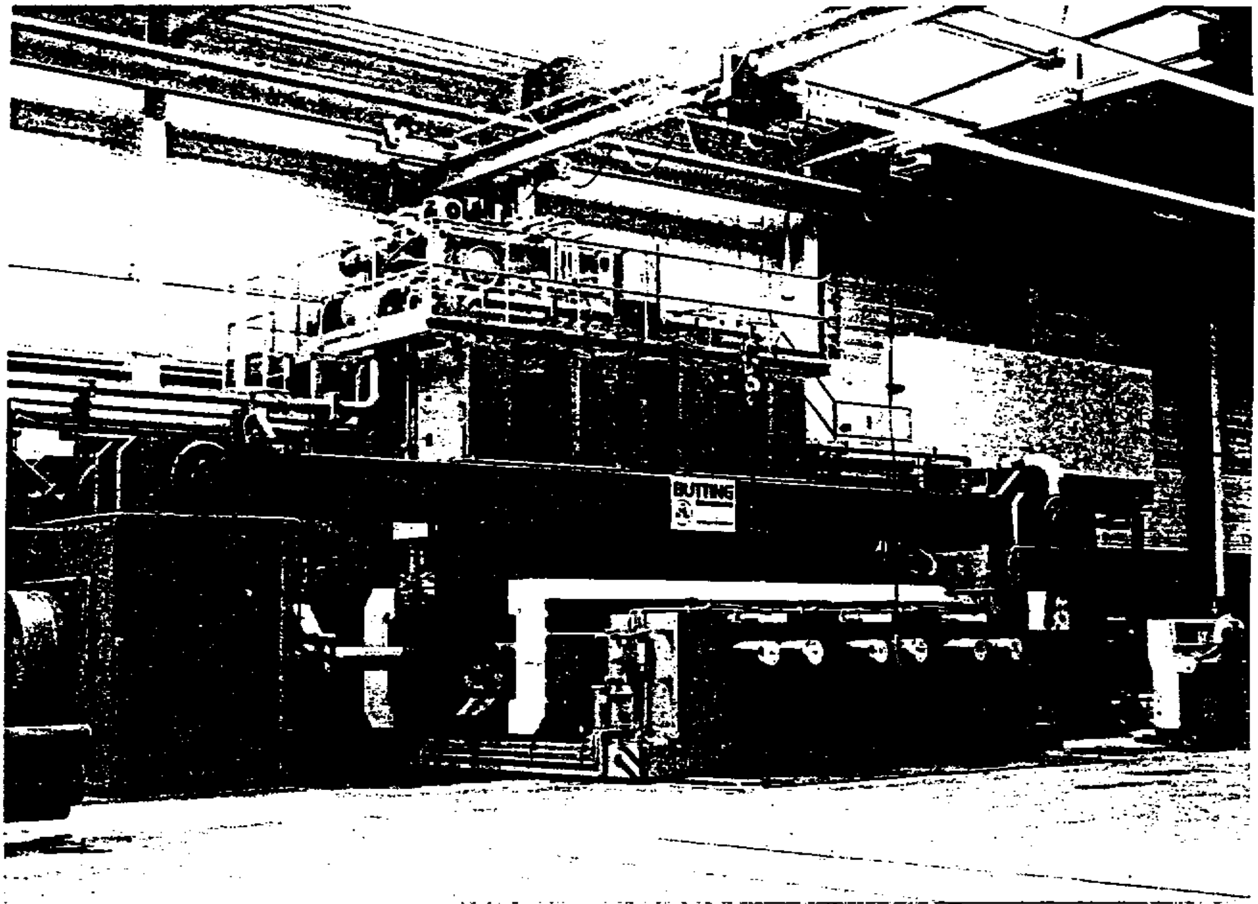

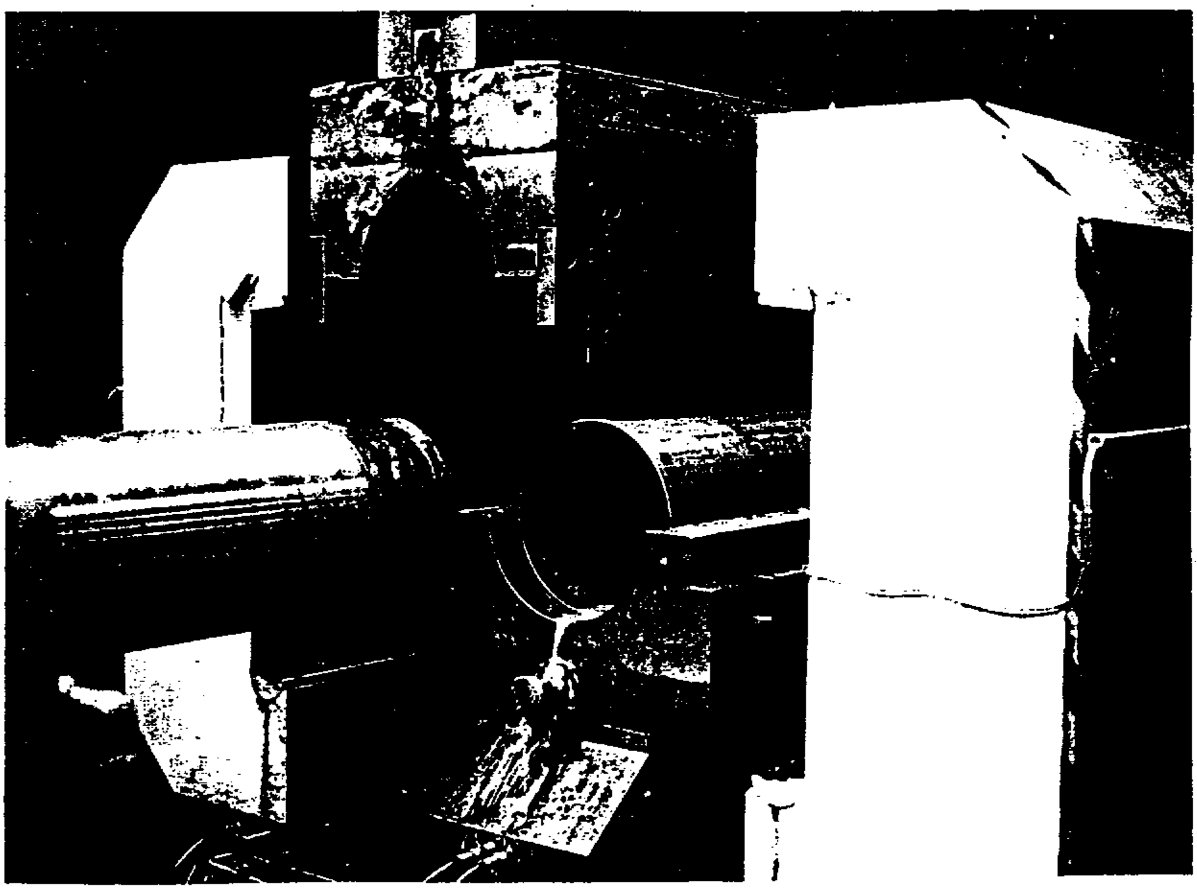

P. Kneisel / CEBAF

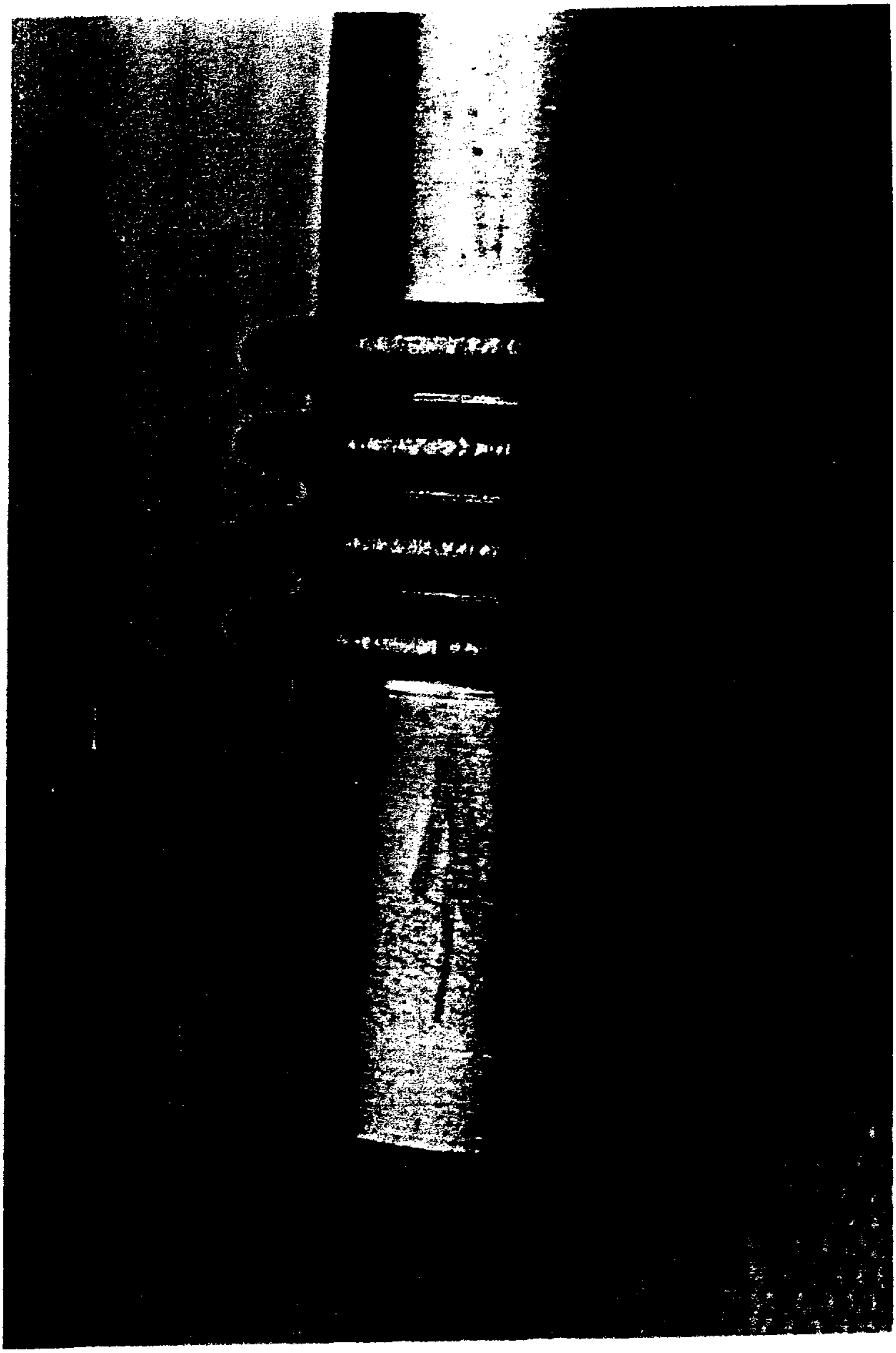

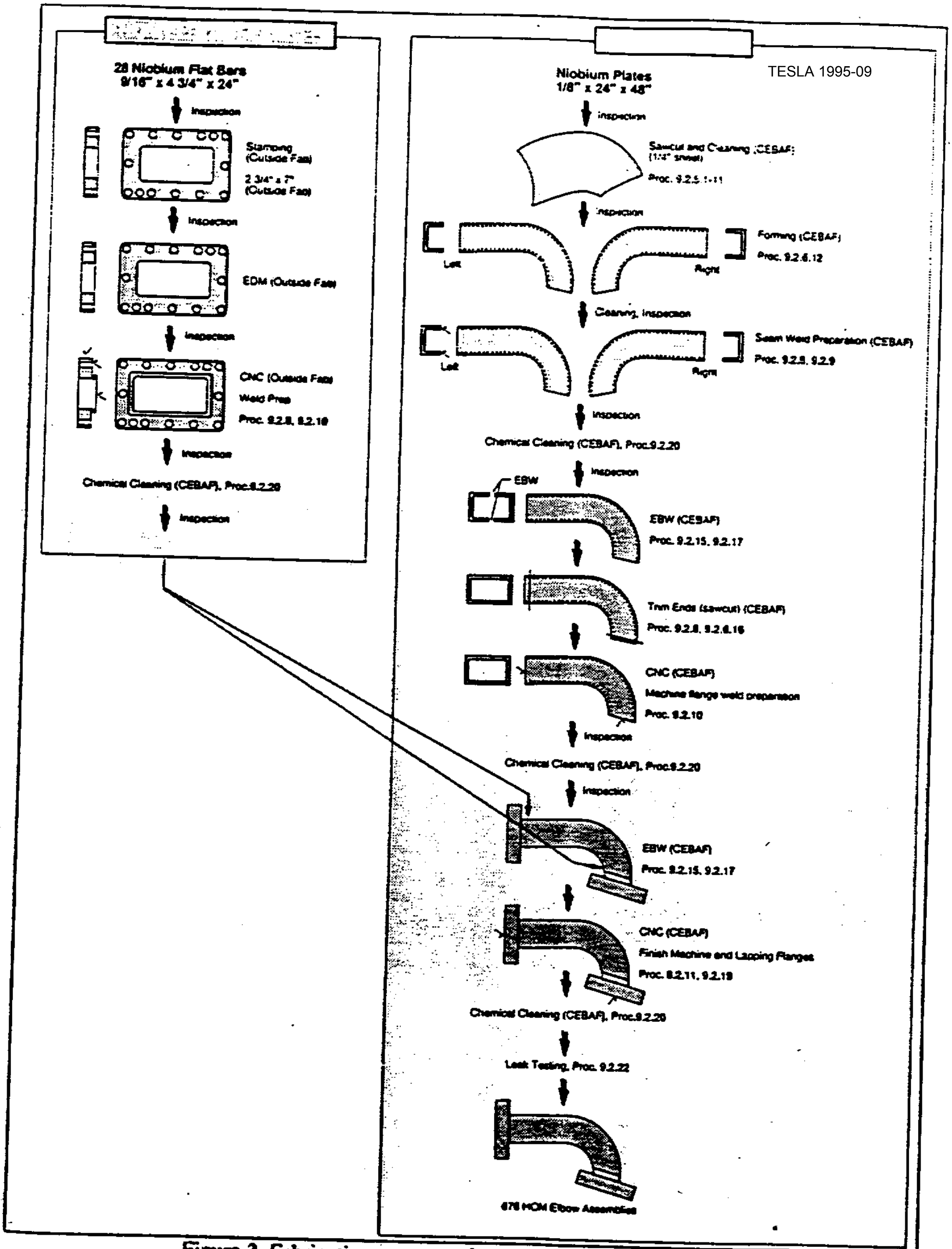

Figure 2. Fabrication sequence for niobium HOM elbows.

Deep Drawing of Niobium

General Rules:

a). Dies made from Al 7075-T6 work well

b). Generous lubrication (Motor Oil, "Never Seez") should be applied

c). Die clearance is equal to material thickness. For non uniform thickness the material gets "squeezed", leaving marks.

d). A slow hydraulic press gives good results and avoids any work-hardening of the material due to "stress-rate' effects.

e). Appropriate shaping of the "templates" is very important to avoid tearing.

f). Appropriate metallurgical conditions of the material is important (grain size > 4 ASTM, stress relieved, homogeneous...)

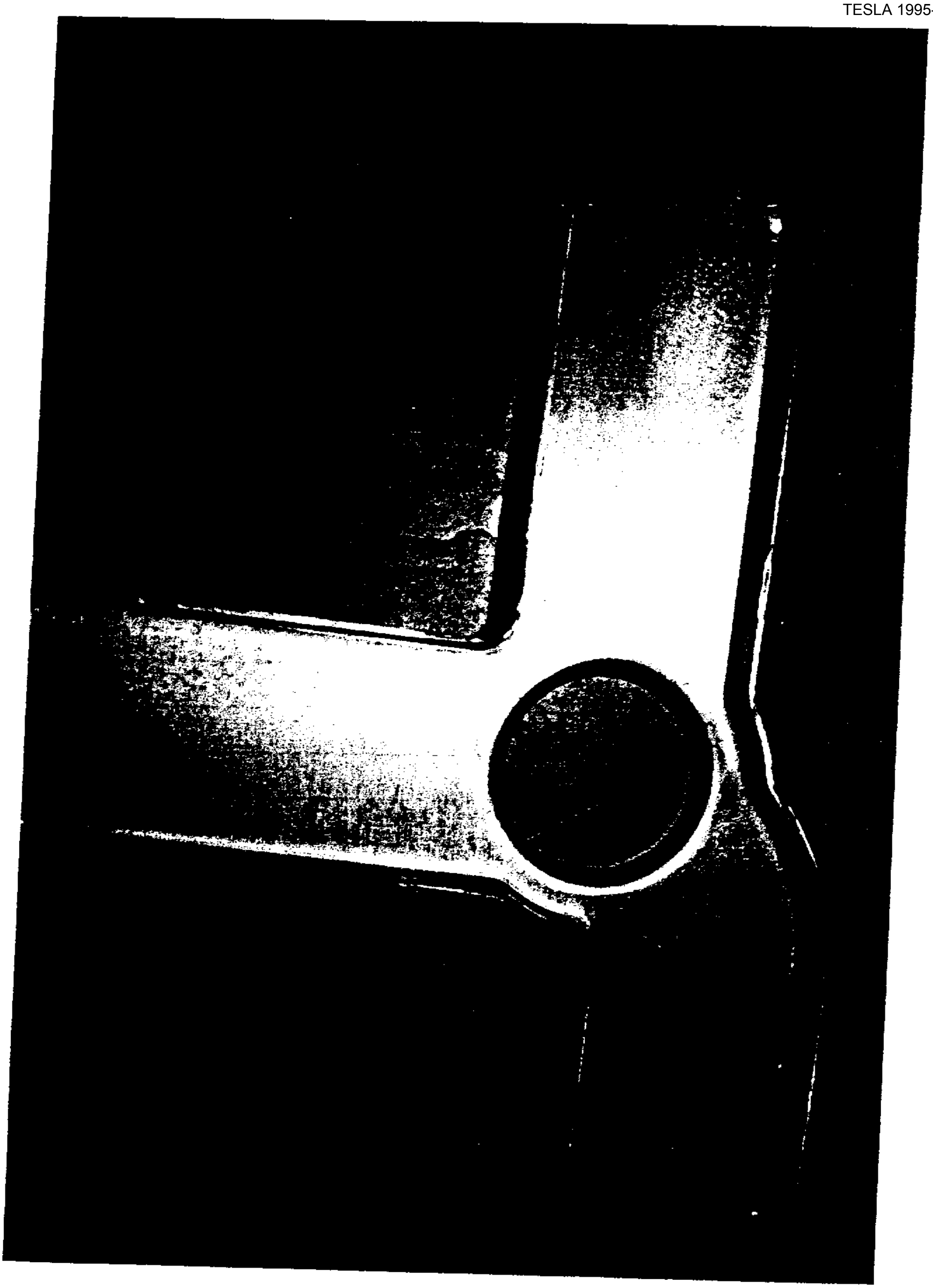

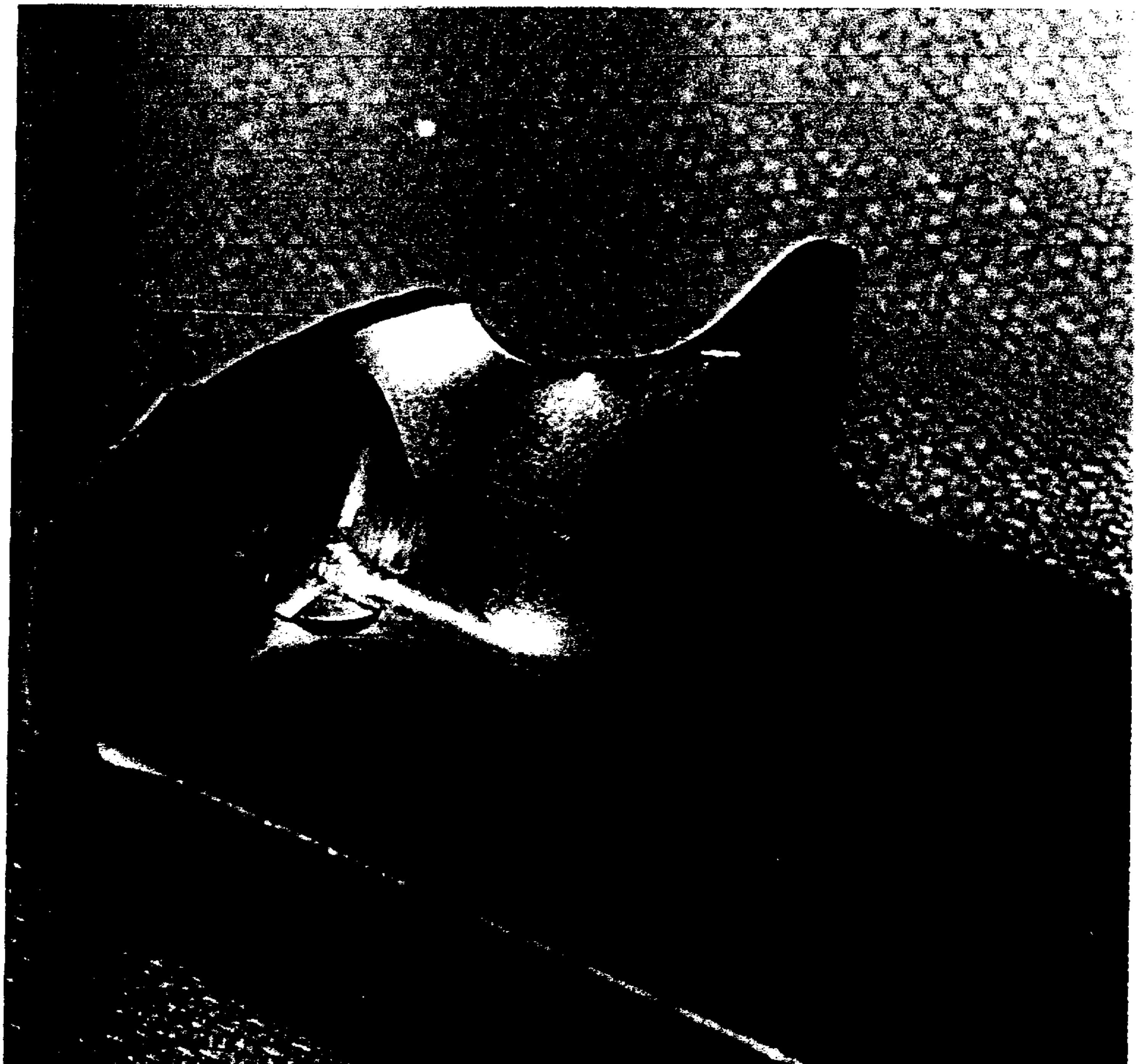

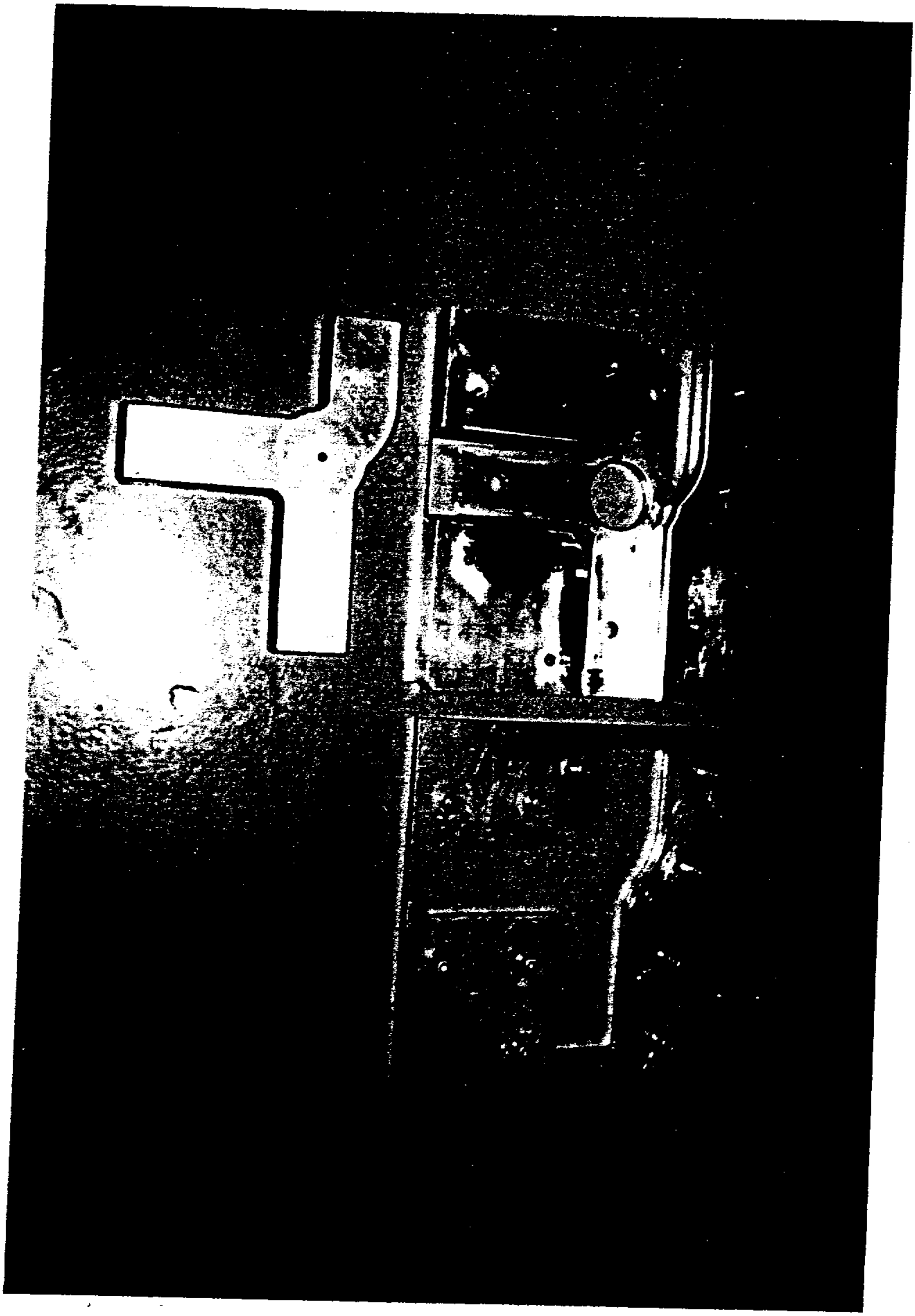

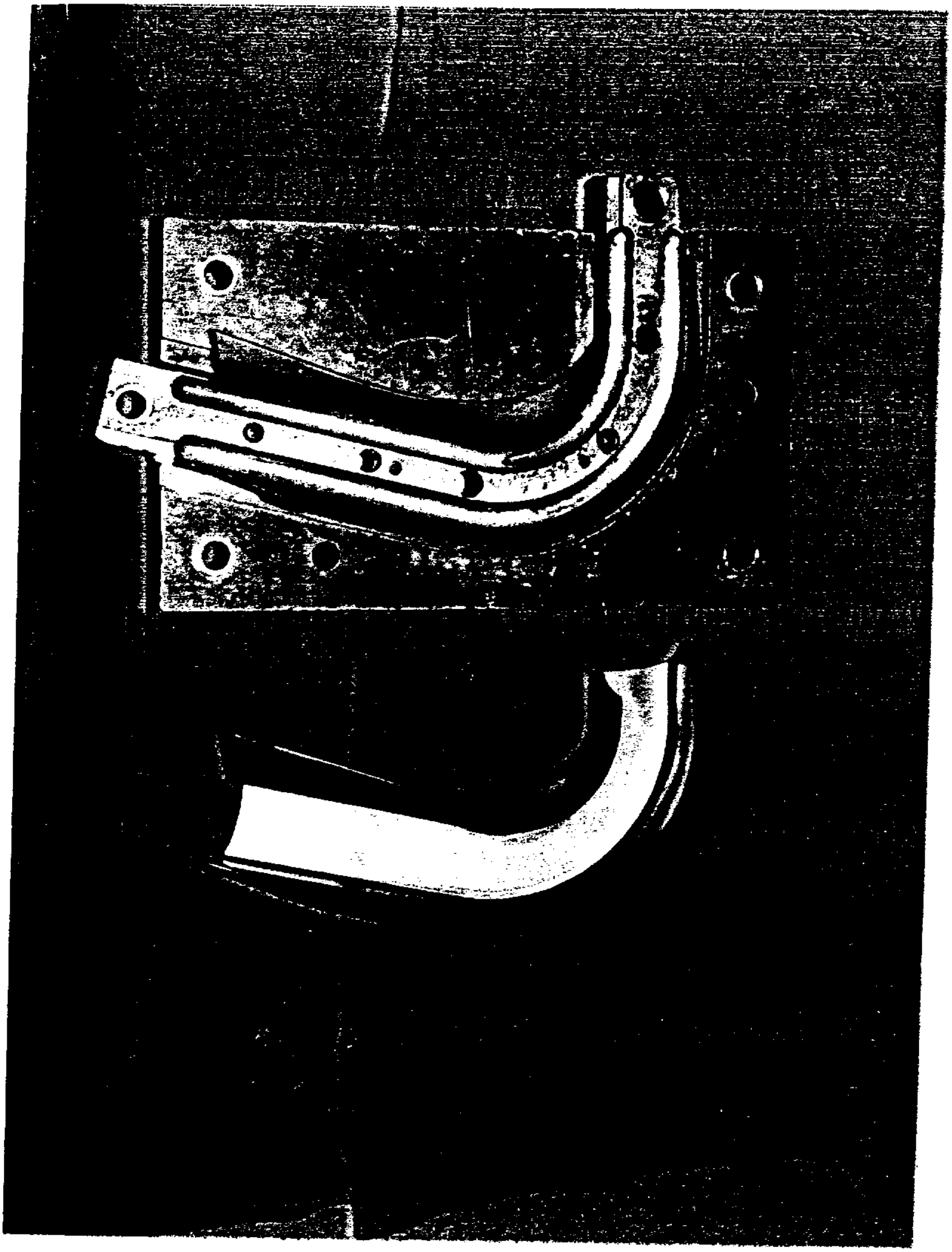

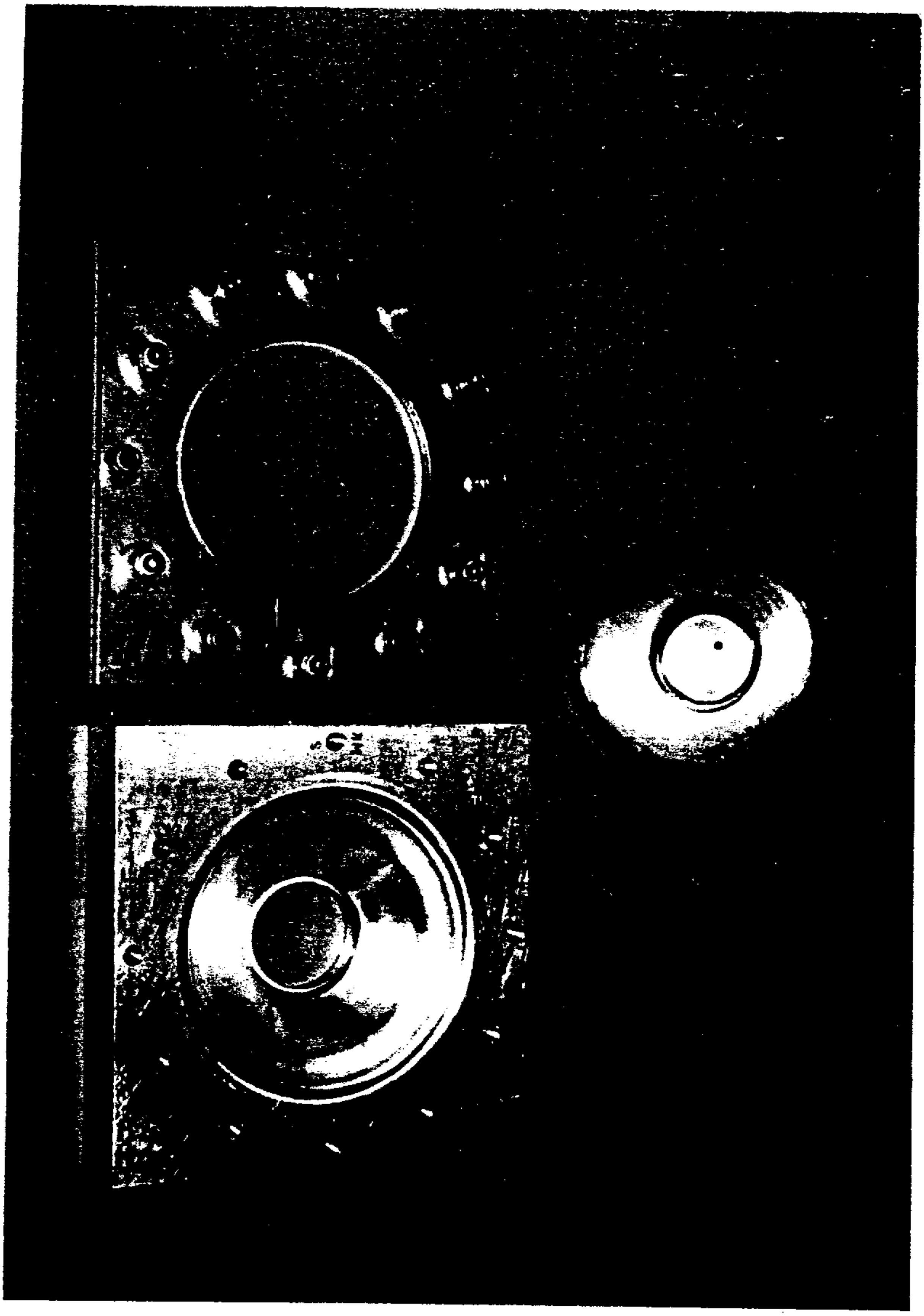

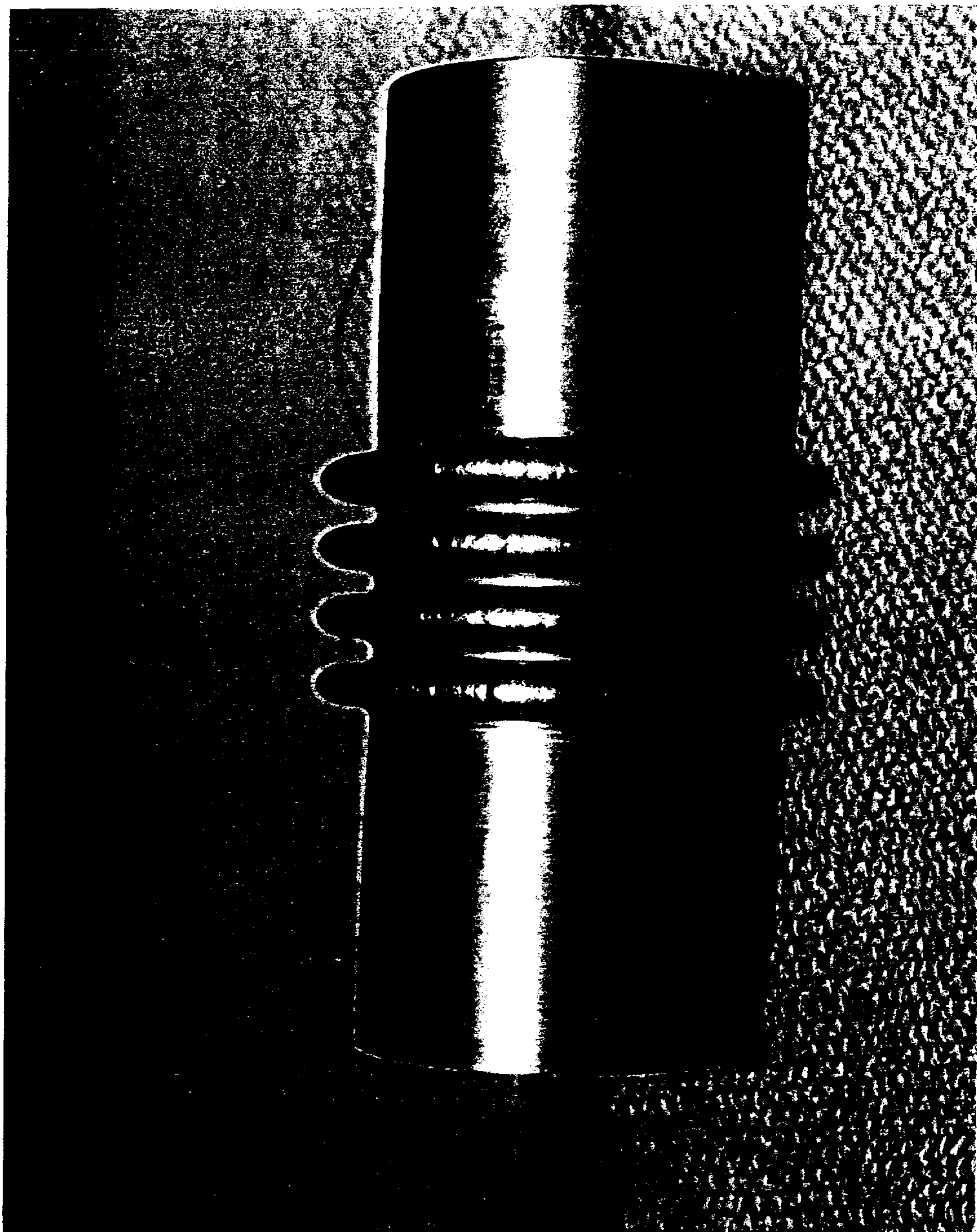

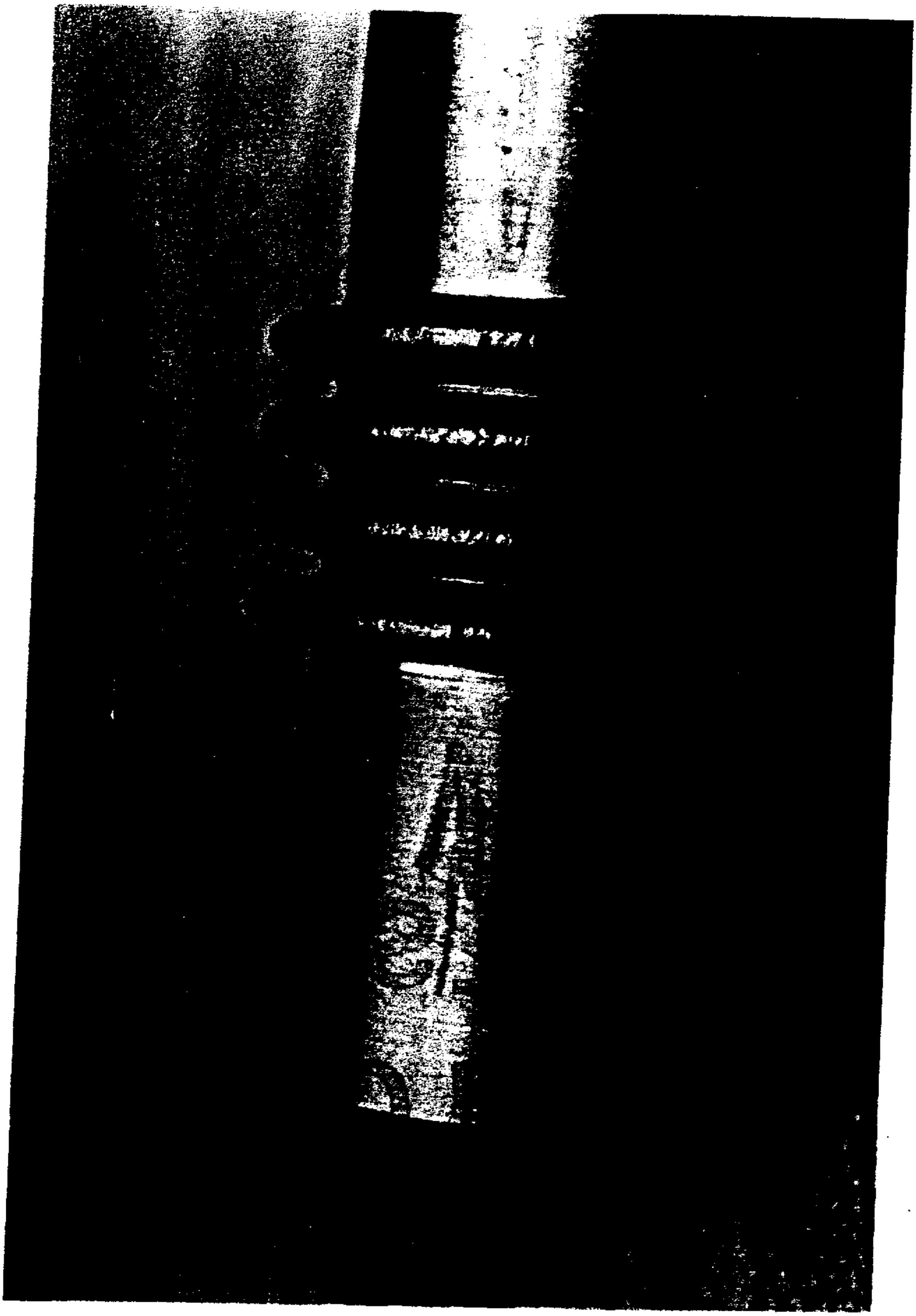

Working group on Niobium properties

C. Antoine, M. Minestrini, M. Kuchnir, F. Schölz, J. Kuzminski, A. Stefanov, W. Singer, G. Rao, B. Bonin.

1. Database on Nb mechanical properties

   What parameters?
   look for correlations between parameters
   determine input parameters for codes

2. Is Nb superplastic?

3. Determine the best parameters for restoration annealing

4. What experiments?

5. List the appropriate codes

Rm 204, Bldg 55
Sem R 1 Bldg 1

Parameters for a database on Nb mechanical properties

Mech. properties
- 1 dim. tract. expt
  - TS
  - YS
  - Al % — max / useful (at necking or at max stress)
- 2 dim tract. expts.
  - Erichsen
  - Swift
  - Guyot

  tests → $(\varepsilon_1 \varepsilon_2)_{max}$
- Hv Vickers hardness

Conditions
- RRR (specify main impurity content)
- a (grain size)
- Sample direction w/r rolling
- Annealing conditions T, t
- Elongation conditions $\dot{\varepsilon}, T$

→ Input for codes
- σ_0, A, n $\quad \sigma = \sigma_0 + A\,\varepsilon^{n}$ ← strain hardening coefficient

Deformation limit

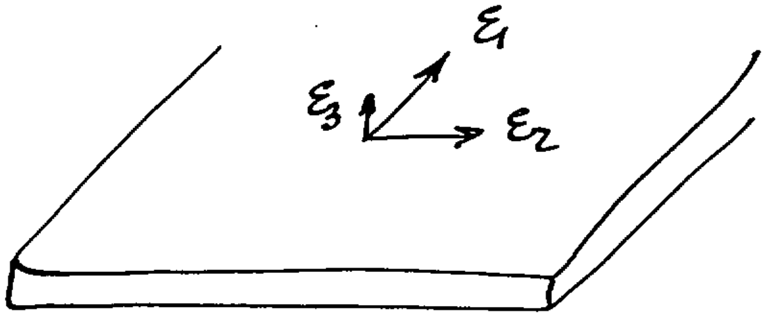

$$\varepsilon_1 + \varepsilon_2 + \varepsilon_3 = 0$$

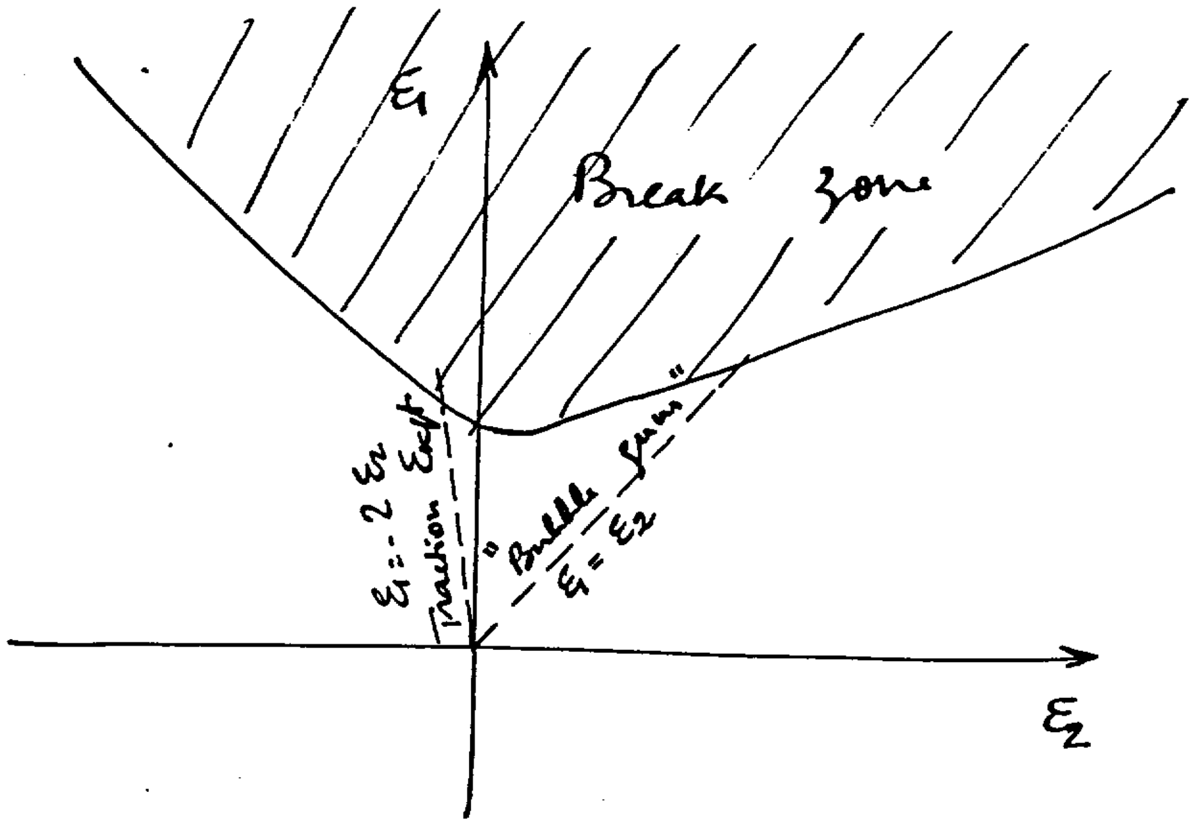

The shape of this curve is not known for niobium. Simple traction expts are not sufficient → { Erichsen, Swift, Guyot } tests.
Need "biaxial" experiments ↗

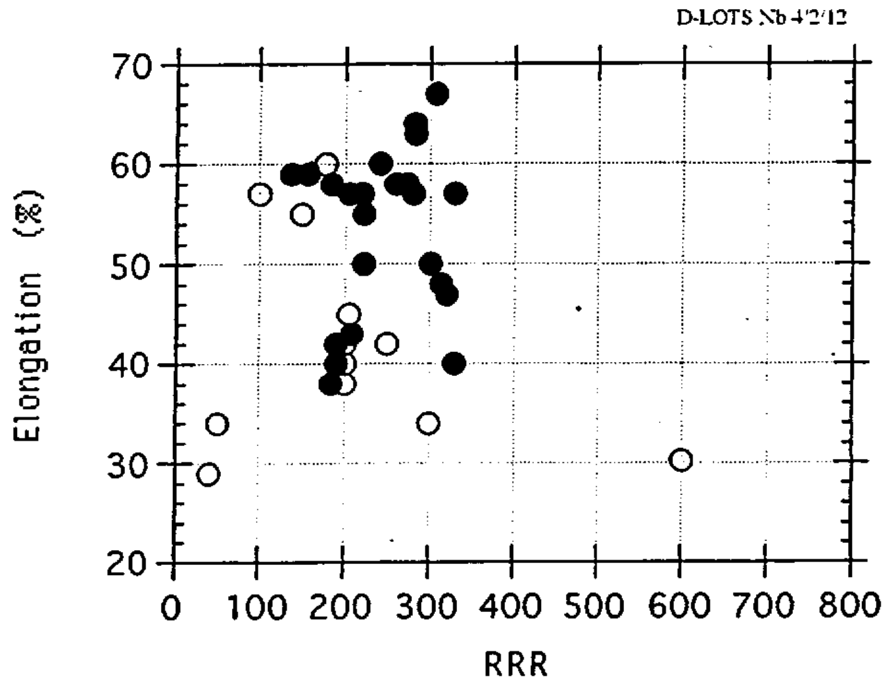

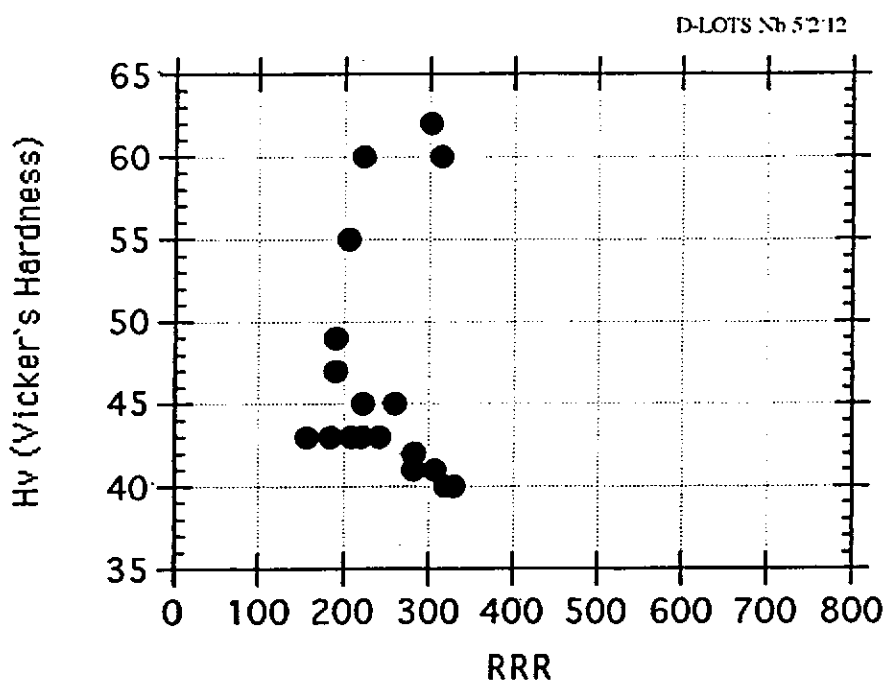

No correlation between parameters.

How to contribute to the database

- Contributions from Cebaf, Saclay, Desy, Los Alamos have been acknowledged.

- Use a common program, easily available in all institutes, and able to select subdatasets and draw correlation plots (Oracle ? Excel)

- Meet periodically (TESLA meetings) to update the database in all institutes.

Annealings of niobium

Forming will imply large deformations
→ probably several steps, with
recrystallisation annealings between steps.

Purpose of the annealing: regain the original mechanical properties (ductility) of the strained material

Mechanism: go back to thermodynamic equilibrium

Expts are needed.

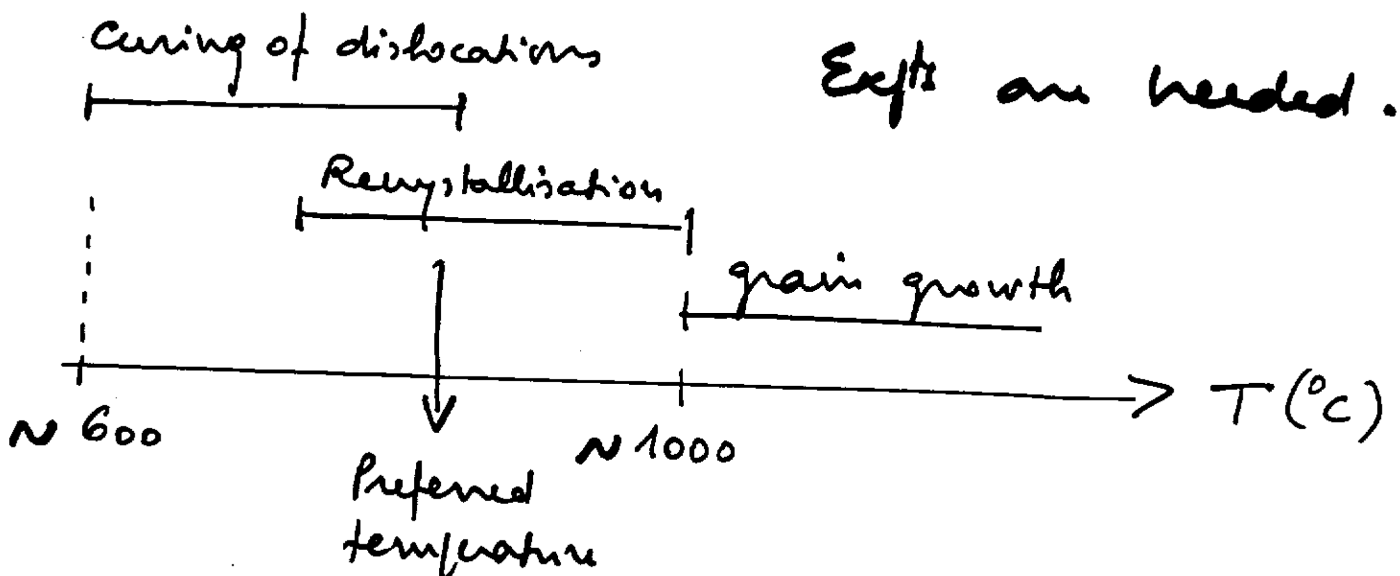

(depends on the degree of work hardening, and on the purity of the material)

~ 770 °C, ref Suppliers

Preliminary result, Saclay.

1 Hour Annealing

$\langle P \rangle \lesssim 10^{-3}$ Pa ($\lesssim 10^{-5}$ Torr)

$\dot{\varepsilon} = 1{,}1 \cdot 10^{-3}$

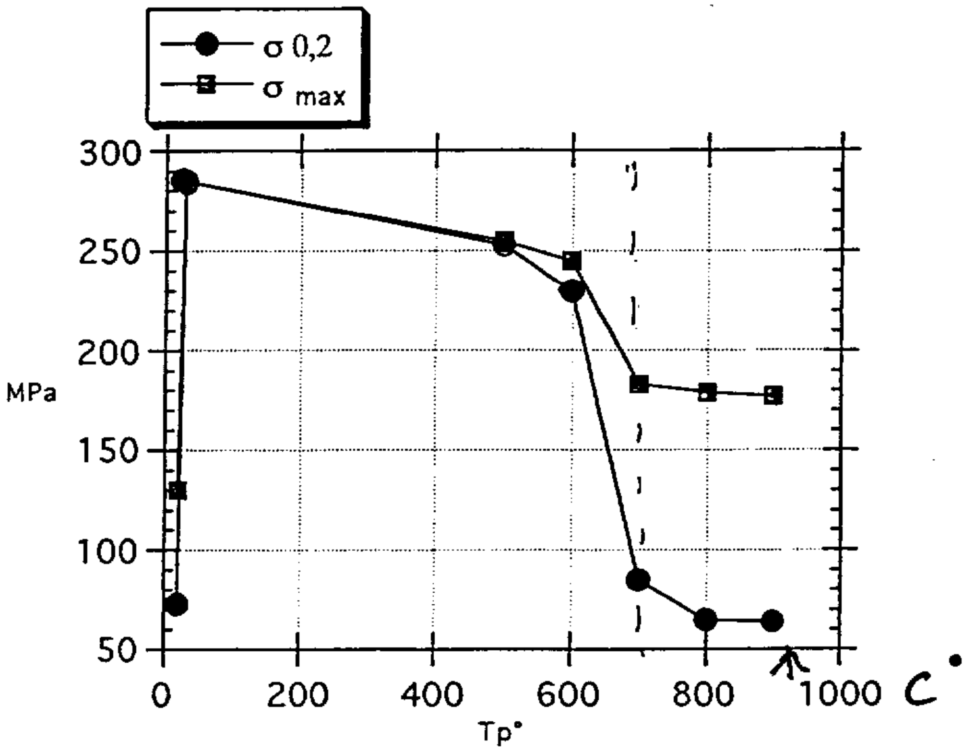

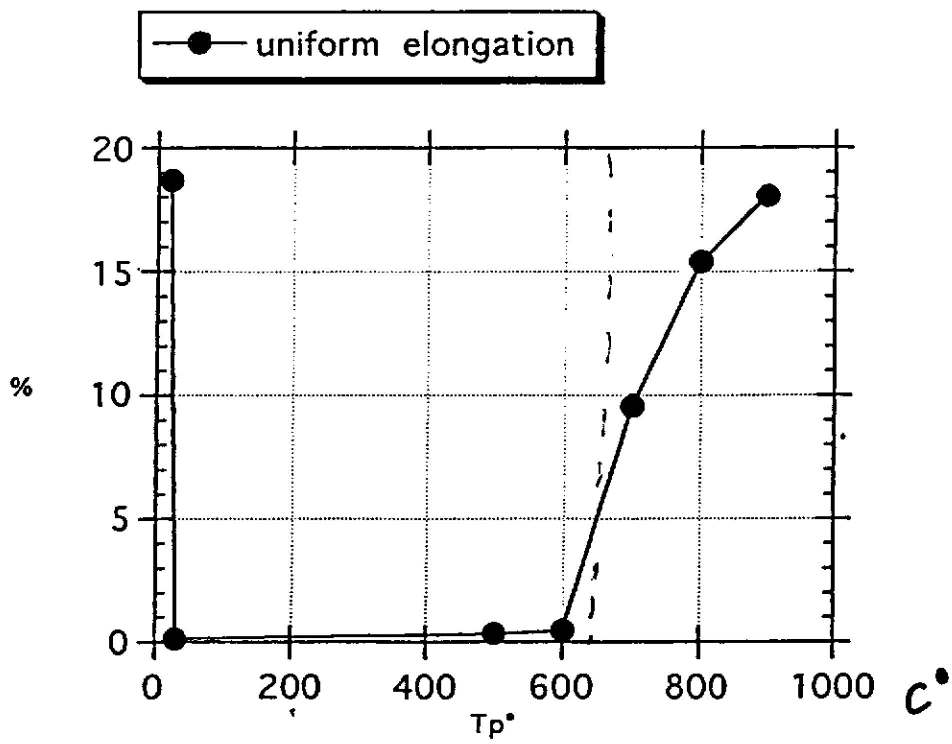

Sample deformed 73% by rolling

Needed experiments

(1) Elongation experiments (for the database)

at weld seams
$\dot{\varepsilon}$ dependence
Sample direction vs rolling

} Uniaxial expts

Erichsen tests
Swift

} Biaxial expts

(2) Deformation - annealing experiments
(to determine the best annealing parameter
T, t)

Deform – anneal – deform
(%) (T, t) (%)

Contributors: DESY, Saclay, Cebaf ....

Preferred :  Exchange results during TESLA meetings

"Triangular" structure

BODY CENTERED CUBIC METALS

Ref A : J.F. FRIES PhD Thesis (1972)
"Influence des el^{ts} interstitiels (O, C, N) sur le comportement plastique en traction du Nb polycristallin entre -253°C et +850°C"

• For BCC Metals, $\sigma = f(\varepsilon)$ [i.e. traction curve] depends strongly from:

- structural state (cold worked, restaured, recrystallised) and/or texture (preferential orient^{ts})
- chemical composition
- mean grain size
- deformation speed
- tp° "

⇒ Hazardous to compare ≠ results unless all these parameters are well defined.

TRACTION CURVES

$\frac{F}{A} \neq \frac{F}{A_0} = \sigma$ (MPa)

Tensile Strength σ_{Max}

Yield stress σ_0 $\left\{ \begin{array}{l} \sigma_{0,2} \\ \sim \\ \sigma_E \end{array} \right.$

Note : σ_E (≡ proportion-nal limit) is delicate to measure accurately (it depends to expl. conditions)

⇒ Intl. convention s to measure σ_0 at 0,2 % deformation

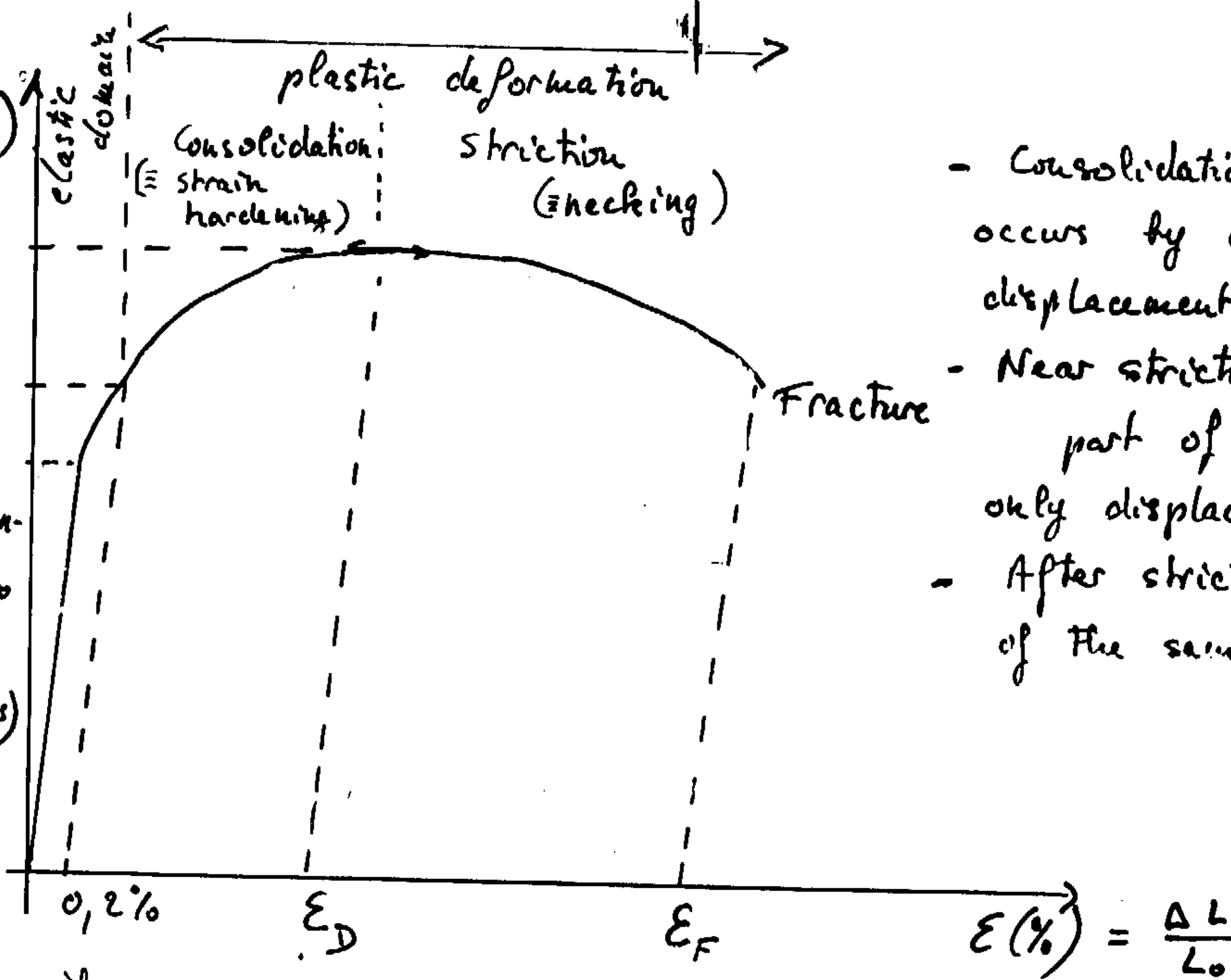

- Consolidation : deformat. occurs by creation & displacement of dislocation
- Near striction (horizontal part of the curve) ⇒ only displacement of dislocat.
- After striction : thinning of the sample to fracture.

ε_D : "distributed elongation" (uniform)
more accurate than ε_F for prediction in deformation but uneasy to measure (flat part of the curve)

ε_F = "Fracture Elongation" → ⚠ depends strongly on localized defects ⇒ varies a lot from a sample to another

A) $\sigma = f(\varepsilon)$

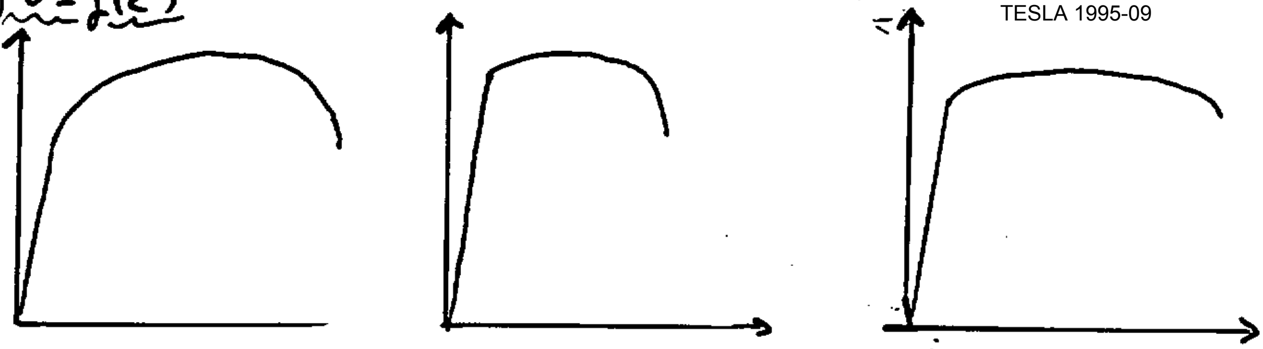

Well annealed sheet → Deformed (rolling or forming) → Partially annealed

↓

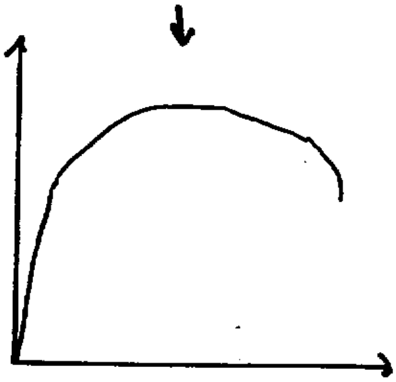

Well Annealed

Note: • Y.S. (σ_0) of sheets are not significant of Y.S. of a formed cavity

B) ROLLING & RECRYSTALLISATION

- same batch (i.e. same purity)
- ~ same mean grain size
- slight ≠ in rolling ⇒ ≠ in recrystallisation!

Isotropic →

ASTM 6-7 (50-35 µm)

⇓

NO DEFORMATION PROBLEM (good strain distribution)

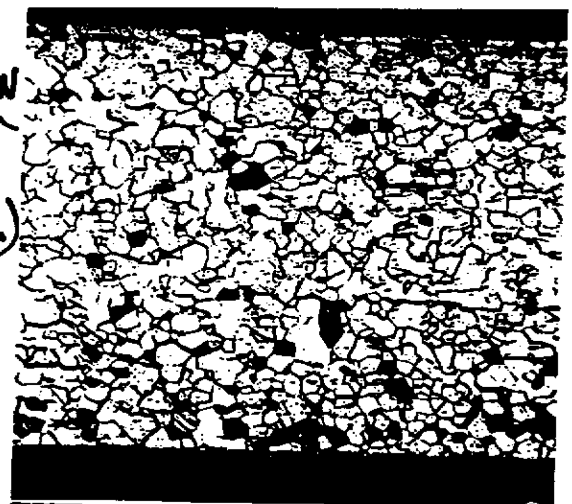

$\phi \leq 30\,\mu m$

$\phi \sim 100\,\mu m$

⇓

EARLY FRACTURE

local strain accumulation.

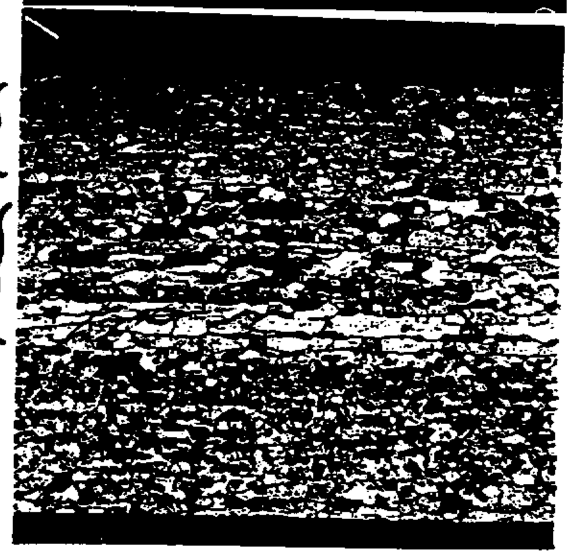

INFLUENCE OF STRAIN RATE ($\dot{\varepsilon}$)

TESLA 1995-09

BCC met

for a given ε : $\boxed{\sigma(\dot{\varepsilon}) \sim A\,\dot{\varepsilon}^{\,n}}$ $A = cst$

n = strain rate sensitivity coeff.

φ origin: interaction with impurities (C, O, N, H)

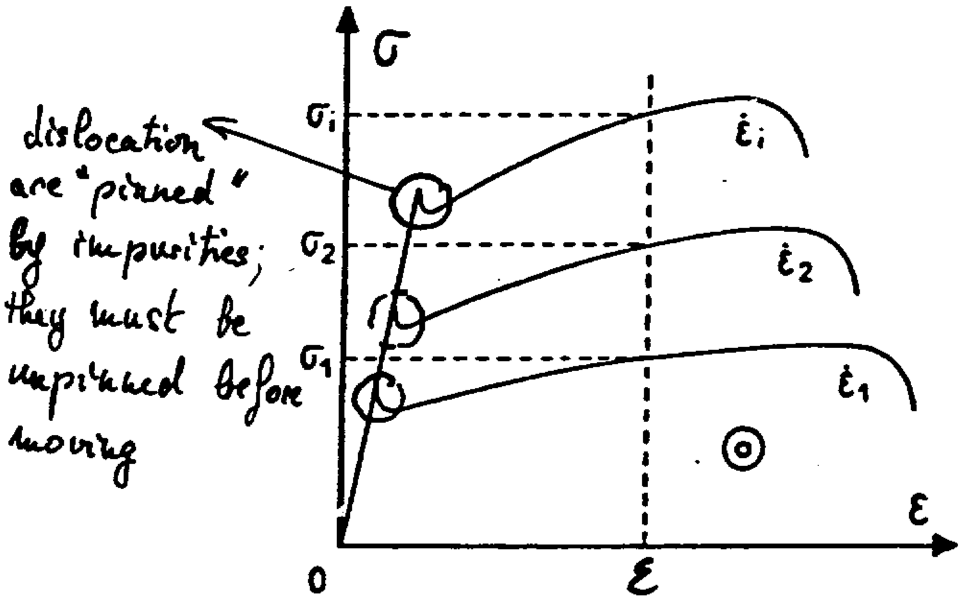

Note: $\dot{\varepsilon}_1 \ll \dot{\varepsilon}_2$ $= f(tp°)$ ⚠

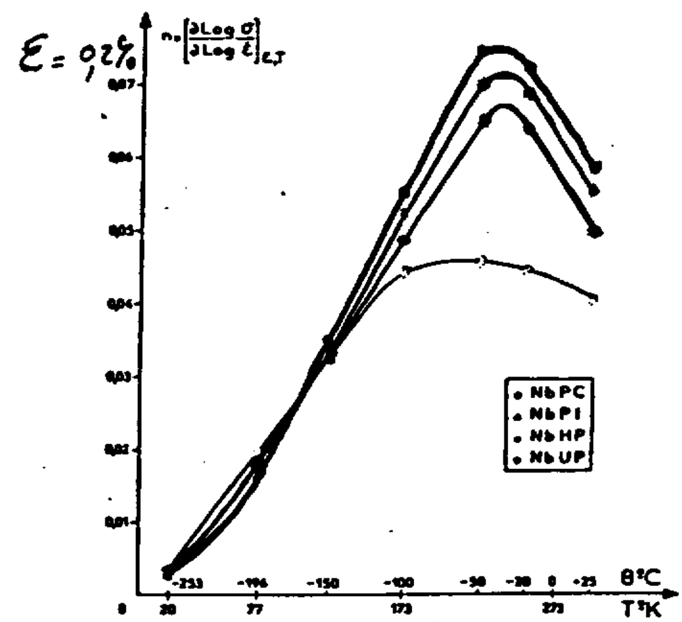

ELEMENT ppm / PURETE	O	C	N	H	W	Ta	Zr	Mo	Fe	Ti	Al
Commerciale	330	70	120	1	400	400	50	100	20	50	50
Intermédiaire	130	50	30	2	320	400	50	30	20	70	50
Haute pureté	55	45	20	<1	20	35	<50	<20	<10	<20	<30
Ultra pur	30	30	<20	<1	<10	<10	<50	<20	<10	<20	<30

ϕ = 30 μm

Ref A

× RRR > 200 (Heraeus)

INFLUENCE OF TEMPERATURE (and PURITY) (Ref A)

(SAME SPEED - SAME SAMPLE GEOMETRY - SAME FACILITY...)

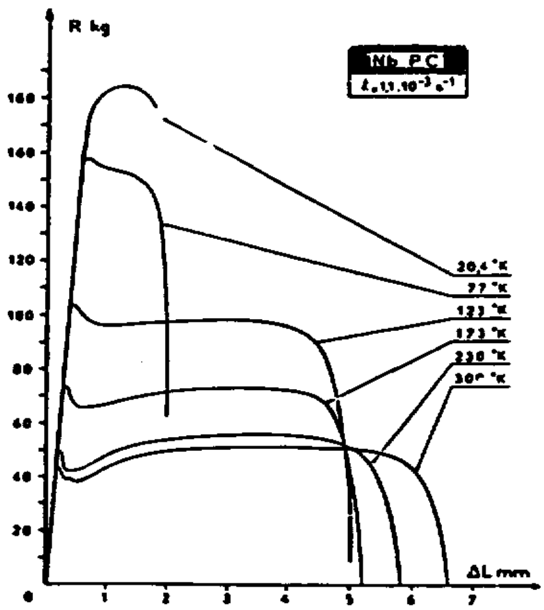

a

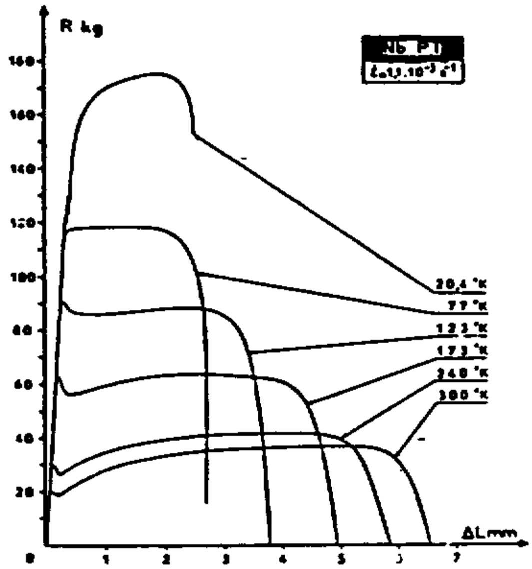

b

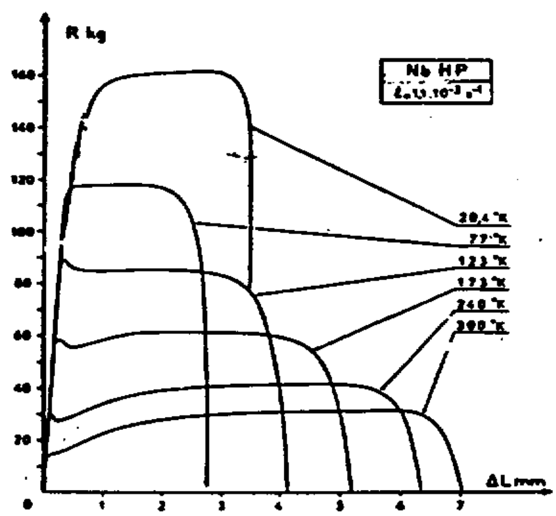

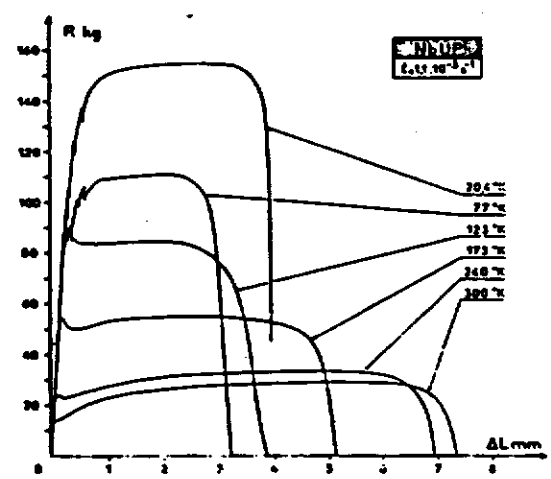

As purity ↗ ⟹ σ_0, σ_{max}, H_V ↘↘, ε_F ↗

ELEMENT ppm / PURETE	O	C	N	H	W	Ta	Zr	Mo	Fe	Ti	Al
Commerciale	330	70	120 (x)	1	400	400	50	100	20	50	50
Intermédiaire	130	50 (x)	30	2	320 (x)	400	50	30	20	70	50
Haute pureté	55 (x)	45	20	<1	20	35 (x)	<50 (x)	<20 (x)	<10	<20	<30
Ultra pur	30	30	<20	<1	<10	<10	<50	<20	<10	<20	<30

[illegible]SAME grain [illegible] (~30 μm) [illegible]SAME [illegible]ruct. state [illegible] well recrystallized)

(x ~ RRR) 200 Heraeus)

RECOVERING ANNEALINGS

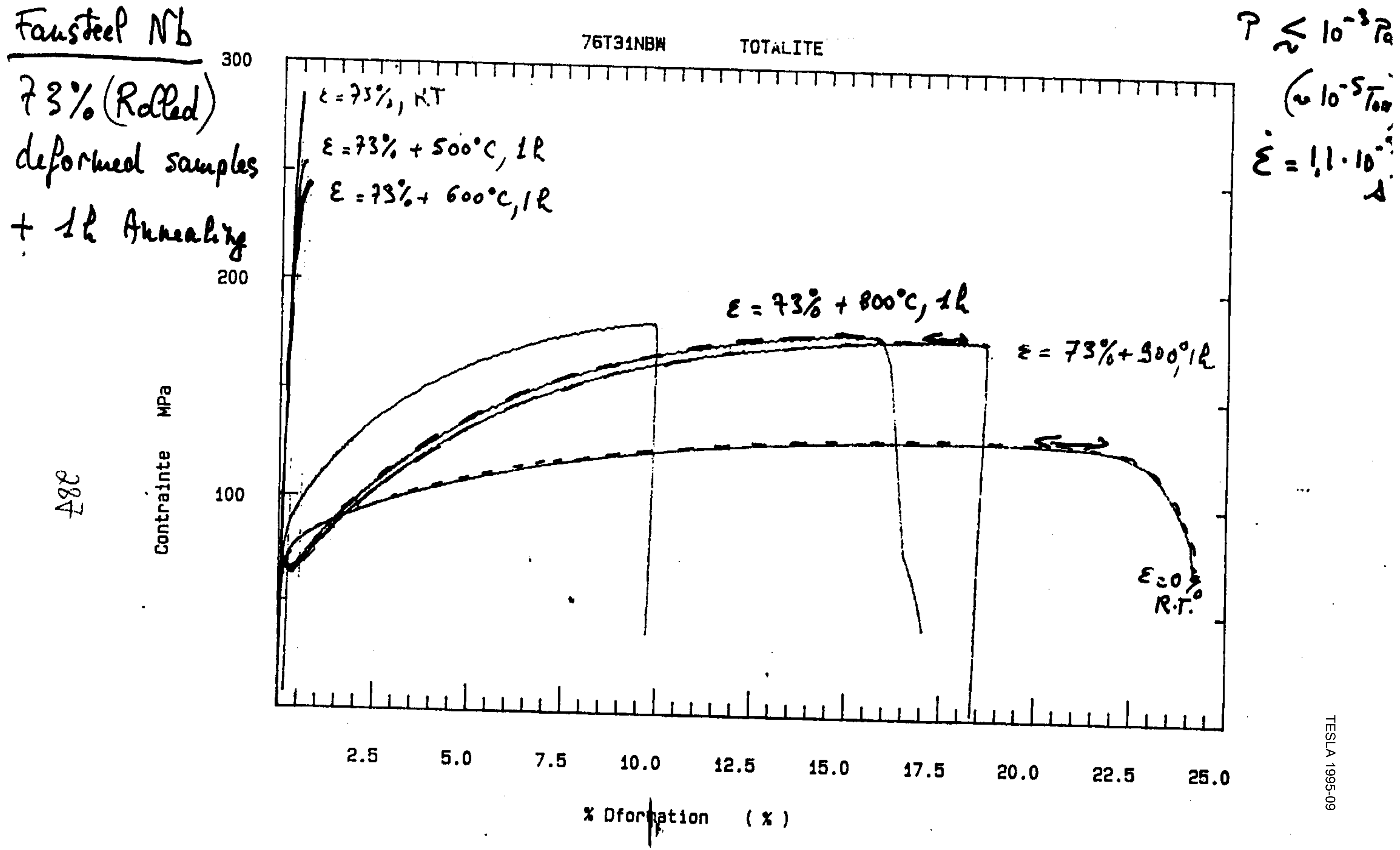

287

DEGRADATION OF RRR

- with deformation

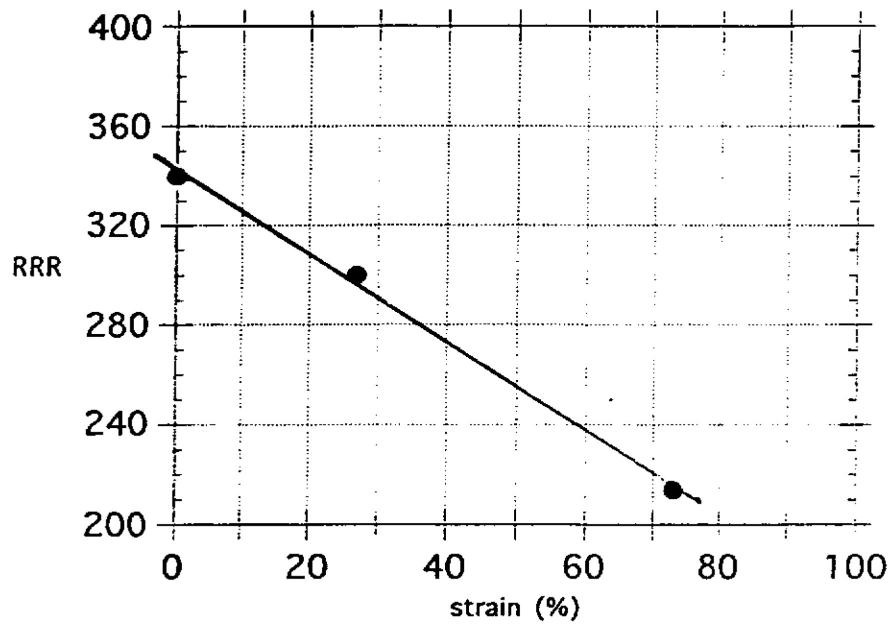

Rolled samples.

- with recovering annealings

1 hour heat treatment at ≤ 10^{-3} Pa on 73% strained samples

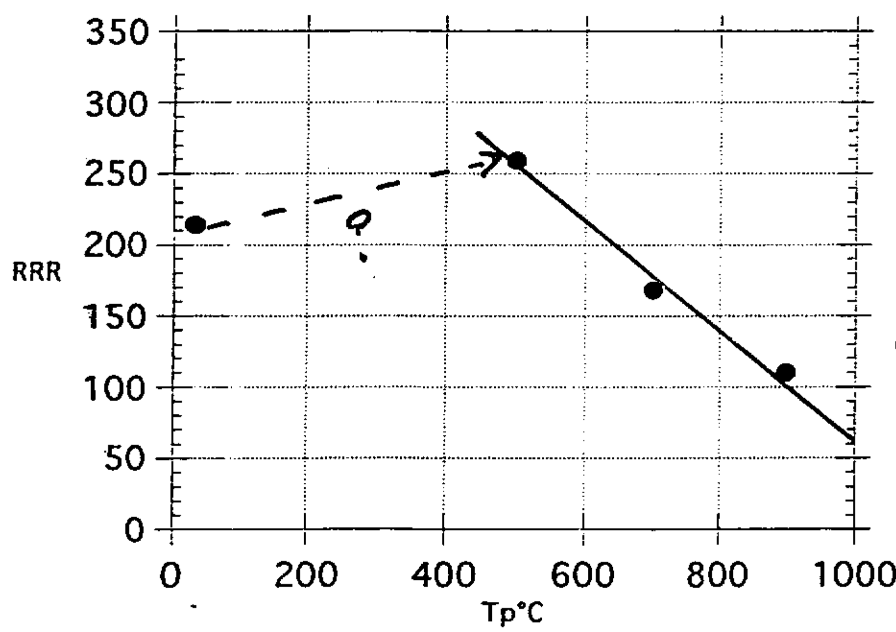

BUT!
very low decrease in Tp.

Working Group on Cavity Fabrication

a). Fabrication Methods

- Spinning
  - External
  - Internal
- Hydroforming
- Superplastic forming
- Hot forming
- Explosion forming
- Electroforming
- "Conventional" Fabrication
  - Hybrid : ebw of n+n-cells
- Nb sputtered on Cu

b). Fabrication of Nb-tube

- Flow Pressing
- Rolling + welding
- Spinning
- Internal / External rollers
- Multi Stage Deep Drawing

c) Material Problems

- Total achievable elongation for Nb
- Surface problems (fissures, surface damage, inclusion
- Appropriate microstructure
- Material tests (Tensile, Erichsen ...)

d). Fabrication costs

e). Who is doing what?

(2)

Method	who	accomplishments	remarks
External Spinning	INFN (V. Palmieri..)	1-cell, 5-cell } Al 1-cell*, 2-cell } Nb 3-cell Cu *will be tested soon	cheap - 20 man hrs / 5 cell Questions: a). thickness variation iris thin 1:4 equator thick 1:1.5 ? Can this be reversed by moving material What d at iris eliminate stiffening ring? What d_{min} is needed to avoid "buckling"? Optimized thickness profile b). Tolerances c). Contamination of material
Internal Spinning rolling	INFN	"single" cell	preliminary attempt showed possibility Questions: Contamination Tolerances Internal surface roughness
	DORNIER	proposed	

Method	who	accomplishments	remarks
Hydroforming	CERN (Hauviller)	Multi-cells @ 352 MHz, @ 1.5 GHz, @ 2.1 GHz } Cu	2–3 intermediate annealing steps; Forming of coupler extrusions possible
	Cornell (1992) (Kirchgessner)	1-cell @ 3 GHz, 2-cell @ 3 GHz } Nb	Tested: $E_{acc} \approx 7$ MV/m, $Q_0 = 8 \times 10^8$; Problems: Ruptures, fixed by TIG
	INR / DESY (Jelezov)	2-cell @ 1.3 GHz Nb proposed	"Magnetic Hammering" of iris considered to be a good approach
	DESY (Stephanov)	2-cell @ 1.3 GHz Nb proposed	
	Butting (DESY	Multi-cell @ 1.3 GHz Nb proposed	use of existing calibrati press with appropriate tooling

Method	who	accomplishments	remarks
Superplastic forming	Dornier	proposed	Questions: Does Nb show superplastic behavior? Important: measurement of m-value (DORNIER). Possible Problems: High temperature (≥1100°C); Reactivity of Nb; Thinning
Hot forming	Cornell (~1983) (Kirchgessner)	at 1500°C reactor grade Nb-tube "blown up" with pressurized gas	Problems: gas purity; high temperature
Explosive forming	INFN (V. Palmieri)	"1-cell" Cu from welded tube	no problems at EBW
	Cornell (~1983) (Kirchgessner)	3mm wall tube of ⌀25mm external spherical cavity	4% expansion okay; >20% expansion → rupture. Conclusion: rapid cold work decreases elongation
	Atlas Ind/CEBAF	proposed, funding pending	
Electroforming	HEPL/Union Carbide (~1968)	X-band cavities	deposition from molten salts slow, too costly
	Siemens/KfK	endplates of S-band cavities	

Method	Who	Accomplishments	Remarks (5)
"conventional" fabrication	everybody	> 20 years of experience > 400 m of cavities	costly possible defects at welds reduction of RRR
Nb sputtered on Cu	CERN + industry INFN Saclay	100 MHz ≤ f ≤ 3 GHz	Fabrication of Cu-structure needs same effort as for Nb-structure Field dependence of Q

Tube fabrication (6)

Method	who	accomplishments	remarks
"Flow Pressing"	W.C. Heraeus	$l = 150$ mm $\phi = 78$ mm $d = 3$ mm	increase of length possible
Rolling + welding	DESY SACLAY	first attempts on samples	microstructure in weld has to be matched to other material mech. properties
Spinning	INFN	$l = 200$ mm $\phi = 78$ mm	needed for Hydroforming of TESLA-cavities $l = 760$ mm $\phi = 126$ mm $d = 2$ mm $\pm$ 0.12 mm Problems: Contamination Thickness variation
Multi Stage deep drawing	Cornell (~1983)	17 stage process $L/D = 13$	no annealing necessary
Combination Spinning / Deep drawing			would calibrate diameter / wall thickness

Fabrication Costs – 9 cell

(+)

"Conventional" Present –	Spinning	Hydroforming	Nb/Cu
Material : DM 18.000	DM 9000.–	Additional cost due to:	even if technology would be available,
Fabrication : DM 30.000	DM 3000.–	• Cleaning	no cost savings expected
	[Tooling: DM 500.– Labor: 30 man hrs]	• Annealing	
DM 48.000	DM 12 000.–	↗ ≈ 1000 - 2000 DM	
without couplers ...			

Workshop on Cavity Fabrication Techniques

Closing remarks

TESLA : 20000 times cavity unit price

- **Joint effort:**

-supply of Nb material

⇒-metal forming technology

-material characteristics (mechanics)

-recover mechanical fabrication damage

-superconducting cavity performance

- **Exchange of ideas, e.g.:**

-electro-magnetic hammer

-inner rolling

-tube forming (recover weld area)

- surface "meshing"

- **Action items**

-make tubes for hydroforming / rolling technique

-make (understand) hydroforming process

-measure spun cavity

- **Nb is a good formable metal**

don't detour with Cu, Al,...(too long)

DK 669.1/.8 : 620.172

März 1986

Prüfung metallischer Werkstoffe	DIN
Zugproben	50 125

Testing of metallic materials; tensile test pieces
Essais des matériaux métalliques; éprouvettes d'essai de traction

Ersatz für Ausgabe 04.51

Zusammenhang mit der von der International Organization for Standardization (ISO) herausgegebenen Internationalen Norm ISO 6892 – 1984 und mit der von der Europäischen Gemeinschaft für Kohle und Stahl (EGKS) herausgegebenen EURONORM 2-80, siehe Erläuterungen.

Maße in mm

1 Anwendungsbereich und Zweck

In dieser Norm sind

a) Formen und Maße von Zugproben aus metallischen Werkstoffen angegeben,

b) Hinweise zusammengestellt, die bei der Herstellung der Zugproben beachtet werden müssen.

Die Norm ist anzuwenden, falls nicht in anderen Normen für bestimmte metallische Werkstoffe und Erzeugnisformen besondere Formen und Maße von Zugproben festgelegt sind. Beispiele siehe Verzeichnis „Weitere Normen".

2 Begriffe

2.1 Proportionale Zugproben (Proportionalproben)

Proportionale Zugproben (Proportionalproben) sind Zugproben, bei denen zwischen der Anfangsmeßlänge L_0 und dem Anfangsquerschnitt S_0 die Beziehung

$$L_0 = 5 \cdot \sqrt{\frac{4}{\pi}} \cdot \sqrt{S_0} = 5{,}65 \cdot \sqrt{S_0} \qquad (1)$$

besteht.

Für Zugproben kreisförmigen Anfangsquerschnitts mit dem Probendurchmesser d_0 (Rundproben) bedeutet dies

$$L_0 = 5 \cdot d_0 \qquad (2)$$

Anmerkung: Im Grundsatz sind alle Zugproben, deren Anfangsmeßlänge nach der Funktion $L_0 = k\sqrt{S_0}$ vom Anfangsquerschnitt abhängt, proportionale Zugproben. Beispielsweise sind auch Zugproben gebräuchlich, bei denen $k = 11{,}3$ oder 4,52 ist. Für Rundproben bedeutet dies $L_0 = 10 \cdot d_0$ oder $L_0 = 4 \cdot d_0$. Die Einschränkung, künftig nur diejenigen Proben proportionale Zugproben zu nennen, bei denen $k = 5{,}65$ ist, soll dazu beitragen, die Formen der Zugproben zu vereinheitlichen.

2.2 Nichtproportionale Zugproben

Nichtproportionale Zugproben sind Zugproben verschiedenen Anfangsquerschnitts S_0, deren Anfangsmeßlänge L_0 unabhängig vom Querschnitt ist.

2.3 Versuchslänge L_c

Die Versuchslänge L_c ist bei spanend bearbeiteten Zugproben die Länge des zylindrischen oder prismatischen Mittelteils der Probe mit dem Anfangsquerschnitt S_0.

Sie ist

a) bei Proben mit rechteckigem Anfangsquerschnitt

$$L_c \geq L_0 + 1{,}5\sqrt{S_0} \qquad (3)$$

b) bei Proben mit kreisförmigem Anfangsquerschnitt

$$L_c \geq L_0 + d_0 \qquad (4)$$

3 Formen und Maße, Bezeichnung

Formen und Maße der Zugproben müssen den Festlegungen nach Abschnitt 2 entsprechen.

Bei rechteckigem Anfangsquerschnitt soll das Verhältnis von Probenbreite b zur Probendicke a nicht größer als 4 : 1 sein. Diese Zugproben werden aus den Probestücken im Regelfall so herausgearbeitet, daß die Probendicke a gleich der Probestück-Dicke ist.

Bei Flachproben mit einer Probendicke unter 5 mm darf das Verhältnis von Probenbreite b zu Probendicke a bis 8 : 1 sein.

Anmerkung: Falls die Probestück-Dicke so groß ist, daß auch bei einem Verhältnis der Probenbreite b zur Probendicke a von 1 : 1 die größte Prüfkraft der Zugprüfmaschine nicht ausreicht, um die Zugfestigkeit zu bestimmen, darf nach Vereinbarung die Probenbreite b kleiner als die Probendicke a gewählt werden. Sie darf aber nicht kleiner als ¼ der Probendicke a sein.

Für eine Auswahl von Zugproben sind in den Abschnitten 3.1 bis 3.7 weitere Angaben über Formen und Maße gemacht sowie Bezeichnungen festgelegt, um die Herstellung dieser Zugproben und die Dokumentation der Prüfergebnisse zu erleichtern. Diese Angaben sind sinngemäß auch auf solche Zugproben zu beziehen, für die keine Einzelangaben gemacht sind.

Bei spanend bearbeiteten Zugproben ist der Anfangsquerschnitt S_0 in der Versuchslänge L_c rechteckig oder kreisförmig. Als Formen A, B, C, D und E sind proportionale Zugproben mit verschiedener Ausbildung der Probenköpfe angegeben. Andere Formen der Probenköpfe können vereinbart werden. Dabei müssen die Mindestwerte der Übergangsradien für die jeweilige Form der Zugprobe eingehalten werden.

Die Formen F und G können gewählt werden, wenn aus unbearbeiteten Abschnitten von Rundstangen, Flachstäben oder Profilen Proportionalproben hergestellt werden sollen.

In den Darstellungen nicht angegebene Einzelheiten sind zweckentsprechend zu wählen. Die Zylinderformtoleranz bei Rundproben und die Parallelitätstoleranz bei Flachproben für die Versuchslänge L_c ist in Tabelle 1 festgelegt. Maßtoleranzen sind nicht angeführt, weil vorausgesetzt wird, daß bei jeder Zugprobe die Maße, die auf das Versuchsergebnis Einfluß haben, vor dem Versuch gemessen werden. Die mindestens erforderliche Oberflächenbeschaffenheit ist nach DIN ISO 1302 angegeben.

Fortsetzung Seite 2 bis 9

Normenausschuß Materialprüfung (NMP) im DIN Deutsches Institut für Normung e.V.

Tabelle 1. Formtoleranzen für die Quermaße der Zugproben

Zugproben	Quermaß	Zylinderformtoleranz oder Parallelitätstoleranz
Formen A, B, C, D	$d_0 \leq 6$ $6 < d_0 \leq 16$ $d_0 > 16$	0,03 0,04 0,05
Form E, zweiseitig bearbeitet	$b \leq 10$ $10 < b \leq 18$ $18 < b \leq 30$ $b > 30$	0,20 0,25 0,30 0,35
Form E, allseitig bearbeitet	$a, b \leq 6$ $6 < a, b \leq 16$ $a, b > 16$	0,03 0,04 0,05

3.1 Zugproben Form A

Rundproben mit glatten Zylinderköpfen zum Einspannen in Spannkeile

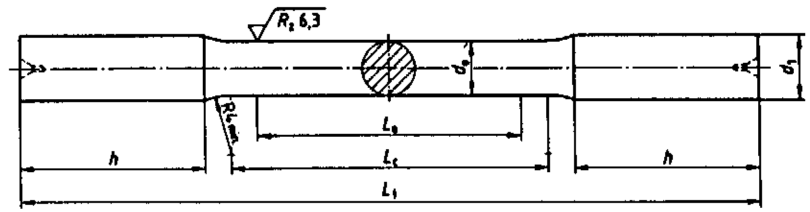

d_0 Probendurchmesser
d_1 Kopfdurchmesser ($\approx 1{,}2\, d_0$)
h Kopfhöhe

L_0 Anfangsmeßlänge ($L_0 = 5\, d_0$)
L_c Versuchslänge ($L_c \geq L_0 + d_0$)
L_t Gesamtlänge

Bezeichnung einer Zugprobe Form A mit Probendurchmesser $d_0 = 12$ mm und Anfangsmeßlänge $L_0 = 60$ mm:

Zugprobe DIN 50125 – A 12 × 60

Tabelle 2. Beispiele für Maße von Zugproben Form A

d_0	L_0	d_1 ≈	h min.	L_c min.	L_t min.
3	15	4	12	18	50
4	20	5	16	24	65
5	25	6	20	30	80
6	30	8	25	36	95
8	40	10	30	46	115
10	50	12	35	60	140
12	60	15	40	72	160
14	70	17	45	84	185
16	80	20	50	96	205
18	90	22	55	108	230
20	100	24	60	120	250
25	125	30	70	150	300

3.2 Zugproben Form B

Rundproben mit Gewindeköpfen

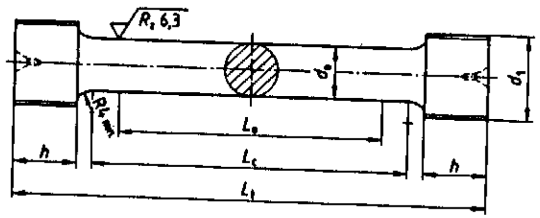

d_0 Probendurchmesser
d_1 Metrisches ISO-Gewinde
h Kopfhöhe
L_0 Anfangsmeßlänge ($L_0 = 5\,d_0$)
L_c Versuchslänge ($L_c \geq L_0 + d_0$)
L_t Gesamtlänge

Bezeichnung einer Zugprobe Form B mit Probendurchmesser $d_0 = 14$ mm und Anfangsmeßlänge $L_0 = 70$ mm:

Zugprobe DIN 50 125 – B 14 × 70

Tabelle 3. **Beispiele für Maße von Zugproben Form B**

d_0	L_0	d_1	h min.	L_c min.	L_t min.
3	15	M 5	5	18	32
4	20	M 6	6	24	40
5	25	M 8	7	30	50
6	30	M 10	8	36	60
8	40	M 12	10	48	75
10	50	M 16	12	60	90
12	60	M 18	15	72	110
14	70	M 20	17	84	125
16	80	M 24	20	96	145
18	90	M 27	22	108	160
20	100	M 30	24	120	175
25	125	M 33	30	150	220

299

3.3 Zugproben Form C

Rundproben mit Schulterköpfen

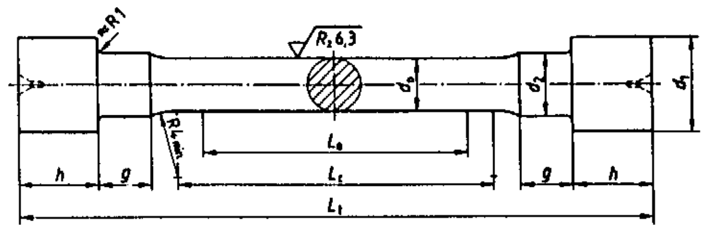

d_0 Probendurchmesser
d_1 Kopfdurchmesser ($\approx 1{,}75\,d_0$)
d_2 Durchmesser des Ansatzes ($\approx 1{,}2\,d_0$)
g Länge des Ansatzes ($\approx d_0$)
h Kopfhöhe ($\approx d_0 + 5$ mm)
L_0 Anfangsmeßlänge ($L_0 = 5\,d_0$)
L_c Versuchslänge ($L_c \geq L_0 + d_0$)
L_t Gesamtlänge

Bezeichnung einer Zugprobe Form C mit Probendurchmesser $d_0 = 16$ mm und Anfangsmeßlänge $L_0 = 80$ mm:

Zugprobe DIN 50 125 – C 16 × 80

Tabelle 4. **Beispiele für Maße von Zugproben Form C**

d_0	L_0	d_1 min.	d_2	g	h min.	L_c min.	L_t min.
3	15	6	4	3	6	18	40
4	20	7	5	4	7	24	50
5	25	9	6	5	8	30	60
6	30	11	8	6	11	36	80
8	40	14	10	8	13	48	100
10	50	18	12	10	15	60	120
12	60	21	15	12	17	72	140
14	70	25	17	14	19	84	160
16	80	28	20	16	21	96	180
18	90	31	22	18	23	108	200
20	100	35	24	20	25	120	220
25	125	44	30	25	30	150	270

3.4 Zugproben Form D

Rundproben mit Kegelköpfen

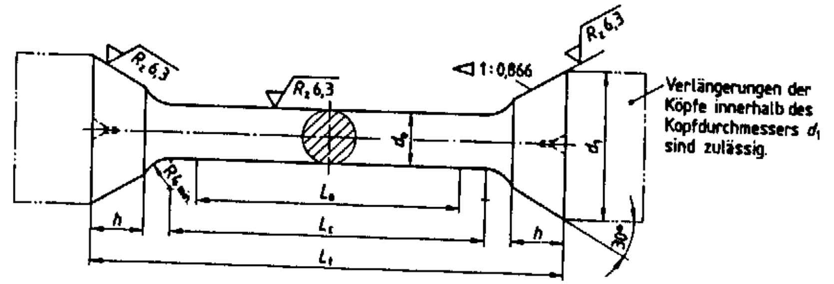

d_0 Probendurchmesser
d_1 Kopfdurchmesser ($\approx 2\,d_0 + 8$ mm)
h Kopfhöhe ($\approx d_0$)

L_0 Anfangsmeßlänge ($L_0 = 5\,d_0$)
L_c Versuchslänge ($L_c \geq L_0 + d_0$)
L_t Gesamtlänge

Bezeichnung einer Zugprobe Form D mit Probendurchmesser $d_0 = 12$ mm und Anfangsmeßlänge $L_0 = 60$ mm:

Zugprobe DIN 50125 – D 12 × 60

Tabelle 5. Beispiele für Maße von Zugproben Form D

d_0	L_0	d_1	h ≈	L_c min.	L_t min.
3	15	10	3	18	30
4	20	12	4	24	38
5	25	14	5	30	46
6	30	20	6	36	60
8	40	24	8	48	75
10	50	28	10	60	90
12	60	32	12	72	105
14	70	36	14	84	120
16	80	40	16	96	140
18	90	44	18	108	155
20	100	48	20	120	170
25	125	58	25	150	210

300

3.5 Zugproben Form E

Flachproben mit Köpfen für Spannkeile

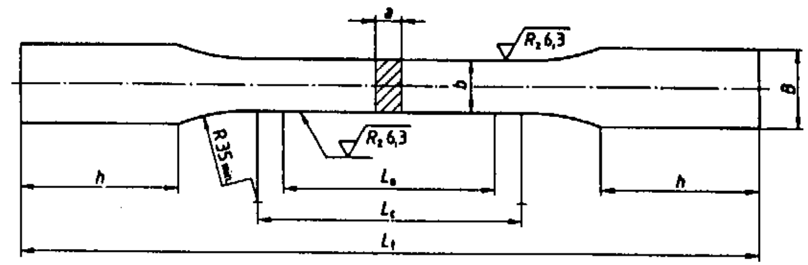

a Probendicke
b Probenbreite
B Kopfbreite ($\approx 1{,}2\,b + 3$ mm)
h Kopfhöhe ($\approx 2\,b + 10$ mm)

L_0 Anfangsmeßlänge
L_c Versuchslänge ($L_c \geq L_0 + 1{,}5\sqrt{S_0}$)
L_t Gesamtlänge

Bezeichnung einer Zugprobe Form E mit Probendicke $a = 5$ mm, Probenbreite $b = 16$ mm und Anfangsmeßlänge $L_0 = 50$ mm:

Zugprobe DIN 50125 – E 5 × 16 × 50

Tabelle 6. Beispiele für Maße von Zugproben Form E

a	b	L_0	B min.	h min.	L_c min.	L_t min.
3	8	30	12	26	38	115
4	10	35	15	30	45	135
5	10	40	15	30	50	140
5	16	50	22	40	65	175
6	20	60	27	50	80	210
7	22	70	29	55	90	230
8	25	80	33	60	105	260
10	25	90	33	60	115	270
10	30	100	40	70	125	300
12	26	100	34	65	125	295
15	30	120	40	70	150	325
16	30	130	40	70	160	335

Anmerkung 1: Flachproben werden vorwiegend aus Bändern, Blechen, Flachstäben und Profilen entnommen. Die Kanten sind zu entgraten. Die Walzhaut ist möglichst nicht abzuarbeiten, die Probendicke a ist dann gleich der Erzeugnisdicke.

Anmerkung 2: Bei allseitig bearbeiteten Flachproben gilt die geforderte Oberflächenrauheit für alle Flächen mit Ausnahme der Probenköpfe.

3.6 Zugproben Form F

Unbearbeitete Abschnitte von Rundstangen

Bezeichnung einer Zugprobe Form F mit Probendurchmesser $d_0 = 10$ mm und Anfangsmeßlänge $L_0 = 50$ mm:

Zugprobe DIN 50125 – F 10 × 50

Tabelle 7. **Beispiele für Maße von Zugproben Form F**

Probendurchmesser d_0	Anfangsmeßlänge L_0	Gesamtlänge L_t min.
6	30	100
8	40	120
10	50	140
12	60	170
14	70	190
16	80	210
18	90	240
20	100	260
25	125	310

3.7 Zugproben Form G

Unbearbeitete Abschnitte aus Flachstäben und Profilen

Bezeichnung einer Zugprobe Form G mit Anfangsquerschnitt $S_0 = 314$ mm² und Anfangsmeßlänge $L_0 = 100$ mm:

Zugprobe DIN 50125 – G 314 × 100

Tabelle 8. **Beispiele für Maße von Zugproben Form G**

Anfangsquerschnitt S_0 mm²	Anfangsmeßlänge L_0	Gesamtlänge L_t min.
50	40	130
78	50	150
113	60	170
154	70	190
200	80	210
254	90	230
314	100	250
380	110	270
452	120	290
530	130	310

4 Bearbeitung der Zugproben

Die Zugproben sind so zu entnehmen und zu bearbeiten, daß die Werkstoffeigenschaften nicht beeinflußt werden. Bei der Entnahme durch thermisches Schneiden (z. B. Brennschneiden) oder stark verformende Schneidverfahren (z. B. Scherschneiden) sind je Probenseite Mindestbearbeitungszugaben nach Tabelle 9 vorzusehen.

Tabelle 9. **Bearbeitungszugaben je Probenseite**

Bearbeitungszugabe je Probenseite min. bei Erzeugnisdicke		
unter 30	30 bis 50	über 50
5	7	10

Stauchen oder Strecken der Zugproben ist nicht zulässig. Richten der Zugproben soll möglichst vermieden werden. Ist es unumgänglich, muß ein Vermerk darüber im Prüfbericht angegeben werden.

Zentrierbohrungen für das Abdrehen sind vorzubohren und zu belassen, damit die Zugproben nötigenfalls nachgearbeitet werden können.

Beim Fertigbearbeiten mit spanenden Werkzeugen sind Schnittgeschwindigkeiten, Vorschub und Spantiefe dem Werkstoff anzupassen, um eine unzulässige Erwärmung oder Kaltverfestigung des Werkstoffs und damit eine Beeinflussung seiner Eigenschaften zu vermeiden.

Die Angabe R_z 6,3 für die Oberflächenrauheit gilt für metallische Werkstoffe, die gut verformbar und zäh sind. In besonderen Fällen (z. B. bei hochfesten oder besonders kerbempfindlichen Werkstoffen) sind höhere Anforderungen an die Oberflächenrauheit zu stellen. Dies ist in den entsprechenden Qualitätsnormen anzugeben oder besonders zu vereinbaren.

301

5 Kennzeichnung

Die Kennzeichnung der Zugproben ist so zu wählen, daß aus ihr auch nach dem Versuch zu ersehen ist, welchem Probestück sie entnommen wurden und, wenn erforderlich, wie ihre Lage und Richtung im Probestück war. Die Kennzeichnung ist auf der Stirnfläche oder auf der Seitenfläche eines Kopfes oder, nötigenfalls, auf den Seitenflächen beider Köpfe anzubringen.

Zitierte Normen

DIN ISO 1302 Technische Zeichnungen; Angabe der Oberflächenbeschaffenheit in Zeichnungen

Weitere Normen

DIN 13912 Zahnheilkunde; Cobalt-Chrom-Gußlegierungen, Anforderungen, Prüfung
DIN 50109 Prüfung von Gußeisen mit Lamellengraphit (Grauguß); Zugversuch
DIN 50114 Prüfung metallischer Werkstoffe; Zugversuch ohne Feindehnungsmessung an Blechen, Bändern oder Streifen mit einer Dicke unter 3 mm
DIN 50140 Prüfung metallischer Werkstoffe; Zugversuch an Rohren und Rohrstreifen
DIN 50148 Zugproben für Druckguß aus Nichteisenmetallen
DIN 50149 Prüfung von Temperguß; Zugversuch
DIN 50154 Zugversuch ohne Feindehnungsmessung an Folien und Bändern aus Aluminium und Aluminium-Knetlegierungen mit einer Dicke bis zu 0,179 mm
DIN 51210 Teil 1 Prüfung metallischer Werkstoffe; Zugversuch an Drähten, ohne Feindehnungsmessung
DIN 51210 Teil 2 Prüfung metallischer Werkstoffe; Zugversuch an Drähten, mit Feindehnungsmessung

Frühere Ausgaben

DIN DVM 125 – DIN 50125: 08.40, 04.51

Änderungen

Gegenüber der Ausgabe April 1951 wurden folgende Änderungen vorgenommen:

a) Der Text wurde gekürzt, indem auf allgemeine Ausführungen verzichtet wurde.
b) Auf die früher als langer Proportionalstab bezeichnete Probe mit dem Faktor $k = 11{,}3$ wird in den Tabellen nicht mehr eingegangen. Diese Probe soll nicht mehr als proportionale Zugprobe bezeichnet werden.
c) Die Mindestbearbeitungszugaben je Probenseite bei der Entnahme durch Brennschneiden oder Scherschneiden sind in Anlehnung an DIN 50121 Teil 1 verringert worden.
d) Die als Beispiele angeführten tabellarischen Maßangaben der Zugproben Form A, B, C, D und E wurden zu kleinen Querschnitten hin erweitert.

Erläuterungen

Diese Norm wurde vom Arbeitsausschuß NMP 142 „Prüfverfahren mit zügiger Beanspruchung für Metalle" im Normenausschuß Materialprüfung (NMP) ausgearbeitet.

Von der International Organization for Standardization (ISO) ist eine Norm ausgearbeitet worden, die ebenfalls Festlegungen über Zugproben enthält:

ISO 6892 – 1984
E: Metallic materials – Tensile testing
D: Metallische Werkstoffe – Zugversuch
1. Ausgabe 15. Juli 1984

Die Europäische Gemeinschaft für Kohle und Stahl (EGKS) hat die EURONORM 2-80 Zugversuch an Stahl, Ausgabe März 1980, herausgegeben [1]).

Diese internationalen Normen enthalten unter anderem auch Angaben über Form, Maße und Bearbeitung von Zugproben. Eine besondere Norm über Zugproben aus metallischen Werkstoffen gibt es im internationalen Bereich nicht.

In ISO 6892 – 1984 wird unter anderem ausgeführt, daß die Zugproben, bei denen zwischen der Anfangsmeßlänge L_0 und dem Anfangsquerschnitt S_0 die Beziehung $L_0 = k \cdot \sqrt{S_0}$ besteht, proportionale Zugproben genannt werden und international für k der Zahlenwert 5,65 angenommen worden ist. Anschließend wird auf die spanend bearbeiteten und die unbearbeiteten Zugproben eingegangen und empfohlen, die Größe des Übergangsradius von der Versuchslänge L_c zu den Probenköpfen in den Werkstoffnormen festzulegen, soweit nicht ISO 6892 – 1984 Angaben darüber enthält.

Tabelle 10. **Festlegungen über Proben in ISO 6892 – 1984 und DIN-Normen**

Erzeugnisform	ISO 6892	DIN-Norm
Blech oder Band mit einer Dicke von 0,1 bis ≤3,0 mm	Anhang B	DIN 50114
Draht mit einem Durchmesser oder einer Seitenlänge < 4 mm	Anhang C	DIN 51210 Teil 1
Erzeugnisse mit einer Dicke ≥3,0 mm oder einem Durchmesser ≥4 mm	Anhang D	DIN 50125
Rohre	Anhang E	DIN 50140

[1]) Zu beziehen beim Beuth Verlag GmbH, Burggrafenstraße 6, 1000 Berlin 30.

TESLA 1995-09